Les effets de l'augmentation de la masse adipeuse sur la fonction cardiovasculaire ex vivo en fonction du stress oxydant et de la fonction mitochondriale : rôle du vieillissement du régime alimentaire

Evangelia Mourmoura

UNIVERSITÉ DE GRENOBLE

THESIS

To obtain the degree of

DOCTOR OF PHILOSOPHY OF UNIVERSITE DE GRENOBLE

Specialty: **Physiology Physiopathology Pharmacology**

Ministerial order: 7 August 2006

Presented by

« Evangelia MOURMOURA »

PhD thesis supervised by « Luc DEMAISON »

in the **Laboratory of Fundamental and Applied Bioenergetics (LBFA)**

in the **École Doctorale Chimie et Sciences du Vivant**

The effects of the increase in the adipose tissue mass on the cardiovascular function *ex vivo* in association with the oxidative stress and mitochondrial function: role of aging and diet

Public PhD thesis defense « 5 Novembre 2012 »,
In front of the jury composed of:

Dr Luc DEMAISON
Researcher of INRA, Université de Grenoble I, PhD supervisor
Pr Catherine GHEZZI
Professor, Université de Grenoble I, Member
Dr Beatrice MORIO
Director of Research, INRA Clermont-Ferrand, Reviewer
Pr Christophe RIBUOT
Professor, Université de Grenoble I, Member
Pr Luc ROCHETTE
Professor, Université de Bourgogne, Member
Pr Catherine VERGELY
Professor, Université de Bourgogne, Reviewer

UNIVERSITÉ DE GRENOBLE

THÈSE

Pour obtenir le grade de

DOCTEUR DE L'UNIVERSITÉ DE GRENOBLE

Spécialité : **Physiologie Physiopathologies Pharmacologie**

Arrêté ministériel : 7 août 2006

Présentée par

« Evangelia MOURMOURA »

Thèse dirigée par **« Luc DEMAISON »**

préparée au sein du **Laboratoire de Bioénergétique Fondamentale et Appliquée (LBFA)**
dans **l'École Doctorale Chimie et Sciences du Vivant**

Les effets de l'augmentation de la masse adipeuse sur la function cardiovasculaire *ex vivo* en fonction du stress oxydant et de la fonction mitochondriale : rôle du vieillissement et du régime alimentaire

Thèse soutenue publiquement le « 5 Novembre 2012 »,
devant le jury composé de :

Dr Luc DEMAISON
Chargé de Recherches INRA, Université de Grenoble I, Directeur

Pr Catherine GHEZZI
Professeur, Université de Grenoble I, Examinateur

Dr Beatrice MORIO
Directeur de Recherches, INRA Clermont-Ferrant, Rapporteur

Pr Christophe RIBUOT
Professeur, Université de Grenoble I, Examinateur

Pr Luc ROCHETTE
Professeur, Université de Bourgogne, Examinateur

Pr Catherine VERGELY
Professeur, Université de Bourgogne, Rapporteur

« Πάντες ἄνθρωποι τοῦ εἰδέναι ὀρέγονται φύσει »

Αριστοτέλης

« Tous les hommes ont naturellement le désir de savoir »

Aristote

Remerciements

Je tiens à remercier d'abord le Ministère de la Recherche qui m'a accordé une bourse et ainsi permis de mener à bien ce projet de thèse.

J'exprime tous mes remerciements à mon directeur de Thèse, le Docteur Luc Demaison, qui m'a prise sous son aile pendant mon stage de Master 2 Recherche et qui m'a fait confiance pour mener à bien ce travail de thèse tout en mettant à ma disposition les moyens d'y parvenir. Un grand merci pour son accompagnement et son encadrement tout au long de ce trajet ainsi que pour la confiance qu'il m'a accordé.

Mes remerciements s'adressent aussi à Xavier Leverve et Uwe Schlattner, qui m'ont acceptée au sein du Laboratoire de Bioénergétique Fondamentale et Appliquée.

Je tiens à remercier les membres du jury pour le temps ainsi que l'intérêt qu'ils portent à juger ce travail :

- *Aux Docteur Béatrice Morio et Professeur Catherine Vergely, qui me font l'honneur de jouer le rôle de rapporteurs. Je suis consciente de l'effort que cela implique et je vous remercie d'avoir consacré du temps à examiner et juger ce travail, malgré l'envoi tardif du manuscrit. J'espère sincèrement que vous trouverez ce travail intéressant ;*
- *Aux Professeurs Catherine Ghezzi, Christophe Ribuot et Luc Rochette pour l'intérêt qu'ils ont porté à cette étude en acceptant d'examiner ces travaux.*

Je suis très honorée de votre participation à l'examen de cette Thèse et je vous prie de trouver ici l'expression de ma profonde gratitude et de mon respect.

Merci aux Docteurs Karine Couturier, Hervé Dubouchaud, Isabelle Hininger et Guillaume Vial pour avoir participé aux travaux de cette thèse.

Je remercie également Cindy Tellier pour avoir pris soin des animaux utilisés pendant toutes ces années ainsi que Joelle Demaison et Mireille Osman pour les différents dosages biochimiques effectués.

Je remercie tous les membres de LBFA. Merci de m'avoir accueilli chaleureusement, merci pour votre sympathie, votre soutien et votre aide!

Un très grand merci aussi aux thésards du laboratoire. Merci aux anciens, Guillaume, Anna, Sacnicte, Severine et Zineb et merci aux « co-thesards » d'aujourd'hui… Merci à Marie et Sarah pour les cours de francais, merci à Marcela pour sa brise mexicaine, merci à Shuijie pour m'avoir appris à dire « j'ai faim » en Chinois ! Merci pour les vendredis après midi, merci pour les soirées, merci pour les journées au labo, merci pour votre soutien, merci pour les discussions... Un grand merci…

A Christos, un grand merci pour sa patience, son soutien et sa présence… Et bien plus encore…

Un merci également à mes amis de Grenoble, de Grèce, de partout, qui m'ont aidé, supporté et surtout m'ont changé les idées quand j'en avais besoin. Merci pour votre support et votre présence dans ma vie!

Je tiens également à dire un merci spécial à ma famille pour son soutien et ses encouragements durant mes multiples années d'études. Un merci à mon frère, Dimitris, pour les discussions téléphoniques quand j'en avais besoin. Merci à mes parents, Panagiotis et Tsampika, qui ont toujours eu confiance en moi et me poussent toujours vers l'avant. Grâce à eux j'ai développé un amour de la science qui m'a mené jusqu'à cette grande réalisation.

Ευχαριστώ…

Abstract

The prevalence of overweight and obesity is increasing worldwide at an alarming rate leading to the development of metabolic syndrome and diabetes mellitus. Previous studies have highlightened the association between fat accumulation, especially in the abdominal area, and the development of cardiovascular diseases. An increase in body and fat mass characterizes normal aging, which is considered *per se* the major risk factor for cardiovascular diseases. In the industrialized societies, the incidence of cardiovascular diseases occurring with age is even more increased due to the Western-world lifestyle habits (e.g. obesogenic diets, sedentariness) that contribute to excess fat accumulation. Accordingly, the overall goal of this work was to understand how body changes occurring from youth to middle age were related to middle age cardiovascular complications and how diet-induced obesity altered these aspects.

Initially, we demonstrated that in normal aging middle-aged hearts of Wistar rats were characterized by lower restoration of the cardiac mechanical activity during reperfusion *ex vivo* due to impaired recovery of the coronary flow and insufficient oxygen supply. This was also related to the presence of increased systemic oxidative stress following the increase in fat mass that occurred from youth to young adulthood. A progressive decline in the endothelium-dependent dilatation of the coronary microvasculature also occurred with aging, which was due to different functional behaviours of the endothelial and smooth muscular cells, which appeared to be related to the energy metabolism and oxidative stress.

High-fat diet-induced obesity triggered a number of alterations in the body, metabolic and cardiovascular characteristics of the animals during this aging period. The excess abdominal fat accumulation provoked the increase of oxidative stress at the systemic, cytosolic and mitochondrial levels accompanied by biochemical alterations in the glucose and lipid metabolisms such as hypercholesterolemia and hypertriglyceridemia. The hyperphagia-induced obesity and the related type 2 diabetes in the Zucker diabetic fatty rats provoked also severe insulin resistance. Both models of diet-induced obesity were characterized by decreased *ex vivo* cardiac function related to mitochondrial energy metabolism and oxidative stress. Furthermore, they were both characterized by an adaptation of the coronary microvasculature whose reactivity was enhanced in the first case and maintained in the second, in order to meet the elevated metabolic demands of the hearts due to obesity. These adaptations were due to different mechanisms in these two models of obesity.

In conclusion, our work revealed a temporal pattern of changes concerning the body and metabolic characteristics, mitochondrial energy metabolism, cardiac function and coronary microvascular reactivity that occur from youth to middle age either under normal or obesogenic-related conditions. These results encourage further research in order to explain the mechanisms related to these alterations. Interventions aiming at reducing the fat mass that increases with age or diet would be of great interest in an effort to delay the cardiovascular complications occurring at middle age.

Keywords: adiposity, aging, diabetes, oxidative stress, mitochondria, coronary microvascular reactivity, ischemia, reperfusion

Résumé

Le surpoids et l'obésité, en constante augmentation à l'échelle mondiale à un rythme exponentiel, conduit au développement du syndrome métabolique et du diabète de type 2. Plusieurs études ont mis en évidence l'association entre l'excès de masse grasse, en particulier dans la région abdominale, et le développement des maladies cardiovasculaires. Une telle augmentation de masse grasse corporelle caractérise le vieillissement normal, qui est considéré *per se* comme un facteur de risque majeur pour les maladies cardiovasculaires. De plus, dans le monde industrialisé, l'incidence des maladies cardiovasculaires est encore plus élevée et fortement liée aux habitudes occidentales (régimes obésogènes, sédentarité) qui contribuent à l'accumulation de la graisse abdominale. L'objectif général de ce travail consiste à suivre les changements corporels qui surviennent entre la jeunesse et l'âge moyen où commence à survenir les complications cardio-vasculaires et à savoir comment l'obésité induite par l'alimentation peut modifier ces aspects.

Dans un premier temps, nous avons montré que les cœurs des rats Wistar d'âge moyen sont caractérisés par une moindre restauration de l'activité mécanique cardiaque au cours de la réperfusion post-ischémique en raison de perturbations de la perfusion coronaire et d'une insuffisance de l'apport en oxygène. La présence d'un stress oxydant systémique suite à l'augmentation de la masse grasse survenant entre la jeunesse et l'âge adulte est également en cause. Une diminution progressive de la dilatation endothélium-dépendante des microvaisseaux coronaires est également observé avec le vieillissement, ce qui résulte d'une évolution différentielle du comportement fonctionnel des cellules endothéliales et musculaires lisses apparemment liée au métabolisme énergétique et au stress oxydant.

L'obésité induite par un régime riche en graisse provoque un certain nombre de modifications corporelles, métaboliques et cardiovasculaires au cours de cette période du vieillissement. L'excès de masse grasse abdominale induit une augmentation du stress oxydant aux niveaux systémique, cytosolique et mitochondrial accompagné par des altérations biochimiques concernant le métabolisme du glucose et les niveaux plasmatiques de cholestérol et de triglycérides. L'obésité induite par une hyperphagie et la présence d'un diabète de type 2 chez les rats Zucker obèses diabétiques provoque également une insulino-résistance sévère. Ces deux modèles d'obésité sont caractérisés par une diminution de la fonction cardiaque *ex vivo* liée au métabolisme énergétique mitochondrial et au stress oxydant. En outre, ils sont tous les deux caractérisés par une adaptation des microvaisseaux coronaires dont la réactivité est augmentée dans le cas de régime riche en graisse et maintenue dans le cas du diabète. Ces adaptations sont dues à des mécanismes différents dans les deux modèles d'obésité. Elles permettent de mieux répondre aux exigences métaboliques élevées liées à l'obésité.

En conclusion, notre travail montre que les caractéristiques corporelles et métaboliques, le métabolisme énergétique mitochondrial, la fonction cardiaque et la réactivité coronaire sont modifiés lors du vieillissement dans les conditions normales ou obésogènes. Ces résultats encouragent la recherche ultérieure des mécanismes mis en jeu. Les interventions visant à réduire la masse grasse, qu'elle soit spontanément accrue par l'âge ou qu'elle résulte du régime alimentaire, seraient d'un grand intérêt pour retarder les complications cardiovasculaires.

Mots clés: adiposité, vieillissement, diabète de type 2, stress oxydant, mitochondries, réactivité microvasculaire coronaire, ischémie, réperfusion

List of abbreviations

AA:	arachidonic acid
ACE:	angiotensin converting enzyme
Ach:	acetylcholine
ADP:	adenosine diphosphate
ADRB3:	gene encoding for beta 3 adenergic receptor
AngII:	angiotensin II
AP-1:	activator protein I
ASK1:	apoptois signal-regulating kinase
ATP:	adenosine triphosphate
BAT:	brown adipose tissue
BDNF:	brain derived neurotrophic factor
BH_2:	dihydrobiopterin
BH_3:	trihydrobiopterin
BH_4:	tetrahydrobiopterin
BMI:	body mass index
cAMP:	cyclic adenosine monophosphate
CAT:	catalase
Ca^{2+}:	calcium ion
cGPDH:	cytoplasmic glycerol-3-phosphate dehydrogenase
CHD:	coronary heart disease
Cl^-:	chloride anion
CNP:	C-type natriuretic peptide
COX:	cyclooxygenase
$CO_3^{\bullet -}$:	carbonate
CPT:	carnitine palmitoyl transferase
CRP:	C-reactive protein
CT:	carnitine:acylcarnitine translocase
Cu:	copper
CVD:	cardiovascular disease
CI:	complex I; NADH dehydrogenase; NADH:ubiquinone oxidoreductase
CII:	complex II; succinate dehydrogenase
CIII:	complex III; cytochrome bc_1 complex
CIV:	complex IV; cytochrome c oxydase
CV:	complex V; ATP synthase
DHODH:	dihydroorotate dehydrogenase
DIO:	diet-induced obesity
DNA:	deoxyribonucleic acid
ECs:	endothelial cells
ECVA:	endothelial cell vasodilatation activity
EDHF:	endothelium-derived hyperpolarizing factor
EDRF:	endothelium-derived relaxing factor
EET:	epoxyeicosatrienoic acid
eNOS:	endothelial nitric oxide synthase; NOS3
EPA :	eicosapentaenoic acid
ETC:	electron transport chain
ETF:	electron transfer flavoprotein
ET-1:	endothelin-1
FA:	fatty acids
FABPpm:	plasma membrane isoform of fatty acid binding protein
FACS:	fatty acyl coA synthetase
FAD/CD36:	fatty acid translocase
$FADH_2$:	flavin adeninde dinucleotide
FATP1/6:	fatty acid transport protein
FMD:	flow mediated dilatation
FMN:	flavin mononucleotide
FFA:	free fatty acids
GH:	ghrelin
GLUT:	glucose transporter
GPx:	glutathione peroxidase
GSH:	glutathione
GSSG:	oxidized glutathione
GTP:	guanosine triphosphate
GTPCH I:	GTP cyclohydrolase I
HF:	high fat
HNE:	4-hydroxy-trans-2-nonel
H(P)ETE:	hydroperoxyeicosatetraenoic acid
HPL:	hormone sensitive lipase
HRP:	horseradish peroxidase
$HO^{\bullet}$:	hydroxyl radical
HO^-:	hydroxide anion
HOCl:	hyperchlorous acid
H_2O_2:	hydrogen peroxide
I_{Ca}:	calcium current
ICAM:	intracellular adhesion molecule
IDF:	International Diabetes Federation
IL:	interleukin
IMM:	inner mitochondrial membrane
iNOS:	inducible nitric oxide synthase; NOS2
IP3:	inositol triphosphate
IRS:	insulin receptor substrate
kDA:	kilodaltons
K^+:	potassium ion
l:	length
LDH:	lactate dehydrogenase
LDL:	low density lipoprotein
LEPR:	leptin receptor
L-NAME:	L-N^G-Nitroarginine methyl ester
LVDP:	left ventricle developed pressure

LO:	lipoxygenase
LPL:	lipoprotein lipase
LV:	left ventricular
LVH:	left ventricle hypertrophy
MAO:	monoamine oxidase
MAPK:	mitogen activated protein kinase
MCP-1:	monocyte chemotactic protein
MC4R:	gene encoding for melanocortin 4 receptor
MDA:	malondialdehyde
MEGJ:	myoendothelial gap junctions
MetS:	metabolic syndrome
MI:	myocardial infarction
MMP:	matrix metalloproteases
Mn:	manganese
MPP:	mitochondrial permeability pore
mtDNA:	mitochondrial DNA
mtGPDH:	mitochondrial glycerol-3-phosphate dehydrogenase
MUFA:	monounsaturated fatty acid
$NADH_2$:	nicotinamide adenine dinucleotide
NADPH:	nicotinamide adenine dinucleotide phosphate
ND:	NADH dehydrogenase
NF-κB:	nuclear factor kappa B
NHE:	sodium hydrogen exchanger
nNOS:	neuronal nitric oxide synthase; NOS1
NO:	nitric oxide
$NO2•^-$:	nitrogen dioxide
NOS:	nitric oxide synthase
NOX:	NADPH oxydases
NPR-C:	natriuretic peptide recptor-C
NWO:	normal weight obesity
OA:	oleic acid
OGTT:	oral glucose tolerance test
ONOOH:	peroxynitrous acid
$ONOO^-$:	peroxynitrite anion
OXPHOS:	oxidative phosphorylation
O_2 :	oxygen
$O_2•^-$:	superoxide radical
PAI-1:	plasminogen activator inhibitor 1
PCSK1:	prohormone convertase 1
PGI2:	prostacyclin
PFK-1:	phosphofructokinase-1
Pi:	inorganic phosphate
PI3K:	phosphatidylinositol 3-kinase
PKA:	protein kinase A
PKG:	protein kinase G
PLC:	phospholipase C
PPARγ:	peroxisome proliferator receptor gamma
PUFA:	polyunsaturated fatty acid
P/O ratio:	phosphate to oxygen ratio
QH_2:	ubiquinol
R:	resistance
r:	radius of the tube
RCR:	respiratory control ratio
RNS:	reactive nitrogen species
ROS:	reactive oxygen species
Sec:	selenocysteine
SERCA:	sarcoplasmic reticulum Ca^{2+}-ATPase
SFA:	saturated fatty acid
sGC:	soluble guanylyl cyclase
SNO:	S-nitrosothiol
SNP:	sodium nitroprusside
SOD:	superoxide dismutase
SR:	sarcoplasmic reticulum
TAG:	triacylglycerol
TBARS:	thiobarbituric acids
TEA:	tetraethylammonium
TG:	triglyceride
TNF-α:	tumor necrosis factor-alpha
TTFA:	thenoyltrifluoroacetone
T2D:	type 2 diabetes; diabetes mellitus
UCP-1:	uncoupling protein-1
VAT:	visceral adipose tissue
VCAM:	vascular cell adhesion molecule
VSMC:	vascular smooth muscle cell
WAT:	white adipose tissue
WHO:	World Health Organization
WHR:	waist-to-hip ratio
XDH:	xanthine dehydrogenase
XO:	xanthine oxidase
XOR:	xanthine oxidoreductase
ZDF:	Zucker diabetic fatty rat
Zn:	zinc
ΔP :	pressure difference
Δp:	proton gradient
ΔpH:	pH gradient
Δψ:	electric membrane potential
H:	solution's viscosity
Φ:	coronary flow
$[Ca^{2+}]i$:	calcium concentration

List of Figures and Tables

CONTENTS

PART I INTRODUCTION

1. The problem of overweight and obesity

1.1 Defining the problem

Overweight and obesity are both labels for ranges of weight that are greater than what is generally considered healthy for a given height. Obesity is defined as the condition of abnormal or excessive fat accumulation in adipose tissue to such an extent that health may be adversely affected [1]. It is an important risk factor for premature death [2-4] and health problems like metabolic syndrome, diabetes and coronary heart disease [5, 6]. Thus, the need to identify individuals and groups at increased risk of morbidity and mortality was raised. In order to classify underweight, overweight and obesity in adult humans, a tool commonly used is the Body Mass Index (BMI). BMI is calculated by the weight in kilograms divided by the square of the height in meters (kg/m^2). The classification of obesity according to BMI is shown in Table 1.

Table 1. *BMI classification*

Classification	BMI (kg/m^2) (Principal cut-off points)
Underweight	**<18.50**
Severe thinness	<16.00
Moderate thinness	16.00-16.99
Mild thinness	17.00-18.49
Normal range	**18.50-24.99**
Overweight	**≥25.00**
Pre-obese	25.00 - 29.99
Obese	**≥30.00**
Obese class I	30.00 - 34.99
Obese class II	35.00 - 39.99
Obese class III	≥40.00

Source: Adapted from WHO 1995, WHO 2000 and WHO 2004.

It should be noted that these values are age-independent and the same for both sexes.

However, the amount of excessive fat stored within the body differs among individuals and BMI may not correspond to the same degree of fatness in different populations due, in part, to different body proportions, since it does not distinguish between weight associated with muscle and weight associated with fat.

The regional distribution of excessive fat within the body of individuals affects also the risks of obesity. The excess abdominal fat mass consists a great risk factor for disease while the "gynoid" fat distribution (fat is more equally and peripherally distributed around the body) is less serious. There is the need to use other methods in addition to the measurement of BMI to identify individuals at increased risk from obesity-related illness due to abdominal fat accumulation, such as the waist-to-hip ratio (WHR). A high WHR with values >1.0 in men and >0.85 in women is an indicator of abdominal fat accumulation [7]. Waist circumference is also a simple measurement unrelated to height that correlates with BMI and WHR and is used as an index of intra-abdominal fat mass [8-10] and total body fat [11]. It has been evidenced that BMI classification misses subjects with elevated adiposity and it has been suggested that elevated adiposity rather than BMI determines metabolic risk.

Increased general obesity estimated by BMI has been associated with the risk of death [12] with higher risks in the lower and upper BMI categories. However, abdominal adiposity, estimated by the waist circumference or the WHR, is also an important predictor of the risk of death independently of general obesity (Fig. 1).

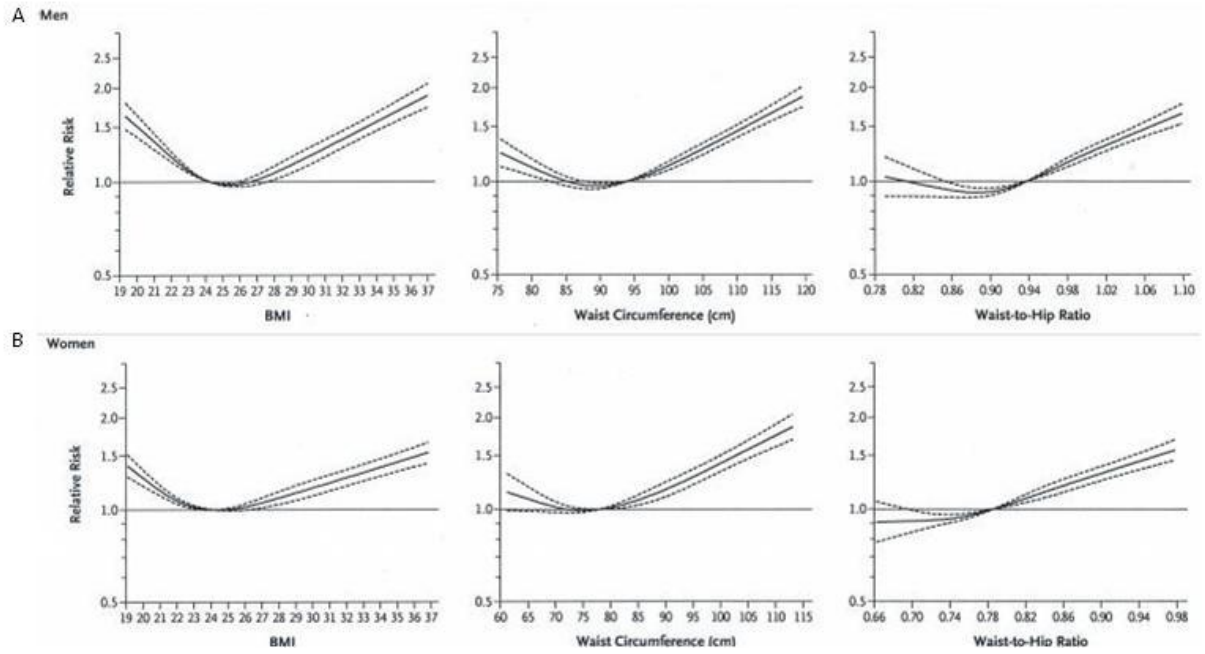

Figure 1 . *The relative risk of death in association with BMI, waist circumference and WHR* ***A*** *for men and* ***B*** *for women. Solid lines indicative relative risks and dashed lines 95% confidence intervals [12]*

Thus, it is extremely important to assess the distribution of body fat even among persons of normal weight. Persons defined as BMI-normal subjects but with elevated body fat percentage display clustering of cardiometabolic abnormalities and have increased risk for future

development of obesity-related diseases, including cardiovascular diseases (CVDs) [13]. These observations have led to the description of a new syndrome, the normal weight obesity syndrome (NWO), which is defined as an excessive body fat associated with a normal body mass index and has captured the interest of researchers.

1.2 Prevalence of overweight and obesity

The prevalence of overweight and obesity is increasing worldwide at an alarming rate. According to World Health Organization, at least 2.8 million people die each year as a result of being overweight or obese. In 2008, 35% of adults aged 20+ were overweight (BMI ≥ 25 kg/m2) (34% men and 35% of women). The worldwide prevalence of obesity has more than doubled between 1980 and 2008. In 2008, 10% of men and 14% of women in the world were obese (BMI ≥30 kg/m2), compared with 5% for men and 8% for women in 1980. An estimated 205 million men and 297 million women over the age of 20 are obese; a total of more than half a billion adults worldwide.

In Europe, the prevalence of obesity has also significantly increased over the past several decades. The rate of obesity has increased by approximately 30% over the past 10 to 15 years [14] and predictions by 2015 suggest a sizeable further increase in European populations [15]. A study of the most recently available national data reveals that 25–70% of adults are overweight, depending on the country; 5–30% are obese, and 41% do not engage in any moderate physical activity in a typical week (WHO).

In France, the prevalence of overweight reaches 30.1% while obesity accounts for 16% (WHO) as shown also in the Fig. 2 below.

Figure 2. *Prevelance of overweight and obesity in France (source: WHO)*

More specifically, according to the results of the Obepi-Roche study in 2009[1], 31.9% of French adults aged 18 or more are overweight (25≤BMI<30kg/m^2) and 14.5% obese (BMI

[1] Enquête épidémiologiquenationale sur le surpoidset l'obésité, INSERM/TNS HEALTHCARE(KANTARHEALTH)/ROCHE, 2009).

$\geq$30kg/m^2). In the same study, it was also shown that obesity increases with age independently of the sex.

1.3 Obesity in rats

Obesity can also be assessed in animal models as in humans even though no classification like the BMI has been established until now. Criteria for the assessment of animal obesity are the gain of body weight, the Lee obesity index and/or the increase of body fat content.

Many studies have used the increase of body or fat weight of the group fed a hypercaloric diet compared to control animals fed chow diets as an indicator of obesity [16-19] but there was a great variability of values between research groups. Harrold et al. [18] defined values of 10-25% greater body weight than controls as moderate obesity and Levin et al. [20] values greater than 40% as severe obesity. The Lee obesity index in rats was defined by Lee in 1929 and is considered to be similar to BMI in humans. It is calculated as the cube root of body weight (g) divided by the naso-anal length (cm) and multiplied by 1000 and values greater than 310 are considered as indicator of obesity. However, Woods et al. showed that measuring the body fat is a more sensitive criterion for assessing animal obesity [19]. In this study, when the rats fed a high-fat diet over 10 week period were compared to those fed a low-fat diet, their body weight was increased only by 10% but their fat content by 50%.

1.4 Adipose tissue

Adipose tissue was traditionally considered as a passive reservoir of energy storage. This view changed in 1994 when the hormone leptin secreted by the adipose tissue was identified and characterized. This established the adipose tissue as a complex and highly active metabolic and endocrine organ [21-23] that expresses and secretes mainly the adipokines, which are bioactive peptides acting at a local (autocrine/paracrine) or a systemic (endocrine) level.

Adipocytes specialize in storing energy as fat in form of triglycerides (TGs) and in releasing it according to the organism needs. For the TGs to be stored in the adipocytes, they must separated first into their parts (one glycerol molecule and three free fatty acids) by the lipoprotein lipase (LPL), which is released by the adipocyte. Glycerol stays in the blood while the free fatty acids are transported into the adipocyte where are reformed in TGs and stored in lipid droplets. Their release is activated by the hormone sensitive lipase (HPL) and after their breakdown, free fatty acids are transferred into the blood stream.

Adipocytes are grouped into two different adipose tissue categories; the white adipose tissue (WAT) and the brown adipose tissue (BAT). WAT is highly adapted to store energy in form of triglycerides whereas BAT oxidizes lipids to produce heat, through the activity of uncoupling protein 1 (UCP1) found in the inner membrane of the mitochondria in this tissue. BAT in humans is found mainly in the newborns while it is highly abundant in hibernating mammals. In contrast to the WAT adipocytes that contain one single lipid droplet, BAT adipocytes contain numerous smaller droplets and many mitochondria that give them a characteristic brown colour. However, the classical WAT adipocytes are considered recently to be of two types: the brown-in-white ("brite or beige) adipocytes, which upon stimulation by cold acclimation or sympathetic agonists can differentiate into cells capable of expressing UCP1 and are particularly observed in the subcutaneous inguinal adipose tissue (iWAT); and the "true" WAT adipocytes incapable of expressing UCP1 physiologically [24, 25].

Aside from adipocytes, adipose tissue contains also connective tissue matrix, nerve tissue, stromovascular and vascular cells and immune cells [26]. Although the adipocytes are the main source of secreted hormones, many proteins are also derived from the non-adipocyte fraction of adipose tissue [27].

1.5 Adipose tissue-secreted proteins

Adipose tissue secrets a number of proteins such as:

Leptin (from the Greek *leptos*, meaning thin), which is a polypeptide of 16-kDa containing 167 amino acids and its secretion is in direct proportion to adipose tissue mass and nutritional status. Leptin's main role is to serve as metabolic signal of energy sufficiency than excess and its effects on energy intake and expenditure are mediated by hypothalamic pathways. Its levels decline with caloric restriction and weight loss. Its expression and secretion are increased by insulin, glucocorticoids, tumor necrosis factor-α (TNF- α) or estrogens and decreased by β-3 adrenergic activity, androgens, ghrelin (GH) or peroxisome proliferator-activated receptor γ (PPARγ) agonists [28, 29];

Adiponectin, which is a 30-kDa polypeptide, highly and specifically expressed in differentiated adipocytes and circulating at high levels in the blood stream. Its biological effects depend on the relative circulating concentrations of its isoforms and the tissue specific expression of its receptor subtypes. It exists an inverse association between adiponectin and both insulin resistance and inflammatory states. Its levels decline before the onset of obesity and insulin resistance whereas they are increased when insulin sensitivity improves [30, 31];

TNF-α, which is a 26-kDa transmembrane protein that is cleaved into a 17-kDa biologically active protein exerting its effects via type I and II TNF-α receptors. Within adipose tissue, it is expressed by adipocytes and stromovascular cells [27]. Its expression is increased in obese rodents and humans and is positively correlated with adiposity and insulin resistance [32];

IL-6, which is a cytokine circulating in multiple glycosylated forms ranging from 22 to 27 kDa in size. Within adipose tissue it is expressed by adipocytes and adipose tissue matrix [27]. Adipose tissue IL-6 expression and circulating levels are positively correlated with obesity, impaired glucose tolerance and insulin resistance [33];

Resistin, which is a 12-kDa polypeptide of a unique family of cysteine-rich C-terminal domain proteins called the resistin-like molecules. Resistin has significant effects on insulin action while its plasma concentration is correlated with insulin-resistance [34].

Other proteins expressed by the adipose tissue are apelin, macrophages and monocyte chemoattractant protein-1 (MCP-1), plasminogen activator inhibitor-1 (PAI-1), adipsin and proteins of the renin-angiotensin system.

1.6 The causes of overweight and obesity

1.6.1 Age

In Western populations, weight gain from youth is the norm. As we age, a decrease in our physical abilities leads to a decrease in our metabolic rate (amount of energy used in a given period), which in turn contributes to weight gain. Studies have shown that body weight increases during the transition from early to middle adulthood independently of sex and that BMI (obesity prevalence) is predicted to grow about 0.12 kg/m^2 (0.6 percentage points) per year [35]. Increases in weight largely reflect accumulated fat mass; the proportion of body weight that is fat increases even when total body fat does not change [35]. A significant positive trend of increased central adiposity and fat distribution with increasing age has been shown in some populations independently of BMI [36].

1.6.2 Lifestyle

Obesity is a result of energy intake exceeding energy expenditure. Despite the strong genetic background of obesity [37], environmental factors are commonly considered to be the underlying cause of the increases in the prevalence of obesity by promoting or exacerbating

the problem [37, 38]. The "obesogenic" environment of our societies promotes sedentariness and excessive food intake that are strongly associated with obesity and higher body weight [39].

1.6.3 Genetic factors

Although it is commonly recognized that environmental factors play a significant role in the development of obesity, genetic susceptibility has been identified as a major contributing factor [40]. Studies have shown that the risk of obesity is about two to three times higher for an individual with a family history of obesity and increases with the severity of obesity. However, not everyone becomes obese in present day despite the overall obesogenic environment, indicating the multifactorial nature of the condition.

Recent progress in genetics has helped to identify candidate genetic loci related to the obesity risk. One of them is MC4R that is expressed in central nervous system and plays a key role in the regulation of food intake and energy homeostasis. Prohormone convertase 1/3 (*PCSK1*) is also another strong candidate as it encodes an enzyme that converts pro-hormones into hormones involved in energy metabolism regulation. Brain-derived neurotrophic factor (*BDNF)* has a role in the regulation of development, stress response, survival, and mood disorders. However, in rodent studies it is implicated in eating behavior, body weight regulation and hyperactivity [41, 42]. *ADRB3* is also a candidate gene given its involvement in the regulation of lipolysis and thermogenesis and its variant Arg64Trp *ADRB3* is one of the first genetic variants for which association with obesity was reported [43]. Mutations in these genes have been related to severe forms of obesity [43-45].

In 1994, the *ob* gene that encodes the protein hormone leptin was cloned in mice. Leptin is a hormone produced and secreted by the white adipose tissue, and its circulating levels are closely related to body fat mass [46, 47]. Leptin deficiency in mice homozygous for a mutant *ob* gene (*ob/ob* mice) causes morbid obesity, diabetes, and various neuroendocrine anomalies, and leptin replacement leads to decreased food intake, normalized glucose homeostasis, and increased energy expenditure [48, 49]. Congenital deficiency of leptin in human subjects results in a phenotype with striking similarities to that seen in *ob/ob* mice. Furthermore, the human leptin receptor (LEPR) is also a candidate genetic locus related to obesity risk but until now no association of its three alleles (K109R, Q223R and K656N) with body mass index and waist circumference has been found in humans [50].

However, in rodents several molecules have been identified to be involved in control of energy intake and energy expenditure. These include *agouti*, a secreted melanocyte-stimulating hormone-receptor antagonist whose ectopic expression leads to severe obesity in mice [51], *tubby/tubby* mice harbor homozygous mutations for a phosphodiesterase (EC 3.1.4.1-like molecule) which is expressed in the hypothalamus [52], fat/fat mouse has a genetically defective form of carboxypeptidase E that results in the impaired processing of hormones [53] and as previously said, the *ob/ob* and *db/db* mice. The *ob/ob* mice have normal weight at birth, then become hyperphagic, markedly obese, hyperinsulinemic and remain infertile with evidence of hypogonadotropic and hypogonadism [54]. The very obese *db/db* mice harbor a homozygous mutation in the hypothalamic form of the cell surface receptor of leptin [55].

In rats, the adult obese Zucker fatty model has a *fa* mutation, the homologue of the mouse *db* mutation. It is a missence mutation in the extracellular domain of the leptin receptor [56, 57]. It has also been shown that the fa-type receptor not only exhibits a slightly reduced leptin-bindig affinity, but also performs reduced signal transduction [58]. This results to insulin resistance, hypertension and dyslipidemia. The obese Zucker diabetic fatty model (ZDF) rat has similar characteristics of the Zucker obese rats and is also hyperglycemic. It was derived from the Zucker obese rat by inbreeding for the hyperglycemia phenotype, which occurred in a subpopulation of the Zucker rat when fed a high-fat diet. Furthermore, the ZDF rat carries a genetic defect in beta cell gene transcription that is inherited independently from the leptin receptor mutation and contributes to the development of diabetes in the setting of insulin [59].

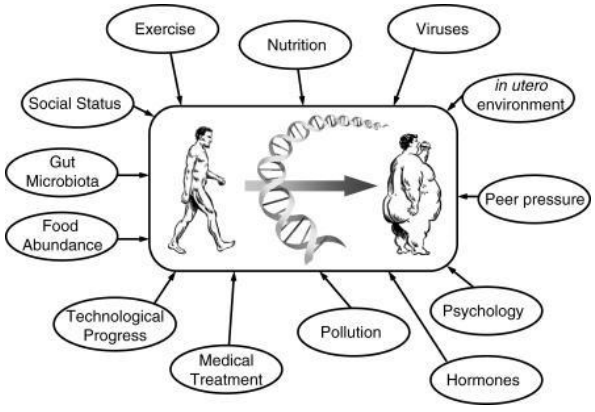

Figure 3. *Genetic and environmental interactions influencing the obese phenotype [60]*

1.7 Consequences of overweight and obesity

Regardless of its origin (genetic or environmental), obesity is related to several metabolic disturbances such as disturbed glucose homeostasis, insulin resistance, impaired insulin secretion, hypertension and dyslipidemia [61, 62]. It has been reported that the metabolic risks associated with obesity are more correlated with a central (abdominal) rather than a peripheral (gluteo-femoral) fat pattern. These complications of obesity have been attributed to increases in visceral adipose tissue (VAT) with an associated increase in portal vein free fatty acid levels [63].

1.7.1 Glucose homeostasis and insulin resistance

The concentration of glucose in the plasma depends on the rate of glucose entering the circulation balanced by the rate of glucose removal from the circulation. A finely regulated balance between these processes defines glucose homeostasis.

Three are the major sources of circulating glucose: intestinal absorption during the fed state, glycogenolysis, and gluconeogenesis. The two last processes happen at the hepatic level. Glycogenolysis is the breakdown of glycogen, which is the polymerized storage form of glucose while gluconeogenesis is the formation of glucose primarily from lactate and amino acids during the fasting state. These processes are under the control of the hormone glucagon, which is produced in the α cells of the pancreas. Thus, glucagon facilitates the appearance of the glucose in the circulation.

Insulin is also a glucoregulatory hormone derived from the pancreas, and in particular from the β pancreatic cells. The primary action of insulin is to lower blood glucose levels. This happens initially by transferring the signal to cells of insulin-sensitive peripheral tissues (primarily skeletal muscle and fat) to increase their glucose uptake [64]. Muscle is the major site of insulin-stimulated glucose uptake *in vivo* while the adipose tissue contributes relatively little to total body glucose disposal. Insulin acts also on the liver to promote glycogenesis, which is the process of glycogen synthesis. Finally, insulin inhibits glucagon secretion from the pancreas and signals the liver to stop producing glucose via glycogenolysis and gluconeogenesis.

The term “insulin resistance” usually implies resistance to the effects of insulin on glucose uptake, metabolism, or storage. In cases of insulin resistance, there is a decreased insulin-stimulated glucose transport and metabolism in adipocytes and skeletal muscle and an impaired suppression of hepatic glucose output [65]. Thus, a corresponding rise in insulin

output in order to maintain normal glycemia is demanded. In obese individuals and those predisposed to type 2 diabetes, this compensation is lost resulting in overt hyperglycemia. Moreover, insulin resistance related to excess adiposity is linked to abnormalities that impact pancreatic β cell function and viability. Some of these abnormalities are glucotoxicity, lipotoxicity, increased oxidative stress, and inflammation that can eventually lead to failure of insulin secretion and hyperglycemia. Defects in phosphorylation/activation of insulin receptor substrates (IRS) proteins are responsible for insulin resistance in the β cell resulting to impairment in glucose sensing, glucose stimulated insulin secretion and to increased loss of β cells.

1.7.2 Dyslipidemia

Obesity is frequently associated with a dyslipidemic state characterized by increased triglycerides, decreased HDL levels and abnormal LDL composition. Dyslipidemia is associated with increased plasma free fatty acids (FFA) levels, which are elevated in most obese subjects [66] due to their increased release by the enlarged adipose tissue and reduction of FFA clearance [67]. Furthermore, elevated levels of FFA inhibit insulin's antilipolytic action, which will further increase FFA release into the circulation [68]. Increased FA levels in blood and increased fatty acid flux to the liver have been known to occur in humans with insulin resistance with and without type 2 diabetes.

1.7.3 Oxidative stress

Reactive Oxygen Species (ROS) occur under physiological conditions and in many diseases causing direct or indirect damage in different organs. Oxidative stress is also involved in pathological processes such as obesity, diabetes and cardiovascular diseases. Biomarkers of oxidative damage, e.g. the sensitivity of C-reactive protein (CRP), have been found to be higher in obese individuals. They are also directly correlated with the BMI and the percentage of body fat, LDL oxidation, and TG levels [69]. In contrast, antioxidant defense markers are lower and inversely related to the amount of body fat and central obesity [70, 71]. Moreover, when obesity is present for a long time, antioxidant sources can be eliminated, leading eventually to the decreased activity of enzymes such as superoxide dismutase (SOD), catalase (CAT) and glutathione peroxidase (GPx) [72, 73].

The increase of oxidative stress in obesity is probably due to the presence of excessive adipose tissue itself. Adipose tissue is considered an important source of proinflammatory cytokines such as the tumor necrosis factor (TNF-α) and the interleukins IL-1, and IL-6. These cytokines stimulate the ROS production by macrophages and monocytes while TNF- α inhibits the activity of CRP resulting to increased generation of superoxide anion [74]. Adipose tissue also secretes angiotensin II that stimulates nicotinamide adenine dinucleotide phosphate (NADPH) oxidase activity, the main source of ROS production in adipocytes [72, 75].

1.7.4 Inflammation

As previously described, adipose tissue is a source of proinflammatory cytokines; thus, obesity is considered to be a state of chronic inflammation that accompanies the accumulation of excess lipid in adipose tissue and liver. The concentrations of circulating fibrinogen, TNF-α, IL-1, IL-6 and CRP are elevated in obese indivinduals [76]. This is due to the expansion of adipose tissue by the dietary excess resulting to hypertrophic adipocytes and increased production of pro-inflammatory cytokines (e.g. TNF-α, IL-6, MCP-1 and PAI-1). These substances have not only local effects leading to upregulation of adhesion molecule synthesis (VCAM, ICAM) but they also affect circulating monocytes contributing altogether to the enhancement of the inflammatory signal.

1.8 Obesity and Type 2 Diabetes

Obesity is associated with an array of secondary metabolic abnormalities, including insulin resistance, T2D and hyperlipidemia. T2D affects 180 million people worldwide and its complications such as diabetic nephropathy, extremity amputation and heart failure have become the principal causes of morbidity and mortality in the western world [77].

Dynamic interactions among different metabolic organs, such as the pancreas, skeletal muscle, liver and adipose tissue, have a key role in the pathogenesis of obesity and diabetes. The hallmark events in the development of obesity-linked diabetes include elevation of plasma FFA, ectopic lipid accumulation in metabolic organs, and chronic low-grade inflammation in adipose tissue, peripheral insulin resistance, chronic hyperglycemia and eventual pancreatic β cell dysfunction [78].

1.9 Obesity and Metabolic syndrome (MetS)

In 1988, Reaven proposed that insulin resistance was a fundamental "disorder" associated with a set of metabolic abnormalities, which not only increased the risk of T2D but also contributed to the development of cardiovascular diseases (CVD) before the appearance of hyperglycemia [79]. This syndrome was first defined as syndrome X but later it was called metabolic syndrome. Since then, many studies have shown that insulin resistance is an important factor related to atherogenic abnormalities such as a prothrombotic profile, inflammation and a typical atherogenic dyslipidemic state characterized by high triglyceride and apolipoprotein B concentrations, increased proportion of small dense LDL particles and reduced concentration of HDL-cholesterol [80]. Insulin resistance contributes further to an dysglycemia, systemic hypertension and T2D.

Various clinical criteria have been developed for the metabolic syndrome. The most widely accepted of these were produced by the World Health Organization (WHO), the European Group for the Study of Insulin Resistance (EGIR), and the National Cholesterol Education Program – Third Adult Treatment Panel (NCEP ATP III)[2]. All groups agreed on the main components of the metabolic syndrome: obesity, insulin resistance, dyslipidemia and hypertension. However, the existing guidelines created difficulties when attempting to identify individuals with MetS in clinical practice. International Diabetes Federation (IDF) gave a new IDF definition that addresses both clinical and research needs. According to this definition of 2006 for a person to be defined as having the MetS they must have:

- central obesity (defined as waist circumference with ethnicity specific values)

If BMI is >30kg/m², central obesity can be assumed and waist circumference does not need to be measured.

- plus any two of the following four factors:

1. Raised triglycerides :	≥ 150 mg/dL (1.7 mmol/L)
	or specific treatment for this lipid abnormality
2. Reduced HDL cholesterol :	< 40 mg/dL (1.03 mmol/L) in males
	< 50 mg/dL (1.29 mmol/L) in females
	or specific treatment for this lipid abnormality

[2] World Health Organization. Definition, diagnosis and classification of diabetes mellitus and its complications. Report of a WHO consultation 1999, Executive summary of the Third Report of The National Cholesterol Education Program (NCEP) Expert Panel on detection, evaluation, and treatment of high blood cholesterol in adults (Adult Treatment Panel III). JAMA 2001;285:2486-97 , Balkau B, Charles MA. Comment on the provisional report from the WHO consultation. Diabetic Medicine 1999;16:442-3.

3. Raised systolic blood pressure :	systolic BP ≥ 130 or diastolic BP ≥ 85 mm Hg *or treatment of previously diagnosed hypertension*
4. Raised fasting plasma glucose (FPG):	≥ 100 mg/dL (5.6 mmol/L), or previously diagnosed type 2 diabetes *If above 5.6 mmol/L or 100 mg/dL, OGTT is strongly recommended but is not necessary to define presence of the syndrome.*

The probability of having metabolic abnormalities, including MetS, increases with the level of obesity [81] and is translated into a higher risk of all-cause and CVD mortality compared to that of normal weight, metabolically normal men [82].

1.10 Obesity and Cardiovascular Diseases

Major CVD feature among numerous comorbidities related to obesity. The adverse affects of obesity on cardiovascular health have been related to hypertension, insulin resistance, dyslipidemia, endothelial dysfunction, inflammation, systolic and diastolic dysfunction, heart failure, coronary heart disease and atrial fibrillation.

The adipocyte is an endocrine organ playing an important role in the development of obesity-related CVD. Recently, increased levels of CRP and leptin were associated with increased risk of CV events [83] and various inflammatory markers were related to insulin resistance, obesity and CVD [84].

Obesity affects significantly the hemodynamics and cardiovascular structure and function [85]. In obese individuals, the augmented body or fat mass results to increased total blood volume, cardiac output and cardiac workload but to a lower level of peripheral resistance at any given level of arterial pressure [85, 86]. The increased cardiac output is mostly caused by stroke volume even though the heart rate is mildly increased due to increased sympathetic activation [87]. Increases in filling pressure and volume shift the Frank-Starling curve to the left indicating increasing cardiovascular work. This often results to left ventricular (LV) and chamber dilation [85, 88, 89]. Obesity increases the risk for left atrial enlargement, abnormal LV diastolic filling and LV hypertrophy, independently of arterial pressure and age [85, 90]. It also affects the LV diastolic and systolic function. All these abnormalities increase the risk for heart failure and cardiovascular events [91-93].

As previously described, obesity is closely related to the development of MetS and T2D. The metabolic characteristics of these states include atherogenic dyslipidemia, elevated blood pressure, proinflammatory and prothrombotic states that can result to cardiovascular events and more specifically to the occurrence of atherosclerosis. Persons with MetS have at least a 2-fold increase in risk for atherosclerotic CVD, compared with those without [94]. Risk for T2D in both sexes is increased about 5-fold. Atherosclerosis has been shown to have a long preclinical phase, with development of pathological changes in arteries of children and young adults well before clinical manifestations of the disease in adults [95]. The presence of endothelial dysfunction is now regarded as an early pivotal event in atherogenesis [96] and has been shown to precede the development of clinically detectable atherosclerotic plaques in the coronary arteries [97]. Endothelial dysfunction can be defined as the partial or complete loss of balance between vasoconstrictors and vasodilators, growth promoting and inhibiting factors, pro-atherogenic and anti-atherogenic factors, and pro-coagulant and anti-coagulant factors [98].

The assesment of endothelial function in terms of vascular reactivity in people with T2D has shown a dysfunction at this level. They have been found to have abnormal vessel reactivity for both endothelium-dependent and -independent vasodilatory pathways. These data indicate a reduction in nitric oxide pathway and response in vascular smooth musle cells [99, 100]. These abnormalities are often the result of hyperglycemia, dyslipidemia and insulin resistance [101] that can lead to increased oxidative stress and affect directly or indirectly the NO pathway. Similar are the results by the measurement of plasma markers of endothelial activation, coagulation/fibrinolysis, or inflammation.

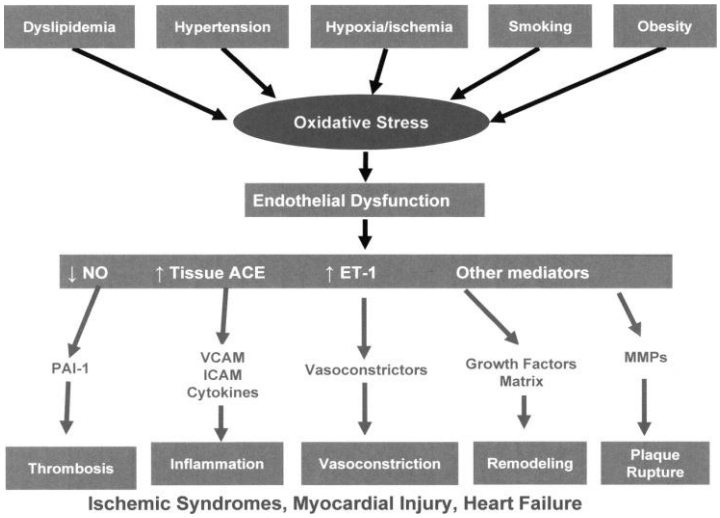

***Figure 4**. Oxidative stress is the prime, common mediator of endothelial dysfunction that can be triggered by risk factors such as hypertension, dyslipidemia, diabetes mellitus, and obesity. It results in decreased bioavailability of nitric oxide, increased production of endothelin-1 (ET-1), increased angiotensin-converting enzyme (ACE), and increased local tissue generation of angiotensin II, which in turn, further increases oxidative stress [102]*

1.11 Obesity paradox

As previously described, obesity has adverse effects on almost all CVDs and affects also adversely all the major risk factors for these events (hypertriglyceridemia, low levels of HDL, metabolic syndrome, diabetes mellitus). Despite these data, recent evidence suggests that among patients with established CVDs, those who are overweight and obese have a better prognosis than their lean counterparts do. This phenomenon has been termed the "obesity paradox".

Studies investigating the effects of obesity on cardiovascular outcomes in treated hypertensive patients have demonstrated a lower mortality in overweight and obese patients after two years [103]. It has also been shown that in a small study of 209 patients with chronic systolic heart failure, both higher BMI and percent body fat were independent predictors of better event-free survival (Fig. 5) [104]. Preliminary data in nearly 1,000 patients with systolic heart failure also showed the prognostic impact of body fat on total survival. Many studies have also reported an obesity paradox in coronary heart disease (CHD), including patients treated with revascularization [105]. In a recent systematic review of over 250,000 patients in 40 cohort studies followed up for 3.8 years, Romero-Corral *et al.* [105] reported that overweight and obese CHD patients have a lower risk for total and CV mortality compared with underweight and normal-weight CHD patients. Importantly, the obesity paradox has also been shown in patients after myocardial infarction (MI) and revascularization, and more recently it has been shown in patients referred for exercise stress testing [106].

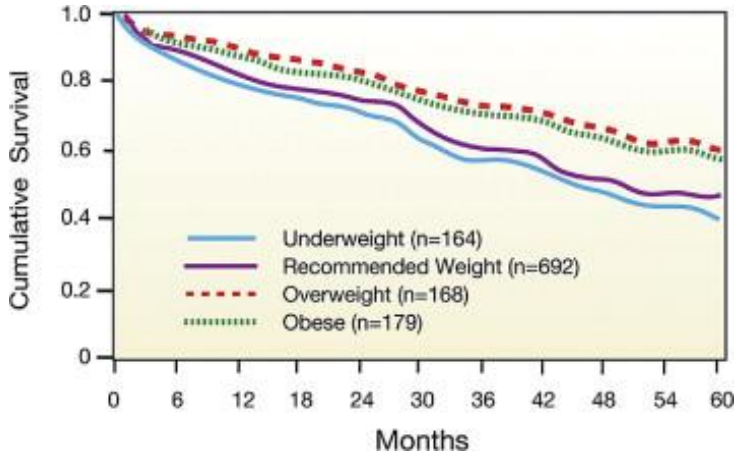

***Figure 5**. Risk-adjusted survival curves for the four BMI categories at 5 years in a study of 1,203 Individuals with moderate to severe heart failure. Survival was significantly better in the overweight and obese categories [107]*

2. Oxidative stress

2.1 Definition

Oxidative stress as defined by Halliwell, is the incapacity of the organism to defend against the attack of ROS [108]. In biological systems oxidative stress occurs when there is an excessive bioavailabilty of ROS as a result of the imbalance between their production and the biological system's ability to detoxify the reactive intermediates or to repair the resulting damage.

ROS are metabolites of molecular oxygen (O_2) that have higher reactivity than O_2. ROS include unstable oxygen radicals such as superoxide radical ($O_2•^-$), singlet oxygen and hydroxyl radical (HO•), and nonradical molecules like hydrogen peroxide (H_2O_2). For organisms living in an aerobic environment, exposure to ROS is continuous and unavoidable. They are generated intracellularly through a variety of processes, for example, as byproducts of normal aerobic metabolism, or as second messengers in signal transduction pathways. They can also derive from exogenous sources and being taken up directly by cells from the extracellular milieu. Finally they can be produced as a consequence of the cell exposure to environmental insult.

A number of defense systems have evolved to combat the accumulation of ROS. These include non-enzymatic molecules (e.g., glutathione, vitamins A, C, and E, and flavonoids) but also enzymatic ROS scavengers (e.g. SOD, CAT and GPx). Unfortunately, these defense mechanisms are not always adequate to counteract the production of ROS resulting in what is termed a state of oxidative stress.

Oxidative stress has been implicated in a wide variety of disease processes including atherosclerosis, ischemia/reperfusion, diabetes, pulmonary fibrosis, neurodegenerative disorders, and arthritis, and is believed to be a major factor in aging [109].

Reactive nitrogen species (RNS) are a family of antimicrobial molecules derived from nitric oxide (•NO) and superoxide ($O_2•^-$) produced via the enzymatic activity of inducible nitric oxide synthase 2 (NOS2/iNOS) and NADPH oxidase respectively. RNS act together with ROS to damage cells, causing nitrosative stress.

2.1.1 Reactive Oxygen Species

Radicals derived from oxygen represent the most important class of radical species generated in living systems [110].

2.1.1.1 Superoxide anion $O_2•^-$

The superoxide anion radical is a radical anion with half-life of 10^{-6} seconds. It is formed by reduction of molecular oxygen mediated by NAD(P)H oxidases and xanthine oxidase or non-enzymatically by redox-reactive compounds such as the semi-ubiquinone compound of the mitochondrial electron transport chain. The production of superoxide occurs mostly within the mitochondria of a cell [111]. During energy transduction, a small number of electrons "leak" to oxygen prematurely, forming the oxygen free radical superoxide, which has been implicated in the pathophysiology of a variety of diseases [112]. This leak occurs at the level of Complex I and III of the mitochondrial respiratory chain.

It is dismutated very rapidly either spontaneously (10^5 $[mol/L]^{-1} \cdot s^{-1}$) or by the SOD action ($10^9$ $[mol/L]^{-1} \cdot s^{-1}$) [113] resulting to the production of hydrogen peroxide H_2O_2.

2.1.1.2 Hydroxyl radical •OH

It is the neutral form of the hydroxide ion (OH^-). The hydroxyl radical has a high reactivity, making it a very dangerous radical with a very short *in vivo* half-life of approx. 10^{-9} s [114]. Thus when produced *in vivo* •OH reacts close to its site of formation.

Under stress conditions, the superoxide radical $O_2•^-$ acts as an oxidant of [4Fe–4S] cluster-containing enzymes and facilitates •OH production from H_2O_2 by making Fe^{2+} available for the Fenton reaction [115]:

$$H_2O_2 + Fe^{2+} \rightarrow OH^- + Fe^{3+}$$

The superoxide radical participates also in the Haber–Weiss reaction ($O_2•^- + H_2O_2 \rightarrow O_2 + •OH + OH^-$) which combines a Fenton reaction and the reduction of Fe^{3+} by superoxide, yielding Fe^{2+} and oxygen ($Fe^{3+} + O_2•^- \rightarrow Fe^{2+} + O_2$) [116]:

$$H_2O_2 + Fe^{2+} \rightarrow OH^- + Fe^{3+}$$

$$H_2O_2 + O_2•^- \rightarrow •OH + OH^- + O_2$$

2.1.1.3 Peroxyl radicals (ROO•)

The simplest peroxyl radical is HOO•, which is the protonated form (conjugated acid; pK_a ~ 4.8) of superoxide (O_2•$^-$) and is usually termed either hydroperoxyl radical or perhydroxyl radical. Given its pK_a value, only ~0.3% of any superoxide present in the cytosol of a typical cell is in the protonated form [117]. This radical has been demonstrated to be implicated in the peroxidation of fatty acids and in particular that of the unsaturated ones.

2.1.1.4 Hydrogen peroxide H_2O_2

The principal production of H_2O_2 is the dismutation of the superoxide anion by SOD as previously described. It is more stable and easily diffusible than the superoxide anion and is produced in peroxisomes under physiologic conditions. Peroxisomes are major sites of oxygen consumption in the cell and participate in several metabolic functions that consume oxygen. Oxygen consumption in the peroxisome leads to H_2O_2 production, which is then used to oxidize a variety of molecules. The organelle also contains CAT, which decomposes hydrogen peroxide and presumably prevents accumulation of this toxic compound. Thus, the peroxisome maintains a delicate balance with respect to the relative concentrations or activities of these enzymes to ensure no net production of ROS. When peroxisomes are damaged and their H_2O_2 consuming enzymes downregulated, H_2O_2 is released into the cytosol where it significantly contributes to oxidative stress. GPx together with CAT contribute in its neutralisation.

2.1.1.5 Hyperchlorous acid HOCl

In biological systems, hyperchlorous acid is produced in activated neutrophils by myeloperoxidase-mediated peroxidation of chloride anion. It contributes mainly to the defense against bacteria [118].

2.1.2 Reactive Nitrogen Species (RNS)

2.1.2.1 Nitric oxide •NO

•NO is a small molecule that contains one unpaired electron and is, therefore, a radical. •NO is generated in biological tissues by specific nitric oxide synthases (NOSs), which metabolise arginine to citrulline with the formation of •NO *via* a five electron oxidative reaction [119].

•NO is an abundant reactive radical that acts as an important oxidative biological signalling molecule in a large variety of diverse physiological processes, including neurotransmission, blood pressure regulation, defence mechanisms, smooth muscle relaxation and immune regulation [120]. •NO has a half-life of only a few seconds in an aqueous environment.

Nitric oxide has great affinity for metal ions. Many of its physiological effects are exerted as a result of its initial binding to Fe^{2+}-heme groups in the enzyme soluble guanylate cyclase (sGC) [121]:

$$Fe^{2+}\ (sGC) + \bullet NO \rightarrow Fe^{2+}\ (sGC) - NO$$

Because of its affinity for metal ions, nitric oxide can modulate the activity of various enzymes. During inflammtory processes, nitric oxide and superoxide anion may react together to produce significant amounts of peroxynitrtie anion ($ONOO^-$):

$$\bullet NO + O_2\bullet^- \rightarrow ONOO^-$$

2.1.2.2 Peroxynitrite ($ONOO^-$)

The peroxynitrite ($ONOO^-$) anion is a short-lived oxidant species that is produced by the reaction of nitric oxide (•NO) and superoxide ($O_2\bullet^-$) radicals at diffusion-controlled rates ($\sim 1\times10^{10}\ M^{-1}\ s^{-1}$) [122].

The oxidant reactivity of peroxynitrite is highly pH-dependent and both peroxynitrite anion ($ONOO^-$) and peroxynitrous acid (ONOOH) can participate directly in one- and two-electron oxidation reactions with biomolecules.

A fundamental reaction of $ONOO^-$ in biological systems is its fast reaction with carbon dioxide, which leads to the formation of carbonate ($CO_3\bullet^-$) and nitrogen dioxide ($\bullet NO_2$) radicals (yield ~35%). Nitrogen dioxide can undergo diffusion-controlled radical–radical termination reactions with biomolecules, resulting in nitrated compounds.

Peroxynitrite can promote the oxidation of cofactors either by direct or free-radical-dependent mechanisms. Peroxynitrite-mediated oxidation of tetrahydrobiopterin (BH_4) to quinonoid 5,6-dihydrobiopterin (and subsequently to 7,8-dihydrobiopterin) leads to the dysfunction of NO synthase (NOS), as BH_4 is an essential NOS cofactor. It has been proposed that low levels of BH_4 can, in turn, promote a cycle of its own destruction, which is mediated by the NOS-dependent formation of peroxynitrite [123]. This mechanism might contribute to vascular endothelial dysfunction that is induced by oxidative stress in various diseases.

2.2 Antioxidant defenses

Enzymatic antioxidant defences include superoxide dismutase (SOD), glutathione peroxidase (GPx) and catalase (CAT). Non-enzymatic antioxidants are represented by ascorbic acid (Vitamin C), α-tocopherol (Vitamin E), glutathione (GSH), carotenoids, flavonoids, and other antioxidants.

2.2.1 Superoxide Dismutase (SOD)

The major cellular defense against $O_2\bullet^-$ and peroxynitrite is a group of oxidoreductases known as SODs, which catalyze the dismutation of $O_2\bullet^-$ into oxygen and H_2O_2. There are three isoforms of SOD in mammals: SOD1 [CuZnSOD]; SOD2 [MnSOD] and SOD3 [ecSOD] with distinct subcellular localization [124].

SOD1 is the major intracellular SOD (cytosolic Cu/ZnSOD) mainly localized in the cytosol. Enzymatic activity of SOD1 depends on the presence of the Cu and Zinc (Zn). SOD1 activity requires a catalytic Cu to scavenge $O_2\bullet^-$. SOD2 is a mitochondrial manganese (Mn) containing enzyme (MnSOD), which is composed of a 96 kDa homotetramer and localized in the mitochondrial matrix [125]. Mn at the active site of SOD2 serves to catalyze the disproportionation of $O_2\bullet^-$ to oxygen and H_2O_2 in a similar fashion as SOD1 and SOD3 (Cu/ZnSODs) [126]. It is involved in dismutating $O_2\bullet^-$ generated by the respiratory chain of enzymes. SOD3, a secretory extracellular Cu/Zn-containing SOD, is the major SOD in the vascular extracellular space. In vascular tissue, SOD3 is mainly synthesized by vascular smooth muscle cells and fibroblasts [127].

2.2.2 Catalases

The overall reaction catalyzed by catalases is the degradation of two molecules of hydrogen peroxide to water and oxygen:

$$2H_2O_2 \rightarrow 2H_2O + O_2$$

They are tetrameric enzymes consisting of four identical tetrahedrally arranged subunits of 60 kDa that contains a single ferriprotoporphyrin group per subunit, and has a molecular mass of about 240 kDa [128].

2.2.3 Glutathione peroxidase (GPx)

GPx (80 kDa) is an isoform of a family of enzymes containing a selenium atom. It contains a single selenocysteine (Sec) residue in each of the four identical subunits, which is essential for the enzyme activity. It protects mammalian cells against oxidative damage by catalysing the reduction of hydroperoxides using glutathione (GSH) [128]:

$$ROOH + 2GSH \rightarrow ROH + GSSG + H_2O$$

2.2.4 Glutathione (GSH)

GSH is a major thiol antioxidant and redox buffer of the cell [129]. The oxidised form of glutathione is GSSG, the glutathione disulphide. GSH is highly abundant in the cytosol (1–11 mM), nuclei (3–15 mM) and mitochondria (5–11 mM), and is the major soluble antioxidant in these cell compartments. GSH is a cofactor of GPx. It scavenges directly hydroxyl radical and singlet oxygen, detoxifying hydrogen peroxide and lipid peroxides by the catalytic action of glutathionperoxidase. GSH is able to regenerate the most important antioxidants, vitamins C and E, back to their active forms. GSH in the nucleus maintains the redox state of critical protein sulphydryls that are necessary for DNA repair and expression. Oxidised glutathione is accumulated inside the cells and the ratio of GSH/GSSG is a good measure of oxidative stress of an organism. A really high concentration of GSSG may damage many enzymes oxidatively.

2.3 Damages

2.3.1 DNA damage

The hydroxyl radical reacts with all components of the DNA molecule resulting to the damage of both purine (adenine, guanine) and pyrimidine (cytocine, thymidine and uracile) bases and also the deoxyribose backbone. One consequence is the formation of 8-OH-G, which is used as a marker of DNA oxidative damage [130]. Permanent modification of genetic material resulting from these oxidative damages incidents represents the first step involved in mutagenesis, carcinogenesis, and ageing. The mitochondrial DNA (mtDNA) has also a susceptibility to oxidative stress 10 times greater than that of nuclear DNA. Its genome doesn’t have introns or protective histons and disposes limited reparation mecanisms. This predisposes the mtDNA to oxidative damage.

2.3.2 Lipid damage (lipid peroxidation)

Polyunsaturated fatty acid residues of phospholipids are extremely sensitive to oxidation. This can modify the membrane fluidity and consequently the homeostasis and metabolic activity of the organism.

Peroxyl radicals (ROO•) can be rearranged *via* a cyclisation reaction to endoperoxides (precursors of malondialdehyde) with the final product of the peroxidation process the malondialdehyde (MDA) [131]. 4-hydroxy-2-nonenal (HNE) is also produced, which with the thiobarbituric acids (TBARS) consist the most common markers of lipid peroxidation. MDA is mutagenic in bacterial and mammalian cells and carcinogenic in rats. HNE is weakly mutagenic but appears to be the major toxic product of lipid peroxidation.

2.3.3 Protein damage

The side chains of all amino acid residues of proteins, in particular cysteine and methionine residues of proteins are susceptible to oxidation by the action of ROS/RNS [132]. In most cases, a carbonyl group is added to the protein. Oxidation of cysteine residues may lead to the reversible formation of mixed disulphides between protein thiol groups (–SH) and low molecular weight thiols, in particular GSH (*S*-glutathiolation). The concentration of carbonyl groups, generated by many different mechanisms is a good measure of ROS-mediated protein oxidation [133].

2.4 Sources of ROS

The sources of ROS can be either endogenous or exogenous. ROS production can be mediated by lysosomes, NADPH oxydases, lipoxygenases, xanthine oxydase or cytochrome P450. Heavy metals, gamma rays and UV light can also result in ROS formation. However, the primary site of ROS production is considered the mitochondrial respiratory chain [134].

2.4.1 NADPH oxydases

NADPH oxydases are multiproteic enzymatic complexes related to many physiological and pathological processes in the heart, such as hypertrophy, apoptosis, heart failure, and hypoxic adaptation [135]. NADPH oxidase-based enzyme complexes have seven catalytic subunits (i.e., Nox1–5 and Duox1 and 2) that are widely expressed. In the heart and vasculature, Nox1,

Nox2, Nox4, and Nox5 are of relevance. Nox-based enzymes generate ROS ($O_2^{\bullet -}$ and H_2O_2) by transferring electrons from NADPH to molecular oxygen.

2.4.2 Xanthine oxidase (XO)

Under normal physiological conditions, XO exists as xanthine dehydrogenase (XDH), which can be converted into XO by oxidation of sulfhydryl residues or limited proteolysis. XO and XDH are both isoenzymes of xanthine oxidoreductase (XOR). XO generates both $O_2^{\bullet -}$ and H_2O_2 through the catalytic oxidative hydroxylation of purine substrates.

2.4.3 Nitric Oxide Synthases (NOS)

NOSs produce nitric oxide from the conversion of L-arginine to L-citrulline. Three isoforms have been identified: neuronal NOS (nNOS, NOS1), inducible NOS (iNOS, NOS2) and endothelial NOS (eNOS, NOS3) [136].

Increased $O_2^{\bullet -}$ interacts with NO to form peroxynitrite. An increase in peroxynitrite levels suggests a compromising of NO bioavailability and physiology. The essential cofactor of NOS is BH_4. Guanosine triphosphate cyclohydrolase I (GTPCH I) is the rate-limiting enzyme of the biosynthesis of BH_4. In the presence of subsaturating levels or deficiency of BH_4, electron transfer in NOS becomes uncoupled from L-arginine oxidation and NO formation, with subsequently less NO and more ROS generation, the so-called NOS uncoupling [137]. Furthermore, ROS serve as an amplifying mechanism to further exacerbate NOS uncoupling. Superoxide rapidly reacts with NO to form the highly reactive intermediate peroxynitrite. Increased formation of peroxynitrite in turn oxidizes BH_4 to the BH_3 radical. In addition, the oxidized form, BH_2, may compete with BH_4 for binding at NOS as well [138].

2.4.4 Myeloperoxidases (MPO)

Myeloperoxidases are heme-containing enzymes in activated neutrophils and monocytes [139] and are used against bacteria and other pathogens. MPO produces hypochlorous acid (HOCl) from hydrogen peroxide (H_2O_2) and chloride anion (Cl^-) (or the equivalent from a non-chlorine halide) during the neutrophil's respiratory burst. Respiratory or oxidative burst is the rapid release of ROS ($O_2^{\bullet -}$ and H_2O_2) from various types of cells. Furthermore, it oxidizes tyrosine to tyrosyl radical using hydrogen peroxide as an oxidizing agent.

2.4.5 Lipoxygenases (LO)

Lipoxygenases (LOs) are nonheme iron dioxygenases that stereospecifically insert molecular oxygen into polyunsaturated fatty acids, resulting in the formation of hydro(pero)xy-eicosatetraenoic acid (H(P)ETE) molecules [140]. The conventional nomenclature classifies animal LOXs with respect to their positional specificity of arachidonic acid oxygenation as 5-LOs, 8-LOs, 11-LOs, 12-LOs or 15-LOs.

12/15-LOXs are mainly in the brain, kidney and blood vessels [141] and participate in the leucotrienes biosynthesis and the side production of ROS. LOXs contribute also in CVDs. As documented, two LOXs in particular, 15-LO type 1 (15-LO-1) in humans and its closely related ortholog in mice, 12/15-LO, as well as the 5-LO pathway are the prime candidates implicated in atherosclerosis [142].

2.4.6 Cytochrome P450

Mammalian cytochromes *P*450 (P450) are a family of heme-thiolate enzymes involved in the oxidative metabolism of a variety of endogenous and exogenous lipophilic compounds. Poor coupling of the P450 catalytic cycle results in continuous production of ROS.

2.4.7 Mitochondria

Mitochondria are a constant source of ROS such as $O_2^{\bullet -}$ and H_2O_2, as a consequence of their normal aerobic metabolism to meet the demand of ATP synthesis by oxidative metabolism.

The mitochondrial electron transport chain (ETC) has been recognized as one of the major cellular generators of ROS, which include $O_2^{\bullet -}$, H_2O_2 and •OH. It was found that some of the electrons passing through the mitochondrial ETC leak out to molecular oxygen to form $O_2^{\bullet -}$, which is quickly dismutated by the mitochondrial SOD (Mn-SOD) to H_2O_2 [143]. It has been estimated *in vitro* (in isolated mitochondria) that 1 to 3% of consumed oxygen is not completely reduced but directed to the radical production [144]. However, it seems that *in vivo* this percentage is 0.4 to 0.8 % [145].

ROS are also produced within mitochondria at sites other than the inner mitochondrial membrane, for example, by monoamine oxidase (MAO) activity [146]. MAOs are flavoenzymes located within the outer mitochondrial membrane, which catalyze the oxidative deamination of catecholamines and biogenic amines such as serotonin. While undergoing this process MAOs generate H_2O_2.

2.5 Physiological role of reactive species

Even though reactive oxygen species are predominantly implicated in causing cell damage, they also play a major physiological role in several aspects of intracellular signalling and regulation [147]. Cells are capable of generating endogenously and constitutively ROS which are utilized in the induction and maintenance of signal transduction pathways involved in cell growth and differentiation.

ROS can play a very important physiological role as secondary messengers, especially in the mitogen-activated protein kinase (MAPK) pathways. In the heart, ROS provoke cardiac growth, remodeling, and dysfunction. They activate the hypertrophy signaling cascade and transcription factors. A low concentration of H_2O_2 (50 μmol/L) has been shown to evoke significant reduction in cardiac contractile function in neonatal and adult rat cardiomyocytes. It has been reported that H_2O_2-induced hypertrophy needs activation of PI3K in a time- and dose-dependent manner. G-protein-coupled receptor-induced ROS activate NF-κB and apoptosis signal-regulating kinase 1 (ASK1) to stimulate cardiomyocyte hypertrophy, whereas genetic depletion of ASK1 inhibits the hypertrophy.

ROS also affect the connective tissue [148], by stimulating myocardial fibroblasts, regulating collagen synthesis , and activating matrix metalloproteases (MMPs) in several ways. ROS also are a critical factor for apoptosis stimulation in myocytes, endothelial cells, and fibroblasts. ROS-influenced apoptosis is concentration dependent; at low concentrations ROS inhibit apoptosis, whereas at high concentrations they provoke the opposite. ROS can also modulate directly components of cardiac excitation-contraction coupling, such as SERCA and I_{Ca} [149].

Finally, the most prominent cases of NO-mediated regulation are in the control of vascular tone and platelet adhesion. Nitric oxide (NO) has also anti-inflammatory and anticoagulant properties. H_2O_2 has also been shown to act as an endothelium-derived hyperpolarizing factor in the process of vasodilatation [150].

2.6 ROS in association with aging, obesity and CVD

Oxidative stress has been implicated in various pathological conditions involving cardiovascular disease, cancer, neurological disorders, diabetes, ischemia/reperfusion and ageing.

The free radical theory of aging was first introduced in 1956 by Denham Harman who proposed the concept of free radicals playing a role in the aging process [151]. This theory is

based on the fact that the random deleterious effects of free radicals produced during aerobic metabolism cause damage to DNA, lipids, and proteins and accumulate over time.

The production of ROS has been shown to be increased in obesity and T2D [152]. Hyperglycemia and hyperlipidemia that characterize obesity and diabetes can stimulate ROS formation from various sources, resulting finally in tissue damage and pathophysiological complications.

The ROS-induced oxidative stress in cardiac and vascular myocytes has been linked with cardiovascular tissue injury [153]. ROS-induced oxidative stress plays a role in various cardiovascular diseases such as atherosclerosis, ischemic heart disease, hypertension, cardiomyopathies, cardiac hypertrophy and congestive heart failure [154]. Major sources of oxidative stress in cardiovascular system are the enzymes xanthine oxidoreductase (XOR), NAD(P)H oxidase (multisubunit membrane complexes), NOS, mitochondrial cytochromes and hemoglobin. NOSs and hemoglobin are also principal sources of RNS, including NO and SNOs (NO-modified cysteine thiols in amino acids, peptides, and proteins), which together with ROS convey NO bioactivity. ROS have also a major role in ischemia and reperfusion. Massive production of ROS during ischemia/reperfusion leads to tissue injury causing thus serious complications in organ transplantation, stroke, and myocardial infarction.

3. Mitochondria

3.1 Overview of the Cellular Energy Metabolism

Many tasks that a cell must perform, such as movement and the synthesis of macromolecules, require energy. ATP plays a central role in this process by acting as a store of free energy within the cell.

Carbohydrates: The major source of cellular energy is the breakdown of carbohydrates and particularly of glucose. Glycolysis is the initial stage in the breakdown of glucose and it is a procedure common to practically all organisms. In eukaryotic cells glycolysis happens in the cytosol. The complete oxidative breakdown of glucose to CO_2 and H_2O (glycolysis) can be written as follows:

$$C_6H_{12}O_6 + 6O_2 \rightarrow 6CO_2 + 6H_2O.$$

Glycolysis occurs in the absence of oxygen and can provide all the metabolic energy of anaerobic organisms. The reactions of glycolysis result in the breakdown of glucose into pyruvate, with the net gain of two molecules of ATP. Phosphofructokinase is the key control enzyme of glycolysis and is inhibited by high levels of ATP. Thus, the breakdown of glucose is inhibited when an adequate supply of metabolic energy in the form of ATP is available in the cell. In addition to ATP production, glycolysis converts two molecules of the coenzyme NAD^+ to NADH. The majority of pyruvate is converted to acetyl-CoA and fed into the citric acid cycle. The most important product of this cycle is NADH, which is made from NAD^+ as the acetyl-CoA is oxidized, even though some more ATP is also generated. The acetyl-CoA oxidation releases carbon dioxide as a waste product. In anaerobic conditions, glycolysis produces lactate, through the enzyme lactate dehydrogenase re-oxidizing NADH to NAD^+ for re-use in glycolysis. The pentose phosphate pathway is an alternative route for glucose breakdown. During this process, the coenzyme NADPH is reduced and pentose sugars are produced including ribose, the sugar component of nucleic acids.

Lipids: Fats are catabolised by hydrolysis to free fatty acids and glycerol. The glycerol enters glycolysis and the fatty acids are broken down by β oxidation to release acetyl-CoA, which then enters the citric acid cycle. Every cycle produces one molecule of NADH and one $FADH_2$. Fatty acids release more energy upon oxidation than carbohydrates because carbohydrates contain more oxygen in their structures and thus require less oxygen for their oxidation.

Aminoacids: Aminoacids are used to synthesize proteins and other biomolecules but are also oxidized to urea and carbon dioxide as a source of energy. The first step of the oxidation pathway is the removal of the amino group by a transaminase, which is then transferred into the urea cycle, leaving a deaminated carbon skeleton in the form of a keto acid. Several of these keto acids are intermediates in the citric acid cycle, for example the formation of α-ketoglutarate by the glutamate deamination. The glucogenic amino acids can also be converted into glucose, through gluconeogenesis.

The produced coenzyme NADH from these catabolic pathways and the citric acid cycle contains electrons that have a high transfer potential. These electrons will pass by the mitochondrial electron transport chain at the level of complex I with final product the ATP. Succinate, a component of citric acid cycle, is also oxidized by the ETC but at the level of complex II.

3.2 General

The name mitochondrion originates from the Greek *μίτος* "mitos" (thread) and *χονδρίον* "chondros" (granule), referring to the appearance of these structures during spermatogenesis. Mitochondria are membrane-enclosed organelles found in the cytosol of most eukaryotic cells localized in parts of cells with active processes. Mitochondria form a functional reticulum whose steady-state morphology is regulated by dynamic fission, fusion and motility events. The mitochondrion contains two membranes that separate four distinct compartments, the outer membrane, intermembrane space, inner membrane and the matrix.

The outer membrane is a relatively simple phospholipid bilayer, containing protein structures called porins or VDAC (Voltage-Dependent Anion Channel) which render it permeable to molecules of about 10 kilodaltons or less (the size of the smallest proteins) [155]. Ions, nutrient molecules, ATP, ADP, etc. can pass through the outer membrane easily. It contains also translocases or proteic transporters for the import of cytosolic proteins.

The inner membrane is freely permeable only to oxygen, carbon dioxide, and water. Its lipid composition consists from phosphatidylcholine and cardiolipin that makes it impermeable to ions. It is highly folded into cristae that increase greatly the total surface area of the inner membrane. Cristae house the megadalton complexes of the electron transport chain and ATP synthase that control the basic rates of cellular metabolism. It also disposes translocases for the protein import.

The matrix contains the mitochondrial DNA (mtDNA) and the enzymes responsible for the citric acid cycle and β-oxidation reactions [156]. The matrix also contains dissolved oxygen, water, carbon dioxide and the recyclable intermediates that serve as energy shuttles. Due to the folds of the cristae, no part of the matrix is far from the inner membrane. This way, matrix components can diffuse to inner membrane complexes and transport proteins within a relatively short time.

The process of energy production by mitochondria and the electron transport chain is called oxidative phosphorylation (OXPHOS), because it involves the coupling of oxygen to phosphorylation of ADP into ATP [157]. The human heart daily synthesizes approximatively 30 kg of ATP.

3.3 Electron Transport Chain (ETC) and ATP synthase

The classic electron-transfer chain was first described as a sequence of prosthetic groups (flavins and cytochromes) embedded in a protein matrix in the inner mitochondrial membrane (IMM), transferring electrons in order of increasing redox potential [158].

Five membrane-embedded enzymes constitute an oxidative phosphorylation (OXPHOS) system in the inner mitochondrial membrane. Four of these protein complexes compose the "respiratory chain" and are involved in electron transfer reactions, which in three cases are coupled to proton translocation across the inner mitochondrial membrane. The resulting proton gradient is used by the ATP synthase complex for the phosphorylation of ADP. These multiproteic complexes either oxidize reduced NADH (complexes I, III, and IV) or reduced $FADH_2$ (complex II). Membrane-bound mitochondrial glycerophosphate dehydrogenase, dihydroorotate dehydrogenase, electron transfer flavoprotein-ubiquinone oxidoreductase (ETF:QO) may also transfer electrons to oxygen.

Complex I or NADH dehydrogenase is the main entrance point of electrons to the respiratory chain. It uses NADH molecules generated by catabolic reactions within the mitochondrial matrix as a source of electrons and transfers them to ubiquinone within the membrane. Succinate dehydrogenase or complex II represents an alternative entrance point of electrons to the respiratory chain, which transfers electrons from succinate to ubiquinone and directly connects the Krebs cycle to the respiratory chain. This electron transfer is not coupled to proton translocation. The central component of the OXPHOS system, cytochrome *c* reductase or complex III, is a functional dimer. It transfers electrons from reduced ubiquinone (which is referred to as "ubiquinol") to cytochrome *c*, which is a small mobile electron carrier

associated with the outer surface of the inner membrane. Complex IV or cytochrome *c* oxidase represents the terminal complex of the respiratory chain and was described as a monomer upon solubilization of the inner mitochondrial membrane by mild detergent treatment but as a dimer within protein crystals. It catalyses electron transfer from cytochrome *c* to molecular oxygen thereby reducing the latter to water. By translocating protons across the inner mitochondrial membrane this complex makes a final contribution to the proton gradient across the inner membrane, which is used by the ATP synthase for ATP formation. The ATP synthase is composed of two domains: a hydrophobic F_0 membrane part that is connected to a water-soluble *F1*-headpiece by two stalks. In a nutshell, the proton gradient across the membrane domain triggers the rotation of the subunit c ring within the F_0 and γ, δ and within F_1, which causes the phosphorylation of ADP.

For a long time it was believd that the organization of OXPHOS sytem was best described by the "fluid-state" or "random diffusion" model, which was based on the finding that all individual protein complexes of the OXPHOS system can be purified in enzymatically active form and on lipid dilution experiments [159]. According to this model, the respiratory chain complexes freely diffuse in the membrane and that electrons flow between them connected by the mobile carriers CoQ and cytochrome *c* (cyt *c*).

However, in the last decade an alternative view, known as "solid-state" model was proposed based on evidences pointing to stable interactions of the OXPHOS complexes in the form of defined supercomplexe [160]. According to this model the respiratory complexes are assembled into supramolecular structures (supercomplexes) to perform their role ("respirasomes") and ensure a quick and efficient transport of electrons [160].

3.3.1 Complex I or NADH-coenzyme Q reductase

Complex I (CI) catalyzes the first step of the electron-transport chain of mitochondria and several bacteria. The reaction is accompanied by translocation of four protons from the matrix to the intermembrane space.

It is a heteromultimer consisting of 45 subunits for a molecular mass of 1,000 kDa which makes CI the largest enzyme of the respiratory chain. Seven subunits are the products of the mitochondrial genome. The enzyme consists of three different sectors: a dehydrogenase unit and a hydrogenase-like unit, constituting the peripheral arm protruding into the matrix, and a transporter unit deeply embedded in the membrane and involved in proton translocation. The dehydrogenase domain contains the NADH oxidizing site, whereas the hydrogenase

domain binds and reduces CoQ. Several prosthetic groups contribute to electron transfer within the enzyme: FMN is the entry point for electrons that are then transferred to a series of iron–sulfur clusters. It is also one of the two mitochondrial sites of ROS production [161].
CI is inhibited by more than 60 different families of compounds from rotenone, the prototype of this series, to a number of synthetic insecticides/acaricides. Rotenone inhibits CI by blocking the electron transfer between the terminal iron-sulfur (FeS) cluster N2 and ubiquinone [162]. This leads to electron transport chain abnormal function with final result the incapacity of ATP synthase to produce ATP.

3.3.2 Complex II or succinate deshydrogenase

Succinate dehydrogenase, an enzyme of 100 kDa, has a functional role in the Krebs cycle. Beside that, it is also involved in aerobic metabolism by the respiratory chain because it can couple the two-electron oxidation of succinate to fumarate with the electron transfer directly to the quinone pool. Hence complex II (CII) is more precisely termed succinate:quinone oxidoreductase (SQR) [163]. Its 4 subunits are entirely products of the nuclear genome. Mammalian CII is part of a class of ubiquinone-reducing enzymes containing a single *b* heme and anchored to the inner mitochondrial membrane by two hydrophobic subunits. It catalyzes the oxidation of succinate to fumarate with subsequent electron transfer to the ubuiquinone pool which is though not coupled to proton efflux to the intermembrane space.
CII is specifically inhibited by thenoyltrifluoroacetone (TTFA) or malonate. Malonate has a structure close to succinate. Thus, it can bind to CII and inhibit its dehydrogenation. This way, only the hydrogenes from CI pass through complex III. This results to the slowdown of the ETC that decreases the phosphorylation rate of ADP by the ATP synthase.

3.3.3 Complex III or ubiquinol-cytochrome *c* oxidoreductase

Complex III (CIII) is a symmetrical, oligomeric dimer of 300 kDa with 10 subunits, most of them produced by the nuclear genome. The enzyme represents a confluence point for reducing equivalents from various dehydrogenases: it can catalyze the transfer of electrons from hydroxyquinones (ubiquinol, reduced CoQ) to a water-soluble *c*-type cytochrome, and it can, concomitantly, link this redox reaction to translocation of protons across the membrane. CIII is the second site of ROS production [161].

Antimycin A and myxothiazol are inhibitros of CIII activity. Antimycin is an antibiotic that inhibits CIII at the level oriented to the matrix. This way the utilization of the ubiquinol (QH2) (H^+ donor) and the ferric cytochorome c (H^+ receptor) is decreased. The slowdown of the coenzyme Q reoxidation deprives the complexes I and II of their H^+ coenzyme acceptor that leads to inhibition of these two enzymes and therefore of the NADH and succinate use. In the presence of this inhibitor cytochrome c oxydase is deprived from the reduced cytochrome c and use less oxygen. Thus, the ETC expels fewer protons and the membrane potential collapses with further inhibition of ATP synthase.

3.3.4 Complex IV or cytochrome c oxydase

Complex IV (CIV) (400 kDa) belongs to the heme-copper oxygen reductase superfamily. It catalyzes the complete reduction of dioxygen to water and promote proton translocation across the mitochondrial membrane, further contributing to the difference in electrochemical potential [164]. Its activity is inhibited by the carbon oxide and cyanide.

The cyanide anion is the most powerful poison of the electron transport chain. It results to inhibition of CIV by blocking the utilisation of oxygen by this complex (hydrogen acceptor) and the cytochrome c (electron donor). The slowdown of the cytochrome c reoxidation deprives the CIII of its electron acceptor coenzyme that leads to inhibition of the activity of this complex and the utilization of QH2. The lack of the oxidized coenzyme Q deprives the complexes I and II from their hydrogen receptor coenzyme. Thus, the enzymes use less NADH and succinate finally leading to inhibition of ATP synthesis.

3.3.5 Auxiliary enzymes of the respiratory chain

There are also alternative oxidases that deliver electrons from CoQ to oxygen, bypassing CIII and cytochrome oxidase. All these enzymes are characterized by lack of energy-conserving proton-translocation mechanisms. Apart of CII that can be regarded as one of them, there is:

- Glycerol-3-phosphate dehydrogenase (mtGPDH) that shuttles reducing equivalents from cytosol through the respiratory chain to molecular oxygen;
- The electron-transfer flavoprotein (ETF)-ubiquinone oxidoreductase that is a globular protein located on the matrix surface of the inner mitochondrial membrane. The enzyme can accept reducing equivalents from a variety of dehydrogenases, including those involved in

fatty acid oxidation, in amino acid oxidation, and in choline catabolism (dimethylglycine dehydrogenase and sarcosine dehydrogenase), and is oxidized by ubiquinone ;

- Choline dehydrogenase that catalyzes the oxidation of choline to betaine aldehyde. The enzyme is localized at the matrix side of the inner mitochondrial membrane; because its oxidation through the respiratory chain was shown to yield a P/O ratio approaching 2, it was suggested that it feeds electrons to CoQ at a similar position to that of respiratory complex II;
- Dihydroorotate dehydrogenase (DHODH) an iron-containing 43-kDa flavoprotein (FMN) that catalyzes the oxidation of dihydroorotate to orotate, the fourth step in *de novo* pyrimidine biosynthesis;
- Alternative NADH dehydrogenases (NDs), a family of proteins located in the inner membrane of eukaryotic mitochondria, which catalyze oxidation of NAD(P)H from either the cytosol (external enzymes) or the mitochondrial matrix (internal enzymes) and enable quinone reduction. The greatest functional difference from CI is that their oxidoreductase activity is rotenone insensitive and is not coupled to proton pumping.

3.3.6 ATP synthase

ATP synthase is often referred in the literature as Complex V (CV) of the respiratory chain due to coupling between the mitochondrial respiration and the ATP production.

In 1960, Mitchell established the chemiosmotic theory according to which the movement of ions (as the reduced equivalents of NADH and $FADH_2$) across an electrochemical potential (as that derived from the proton transfert of the respiratory chain) could provide the energy needed to produce ATP. ATP synthase forms ATP from ADP and inorganic phosphate (Pi) driven by this motive proton force, a reaction that is reversible.

ATP synthase consists of two regions: the F_O portion that is within the membrane and the F_1 portion that is above the membrane, inside the matrix of the mitochondria. Intact ATP synthase is also called the F_oF_1-ATPase.

The enzyme is composed of at least 8 subunit types, of which 5 form the catalytic hydrophilic F_1-portion. These subunits are named by Greek letters (alpha **α**, beta **β**, gamma **γ**, delta **δ** and epsilon **ε**) in accordance with their molecular weight. The proton translocating F_O portion is composed of subunits of 3 types named ***a, b*** and ***c***. The catalytic portion of ATP synthase (F_1) is formed by $\boldsymbol{\alpha_3\beta_3}$ hexamer with **γ** subunit inside it and **ε** attached to the **γ**. Subunit **δ** is bound to the "top" of the hexamer and to subunits ***b***. The hydrophobic transmembrane segment of subunit ***b*** is in contact with subunit ***a***. Subunits **γ** and **ε** of the catalytic domain are bound to

the ring-shaped oligomer of ***c***-subunits. Proton translocation take place at the interface of subunits ***a*** and ***c.***

Driven by the protonmotive force, protons are transferred through the F_O portion of the enzyme. This transfer drives the rotation of the ***c***-subunit oligomer ring relative to the ***a*** and ***b*** subunits. The rotation is passed to **γ** and **ε** subunits that are bound to the ***c***-subunit oligomer ring. The rotation of asymmetric Gamma subunit mechanically causes conformational changes in $\alpha_3\beta_3$ -hexamer. Each 120 degrees of the **γ** subunit rotation forces one of 3 catalytic sites located at **α-β** interface into an opened conformation. Freshly synthesized ATP molecule is released, and phosphate and ADP are bound instead. High affinity of the opened site to phosphate impairs rebinding of ATP and favours ADP binding. Rotation goes further, **γ** subunit turns another 120 degrees forcing the next site into the opened conformation, and the ADP and phosphate bound to the previous opened site are occluded and ATP synthesis takes place. The ATP molecule formed is released when the **γ** subunit makes one 360 degrees turn and once again opens the site (Fig. 6B).

Oligomycin is a specific inhibitor of ATP synthase by blocking its function. Protons are then accumulated in the intermembrane space which will prevent complexes I, III and IV from pumping protons from the matrix to the intermembrane space. The oxidation reactions are also inhibited finally leading to less utilization of NADH and succinate by complexes I and II respectively.

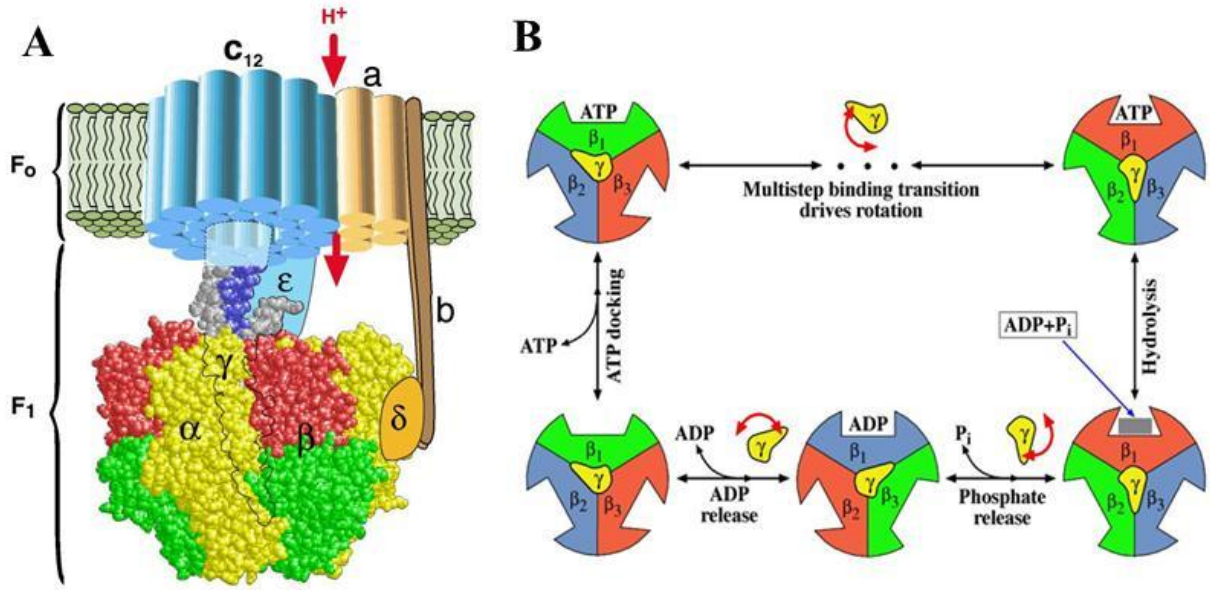

Figure 6*. **A** Structure of ATP synthase [165]. **B** A model of the 'binding-change' mechanism of ATP synthase, as proposed by Boyer [166]*

3.3.7 Organization of complexes

3.3.7.1 Fluid state model

The original model for how the respiratory chain complexes are organized was that complex I to IV diffuse freely in the inner mitochondrial membrane and electron transfer is based on random collisions of the involved components. This model is supported by the fact that all five complexes can be purified in a physiologically active form and by lipid dilution experiments using isolated mitochondrial membranes [159].

3.3.7.2 Supercomplexes and the respirasome

According to the structural model of the mitochondrial inner membrane, initially proposed more than 50 years ago by Chance and Williams [158] and expanded and amplified by Schagger's group [167], the structural support for oxidative phosphorylation is provided by assemblies of the ETC complexes into supercomplexes termed respiratory supercomplexes or respirasomes. Many OXPHOS supercomplexes that function as a respiratory unit were identified and characterized: i) a "I+III_2 supercomplex" including complex I and dimeric complex III, ii) "III_2+$IV_{1–2}$ supercomplexes" consisting of dimeric complex III and one or two copies of monomeric complex IV, and iii) very large "I+III_2+$IV_{1–4}$ supercomplexes" comprising complexes I, dimeric complex III, and one to four copies of complex IV [168].

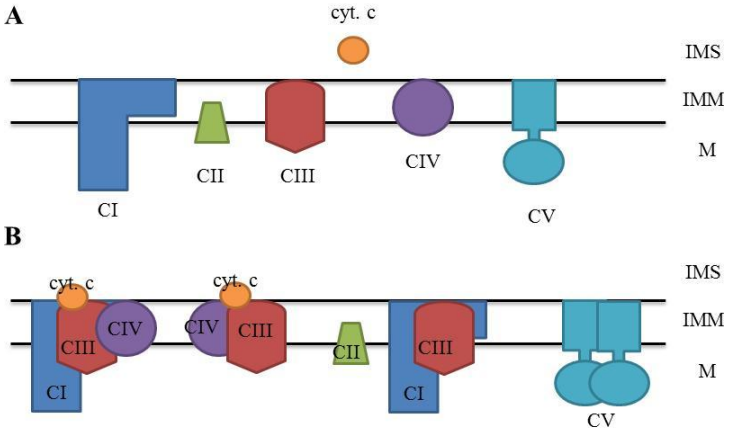

Figure 7. Models of the mitochondrial OXPHOS system. A *The "fluid state model".* ***B*** *Defined interactions of OXPHOS complexes within supercomplexes as predicted by the "solid state model".* M: *Matrix;* IM: *inner mitochondrial membrane;* IMS: *mitochondrial intermembrane space.*
Adapted from Dudkina et al., 2008 [169]

3.4 The leaks and slips of the oxidative phosphorylation

As already seen, mitochondrial membrane contains proton pumps that couple electron transport to the pumping of protons across these membranes. This pumping generates an electrochemical proton gradient (Δp) across the membrane, composed of a pH gradient (ΔpH) and an electrical membrane potential (Δψ). The return of protons down this gradient is coupled to the phosphorylation of ADP by the ATP synthase.

However, the mitochondrial membrane suffers from two major inefficiencies:

- *Proton leak or just leak*: it is the passive leak for protons (and other ions) such that a significant proportion of protons pumped by the redox proton pumps leak back across the membrane without being coupled to ATP synthesis, first measured by Mitchell and Moyle [170];
- *Redox slip or just slip*: the phenomenon occurs when the proton pumps fail to pump protons at all, or pump protons at a reduced proton stoichiometry despite the electron transfer through the respiratory complexes, in particular cytochrome c oxydase.

These processes have a major impact on mitochondrial coupling efficiency and ROS production.

3.5 The respiratory chain as a source of ROS

There is growing evidence that most of the $O_2^{\bullet -}$ generated by intact mammalian mitochondria *in vitro* is produced by CI. This $O_2^{\bullet -}$ production occurs primarily on the matrix side of the IMM. $O_2^{\bullet -}$ production by CI was also found to be markedly stimulated in the presence of succinate, the substrate of CII, indicating that a reverse electron flow is involved. Superoxide anion is unable to cross the IMM and it is rapidly converted to hydrogen peroxide by the MnSOD present in the mitochondrial matrix.

In addition to CI, CIII is regarded as an important site of $O_2^{\bullet -}$ production, especially when mitochondrial respiration is suppressed by antimycin, which is a specific inhibitor of CIII. $O_2^{\bullet -}$ produced at this site appears at both sides of the inner membrane. Ubiquinone, a component of the mitochondrial respiratory chain connecting complex I with III and complex II with III, is regarded as a major participant in formation of $O_2^{\bullet -}$ by CIII. The oxidation of ubiquinone proceeds in a set of reactions known as the Q-cycle, and unstable semiquinone is responsible for $O_2^{\bullet -}$ formation. Specific CIII inhibitors, such as antimycin and myxothiazol, are important tools in deducing both the site and the source of $O_2^{\bullet -}$ production.

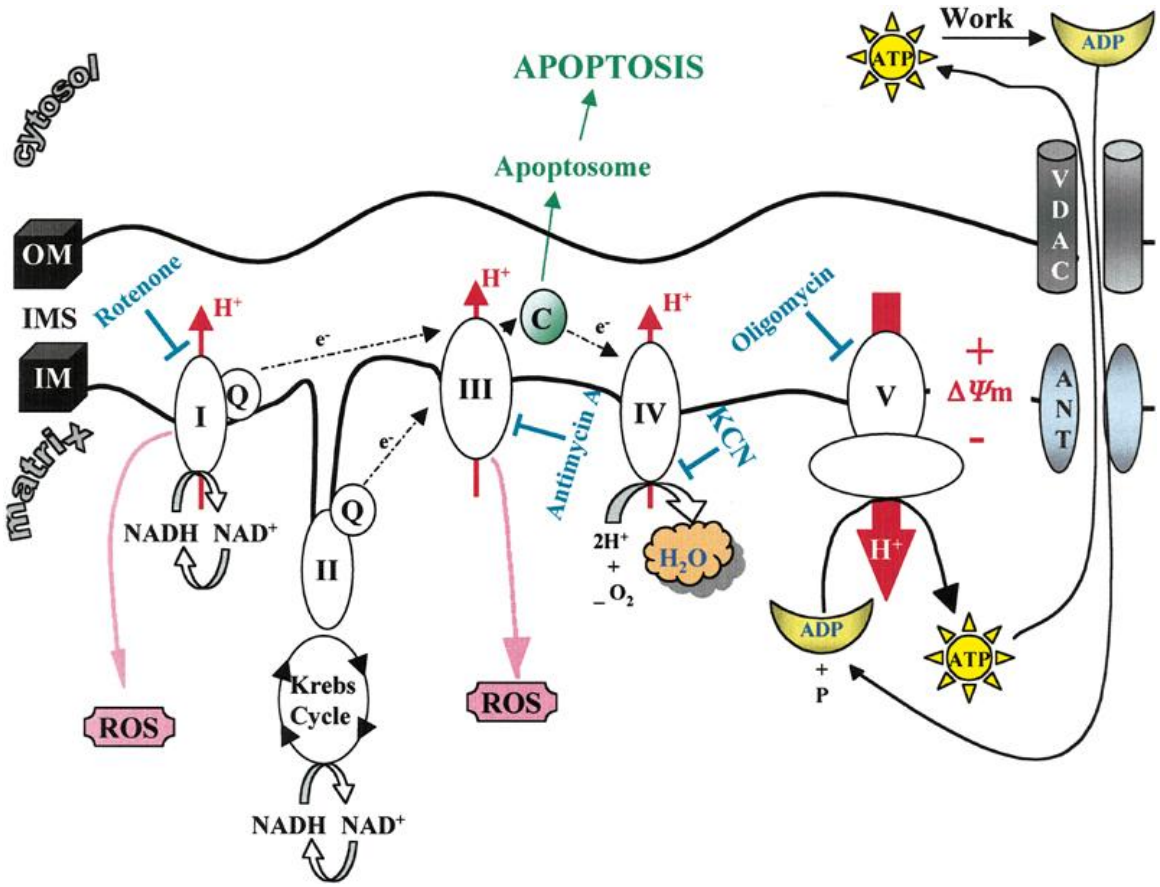

***Figure 8**. Electron transport chain, ATP generation and ROS production. Complexes I-IV are represented in the inner membrane (IM) of the mitochondria. ROS that are produced by the ETC are indicated. Several respiratory inhibitors are represented: rotenone (CI inhibitor), antimycin (CIII inhibitor), potassium cyanide KCN (CIV inhibitor), oligomycin (ATP synthase inhibitor). OM: outer membrane; IMS: intermembrane space; IM: inner membrane [171]*

3.6 Regulation of Mitochondrial Respiration by Substrates

The nature of the cellular substrates (fatty acids, carbohydrates) affects the oxidative phosphorylation stoichiometry by modulating the ratio between NADH + H^+ and $FADH_2$. The oxidation of NADH involves three coupling sites, the complexes I, III and IV. The $FADH_2$ oxidation involves two coupling sites, the complexes III and IV. Thus, when $FADH_2$ is oxidized the yield of ATP synthesis is lowered compared to the NADH oxidation. Carbohydrate metabolism results to two molecules of NADH while the fatty acid β-oxidation to equal amounts of NADH + H^+ and $FADH_2$. Thus, the stoichiometry of ATP synthesis to oxygen consumption is lower when lipids rather than carbohydrates are used.

In order for the NADH to enter the mitochondrion, since the mitochondrial inner membrane is impermeable to this molecule, shuttle systems are used:

- *the malate/aspartate shuttle*: Malate dehydrogenase is the primary enzyme of this shuttle and exist in two forms: the mitochondrial and cytosolic forms, which catalyze the reaction in opposite directions. In the cytosol, malate dehydrogenase reacts with NADH + H^+ and oxaloacetate to produce malate and NAD^+. Two electrons are attached this way to oxaloacetate. Malate is then imported into the mitochondrial matrix in exchange of α-ketoglutarate. Malate is then converted into oxaloacetate by the mitochondrial malate dehydrogenase, during which NAD^+ is reduced with two electrons to form NADH +H^+. Oxaloacetate is then transaminated into aspartate by mitochondrial aspartate aminotransferase and glutamate. Glutamate is thus transformed into α-ketoglutarate. Then the glutamate-aspartate antiporter imports glutamate from the cytosol into the matrix and exports aspartate from the matrix to the cytosol. Once in the cytosol, aspartate is converted by cytosolic aspartate aminotransferase to oxaloacetate;
- *glycerol 3-phosphate/dihydroxyacetonephosphate shuttle*: This shuttle is a mechanism that regenerates NAD^+ from NADH, a by-product of glycolysis. Its importance in transporting reducing equivalents is secondary to the malate-aspartate shuttle. In this shuttle, the enzyme called cytoplasmic glycerol-3-phosphate dehydrogenase 1 (cGPDH) converts dihydroxyacetone phosphate to glycerol 3-phosphate by oxidizing one molecule of NADH to NAD^+. Glycerol 3-phosphate is converted back to dihydroxyacetone phosphate by a membrane-bound glycerol-3-phosphate dehydrogenase 2 (mGPDH) reducing at the same time one molecule of FAD to $FADH_2$.

The first shuttle depends on the mitochondrial transmembrane electrical potential while the latter does not. Moreover, the glycerol phosphate shuttle is energetically less efficient than the malate-aspartate shuttle, because the $FADH_2$ produces one less ATP than NADH in the oxidative phosphorylation.

3.7 Respiration measurements

Measurement of oxygen consumption in mitochondria in the presence of specific substrates that feed electrons into different sites of the ETC [172] is possible. For example, in the presence of pyruvate + malate or succinate (+ rotenone), the electrons fed into CI or CII, are transferred to ubiquinone, CIII, and CIV, where oxygen plus hydrogen are converted into water. Substrates derived from carbohydrate, amino acids, or fatty acids oxidation can also be used to evaluate mitochondrial function. Oxygen consumption in the presence of ADP is coupled to the production of ATP by the phosphorylation system. The measurement of

oxygen consumption in the absence of ATP synthesis by using the ATP synthase inhibitor oligomycin is used as an estimation of the proton leak, i.e., the protons not used to phosphorylate the ADP. Uncouplers also can be added to dissociate the proton gradient in the intermembrane space and to look at the limitation of the electron transport by the phosphorylation system. The measurement of OXPHOS assesses multiple components of mitochondrial metabolism and can uncover defects and differences in mitochondrial function not apparent by other techniques.

3.8 Mitochondria in Aging and Obesity

An overwhelming body of evidence accumulated in the last decades has demonstrated that mitochondria have a central role in the etiology and pathogenesis of most major chronic diseases and in aging itself as described by the mitochondrial (or free radical) theory of aging proposed by Harman in 1956 [151]. This theory proposes that oxidative damage to the mitochondria can lead to a compounding effect whereby damaged mitochondria in turn release more ROS, increasing oxidative damage to the mitochondrial, cytosolic and nuclear compartments and leading eventually to dysfunctional or defective mitochondria establishing a vicious circle of oxidative stress and energetic decline. Numerous studies demonstrate increased oxidative damage to mitochondrial lipids, proteins and DNA with age. Activities of the mitochondrial ETC complexes isolated from variety of tissues in several species have been reported to decrease with age [173, 174]. Decreases have been observed in the activities of CI, III and IV while the CII seems to be more resistant to age-induced changes [174]. The underlying reason is probably the fact that many subunits of CI, III and IV are encoded by mtDNA susceptible to mitochondrial oxidative damage while CII is encoded by nuclear DNA. A decline in oxygen consumption with age has also been reported [175, 176]. Advanced mitochondrial ROS production significantly increases in both heart and vasculature [176, 177] and they may impact endothelium-dependent dilatation. It should be noted though that most of these studies have studied the advanced aging after the cutoff point of middle age (65 years for the human).

Aging is also related to the development of obesity and diabetes. Obesity and diabetes are related to altered myocardial substrate utilization by the heart. It has been shown that in rodents and humans there is a characteristic increase in fatty acid utilization accompanied by a reduction in glucose and lactate utilization [178]. The increased lipid delivery reduces the heart's ability to enhance fatty acid oxidation and its metabolic flexibility. These are

consistent with the observed mitochondrial dysfunction in these states [179]. It has also been shown that the observed decreased cardiac efficiency in obese and diabetic patients is related to increased uncoupled respiration and activation of uncoupling proteins [179]. This may contribute to impair energy requiring processes in the heart such as diastolic relaxation and systolic contraction, and may render the heart susceptible to ischemic injury.

4. Cardiovascular function

4.1 Cardiac metabolism

Life critically depends on the proper heart function, which in its turn relies on high efficiency of energy conversion. Mitochondrial oxygen-dependent processes transfer most of the chemical energy from metabolic substrates into ATP. In order to maintain a continuous supply of ATP to the contractile machinery, the heart has developed an omnivorous attitude and is able to use a wide variety of circulating substrates, including fatty acids, glucose, lactate and ketone bodies. Fatty acids are catabolized by β-oxidation, and account for 60–90% of the total energy production [180]. Metabolized through glycolysis, glucose accounts for 10–40% of the total energy production [181]. However, substrate selection is dictated by their relative abundance at a given time and by regulation according to the developmental, hormonal and pathophysiological status of the organism.

4.1.1 Fatty acid metabolism

The heart has a small capacity for *de novo* fatty acid synthesis and storage, and therefore mainly relies on arterial fatty acid supply. The main sources of fatty acids for the heart are the free fatty acids bound to albumin and triacyglycerols (TAG) found in the core of blood lipoproteins. The majority of fatty acids for the heart are provided by the albumin-bound fatty acids, while the TAG component probably accounts for ≤20–25% of the cardiac FA consumption [182].

FFAs originating from either albumin or lipoprotein-TAG enter the cardiac myocyte either by passive diffusion or via a protein carrier-mediated pathway that includes fatty acid translocase (FAT)/CD36, the plasma membrane isoform of fatty acid binding protein (FABPpm), and fatty acid transport protein (FATP) 1/6. Once in the cytoplasm, fatty acids are converted into long-chain acyl CoA esters by fatty acyl CoA synthetase (FACS) of the mitochondrial outer membrane [183] (Fig. 9). These long-chain acyl CoAs can then be used for synthesis of a number of intracellular lipid intermediates, or the fatty acid moiety can be transferred to carnitine and taken up into the mitochondria. The carnitine palmitoyltranferase system then is used for the long-chain acyl CoAs to overcome the mitochondrial membrane impermeability. Carnitine palmitoyltransferase (CPT) 1 is a key enzyme in the mitochondria and catalyzes the conversion of long-chain acyl CoA to long-chain acylcarnitine, which is subsequently shuttled

into the mitochondria. Following the formation of long-chain acylcarnitine by CPT1, the acylcarnitine is translocated across the inner mitochondrial membrane by a carnitine:acylcarnitine translocase (CT) that involves the exchange of carnitine for acylcarnitine. Once in the matrix, acylcarnitine is converted back to long-chain acyl CoA by CPT2, which is located on the matrix side of the inner mitochondrial membrane. The metabolism of long-chain acyl CoA in the mitochondrial matrix occurs via the β-oxidation pathway, involving the sequential metabolism of acyl CoAs by acyl CoA dehydrogenase, enoyl CoA hydratase, L-3-hydroxyacyl CoA dehydrogenase, and 3-ketoacyl CoA thiolase (3-KAT) [184]. The fatty acids that do not undergo β-oxidation are stored as triglycerides as a potent energy reserve.

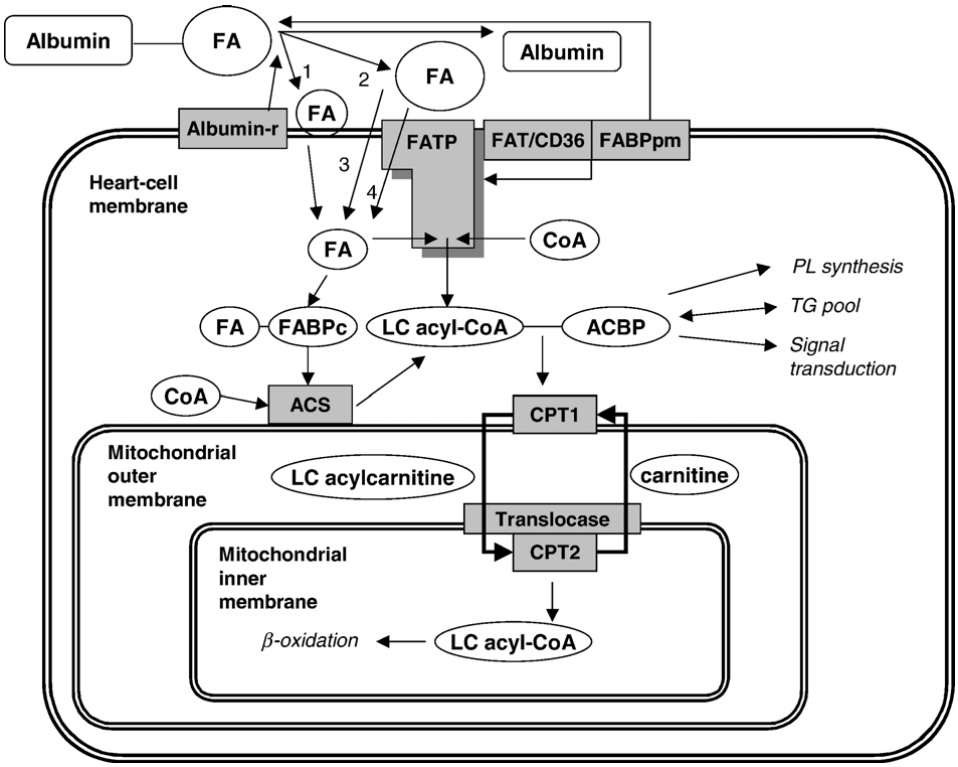

***Figure 9**. Cardiac fatty acid metabolism. 1 = Direct route of FA into outer cell membrane, 2 = Indirect route of FA as source for passive diffusion; 3 = Passive diffusion, 4 = Transfer of FA by FATP. Abbreviations: ACBP=Acyl-CoA binding protein; ACS = Acyl-CoA synthase; Albumin-r = Albumin receptor; CoA = Coenzyme A; CPT1 and CPT2 = Carnitine palmitoyltransferase 1 and 2, respectively; FA = Fatty acids; FABPc = Cytoplasmic fatty acid binding protein; FABPpm = Peripheral membrane fatty acid binding protein; FAT/CD36 = Fatty acid translocase with CD36 antigen; FATP = Fatty acid transport protein; LC acylcarnitine = Long-chain acylcarnitine; LC acyl-CoA = Long-chain acyl-CoA; PL synthesis = Phospholipid synthesis; TG pool = Triacylglycerol pool [185]*

4.1.1.1 Cardiac membrane phospholipids

Myocardial cell membranes are dynamic structures that are always under constant strain. Their composition, in particular their fatty acid content, plays an important role in their function and can be affected by diet and stress. More specifically, it may influence the physical behavior of the membrane bilayer, the membrane permeability and fluidity and the activities of enzyme molecules embedded in it [186-188].

The type of dietary lipids is of crucial importance for the fatty acid composition of cellular membranes. Epidemiological studies have shown the detrimental effects of dietary saturated fatty acids (SFAs) on the cardiovascular health [189, 190] while monounsaturated fatty acids (MUFAs) seems to be either neutral [191] or protective [192] against CVD risk factors. In contrast, n-3 polyunsaturated fatty acids (PUFAs) seem to exert cardioprotective effects [193, 194].

PUFAs include the n-6 and n-3 classes that are considered "essential" FAs since they cannot be synthetized in the human body and are mostly obtained by diet. More specifically, humans lack the Δ12- and Δ15-desaturases necessary to insert a double bond at the n-3 and n-6 position of a FA carbon chain [194]. After their intestinal absorption, they are incorporated into chylomicrons and transferred to the liver, where they can be elongated and desaturated (Fig. 10). Then, they are released into the bloodstream and incorporated into different organs (e.g. heart, lung, kidney, brain, adipose tissue and skeletal muscle) [195-197]. At the cellular level, they can either be oxidized in the mitochondria or incorporated into complex lipids. N-3 PUFAs compete with n-6 PUFAs for phospholipid fatty acid composition [198]. PUFAs also include the n-9 class, derived from oleic acid (OA, 18:1) and the n-7 class, derived from palmitoleic acid (16:1), which are not essential [199].

The n-6 and n-3 PUFAs are also involved in eicosanoid synthesis when incorporated into phospholipids. Through the action of phospholipase A2 they can be released as FFAs and can be transformed by the cyclooxygenase (COX), the lipoxygenase (LOX) or cytochrome P450 monoxygenase enzymes. The COX enzymes lead to the synthesis of 2-series prostanoids (prostaglandins E2, prostacyclin I2 and thromboxane A2) from arachidonic acid, while the LOX generate 5-HPETE (arachidonic acid 5-hydroperoxide), which in turn is used to produce the 4-series leukotrienes. EPA and DHA are converted by the same enzymes, e.g., COX and LOX, to 3-series prostanoids (prostaglandins E3, prostacyclin I3 and thromboxane A3), and 5-series leukotrienes, respectively.

Generallty, the n-6 PUFA-derived eicosanoids are proinflammatory and elicit a wide range of responses including vasoconstriction, vasodilatation, activation of leukocytes, stimulation of platelet aggregation and generation of ROS. Eicosanoids produced from EPA and DHA (n-3 PUFAs) are generally less inflammatory, serve as vasodilators and inhibit platelet aggregation.

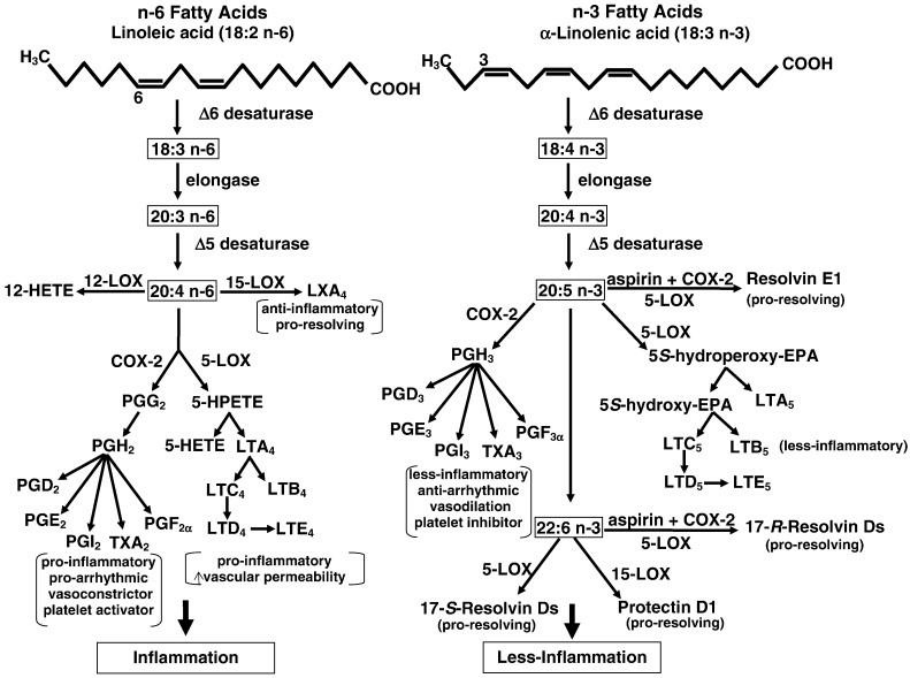

Figure 10. *The metabolism of n-3 and n-6 PUFA and the biosynthesis of their respective eicosanoid and proresolving mediators. HPETE: hydroperoxyeicosatetraenoic acid; LTA_4: leukotriene A_4; LXA_4, lipoxin A_4; LOX: lipoxygenase; COX: cyclooxygenase [194]*

4.1.2 Carbohydrate metabolism

Glucose uptake rises with increasing concentrations of the carbohydrate presented to the myocardium. This glucose uptake into the myocytes is facilitated by the glucose transporters GLUT-1 and GLUT-4. In the adult heart, GLUT-4 is the dominant myocardial isotype in a GLUT- 4/GLUT-1 ratio of 3:1 and it is insulin-sensitive, responding to various environmental influences to meet changing metabolic demands. Once glucose is imported, hexokinase catalyzes the phosphorylation of glucose to glucose-6-phosphate. This reaction is irreversible, because heart, like all muscle tissues, does not contain glucose-6-phosphatase. Afterwards, glucose-6-phosphate can enter three different pathways: glycogenesis (and synthesis of glucose derivatives) where a variable amount of imported glucose is temporarily stored as glycogen being a small energy reserve for the myocytes, pentose phosphate pathway or

glycolysis. The glycolysis pathway generates two pyruvate molecules from one glucose-6-phosphate with phosphofructokinase-1 (PFK-1) as the key-regulating enzyme in this pathway. The next step is the breakdown of one 6-C containing fructose-1,6-bisphosphate into two 3-C containing molecules (glyceraldehyde 3-phosphate), a reversible reaction catalyzed by fructose 1,6-bisphosphate aldolase. Further downstream, glyceraldehyde 3-phosphate is converted into 1,3-bisphosphoglycerate, a reaction catalyzed by glyceraldehyde 3-phosphate dehydrogenase, and generating NADH from NAD^+.

The pyruvate formed from glycolysis passes the outer mitochondrial membrane by the monocarboxylate transporter (MCT). The pyruvate dehydrogenase complex on the IMM transports pyruvate across the membrane and catalyzes the irreversible transformation into acetyl-CoA. Pyruvate can also be converted into two intermediates of the citric acid cycle, malate and oxaloacetate. A third intermediate-producing pathway is transamination of pyruvate with glutamate to form alanine and the citric acid cycle intermediate α-ketoglutarate. The anaplerotic reactions described above are viewed as 'fillup reactions', replenishing citric acid cycle intermediates.

Lactate is also a significant, but often underestimated, source of oxidative fuel for the heart. It mainly crosses the plasma membrane by facilitated transport through monocarboxylate transporters (MCT).

Intracellular lactate reacts with NAD^+ in a reversible reaction catalyzed by lactate dehydrogenase (LDH). This reaction forms pyruvate and NADH and H^+. The flux through the reaction depends on the concentrations of the reagents. Under conditions of adequate oxygenation and a high rate of lactate uptake, the equation proceeds toward pyruvate. During hypoxia, when NADH and H^+ accumulate and pyruvate cannot be metabolized further, the reaction takes place in the lactate direction [185].

4.1.3 Amino acid and ketone bodies metabolism

Under conditions of high-energy substrate demand, unmatched by glucose or fatty acids, protein is degraded and amino acids are released from muscle into the blood stream. Aminotransferases can convert some amino acids into other amino acids that can later be used for energy production or transported to the liver for gluconeogenesis. It has been proposed that amino acid transamination may be an important adaptive process in the immature heart, improving its resistance to ischemic damage [200].

Ketone bodies are a minor substrate for the myocardium since their plasma levels are usually

low. However, in times of starvation, poorly controlled diabetes, chronic heart failure and during high-fat diet consumption their levels can significantly increase [201] and can be used by the heart by inhibiting the other main oxidation pathways in the heart.

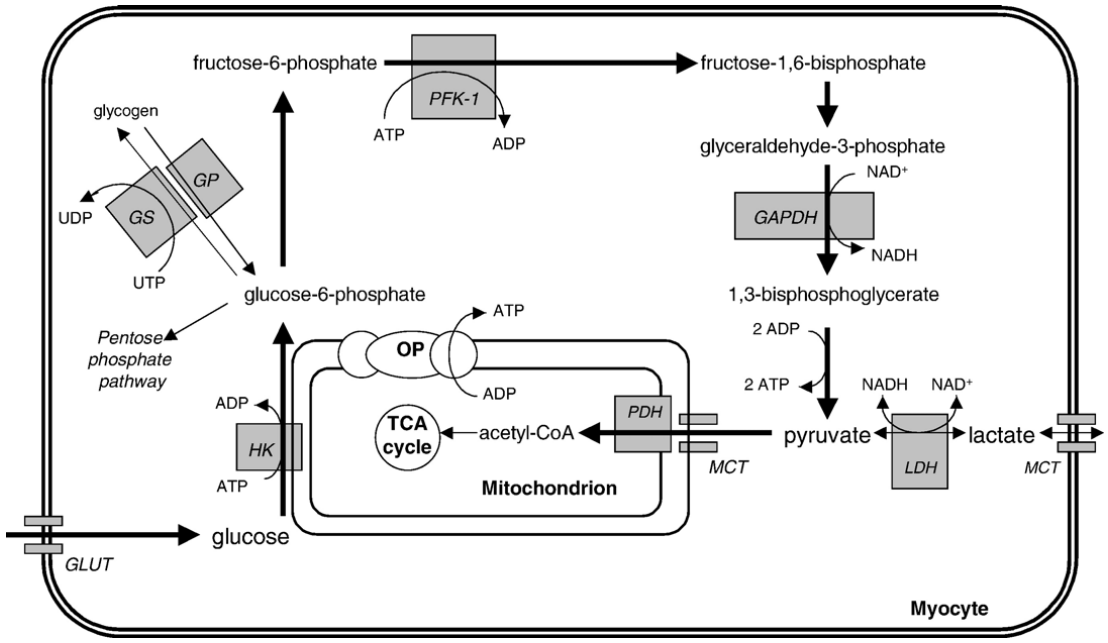

Figure 11. *Cardiac carbohydrate pathways. GAPDH : Glyceraldehyde-3-phosphate dehydrogenase; GLUT :Glucose transporter; GP: Glycogen phosphorylase; GS: Glycogen synthase; HK: Hexokinase; LDH: Lactate dehydrogenase; MCT: Monocarboxylate transporter; OP = Oxidative phosphorylation; PDH: Pyruvate dehydrogenase complex; PFK-1: Phosphofructokinase-1; TCA cycle: Tricarboxylic acid cycle [185]*

4.2 Myocardial Ischemia/Reperfusion

Myocardial ischemia develops when coronary blood supply to myocardium is reduced, either in terms of absolute flow rate (low-flow or no-flow ischemia) or relative to increased tissue demand (demand ischemia) [202]. Ischemia may be followed by reperfusion, which is the re-admission of oxygen and metabolic substrates with washout of ischemic metabolites. The incidence and implications of ischemic injury are enormous since it occurs in many situations including myocardial infarction, stroke and organ procurement injury.

It is recognized that prolonged myocardial ischemia is accompanied by a time-dependent loss of the viability of myocardial cells in the traumatized region of the heart. Reperfusion is necessary to initiate and maintain those functions responsible for reversing the changes induced by ischemia. It is also necessary for the continued survival of the myocardial cells at

risk of permanent damage. Despite these benefits of the blood reperfusion to an ischemic tissue, this can cause a series of adverse reactions that paradoxically injure tissue [203]. Myocardial injury is clinically manifested as combination of myocardial cell death, contractile dysfunction, arrhythmia and microvascular dysfunction.

4.2.1 Cellular effects of ischemia and reperfusion

In non-ischemic hearts, the majority of ATP production (over 95%) results from the mitochondrial oxidative phosphorylation and in particular by beta-fatty acid oxidation [204]. Ischemia results from insufficient blood supply to the myocardium; thus, there is an insufficient oxygen supply to the mitochondria not meeting the oxidative phosphorylation demands. Consequently, cellular oxidative phosphorylation decreases resulting eventually to failure to resynthesize energy-rich phosphates (e.g. ATP and phosphocreatine). An accumulation of reduced substrates at the expense of their oxidative counterparts is observed as evidenced also by the 10-fold increase in the $NADH/NAD^+$ ratio [205]. In response to this decreased oxidative phosphorylation, the cardiac metabolism switches to glycolysis for its energy production, which is a short-term solution since myocardial glycogen stores are limited [206]. This leads to increased lactic acid production and hydrogen ions accumulation with consequent intacellular acidosis within the first 15 minutes of ischemia [207]. Aside form these metabolic changes, the myocardium readjusts its oxygen demands according to the disponibility of oxygen under these conditions by reducing its contractility leading to myocardial hibernation [208].

The excess of protons in the cytoplasm resulting from non-mitochondrial ATP production activates the sodium/hydrogen exchanger (NHE). This leads to an initial intracellular sodium overload and an eventual intracellular calcium overload caused by the functional inability of the sodium/potassium ATPase and the reverse function of the sodium/calcium antiporter [209]. Thus, cytosolic [210] and mitochondrial [211] calcium levels are increased. However, cytosolic calcium overload is exacerbated mostly at the early reperfusion [212]. Myocardial acidosis during ischemia interferes with the normal Ca^{2+}-troponin C interaction resulting in reduced cardiac contractility and arrhythmia [213]. Elevated Ca^{2+} may also activate proteases causing alterations in contractile proteins leading in contractility impairement despite the elevated calcium concentration.

Furthermore, there is progressive membrane damage in the cardiomyocytes during ischemia. The sustained increase in calcium leads to the activation of phospholipase and consequent

degradation of phospholipids and release of FFAs. Since the mitochondrial oxidative phosphorylation is depressed, mitochondrial fatty acid metabolism products are accumulated and can be incorporated into membranes and impair their function. Moreover, ROS produced by the ischemic myocardium [214] can induce peroxidative damage to the fatty acids of membrane phospholipids. Activated proteases may also cleave cytoskeletal filaments leading to membrane permeability, derangement of intracellular electrolytes and ATP exhaustion. All these ischemic conditions contribute eventually to cell death [215] by oncotic necrosis (cell injury with swelling) or apoptosis (cell injury with shrinkage) [216].

Ischemia affects also the endothelium, where it promotes expression of certain proinflammatory gene products (e.g. leucocyte adhesion molecules, cytokines) and bioactive agents (e.g. endothelin, thromboxane A_2) and repression of other 'protective' gene products (e.g. constitutive NOS, thrombomodulin) and bioactive agents (e.g. prostacyclin, NO). Thus ischemia induces a proinflammatory state that increases tissue vulnerability to further injury on reperfusion [202].

At reperfusion, the oxygenation is restored. However, the concept of a unique type of reperfusion injury was first proposed in 1970s [217]. During ischemia, there is an increased accumulation of reducing equivalents that can serve as substrates for oxygen centered ROS generation at reperfusion [214]. The peak of ROS generation with oxygenated reperfusion occurs approximately 20 seconds after its beginning [218]. $O_2\bullet^-$ was identified as the parental radical at reperfusion [218, 219]. The combined presence of high calcium, ROS and increasing pH induces the mitochondrial permeability pore (MPP) opening that results to further ROS production, depletion of ATP and cytochrome C leak into the cytoplasm leading eventually to cell death. Moreover, since some of ATP production is restored there is excessive contractile activation. The mechanical effect can lead to disruption of the sarcolemma, and propagate to adjacent cells through gap junctions. These processes lead to cell death through necrosis and apoptosis, and have a crucial role in reperfusion injury [202].

Potential cellular sources of ROS production during ischemia and reperfusion are the mitochondrial electron transport damage and uncoupling, the NAD(P)H oxidase activity, the uncoupled nitric oxide synthase activity, the cellular P450 activity and the conversion of cellular xanthine dehydrogenase (XDH) to xanthine oxidase. However, mitochondria seem to be especially important in this context since they are abundant in the heart tissue [220], are important sources of $O_2\bullet^-$, $\bullet OH^-$ and •NO [221], contain biomolecules susceptible to ROS reactions and are key regulators of ROS mediated cell death [222]. However, it is possible that the peak of ROS production during the first seconds of reperfusion is associated with the

cellular xanthine oxidase. The cessation of oxidative phosphorylation during ischemia causes ATP degradation to lower energy products of purine catabolism. Hypoxanthine is one of these intermediates. Thus, it accumulates during ischemia and serves as substrate for XDH when oxygen is restored at reperfusion. This reaction provides also xanthine as substrate for xanthine oxidase.

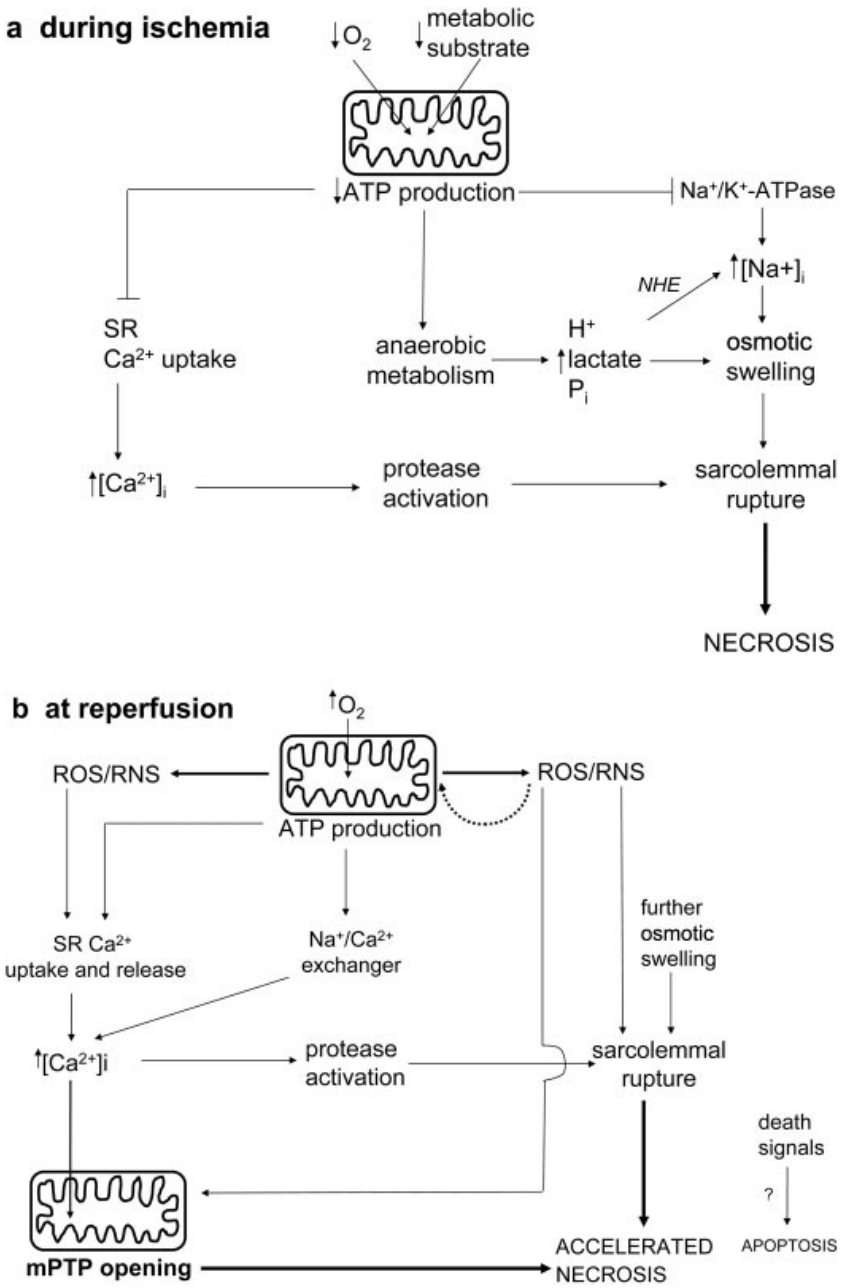

Figure 12. *Major cellular effects of ischemia (**a**) and reperfusion (**b**) leading to irreversible forms of injury [202]*

4.2.2 Role of ROS and reperfusion injury

As already described, reperfusion of ischemic tissues results in formation of toxic ROS (O_2•$^-$, •OH, HOCl, H_2O_2 and peroxynitrite) [223]. Cellular ischaemia results in ATP degradation to form hypoxanthine. Under normal physiological conditions, hypoxanthine is oxidized by xanthine dehydrogenase to xanthine. However, xanthine dehydrogenase is converted to xanthine oxidase during ischaemia. Unlike xanthine dehydrogenase, which uses NAD as its substrate, xanthine oxidase uses oxygen; therefore during ischaemia it is unable to catalyse the conversion of hypoxanthine to xanthine, resulting in a build-up of excess tissue levels of hypoxanthine. With the reintroduction of oxygen during reperfusion, conversion of the excess hypoxanthine by xanthine oxidase results in the formation of toxic ROS.

ROS may cause tissue injury via several mechanisms (as already described in session 2.3 of the Introduction). They can directly damage cellular membranes through lipid peroxidation, stimulate leucocyte activation and chemotaxis by inducing plasma membrane phospholipase A_2 or mediated release of arachidonic acid, an important precursor of eicosanoid synthesis (e.g. thromboxane A_2 and leukotriene B_4). Finally, ROS increase leucocyte adhesion molecule and cytokine gene expression by activating transcription factors such as nuclear factor κB (NF-κB) and activator protein 1 (AP-1).

4.2.3 Clinical manifestations of ischemia-reperfusion injury

4.2.3.1 Myocardial stunning

Myocardial stunning can be defined as myocardial dysfunction persisting after reperfusion despite the absence of irreversible damage. This contractile dysfunction is not permanent and fully reversible with time. Mechanisms of myocardial stunning may include decreased ATP resynthesis, coronary microvasculature spasm or plugging, ROS-mediated cytotoxic injury and altered intracellular calcium release and uptake [224].

4.2.3.2 Reperfusion arrythmias

Reperfusion arrhythmias are frequent in patients undergoing thrombolytic therapy or myocardial surgical revascularization. Ventricular tachycardia, ventricular fibrillation or accelerated idioventricular rhythms are often observed following myocardial I–R in animals

with normal coronary arteries, particularly if reperfusion occurs abruptly after 15–20 min of ischaemia. Reperfusion arrhythmias may be in part due to rapid and sudden ion concentration changes within ischaemic tissues upon reperfusion [224].

4.3 Coronary endothelial function

Coronary vessels are required to maintain cardiac homeostasis, as evidenced by the dramatic effects of coronary ischemia. In 1980, Furchgott and Zawadski [225] discovered the obligatory role of the vascular endothelium in vasomotor tone. Since then, the endothelium has emerged as an essential structural and functional element of the cardiovascular system. The endothelium is the largest organ in the body and strategically located between the wall of blood vessels and the blood stream. It regulates vascular permeability, adjusts the caliber of blood vessels to hemodynamic and hormonal demands and maintains blood fluidity. Endothelial cells have a central role in these functions by the expression, activation, and release of powerful vasoactive substances as well as of numerous other bioactive molecules. These substances include vasoconstricting and vasodilating factors, pro- and anticoagulant factors, pro- and antithrombotic factors, growth and antigrowth factors, factors that contribute to angiogenesis and tissue remodeling, as well as to immune reactions and tissue inflammation [226]. Among the vasodilatory substances produced by the endothelium are NO, prostacyclin (PGI2), endothelium-derived hyperpolarizing factors (EDHF), and C-type natriuretic peptide. Vasoconstrictors include endothelin-1 (ET-1), angiotensin II (Ang II), thromboxane A2, and ROS. Inflammatory modulators include NO, intercellular adhesion molecule-1 (ICAM-1), vascular adhesion molecule-1 (VCAM-1), E-selectin, and NF-κB. Modulation of hemostasis includes release of plasminogen activator, tissue factor inhibitor, von Willebrand factor, NO, PGI2, thromboxane A2, plasminogen-activator inhibitor-1 and fibrinogen. The endothelium also contributes to mitogenesis, angiogenesis, vascular permeability, and fluid balance. It also senses mechanical stimuli, such as pressure and shear stress.

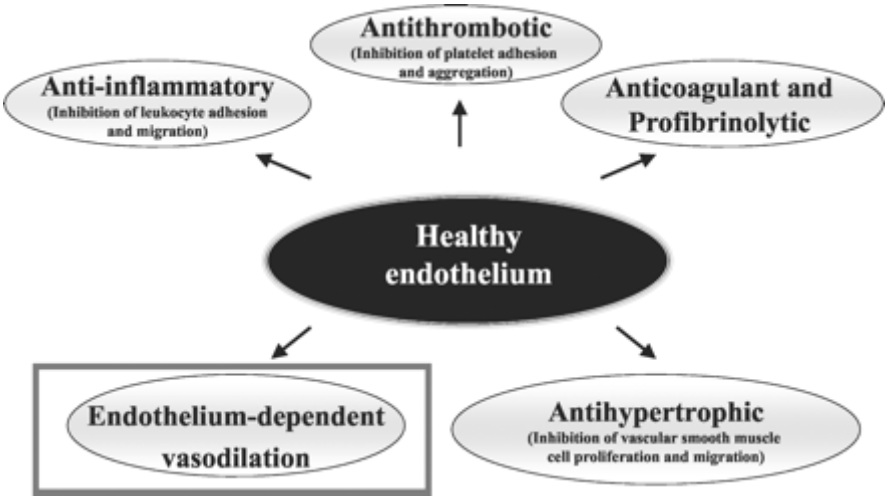

Figure 13. *Functions of healthy endothelium* [227]

Dysfunction of the endothelium has been implicated in the pathophysiology of different forms of cardiovascular disease, including hypertension, coronary artery disease, chronic heart failure, peripheral artery disease, diabetes, and chronic renal failure. It has been shown that a state of endothelial dysfunction is a phenomenon implicated in the atherogenic process, preceding the first clinical manifestations [228]. Endothelial dysfunction was initially identified as impaired vasodilation to specific stimuli such as acetylcholine or bradykinin. Impairement of endothelium-dependent dilatation (EDD) represents the functional characteristic of endothelial dysfunction. It is characterized by a shift of the actions of the endothelium toward reduced vasodilation, proinflammatory state and prothrombic properties [229].

4.3.1 Regulation of the vascular tone

The primary function of the endothelium is the regulation of the vascular tone and blood flow in response to various mechanical or chemical stimuli. The nature of these stimuli determines the secretion of substances from the endothelium that regulate the vasodilatation or vasoconstriction. These vasoactive substances diffuse to the underlying smooth muscle cells where they provoke their relaxation or contraction.

4.3.1.1 Chemical and physical stimuli

In 1980, Furschgott and Zawadski proposed that an endothelium-derived relaxing factor

(EDRF) identified as the NO had a major contribution in the vessel relaxation mediated by acetylcholine (Ach). Since then, many other substances such as noradrenaline, bradykinin and serotonin are used as pharmacological stimuli to assess endothelial function. These substances are recognized by specific G-protein coupled receptors on the endothelial surface [230] and induce vasodilatation. Their administration *in vivo* is done intravenously and in low doses in order to avoid side effects on the vascular neurogenic tone and arterial pressure. Recently, other factors participating in the EDD by these pharmacological stimuli has been described. The EDHF is a substance and/or electrical signal that is generated or synthetized in and released from the endothelium that hyperpolarizes vascular smooth muscle cells (VSMC) and this way causes their relaxation [231].

Shear stress is also widely used as mechanical stimulator of the vasodilator response of the endothelium. Shear stress is the tractive force produced by flowing blood upon the endothelial cell surface. It contributes to the endothelial production of NO and EDHF via activation of the Akt/kinases-dependent pathway. This induces the flow-mediated dilatation (FMD) translated to an increase in the blood flow.

Independently of the nature of these stimuli, the production of NO and EDHF is important for the EDD. However, it must be noted that the contribution of these substances to the EDD depend on the vascular bed, the vessel diameter and the organism pathology. It has been demonstrated that the conribution of EDHF to the EDD increases as the vessel diameter decreases. It has also been reported that it mediates a compensatory adaptation when NO bioavailability is lost in order to maintain the EDD as in states of obesity.

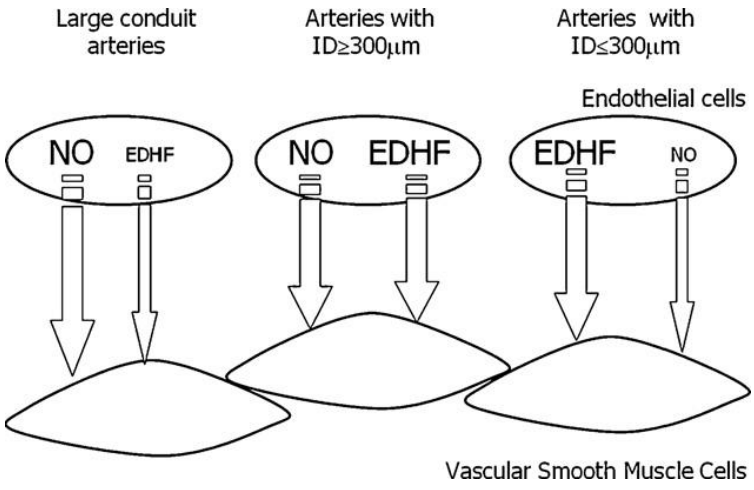

Figure 14. *Balance between NO and EDHF release in arteries depending on their internal diameter (ID) [232]*

4.3.1.2 Endothelial Vasodilator substances

4.3.1.2.1 Nitric oxide (NO)

One of the most important vasodilating substances released by the endothelium is NO, which acts as a vasodilator, inhibits growth and inflammation, and has anti-aggregant effects on platelets. In biological systems, NO can be formed both enzymatically and non-enzymatically. In the tissues, such as the heart, there are numerous pathways for the generation of NO from nitrite, all greatly potentiated during hypoxia, including xanthine oxidoreductase (XOR), deoxygenated myoglobin, enzymes of the mitochondrial chain and protons [233].

The enzyme responsible for NO generation in animals is NOS. The NOS enzymes utilize L-arginine and molecular oxygen to produce the free radical gas •NO and L-citrulline. NO is an autocrine and paracrine signalling molecule whose lifetime and diffusion gradients are limited by scavenging reactions. There are three NOS isofroms : the inducible, the neuronal and the endothelial NOS. nNOS (also known as Type I, NOS-I and NOS-1) being the isoform 1rst found (and predominating) in neuronal tissue, iNOS (also known as Type II, NOS-II and NOS-2) being the isoform which is inducible in a wide range of cells and tissues and eNOS (also known as Type III, NOS-III and NOS-3) being the isoform first found in vascular endothelial cells.

NOS enzymes in their active form are usually referred to as `dimeric'. However, this does not include the required calmodulins (CaMs) for their activity. This would mean that they are tetramers (of two NOS monomers associated with two CaMs) [136]. They contain relatively tightly-bound cofactors ((6R)-5,6,7,8-tetrahydrobiopterin (BH4), FAD, FMN and iron protoporphyrin IX (haem)) and catalyse a reaction of L-arginine, NADPH, and oxygen to the free radical NO, citrulline and NADP .

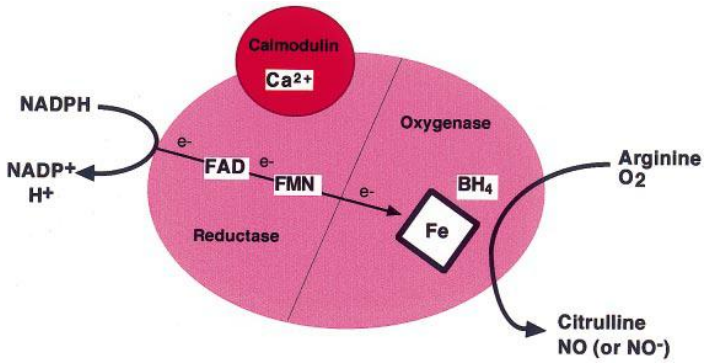

Figure 15. *Overall reaction catalysed and cofactors of NOS [136]*

After the production of NO in the endothelial cells, NO diffuses to the adjacent smooth muscle cells where it reacts with sGC that helps convert guanosine 5′-triphosphate (GTP) to cyclic guanosine 3′,5′-monophosphate (cGMP). Once produced cGMP activates protein kinase G (PKG) that leads to activation of myosin phosphatase. In smooth muscle cells, PKG is known to lower $[Ca^{2+}]_i$ by activating calcium-dependent potassium channels, inhibiting agonist-dependent activation of phospholipase C (PLC), stimulating Ca^{2+} uptake into the sarcoplasmic reticulum (SR) and inhibiting inositol trisphosphate (IP3)-mediated Ca^{2+} release from the SR [234]. This in turn leads to relaxation of the smooth muscle cells. It has also been shown that, apart from the sGC pathway, NO directly activates calcium-dependent potassium channels in VSMCs and leads to their consequent relaxation [235].

The sGC pathway requires only picomolar–nanomolar concentrations of NO which can be effectively generated by the constitutively expressed isoforms of NOS. This reaction requires as a substrate the amino acid L-arginine together with cofactors including BH_4, NADH and O_2. Activation of this mechanism in blood vessels occurs either through the release of Ach at parasympathetic nerve endings or signalling activated by shear stress recognition by the endothelium, both of which result in an increase in calcium flux in endothelial cells.

4.3.1.2.2 Prostacyclin (PGI2)

Prostaglandins were the first endothelium-derived relaxing factors to be discovered. In 1976, Moncada et al. described an anticlotting agent that was also capable of relaxing vascular smooth muscle [236]. This substance was later identified as prostacyclin [237]. Prostacyclin, as nitric oxide, is lipid soluble and highly unstable in the body and thus it leaves the endothelial cell following its production and acts as a local anticoagulant and vasodilator. Interaction between prostacyclin and its receptor in the plasma membrane of vascular smooth muscle leads to activation of adenylyl cyclase and an increase in the production of cyclic AMP (cAMP). cAMP activates protein kinase A (PKA) that continues the cascade by phosphorylating and inhibiting myosin light-chain kinase, which leads to smooth muscle relaxation and vasodilatation.

4.3.1.2.3 EDHF

Based on the place of the events, the basic mechanism of EDHF mediated response can be separated into two stages. The endothelial stage of the EDHF-mediated response include an

increase in calcium concentration $[Ca^{2+}]i$, activation of Ca^{2+}-dependent K^+-channels and K^+ efflux followed by hyperpolarization, synthesis of substance or generation of signals capable of diffusing through membranes or myoendothelial gap junctions (MEGJ) to VSMCs. The following stage reflects the mechanism by which endothelial hyperpolarization is transferred to VSMCs. At the level of VSMCs, EDHF activates K^+-channels and causes endothelium-dependent hyperpolarization accompanied by closure of voltage-sensitive Ca^{2+}-channels that results in relaxation [238].

Classically, EDHF-mediated response is a hyperpolarization with subsequent relaxation maintained after inhibition of NO and prostaglandins, namely PGI2, synthesis. However, it must be noted that since both NO and PGI2 in certain circumstances and in some types of arteries and/or species may also hyperpolarize the VSMCs, theoretically, they could be considered as EDHF.

4.3.1.2.3.1 Epoxyeicosatrienoic acids

Metabolites of arachidonic acid are strong candidates as EDHF mainly in coronary circulation [239]. Epoxygenase CYP-450 products of arachidonic acid, notably 5,6-; 8,9-; 11,12-; or 14,15 epoxyeicosatrienoic acid (EETs) have been suggested to serve as EDHF, at least, in some vascular beds.

4.3.1.2.3.2 Hydrogen peroxide

Endothelial cells (ECs) are capable of producing superoxide anions ($O_2\bullet^-$) from sources such as eNOS, LOX, COX, CYP450 epoxygenases and NAD(P)H oxidase. These anions are precursors of H_2O_2 [240]. Thus, H_2O_2 was considered as a possible EDHF for a long time. Recently, it has been identified as the transferrable factor mediating flow-induced dilation in human coronary arterioles [241].

4.3.1.2.3.3 Potassium ions

The activation of endothelial calcium activated potassium (KCa^{2+}) channels causes an efflux of K^+ from ECs towards the extracellular space. An increase in extracellular K^+ from 1 to 10 mmol/l has been shown to activate an ouabain-sensitive electrogenic Na^+/K^+-ATPase and potassium inward-rectifing-channels followed by hyperpolarization and SMC relaxation

[242].

4.3.1.2.3.4 C-type natriuretic peptide

C-type natriuretic peptide (CNP) has been shown to exert a variety of cardiovascular effects including vasodilatation and hyperpolarization of arteries through the opening of KCa+-channels. CNP is widely distributed in the cardiovascular system and it has been found at high concentrations particularly in ECs. Endothelium-derived CNP has been proposed to act as an EDHF via specific C-subtype of natriuretic peptide receptor (NPR-C) followed by Gi -dependent activation of G protein-gated potassium inward rectifing–channels and Na^+/K^+-ATPase in VSMCs, thus bringing hyperpolarization and, thereby, relaxation [243] .

4.3.1.2.3.5 GAP junctions

The EDHF phenomenon may be further explained by the transmission of endothelial cell hyperpolarization to the vascular smooth muscle via gap junctions [244]. These are myoendothelial and heterocellular. They couple endothelial cells to other endothelial cells and to smooth muscle cells, providing a low-resistance electrical pathway between the cell layers. Gap junctions are formed by the docking of two connexions present in adjacent cells that creates an aqueous pore permitting the transfer of ions and electrical continuity that establishes a uniform membrane potential across cells. Their number increases with diminution in the size of the artery, paralleling the importance of EDHF to vessel size with a greater influence in the resistance than in the conductance vessels [245].

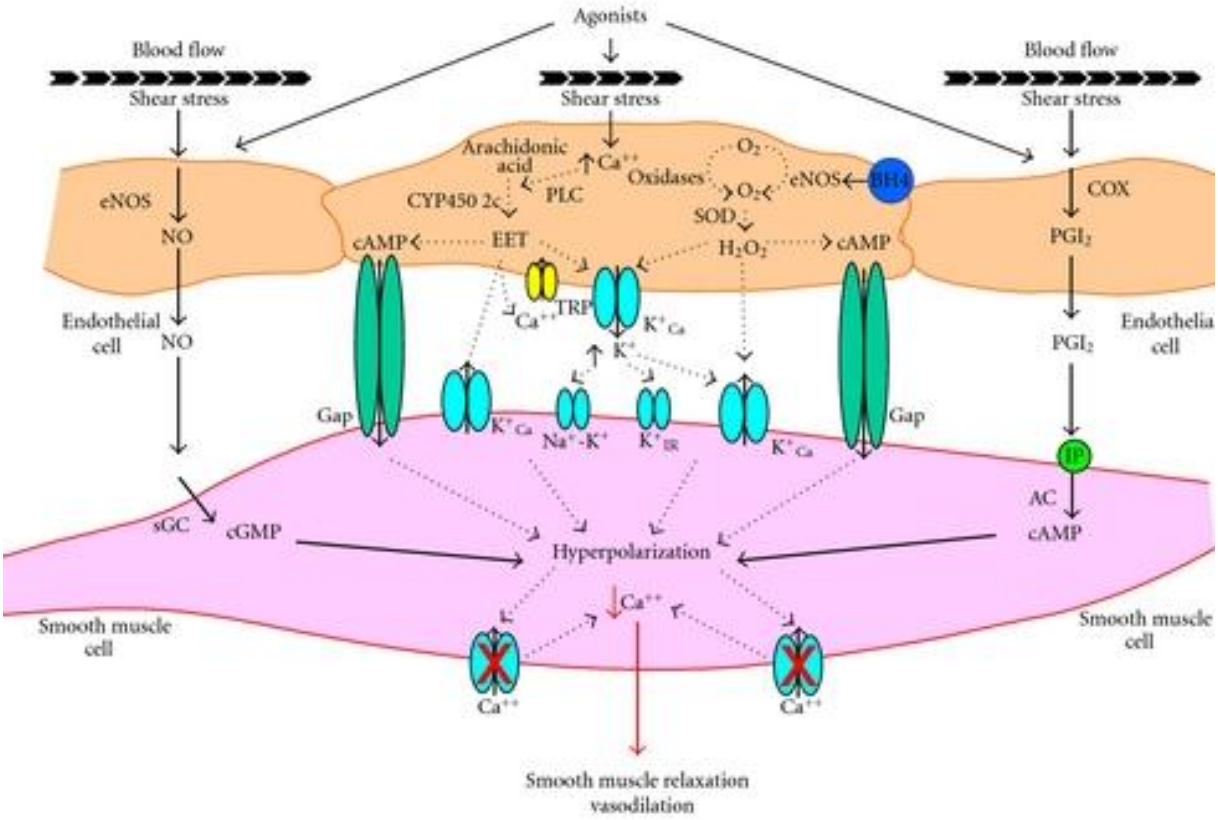

Figure 16. *Mechanisms for endothelial cell mediated relaxation. Adenylyl cyclase: AC; cyclic Adenosine monophosphate: cAMP; cyclic guanosine monophosphate: cGMP; soluble guanylyl cyclase: sGC; prostacyclin receptor, IP [246]*

4.4 Cardiovascular function in aging and obesity

Aging is accociated with changes of cardiovascular structure and function. There is a mild increase in heart weight reflecting some degree of left ventriculrar hypertrophy [247] and even though systolic function, heart rate and cardiac output are not altered [248], there is a reduction in the diastolic function [249]. Catecholamine or exercised induced increases in heart rate and myocardial contractility are blunted in elderly subjects [250]. Large arteries are elongated with enlarged lumen, thickened wall and increased stiffness [251]. Furthemore, studies mostly in animal species demonstrate a reduction of the release of NO and EDHF and an augmentation of the endothelium-derived vasoconstrictor prostanoids. Studies *in vivo* in young and old people also suggest that endothelium-dependent dilatation decreases progressively with advancing age [252]. It must be noted though that most of these studies are focused on advanced ageing (cut off point for advanced age in humans around 65 years and for rats 18 months).

Beyond an unfavorable risk factor profile, overweight and obesity also affects heart structure and function [253]. As excessive adipose tissue accumulates, many adaptations and alterations in cardiac structure and function occur. Circulating blood volume, plasma volume and cardiac output increase to meet the higher metabolic need of the organism [85]. The increased blood volume leads to increased venous return to the ventricles eventually producing dilation of the cardiac cavities and increasing wall tension [89]. This results in left ventricle hypertrophy accompanied by a decrease in diastolic chamber compliance finally leading to increased left ventricular filling pressure and left ventricular enlargement. When the left ventricular hypertrophy fails to keep along with the progressive ventricular dilation, the wall dilation increases and systolic dysfunction occurs. Eccentric LVH is often associated with ventricular diastolic dysfunction [254]. Adipose tissue is also a source of inflammatory cytokines and CRP is a marker of a chronic inflammatory state that can trigger acute coronary syndrome [255]. All these changes predispose to heart failure. Increased risk of arrhythmias and sudden death is present in obese individuals even in the absence of cardiac dysfunction [87]. Furthermore, obesity has been associated with abnormal endothelial function and decreased NO bioavailability related to increased oxidative stress [256, 257]. However, in recent years, studies in animals and patients have demonstrated that obesity might maintain or enhance the dilator function of coronary microvessels to increase coronary blood flow to higher metabolic demand [258-262]. This could indicate an adaptation which may decline with the progression of obesity and development of comorbidities such as diabetes and metabolic syndrome [263].

PART II. EXPERIMENTAL RESEARCH

1. Introduction

According to WHO, 17.3 million deaths occurred in 2008 due to CVDs while it is estimated that 23.6 million people will die from CVDs by 2030. CVDs are considered worldwide as the leading causes of death and disability. Normal aging is closely related to changes in cardiovascular structure and function that make the heart more susceptible to damage. Age *per se* is thus considered the major risk factor for CVDs [264]. In United States, atherosclerosis and hypertension associated with heart failure and stroke, account for over 40% of deaths for the people aged 65 years and above. However, the cardiac susceptibility to injury is apparent at middle age. The consequences of the changes occurring at the cardiovascular level at middle age have been well characterized as well as changes that occur in the body composition. Increased body mass, especially fat mass, hyperlipidemia, glucose intolerance or insulin resistance develop with aging contributing to cardiovascular incidents.

In the industrialized societies, the incidence of CVD is even more increased and related to the lifestyle habits of the Western world (e.g. non-healthy diets and physical inactivity). Data obtained from WHO, indicate that at least 2.8 million people die each year as a result of being overweight or obese. Beyond an unfavorable risk factor profile, overweight and obesity affect heart structure and function [253] in a way that favors heart failure. Furthermore, it has been demonstrated that the risk of developing obesity and related pathologies such as T2D in later life is affected by dietary habits adopted during early life (childhood or adolescence) [265-267].

Thus, the general objectif of this work was to characterize the changes that progressively occur from youth to middle age on the cardiovascular function in association with the mitochondrial function and oxidative stress and to understand the mechanisms involved in the increased susceptibility of the middle aged hearts to ischemia. These parameters were also studied after a high fat diet protocol applied during this aging period in order to better understand the obesity-related alterations on the cardiovascular function at middle age. The study of the reactivity of the coronary microvessels had a prominent role in this work since alterations of the coronary reserve due to vascular dysfunction may lead to eventual ischemic incidents that would compromise the health and welfare of individuals.

Aims of the investigation

Study 1. Earlier studies have demonstrated that advanced aging is associated with a diminished functional and adaptive reserve capacity and an increased susceptibility to incur damage [268]. NADPH oxidase [269] and mitochondrial ROS through a ROS-induced release process [270] have been associated with this pathology. Thus, our first study aimed at determining whether middle-aged hearts demonstrate impaired contractile recovery in the post-ischemic period as found in the advanced aging and whether this is related to an increased mitochondrial ROS release at resumption of the coronary flow. For this reason, the hearts of 10-weeks and 52-weeks old animals were perfused and subjected to ischemia followed by reperfusion. Parameters of cardiac mechanical activity were evaluated *ex vivo* under normoxia, ischemia and reperfusion as well as the mitochondrial function, the mitochondria-derived oxidative stress and the activities of respiratory chain complexes.

Study 2. This study was designed in order to complete and better understand the results from the first study, which demonstrated a lower restoration of the cardiac mechanical activity during reperfusion in the middle aged hearts due to impaired recovery of the coronary flow and an insufficient oxygen supply. Thus, the influence of the aging during the period from youth to middle age on the functional behavior of coronary microvessels and the functional contribution of endothelial cells and smooth muscle cells were examined. The mechanical function and coronary microvascular reactivity were studied in the *ex vivo* Langendorff perfused heart derived from rats of different ages (3, 6 and 11 months for youth, young adulthood and middle age). The results were associated with the state of oxidative stress in the organism and the mitochondrial function in terms of oxidative phosphorylation and H_2O_2 production.

Study 3. The results from the second study revealed that major changes occur from youth to young adulthood affecting the body composition, the mitochondrial oxidative phosphorylation and the coronary microvascular reactivity. Western life is strongly associated with high-fat content dietary habits beginning mostly at the early adulthood. High fat diet is an excellent model for excess caloric intake, which contributes to the development of obesity and metabolic syndrome. Thus, the aim of our study was to characterize and monitor the changes induced by a high-fat diet during adulthood on the i) state of oxidative stress of the organism, ii) cardiac mitochondrial function (oxidative phosphorylation and H_2O_2 production) and iii)

cardiovascular function *ex vivo*. For this reason, we applied a short- and long-term high-fat feeding protocol on Wistar rats during the period from youth to middle age.

Study 4. Our third study revealed some surprising and interesting information concerning the reactivity of the intact coronary microvasculature under high-fat conditions. Thus, we were interested in this study to confirm the results found in study 3 regarding the establishment of a coronary adaptation in response to the high-fat diet but also to investigate the mechanisms involved in this phenomenon. Thus, the hearts of Wistar rats following a 3-month protocol of standard or high-fat diet were perfused *ex vivo* according to Langendorff and the reactivity of the coronary microvessels were once again studied. After finding the same results, we performed the same manipulations but perfused the hearts in the presence of the inhibitors L-NAME, indomethacin and tetraethylammonium in order to investigate the contribution of NO, COX-derived molecules and potassium channels respectively in the coronary adaptation. An evaluation of the fatty acid profile of their cardiac membrane phospholipids was also performed to better understand the results of this work.

Study 5. Study 3 revealed a decreased cardiac mechanical function *ex vivo* after a high-fat diet, which was not accompanied by severe glucose intolerance or diabetes development. In this context a number of adaptations occurred including that of the coronary microvasculature, which was established at the beginning of the diet. Thus, the aim of this study was to determine whether the development of T2D at its early phase can cause this kind of modifications in the cardiovascular level. For this reason, the hearts of young ZDF rats and their lean littermated were perfused *ex vivo* according to Langendorff and their cardiac mechanical activity and coronary reactivity were evaluated. Finally, the results were associated with the diabetic state of the organisms, their levels of oxidative stress and the fatty acid profile of the cardiac membrane phospholipids.

2. Materials and Methods

2.1 Isolated heart perfusion according to a modified Langendorff mode

2.1.1 The Langendorff technique

In 1895, Oscar Langendorff was the first to produce an isolated mammalian heart with full contractile activity and the first to demonstrate that the heart receives its nutrients and oxygen from blood through the coronary arteries and that cardiac mechanical function is reflected by changes in the coronary circulation. The general principle of this method is to provide the isolated heart with oxygen and metabolites (usually by using physiological salt solution containing bicarbonate which mimics the ionic content of the plasma) via a cannula inserted and fixed in the ascending aorta. With the perfusion buffer flowing retrogradely down the aorta, opposite to normall physiologic flow, the aortic valve is closed under pressure. This constant retrograde flow closes the leaflets of the aortic valve and does not permit the perfusion fluid to enter into the left ventricle. Thus, the entire perfusate enters the coronary arteries via the ostia at the aortic root during the diastolic period, just as it flows in the normal cardiac cycle. The perfusion buffer then continues through the coronary system (left and right main coronary arteries → arterial branches → arterioles → capillaries → venules → coronary veins) and is then drained into the right atrium via the coronary sinus. Throughout this procedure, the ventricular chambers remain essentially "dry".

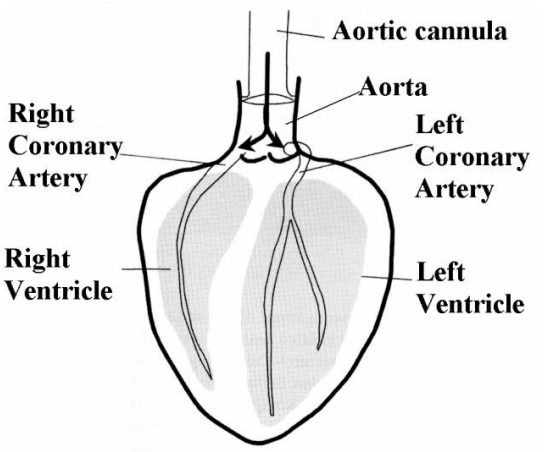

Figure 17. *Scheme of the isolated perfused heart according to Langendorff. Perfusion solution is flowing retrogadely within the aorta and then orthogradely within the coronaries during diastole. A prerequisite is that the aortic valve is closed by the hydrostatic pressure of the perfusion solution.*

2.1.2 Modes of perfusion: constant pressure and constant flow

There are two modes of retrograde perfusion; at a constant hydrostatic pressure or at a constant flow rate with the use of a calibrated roller pump. Both types of perfusions help the researchers monitor the change in the mean radius of the coronary arteries which reflects the mechanical function of the smooth muscles. However, a direct measure of this parameter is difficult. Thus, flow resistance is used for assessing smooth muscle function.

The resistance of the coronary circulation can be described in analogy to Ohms law as:

$$R=\Delta P/\Phi$$

where ΔP= pressure difference (which is in the common Langendorff heart the perfusion pressure, since the outflow pressure is almost zero (this is different in working heart models)) and Φ= coronary flow. As a consequence for calculation of R either both variables have to be measured or only one if the other is kept constant. This has led to the development of two forms of the Langendorff heart, the constant pressure model and the constant flow model. Since the flow resistance can be described according to Hagen-Poiseuille's law by the equation:

$$R = 8\eta l/\pi r^4$$

where l=length, η=viscosity of the solution and r=radius of the tube. A change in the diameter of the vessel caused by vasoconstriction or dilation leads to a change in the radius of the vessel and thereby to a change in resistance which is proportional to l/r^4. Thus, if pressure is kept constant, the term $\Delta P(=\text{constant})/\Phi$ is proportional to l/r^4 in a constant pressure Langendorff model and perfusion flow is the variable which can be measured as an indicator of l/R or of r. On the other hand, if flow is kept constant the term $\Delta P/\Phi(=\text{constant})$ is proportional to l/r^4 and in that case the variable pressure has to be measured as an indicator of l/r or R.

Thus, the flow resistance is directly proportional to coronary perfusion pressure and inversely proportional to coronary flow. This way it can be easily determined with the use of either of these two parameters. The pressure of delivering the perfusion solution can be measured near to the aortic cannula with a transducer connected to the perfusion line by a side arm. The coronary flow can be measured by flowmeters connected to the line near to the aortic cannula.

2.1.3 Experimental procedure of studies 2-5

The day of the perfusion, the animals were anesthetised by an intraperitoneal injection of pentobarbital sodium (60mg/kg) and afterwards heparinised (1500 I.U./kg) via the saphenous vein. 30s later, a rapid thoracotomy was performed and the heart was immediately collected and immersed in cold perfusion solution (4^{o}C to limit any ischemic injury during the period between excision and restoration of vascular perfusion). The cannulation of the aorta and the re-establishment of the vascular perfusion lasted less than one minute in order to avoid any ischemic injury or preconditioning. After the canulation of the aorta, the heart was perfused according to the Langendorff mode (Fig. 17) with Krebs-Heinselett buffer. For the studies 2-5 this buffer containing in (mM) NaCl 119, $MgSO_4$ 1.2, KCl 4.8, $NaHCO_3$ 25, KH_2PO_4 1.2, $CaCl_2$ 1.2 and glucose 11, as sole energy substrate. The buffer was maintained at 37^{o}C and continuously oxygenated with carbogen (95% O_2/5% CO_2). CO_2 allowed the maintaining of the pH at a value of 7.4 with bicarbonates included in the medium.

The heart was first perfused at constant pressure of 59 mmHg for 30 minutes with a pressure gauge inserted into the perfusion circuit just upstream the aortic cannula. A latex balloon connected to a pressure probe was inserted into the left ventricle and filled until the diastolic pressure reached a value of 7–8 mmHg. The signals, obtained through the use of an amplifier connected to a computer, allowed the evaluation of the systolic, diastolic and left ventricle developed pressures as well as the heart rate throughout the perfusion protocol. The coronary flow for each heart was estimated by weight determination of 1-min collected samples at the 25th min of perfusion.

After the 30-min perfusion at constant pressure, the heart was perfused with a peristaltic pump (Gilson, Villiers-Le-Bel, France) at the coronary flow previously determined during the perfusion at constant pressure. The systolic, diastolic and left ventricle developed pressures as well as the heart rates were determined after 10 min of perfusion at forced flow in order to allow the heart a satisfying stabilization. The left ventricle developed pressure was calculated by subtracting the diastolic pressure to the systolic pressure. The rate pressure product (RPP) was defined as the product between the left ventricle developed pressure and heart rate. The perfusion flow equaled the coronary flow in this model of aortic perfusion. In our model of Langendorff perfusion at forced flow, the aortic pressure reflected the coronary pressure and changes in the coronary tone triggered variations of the aortic pressure. All the parameters were recorded and analysed using the HSE IsoHeart software (Hugo Sachs Elektronik).

2.1.4 Measurement of the coronary reactivity

The hearts were perfused at a coronary pressure of about 60-70 mmHg for 20 min. Just before the end of this period, parameters of the cardiac function were monitored and samples of the coronary effluents were collected for determination of lactate and pyruvate concentrations. Thereafter, a solution containing a potent constricting agent (U46619, thromboxane analogue) was continuously infused into the perfusion system near the aortic canula at a rate never exceeding 1.5% of the coronary flow. This allowed the obtainment of a coronary pressure of 110-130 mmHg. At this high coronary pressure, the effect of the different dilatation agents was maximal. After 15-20 minutes of U46619 infusion, injection of the vasodilator agents was performed:

- *acetylcholine (Ach)* was used to estimate the Endothelium Dependent Dilatation (EDD). The action of Ach on the endothelium is mainly mediated through muscarinic receptors, which are members of a G-protein coupled receptor family. This leads to increase in the intracellular Ca^{2+} and to eventual activation of endothelial nitric oxide synthase (NOS), cyclooxygenase (COX), the putative endothelium-dependent hyperpolarization factor(s) EDHF synthase and the synthesis of nitric oxide (NO), prostacyclin (PGI2) and EDHF respectively. NO and PGI2 mediate relaxation of vascular smooth muscle cells (VSMC) via cyclic GMP and AMP-dependent mechanisms respectively and EDHF via, directly or indirectly, opening of a VSMC K^+ channel(s). This results in the dilatation of the vessels. Ach was injected in doses of 4, 10, 20, 40, 60, 80, 100 picomoles (pm)**,** which allowed functional estimation of the two tunica (intima and media) implied in the vascular vasomotricity;
- *sodium nitroprusside (SNP),* in doses of 100 pm, 200 pm, 400 pm, 600 pm, 800 pm, 1000 pm, was used to estimate the Endothelium Independent Dilatation (EID). SNP in aqueous solution spontaneously generates NO that directly acts on the smooth muscle cells resulting in their relaxation through a cGMP-dependent mechanism. This allowed the evaluation of smooth muscle cell function.

The injections of Ach and SNP triggered a decrease in the coronary pressure, simultaneously reflecting reduction of the coronary tone and dilatation (Fig. 18). The dilatation amplitude was calculated as the ratio between the maximal decrease in coronary pressure and the coronary pressure just before the injection of the dilatation agents.

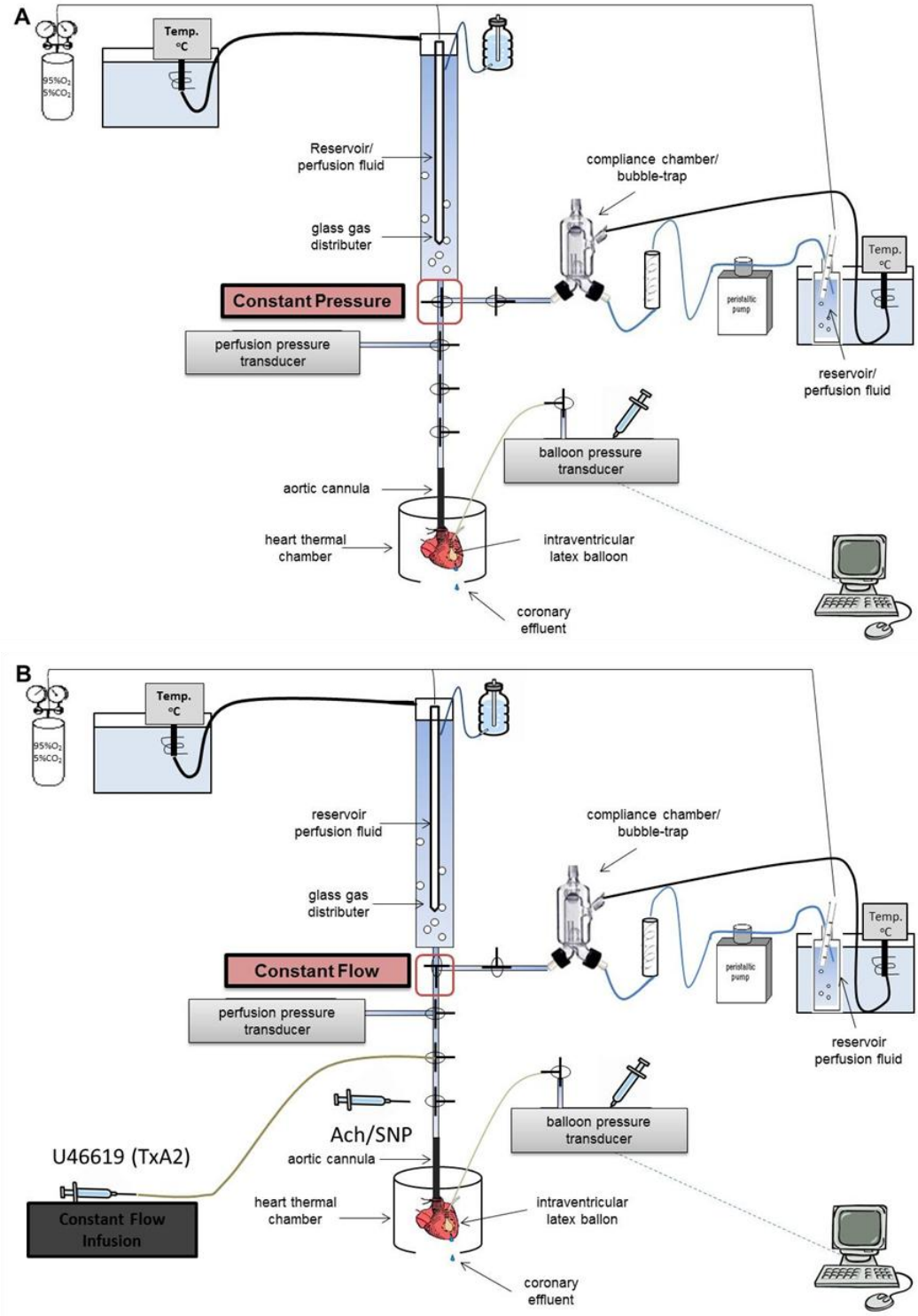

Figure 18. *Experimental apparatus for isolated heart perfusion according to a modified Langendorff technique. The apparatus combines the two possible types of Langendorff heart perfsusion; the constant pressure and constant flow perfusion. Firstly, the position of the switch allows the perfusion of the heart at constant pressure (Panel **A**) where the coronary flow of each heart is determined. Then, the switch changes (Panel **B**) allowing the perfusion of the heart at constant flow rate as previously determined during the constant pressure perfusion. Then, a vasoconstricting agent (U46619) is constantly infused in order to raise the perfusion pressure around 130 mmHg. Finally, injections of acetylcholine (Ach) and sodium nitroprusside (SNP) are performed to evaluate the resistance of the coronary vasculature.*

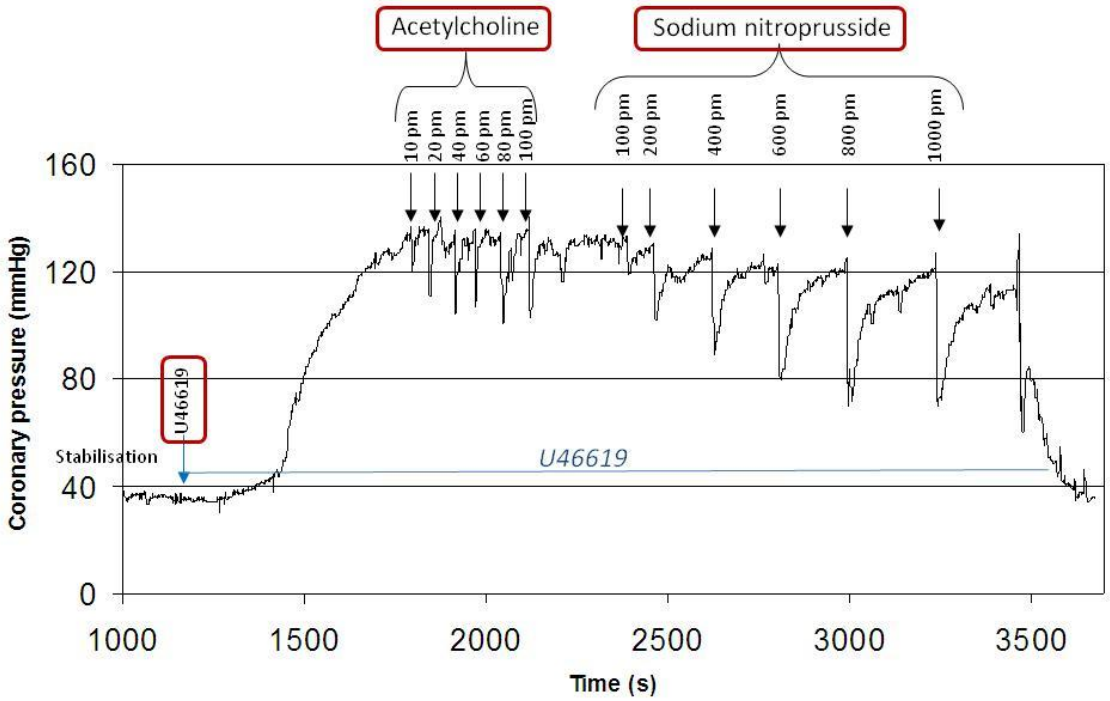

Figure 19. *Evolution of the coronary pressure during the perfusion. →: sudden injections of Ach or SNP. Each injection triggers a reduction in the coronary pressure reflecting a decrease in the flow resistance and thus the vasodilatation*

Since the heart weight and coronary volume varied between subgroups, a correction was performed to normalise the amount of vasodilatation agent visualised by the endothelial cells. The best estimation of the vascular volume was considered to be the coronary flow and hence the amounts of vasodilatation agent were divided by this parameter. The corresponding vasodilatation was thus plotted against corrected amounts of Ach or SNP which were specific to each animal. This prevented statistical calculations. In order to make statistical comparisons between subgroups, the dose-effect curve was fitted to a theoretical curve for each heart (% vasodilatation = α x ln *(corrected vasodilatation agent amount)* + b), where α and b represent the coefficients of the theoretical curve. The regression coefficients (R^2 value) of the theoretical curves of acetylcholine (Ach)- and sodium nitroprusside (SNP)-induced were close to 1, indicating a good linearity between the % vasodilatation and the natural logarithm of the amount of vasodilatation agent. Thereafter, the expected % vasodilatation were recalculated at fixed amounts of vasodilatation agents (4, 10, 20, 40, 60, 80, 100 pm for Ach and 100, 200, 400, 600, 800, 1000 pm for SNP). Since the amounts of vasodilatation agents

became the same in each animal subgroup, this allowed the fulfillment of classical analysis of variance.

In addition to these calculations, the amount of sodium nitroprusside necessary to obtain the observed Ach-induced vasodilatation was also estimated from the corrected EDD and EID curves. For each heart and each injected Ach dose, the amount of sodium nitroprusside (reflecting the amount of all vasodilatation agents) necessary to obtain the same % vasodilatation was extracted from the EID curve according to the formula:

$$\text{endothelial cell vasodilatation activity (ECVA)} = e^{[(\%\ \text{Ach-induced dilatation} - b) / a]}$$

where α and b are the coefficients of the theoretical EID curves. The results were expressed in nitroprusside equivalents.

2.2 Mitochondrial function in isolated organelles

2.2.1 Mitochondrial respiration

The consumption of oxygen by the mitochondria is measured in an oxygraph (Hansatech Instrument) that consists from a closed thermostated and agitated chamber equipped with a Clarke electrode [271]. The signals produced by the electrode are collected to the connected computer and with specific software (Oxygraph Plus Software, Hansatech) are translated into nmol of O_2/ml.

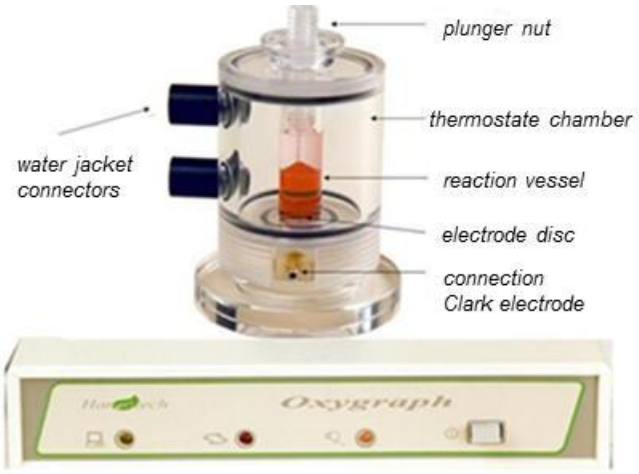

Figure 20. *Oxygraph chamber (Hansatech Instruments)*

The rate of mitochondrial oxygen consumption was measured at 30°C in an incubation chamber with a Clarke-type O_2 electrode filled with 1 ml of incubation medium (KCl 125 mM, Tris–Base 20 mM, EDTA 5 μM, pH 7.2, fatty acid-free bovine serum albumin 0.15%, KH_2PO_4 3 mM, $CaCl_2$ 10 μM). All measurements were performed using mitochondria (0.2 mg mitochondrial protein/ml) incubated with one of the following substrates (at final concentrations):

- glutamate (5.5 mM)/malate (2.5 mM). This substrate combination activates dehydrogenases with reduction of NADH, then feeding electrons into CI and down the thermodynamic cascade through the Q-cycle and CIII of the electron transport system to CIV and O_2;
- succinate (5.5 mM) + rotenone (2.5 μM). These conditions allow the estimation of the respiration rate from CII;
- glutamate (5.5 mM)/malate (2.5 mM)/succinate (5.5 mM). the utilization of these substrates together permits the activation of both CI and CII of the ETC;

- palmitoyl-carnitine (0.05 mM)/ malate (2.5 mM). This substrate is a long-chain fatty acid that can feed the ETC at the levels of CI, CII and ETF.

The rate of oxygen consumption under these conditions is defined as the **state 2** of the respiration rate.

The addition of ADP (1mM) allows the estimation of the **state 3** of the respiration rate. State 3 respiration is the ADP stimulated respiration of isolated coupled mitochondria in the presence of high ADP and Pi concentrations, supported by a defined substrate or substrate combination at saturating oxygen levels [272].

The addition of oligomycin (0.5 µg/ml) permitted the estimation of **state 4** of respiration rate. This state is representative of the "proton leak" of the respiration since oligomycin, which is an inhibitor of ATP synthase, prevents the re-enry of the protons in the matrix.

Coupling of the mitochondrial oxidative phosphorylation was evaluated by the values of the respiratory control ratio (**RCR**), which was calculated by the state 3/state 4 ratio.

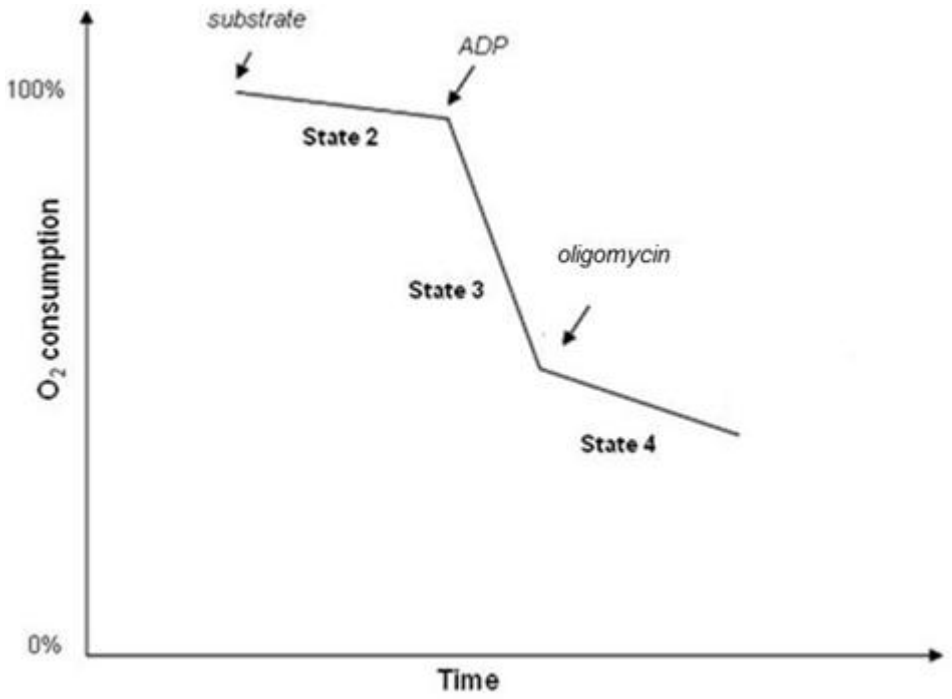

Figure 21. *Schematic diagram of the states of the respiratory rate when substrates and inhibitors are added.*

2.2.2 Fluorimetric study of mitochondrial H_2O_2 release

The mitochondrial ETC-derived ROS production was estimated by the measurement of H_2O_2 production. The Amplex Red (10-acetyl-3,7-dihydroxyphenoxazine) reagent was used to detect H_2O_2 levels. In the presence of horseradish peroxidase (HRP), Amplex Red reacts with H_2O_2 in 1:1 stoichiometry to produce the red fluorescent oxidation product, resorufin ($\lambda_{excitation}$ = 560 nm and $\lambda_{emission}$ = 584 nm). The measured fluorescence is directly proportional to the production of H_2O_2.

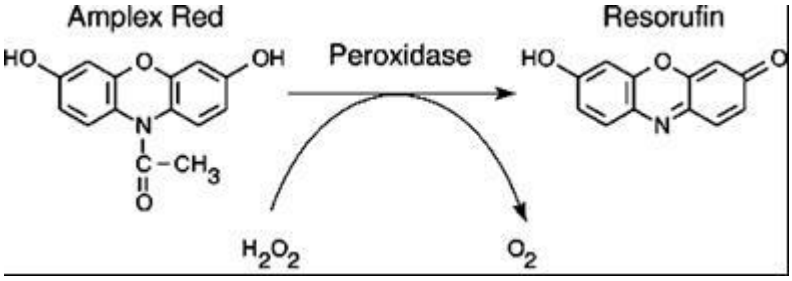

Figure 22.*Oxidation of Amplex Red by H_2O_2*

The rate of mitochondrial H_2O_2 production was measured at 30°C with a thermostated spectrofluorimeter (Hitachi) connected to a computer permitting the data analysis by following kinetically the rate of H_2O_2 production by isolated mitochondria. Reaction conditions were 0.25 mg of mitochondrial protein/ml, 5 U/ml of horseradish peroxidase, 1 μM of amplex red, with:

- glutamate (5.5 mM)/malate (2.5 mM);
- succinate (5.5 mM) (without rotenone);
- glutamate (5.5 mM)/malate (2.5 mM)/succinate (5.5 mM);
- palmitoyl-carnitine (0.05 mM)/ malate (2.5 mM).

They were added in order to start the reaction in the same incubation buffer with that used for measurements of mitochondrial oxygen consumption. Mitochondrial ROS was measured in the absence of ADP (state 2 respiration rate) to measure the basal H_2O_2 production. The CI inhibitor rotenone (1 μM) and the CIII inhibitor antimycin A (0.5 μM) were sequentially added to determine, respectively, the maximum rate of H_2O_2 production of complexes I and III of the respiratory chain. The addition of rotenone inhibits CI by binding to its ubiquinone site; thus, electrons escape and produce $O_2^{\cdot-}$. Rotenone disrupts this way the electron transfer between the terminal Fe-S cluster of CI and ubiquinone [162]. This results to the slowdown of the use of NADH (hydrogen donor) and of the coenzyme Q (hydrogen receptor) by CI. The

slowdown of the coenzyme Q reduction deprives CIII from its coenzyme hydrogen donor, which leads to inhibition of the reduction of the ferric cytochrome c to ferrous cytochrome c. This lack of reduced cytochrome c deprives cytochrome oxidase from its coenzyme donor of electrons and consequently the enzyme uses less oxygen resulting eventually to the slowdown of the respiration. The oxidation reduction at the levels of CI, II and IV are thus disturbed as well as the proton transfer from the matrix to the intermembrane space. Antimycin A inhibits CIII at the level of its Qi ('in') center. It binds to this sit and inhibits the transfer of electrons in Complex III from heme b_H to oxidized Q. This way antimycin A slows down the use of the ubiquinol (QH2), donor of hydrogen, and of the ferric cytochrome c, electron receptor. This slowdown of the coenzyme Q reoxidation deprives CI and II from their coenzyme hydrogen receptor, which leads to inhibition of the activities of these two enzymes activities and of the use of NADH and succinate. In the presence of this inhibitor, cytochrome c oxidase is deprived of reduced cytochrome c and thus uses less oxygen. This way the ETC expels less protons, the membrane potential collapses resulting eventually to diminished phosphorylation of ADP to ATP.

The H_2O_2 production was expressed in pmoles of H_2O_2/mg proteins according to the change in fluorescence caused by the addition to the reaction medium containing the mitochondria of a known amount of H_2O_2 equivalent to 450 pmoles (measured by spectrometry ($\lambda_{absorption}$ H_2O_2 = 240 nm)) obtained by dilution of a stock solution of 30%.

Figure 23. *Schematic diagram of the fluorimetric measurement of mitochondrial ETC-derived ROS production when substrates and inhibitors are added*

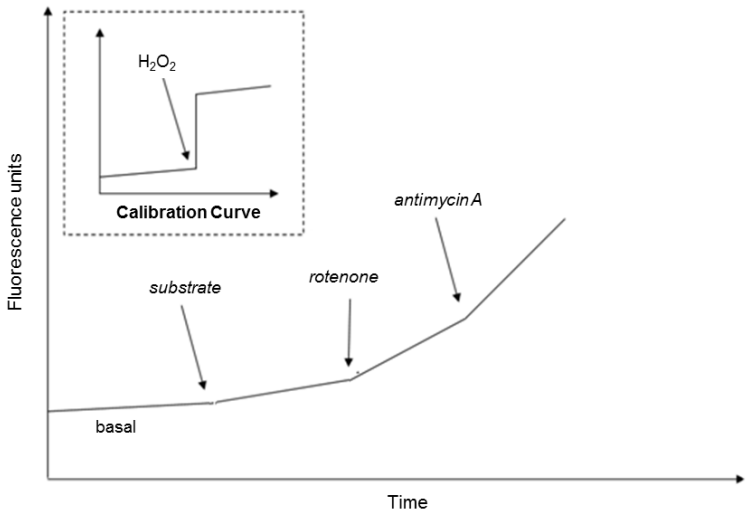

The fluorimetric measurement of the mitochondrial H_2O_2 release varies according to the substrate used (Fig. 24).

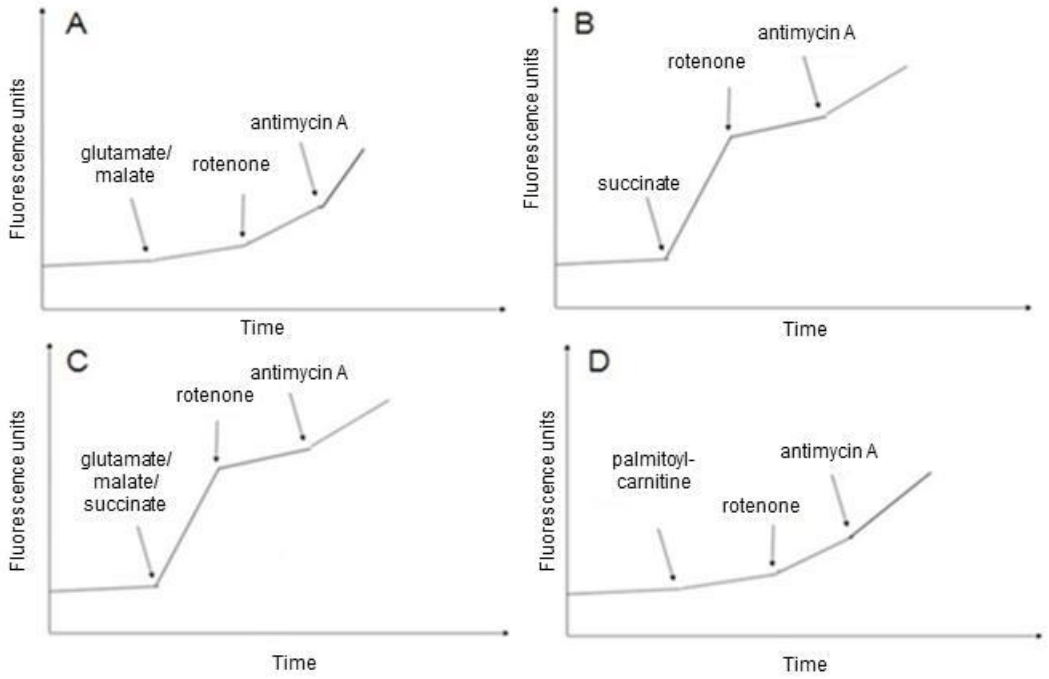

Figure 24. *Schematic representation of the fluorimetric measurement of ROS production in the presence of* ***A****: glutamate/malate;* ***B:*** *succinate;* ***C****: glutamate/malate/succinate and* ***D****: palmitoylcarnitine. When glutamate/malate (panel A) is used as a substrate, dehydrogenses are activated resulting to reduction of NADH that feed electrons into CI and down the thermodynamic cascade through Q-cycle and CIII of the electron transport system to CIV and O_2. The addition of rotenone slowdowns the transfer of electrons from CI and most of them leak at the level of CI producing ROS. Thus, the addition of rotenone indicates the maximum ROS production at the level of CI. The further addition of antimycin indicates the maximum production of ROS of CI+CIII; thus an estimation of ROS production at CIII can be done. The FAD-linked substrate succinate supports the highest rate of H_2O_2 production in the absence of respiratory inhibitors (panel B) that is mediated by the reverse electron flow at CI. When rotenone is added, the reverse electron flow is inhibited resulting to the slower rate of fluorescence increase reflecting the H_2O_2 production. When glutamate/malate plus succinate are used as substrates, electrons are carried to both CI and CII of the ETC giving a more global estimation of the function of the ETC. The substrate palmitoylcarnitine, a long-chain fatty acid, gives NADH and $FADH_2$ produced by both fatty acid β-oxidation and the TCA cycle, which are used by the electron transport chain at the levels of CI, CII and ETF to produce ATP. When it is used as a substrate, a global estimation of the ETC is given.*

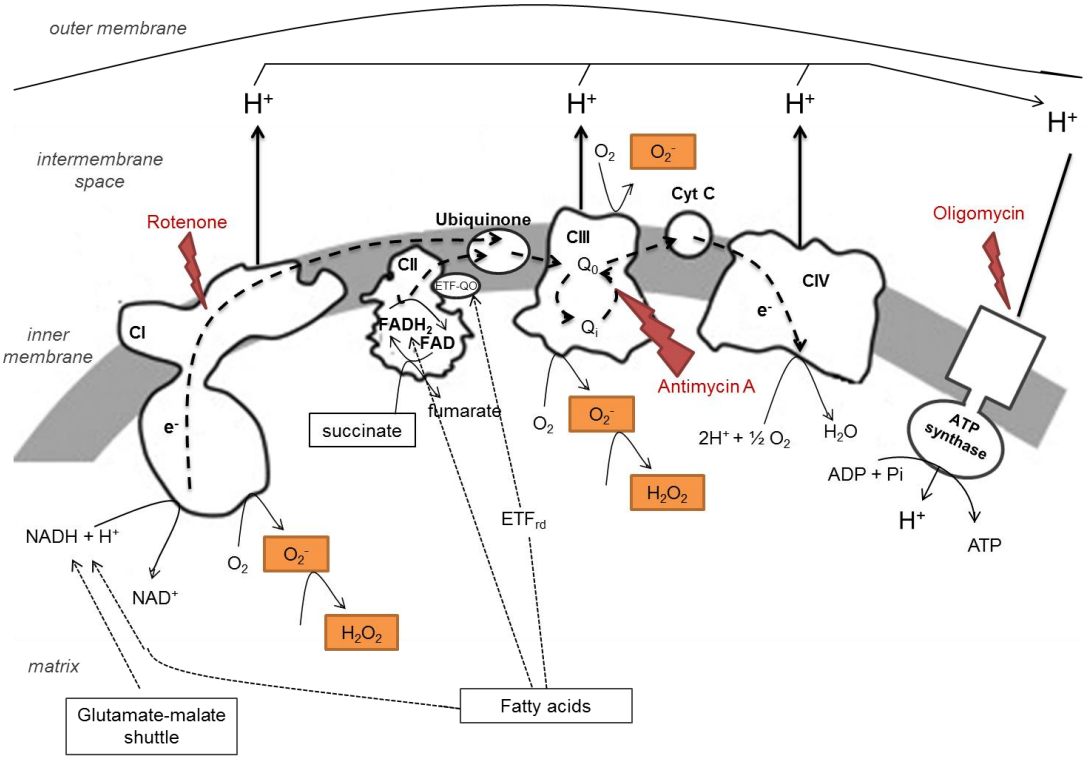

Figure 25. *The mitochondrial electron transport chain (ETC) and ATP synthase. Substrates such as glutamate associated with malate, succinate or fatty acids provide electrons to the respiratoy chain et the levels of CI, CII or ETF. Electrons pass via the ubiquinone to CIV where they are used for H_2O production. The proton gradient that is created during this process is used for generation of ATP by the ATP synthase. CI and CIII are sites of electron escape leading to O_2^- formation. Inhibitors such as rotenone or antimycin A can disrupt the electron transfert via the ETC at CI and CIII respectively. Oligomycin is also an inhibitor of mitochondrial respiration acting at the level of ATP synthase.*

3. Experimental Studies

3.1 ARTICLE I

"Middle age aggravates myocardial ischemia through surprising upholding of complex II activity, oxidative stress, and reduced coronary perfusion"

This work is published in the journal "AGE".

AGE
DOI 10.1007/s11357-010-9186-0

Middle age aggravates myocardial ischemia through surprising upholding of complex II activity, oxidative stress, and reduced coronary perfusion

Evangelia Mourmoura · Marie Leguen · Hervé Dubouchaud · Karine Couturier · Damien Vitiello · Jean-Luc Lafond · Melanie Richardson · Xavier Leverve · Luc Demaison

Received: 20 May 2010 / Accepted: 14 September 2010

Abstract Aging compromises restoration of the cardiac mechanical function during reperfusion. We hypothesized that this was due to an ampler release of mitochondrial reactive oxygen species (ROS). This study aimed at characterising ex vivo the mitochondrial ROS release during reperfusion in isolated perfused hearts of middle-aged rats. Causes and consequences on myocardial function of the observed changes were then evaluated. The hearts of rats aged 10- or 52-week old were subjected to global ischemia followed by reperfusion. Mechanical function was monitored throughout the entire procedure. Activities of the respiratory chain complexes and the ratio of aconitase to fumarase activities were determined before ischemia and at the end of reperfusion. H_2O_2 release was also evaluated in isolated mitochondria. During ischemia, middle-aged hearts displayed a delayed contracture, suggesting a maintained ATP production but also an increased metabolic proton production. Restoration of the mechanical function during reperfusion was however reduced in the middle-aged hearts, due to lower recovery of the coronary flow associated with higher mitochondrial oxidative stress indicated by the aconitase to fumarase ratio in the cardiac tissues. Surprisingly, activity of the respiratory chain complex II was better maintained in the hearts of middle-aged animals, probably because of an enhanced preservation of its membrane lipid environment. This can explain the higher mitochondrial oxidative stress observed in these conditions, since cardiac mitochondria produce much more H_2O_2 when they oxidize $FADH_2$-linked substrates than when they use NADH-linked substrates. In conclusion, the lower restoration of the cardiac mechanical activity during reperfusion in the middle-aged hearts was due to an impaired recovery of the coronary flow and an insufficient oxygen supply. The deterioration

E. Mourmoura · M. Leguen · H. Dubouchaud · K. Couturier · D. Vitiello · X. Leverve · L. Demaison (✉)
Laboratoire de Bioénergétique Fondamentale et Appliquée, INSERM U884, Université Joseph Fourier, BP 53, Grenoble Cedex 09 38041, France
e-mail: luc.demaison@ujf-grenoble.fr

E. Mourmoura · M. Leguen · H. Dubouchaud · K. Couturier · D. Vitiello · X. Leverve · L. Demaison
Université Joseph Fourier, Laboratoire de Bioénergétique Fondamentale et Appliquée, Grenoble Cedex 09 38041, France

J.-L. Lafond
Département de Biologie Intégrée, CHU de Grenoble, Grenoble Cedex 09 38043, France

M. Richardson
Department of Population Health Sciences, School of Medicine and Public Health, University of Wisconsin, Madison, WI 53705, USA

L. Demaison
INRA, Unité CSGA, Dijon Cedex 21065, France

Published online: 29 September 2010

of the coronary perfusion was explained by an increased mitochondrial ROS release related to the preservation of complex II activity during reperfusion.

Keywords Myocardial aging · Ischemia · Oxidative stress · Respiratory chain complexes

Introduction

Amongst subjects admitted in care units for an acute myocardial infarction, in-hospital and long-term mortalities are significantly higher in patients over 65 years old when invasive strategies are not endeavored (Polewczyk et al. 2008). This is probably related to the observed increased incidence of diabetes, hypertension, and heart failure in this population and to the associated activation of the adrenergic drive (Hu et al. 2008). From data presented in the literature, the aged heart has a diminished functional and adaptive reserve capacity, an increased susceptibility to incur damage and a limited practical ability for repair/regeneration (Juhaszova et al. 2005). The reduced tolerance to ischemic insult with aging is also noticed in the laboratory animal with a reduced recovery of the coronary flow and contractility during reperfusion occurring in mice (Azhar et al. 1999; Willems et al. 2003; Willems et al. 2005) and rats (Leichtweis et al. 2001; Xia et al. 2003) as soon as they reach middle age.

Oxidative stress seems to play a central role in the age-associated vulnerability to ischemia/reperfusion. Indeed, administration of superoxide dismutase and catalase during the pathology affords protection to the senescent heart by preventing vasoconstriction and protein oxidation (Besse et al. 2006). Although some authors emphasize the involvement of the vascular NADPH oxidase in this pathology (Oudot et al. 2006), others point out the prominent responsibility of the mitochondrial reactive oxygen species (ROS) (Lesfnefsky and Hoppel 2003) through the well-known ROS-induced release process (Zorov et al. 2006). Due to cardiolipin oxidation by ROS attack, interfibrillar mitochondria of the senescent heart display lower oxidative capacities and increased ROS release (Fannin et al. 1999; Lesnefsky et al. 2001a; Hoppel et al. 2002). Ischemia further amplifies these abnormalities (Lesnefsky et al. 2001b; Lesnefsky and Hoppel 2008; Lesnefsky et al. 2009), but only in the aged myocardium.

The augmented vulnerability to calcium of senescent cardiomyocytes (Tsukube et al. 1996; Hansford et al. 1999; Lakatta et al. 2001; Jahangir et al. 2001) might be responsible for the amplified oxidative stress during ischemia/reperfusion. Indeed, rising levels of matrix calcium favors mitochondrial ROS release (Martin et al. 2007) through a mechanism that can imply succinate accumulation (Sentex et al. 1999). Succinate-ubiquinone reductase (complex II) re-oxidizes succinate, which can support important ROS production at the level of complex I via reverse electron flux (Capel et al. 2005; Lacraz et al. 2008). This mechanism is probably responsible for the huge ROS production that transitorily occurs at early reperfusion in the adult heart (Demaison et al. 2001), which is most likely amplified in the aging heart. Indeed, in ischemia/reperfusion, old hearts have more oxidized proteins than young hearts (Nagy et al. 1996).

Ischemia/reperfusion-induced oxidative stress has a noticeable influence on NADH-ubiquinone reductase (complex I) activity, since it transitorily diminishes it (Paradies et al. 2004). Complex II activity is also robustly reduced by reperfusion-induced oxidative stress (Pasdois et al. 2006; Chen et al. 2008) via deglutathionylation of its 70-kDa flavin protein and tyrosine nitration by peroxynitrite (Chen et al. 2007, 2008). The significance of the decrease in activities of the complexes I and II at resumption of the coronary flow is not known, but these complexes could be used as fuses to prevent perpetuation of the huge ROS release occurring during this period. Nevertheless, the early and important ROS release at the beginning of reperfusion could be responsible for the oxidative modifications of numerous proteins and the alterations of their functioning. It could explain several abnormalities of the senescent reperfused heart including impaired oxidative capacities and cardiac metabolic efficiency through changes in respiratory complex activities, but also the low restoration of the coronary flow via reduction of the NO bioavailability and/or endothelin-1 over-activity through oxidation of its receptors (Amrani et al. 1996; Goodwin et al. 1999; Besse et al. 2001; Nakamura et al. 2003).

This study was aimed at determining whether the impaired contractile recovery observed in the post-ischemic aged heart is related to an augmented mitochondrial ROS release at resumption of the coronary flow and at evaluating the causes and consequences of this phenomenon. The hearts of

young adults (10 weeks) and middle-aged (52 weeks) animals were thus perfused and subjected to ischemia followed by reperfusion. To estimate the ex vivo mitochondrial ROS release during reperfusion, we evaluated the aconitase to fumarase ratios before ischemia and at the end of the reperfusion and we contrasted these values to the rate of H_2O_2 released by mitochondria isolated from the pre-ischemic myocardium. The causes and consequences of the observed changes were determined by measuring the activities of several respiratory complexes known to be reduced through ischemia/reperfusion-induced oxidative stress and by examining scrupulously several parameters of cardiac functioning including mechanical activity, oxidative capacities, metabolic efficiency, and coronary perfusion.

Materials and methods

Animals and treatments

The experiments followed the European recommendation guidelines for the use of laboratory animals and were approved by the local ethics review board (authorization number, 380537). Thirty-six male Wistar rats from an inbred colony were housed in individual cages in an animal facility with controlled temperature, dark/light cycle, and hygrometry. They were fed standard commercial pellets (A04, Safe, Gannat, France) ad libitum with free access to water. Animals were randomly divided into two groups according to their age. The young adult group was composed by 10-week-old rats while the middle-aged group by 52-week-old rats.

Isolated heart perfusion

The animals were anesthetized with sodium pentobarbital (50 mg/kg) and heparinized (1,000 I.U./kg) through the saphenous vein. After rapid excision of the heart, the aorta was cannulated in Langendorff mode of non-recirculating coronary perfusion at constant pressure (60 mmHg) at 37°C. Modified Krebs–Henseleit perfusion buffer contained (in mM): NaCl (119), $MgSO_4$ (1.2), $NaHCO_3$ (25), KCl (4.8), $CaCl_2$ (2.5), and glucose (11) as sole energy source and was equilibrated with 95% O_2–5% CO_2. A latex balloon linked to a pressure probe was inserted into the left ventricle cavity to determine diastolic and systolic pressures. Baseline diastolic pressure was set at approximately 10 mmHg. The coronary flow was estimated by weight determination of 30-s collected samples of effluent. The pulmonary artery was cannulated for a direct coronary sinus sampling of the coronary effluent. Arterial and venous oxygen contents were measured by anaerobic collection of effluent in hermetically closed capillary tubing. The samples were then kept in ice until determination of oxygen concentration with a blood gas analyser (Radiometer™ABL 700, Brønshøj, Danemark). Developed pressure was calculated as the difference between the systolic and diastolic pressures. The rate×pressure product (RPP) was the product between the heart rate and developed pressure. Oxygen consumption was calculated as the product of the arterio-venous oxygen content difference and the coronary flow. Since the blood gas analyser gave results of the oxygen concentration in kPa, the arterio-venous oxygen content difference was calculated assuming that 1 kPa=10 nmoles of oxygen$\times ml^{-1}$ (Gnaiger 2001). Cardiac metabolic efficiency was estimated as the total RPP (expressed in mHg/min) to total oxygen consumption ratio (expressed in µmoles/min) of each heart and was expressed in mHg/µmole.

Ischemia-reperfusion protocol and sampling

In a first set of experiments, isolated hearts issued from ten young adult and ten middle-aged rats were perfused for 30 min to establish stabilized baseline performances before inducing total global normothermic ischemia for 25 min and reperfusion for 45 min. During ischemia, rigorous conditions of temperature verification were applied by bathing the heart in Krebs–Heinseleit buffer maintained at 37°C. At the end of the reperfusion period, the hearts were freeze-clamped in liquid nitrogen and stored at −80°C until determination of cardiac dry weight, aconitase to fumarase ratio, and respiratory chain complex activities.

In a second set of experiments, hearts from young adult and middle-aged rats (eight per group) were perfused in baseline conditions for 30 min. At the end of the perfusion protocol, a piece of myocardium (about 200 mg) from the apex of the heart was immediately freeze-clamped and stored at −80°C in order to measure respiratory chain complex activities and aconitase to fumarase ratio. The other part of the

myocardium was immediately used for isolated mitochondria preparation.

Mitochondria preparation

After the perfusion, atria and the remaining aorta were cut off from the heart. Myocardium was minced with scissors in a cold isolation buffer composed of (in mM) sucrose (150), KCl (75), Tris–HCl (50), KH_2PO_4 (1), $MgCl_2$ (5), and EGTA (1), pH 7.4, fatty acid-free serum albumin 0.2%. The pieces of myocardium were rinsed several times on a filter and put in an Elvehjem potter containing 15 ml of isolation buffer. A protease (subtilisin 0.02%) was added for 1 min to digest myofibrils at ice temperature, and the totality was then homogenized with the potter (300 rpm, 3 to 4 transitions). Subtilisin action was stopped by addition of the isolation buffer (30 ml). The homogenate was then centrifuged (800 g, 10 min, 4°C), and the resulting supernatant was collected and filtered. Mitochondria were then washed through two series of centrifugation (8,000×*g*, 10 min, 4°C). The last pellet of mitochondria was re-suspended in sucrose 250 mM, Tris–HCl 10 mM, EGTA 1 mM, pH 7.4 at a concentration of approximately 20 mg/ml.

Respiration measurements

The rate of mitochondrial oxygen consumption was measured at 30°C in an incubation chamber with a Clarke-type O_2 electrode filled with 1 ml of incubation medium (KCl 125 mM, Tris–HCl 20 mM, KH_2PO_4 10 mM, EGTA 1 mM, pH 7.2, fatty acid-free bovine serum albumin 0.15%). All measurements were performed using mitochondria (0.25 mg mitochondrial protein/ml) incubated either with glutamate (5 mM)/malate (2.5 mM) or/and succinate (5 mM) as substrates, in the presence (state 3) and in the absence (state 4) of ADP 100 mM. The incubation medium was constantly stirred with a built-in electromagnetic stirrer and bar flea. Coupling of the mitochondrial oxidative phosphorylation was assessed by the state 3/state 4 ratio which measures the degree of control imposed on oxidation by phosphorylation (respiratory control ratio (RCR)).

Mitochondrial reactive oxygen species release

The rate of mitochondrial H_2O_2 production was measured at 30°C which followed linear increase in fluorescence (excitation at 560 nm and emission at 584 nm) due to enzymatic oxidation of amplex red by H_2O_2 in presence of horseradish peroxidase, modified to kinetically follow the rate of production of H_2O_2 by isolated mitochondria on a SFM25 computer-controlled Kontron fluorometer. Reaction conditions were 0.25 mg of mitochondrial protein/ml, 5 U/ml of horseradish peroxidase, 1 μM of amplex red, with glutamate/malate or/and succinate (in the same concentrations as in respiration measurements). They were added in order to start the reaction in the same incubation buffer with that used for measurements of mitochondrial oxygen consumption. Mitochondrial ROS was measured in the absence of ADP (state 2 respiration rate). Rotenone (1 μM) and antimycin A (0.5 μM) were sequentially added to determine, respectively, the maximum rate of H_2O_2 production of complexes I and I+III of the respiratory chain.

Measurement of respiratory chain complex activities

Activities of the NADH-ubiquinone oxydo-reductase (complex I), succinate-ubiquinone oxydo-reductase (complex II), ubiquinol cytochrome *c* reductase (complex III), cytochrome *c* oxidase (complex IV), NADH cytochrome *c* reductase (activity of complex I+III) and succinate cytochrome *c* reductase (activity of complex II+III) were determined as commonly performed in this laboratory. Heart samples (100 mg) were homogenized at 4°C with 0.9 ml of a potassium phosphate buffer 100 mM, pH 7.4. The homogenates were centrifuged (1,500×*g*, 5 min, 4°C), and the resulting supernatants were stored at −80°C until determination of the various enzymatic activities.

Complex I activity was determined spectrophotometrically by measuring the disappearance of NADH at 340 nm in the presence of decylubiquinone (Kramer et al. 2005). The reaction medium was a potassium phosphate buffer 47.5 mM, pH 7.4 containing bovine serum-albumin (3.75 mg/ml), NADH (0.1 mM) and decylubiquinone (0.1 mM). The reaction was initiated by adding the 200-times diluted sample and the change in absorbance at 37°C was measured for 2 min with and without rotenone (10 μM) in order to evaluate the specific and non-specific activities.

Complex II activity was also evaluated spectrophotometrically in the presence of succinate by measuring the reduction of dichloro-inophenol

(DCIP) (Miro et al. 1999). In this reaction, succinate oxidation by complex II reduces decylubiquinone which spontaneously transfers its electrons to DCIP. The 200-times diluted sample with the reaction medium (potassium phosphate buffer 45.4 mM, pH 7.4, bovine serum-albumin 2.5 mg/ml, antimycin A 9.3 μM, rotenone 5 μM, DCIP 100 μM and succinate 30 mM) were stirred at 37°C for 10 min, and the reaction was initiated by addition of decylubiquinone (50 μM). The change in absorbance was then measured at 600 nM for 5 min.

Complex III activity was determined by measuring the reduction of cytochrome *c* when decylubiquinol was used as substrate and complexes I and IV were blocked by specific inhibitors (Krähenbühl et al. 1994). The change in absorbance at 550 nm was first evaluated at 30°C for 1 min in the presence of potassium phosphate buffer 90.7 mM, pH 7.4, EDTA 50 μM, bovine serum-albumin (1 mg/ml), KCN 1 mM, oxidized cytochrome *c* (100 μM), decylubiquinol 0.11 mM and the 200 times diluted sample in order to evaluate total activity. The non-specific activity was then measured with antimycin A (5 μg/ml) for 2 min and complex III activity was then calculated by subtraction.

Complex IV assay was performed by determining the oxidation of reduced cytochrome *c* in a medium containing potassium phosphate buffer 50 mM, pH 7.4 and cytochrome *c* 1 mM reduced at 90% with sodium dithionite (Veitch and Hue 1994). The reaction was initiated by addition of the 200-times diluted sample and it was followed at 37°C and 550 nm for 2 min. The non-specific activity was then measured by addition of KCN 1 mM.

Complexes I+III and II+III activities were evaluated by using NADH (0.25 mM) and succinate (25 mM) as substrates and measuring the reduction of cytochrome *c* at 550 nm (Veitch and Hue 1994). The reaction was initiated in a medium containing potassium phosphate buffer 90 mM, pH 7.4, EDTA 0.5 mM, sodium azide 2 mM and oxidized cytochrome *c* 50 μM by addition of the 200-times diluted sample and it was maintained at 30°C for 5 min. In the case of the complex II+III activity determination, rotenone (1 μM) was added to avoid reverse electron flux through complex I. The non-specific activities was evaluated by using specific inhibitors of complexes I and II (rotenone 1 μM and thenoytrifluoroacetone 10 pM, respectively).

Other enzymatic assays

Activity of the citrate synthase was determined according to Faloona and Srere (1969). Aconitase and fumarase activities were determined according to Gardner et al. (1994), with the modification that the extraction medium was supplemented with tri-sodium citrate to stabilize aconitase activity ex vivo. In order to evaluate myocardial mitochondrial density, activity of the citrate synthase was divided by the protein amount of the homogenate. The activities of respiratory chain complexes were expressed in units per mg of proteins. Proteins were measured using the bicinchoninic acid method with a commercially available kit (Thermo Scientific, Rockford, IL).

Statistical analysis

The results are presented as mean±SEM. General data on animal morphology and baseline normoxic cardiac function were contrasted across the animal age by 1-way analysis of variance (ANOVA). Enzymatic measurements were analysed through a two-way ANOVA depicting the effects of aging, ischemia/reperfusion, and the cross-interaction between these two factors. Measurements made during ischemia-reperfusion (diastolic pressure, developed pressure, heart rate, RPP, oxygen consumption, metabolic efficiency) were treated with repeated-measures ANOVA to test the effect of animal age (external factor), perfusion time (internal factor), and their interaction. When required, group means were contrasted with a Fisher's LSD test. A probability (p) less than 0.05 was considered significant. Statistical analyses were performed using the NCSS 2007 software.

Results

General data

Animal size was estimated by measuring the length from insertion of the collarbones on the sternum to the outer sexual organ (Table 1). Middle-aged rats displayed a higher value (+10%) than that of their young adult counterparts. Interestingly, the relative thorax length was increased (+23%) in the older animals, due to a rise in thorax length (+32%) without

AGE

Table 1 General morphological data

	Young adults	Middle aged	ANOVA
Thorax length (cm)	4.4±0.1	5.8±0.1	$p<0.001$
Abdomen length (cm)	9.8±0.1	9.8±0.4	NS
Total length (cm)	14.2±0.1	15.6±0.4	$p<0.001$
Relative thorax length (%)	31±1	38±1	$p<0.001$
Relative abdomen length (%)	69±1	62±1	$p<0.001$
Animal weight (g)	323±5	444±33	$p<0.001$
Heart dry weight (mg)	204±6	262±8	$p<0.001$
Relative heart weight (mg/kg)	634±19	612±5	NS

Thorax length was measured from the insertion of the collarbones on the sternum to the apex of the sternum. Abdomen length was determined by measuring the distance from the apex of the sternum to the penis. Total length was the sum of the thorax and abdominal lengths. Relative heart weight was the ratio between heart dry weight and animal weight. The number of experiments was ten per group

ANOVA analysis of variance, *NS* not significant

any change in abdomen length. Animal and heart weights were augmented by aging (+37 and +28%, respectively), but the ratio between heart and body weight was unaffected.

Basal cardiac functioning

Under pre-ischemic conditions, the systolic pressure, left ventricle developed pressure, heart rate, and rate×pressure product were high and not affected by the animal age (Table 2). Since we aimed at evaluating the global heart functioning, but not the myocardial efficiency to produce its mechanical activity, these parameters were not divided by the cardiac dry weight. Coronary flow and oxygen consumption were similar in young adult and middle-aged rats. However, the cardiac metabolic efficiency was significantly decreased (−17%) by aging.

Cardiac functioning during ischemia

As soon as the coronary flow was stopped, the left ventricle developed pressure and rate×pressure product became null. The heart rate stopped soon after cessation of contraction and the diastolic pressure began to increase from the 5thmin of ischemia (Fig. 1), indicating the occurrence of a progressive contracture. The rise in diastolic pressure was less important in the middle-aged group from the 12th to the 19thmin of ischemia in comparison with the young group (−30, −43, −44, −42, −38, −31, −24, and −10% at the 12th, 13th, 14th, 15th 16th, 17th, 18th,

Table 2 Basal cardiac functioning

	Young adults	Middle aged	ANOVA
Syst P (mmHg)	139±5	155±8	NS
Diast P (mmHg)	12±1	13±1	NS
LVDP (mmHg)	127±5	142±8	NS
Heart rate (beats/min)	271±8	257±14	NS
RPP (mHg/min)	34.3±1.2	36.3±2.3	NS
Coro flow (ml/min/g)	51.8±3.6	53.1±4.6	NS
Ox cons (μmoles/min/g)	32.0±2.2	31.9±2.4	NS
Met. Eff. (mHg/μmole)	5.41±0.24	4.48±0.31	$p<0.05$

The number of experiments was ten per group.

Syst P systolic pressure, *Diast P* diastolic pressure, *LVDP* left ventricle developed pressure, *RPP* rate×pressure product, *Coro flow* coronary flow, *Ox cons* oxygen consumption, *Met. Eff.* metabolic efficiency, *ANOVA* analysis of variance, *NS* not significant

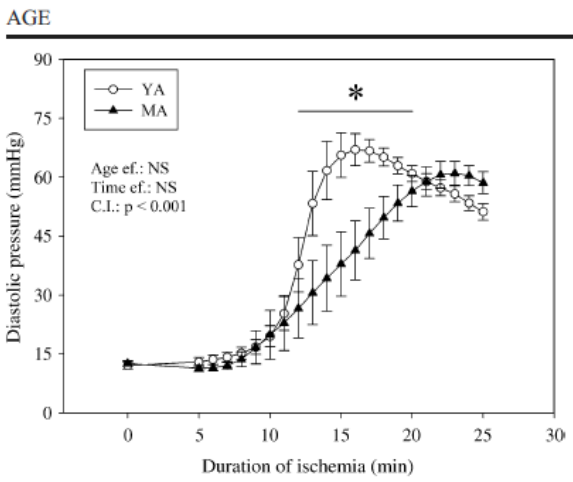

Fig. 1 Effects of aging on myocardial rigor tension evaluated by the diastolic pressure during ischemia. The number of experiments was ten per group. *YA* young adult rats, *MA* middle-aged rats, *Age ef.* effect of the age, *Time ef.* effect of the duration of ischemia, *C. I.* cross-interaction, *asterisk* significantly different

and 19thmin of ischemia, respectively). Thereafter, the diastolic pressure of the middle-aged animals equalized that of their young counterparts until the end of ischemia.

Cardiac mechanical function during reperfusion

As soon as resumption of the coronary flow, the diastolic pressure increased from approximately 54±2 mmHg at the end of ischemia to 104±3 mmHg at the 5thmin of reperfusion (Fig. 2). Thereafter, the diastolic pressure progressively decreased to a value close to 78±3 mmHg at the 45thmin of reperfusion. During the whole reperfusion, values of the diastolic pressure were not affected by aging. The systolic pressure at the 5thmin of reperfusion was slightly lower compared with the pre-ischemic value (−8 and −25% in the young adult and middle-aged rats, respectively), and less restored in the older animals (−10%) than in the youngest rats. This statement was true for the whole duration of reperfusion. The left ventricle developed pressure and rate×pressure product evolved similarly during reperfusion. They gradually recovered from a null value at the end of ischemia to positive values whose magnitude depended on the age of the animals. The restoration of these two parameters was indeed reduced in the middle-aged rats (−73 and −76% for the left ventricle developed pressure and rate×pressure product in comparison with the young animals at the 25thmin of reperfusion). However, although still significantly different, this huge difference tended to be lower at the 45thmin of reperfusion (−33% and −38% for the left ventricle developed pressure and rate×pressure product). Recovery of the heart rate was never significantly affected by the age of the animals.

Cardiac metabolic function during reperfusion

The coronary flow (Fig. 3) was similarly restored in the two age groups at the 5th of reperfusion (42±4 and 42±7% of the pre-ischemic value for the young and mature adults), but evolved differently thereafter. In the group of the young adult animals, the coronary flow continued to increase until the 45thmin of reperfusion to a value equal to 25±3 ml/min/g dry weight. Contrariwise, in the older animals, this parameter tended to decrease until the end of reperfusion to 18±2 ml/min/g dry weight. Consequently, the rate of the coronary flow was significantly lower in the older animals (−28%) compared with that of the younger ones. The oxygen consumption progressed similarly during reperfusion. Although it was similar in the two groups at the 5thmin of reperfusion, it was lower in the middle-aged rats (−28%) compared with their young counterparts at the 45thmin of reperfusion. The metabolic efficiency progressively recovered to achieve the pre-ischemic value at the 45thmin of reperfusion in the younger animals, whereas it remained constantly low in the older ones. At the end of reperfusion, the metabolic efficiency was reduced by 60% by aging.

Aconitase to fumarase ratio of myocardial biopsies

The aconitase to fumarase ratio (Fig. 4) inversely related to the mitochondrial oxidative stress was reduced by ischemia/reperfusion (−22%). Interestingly, the decrease was minimal in the heart of young adult animals (−8%) whereas it was significantly different in the myocardium of middle age rats (−34%, $p<0.05$).

Mitochondrial oxygen consumption and ROS release

Cardiac mitochondria were purified after a 30-min normoxic perfusion and their respiration properties were determined using several substrates (glutamate/malate as NADH-linked substrate, succinate/rotenone

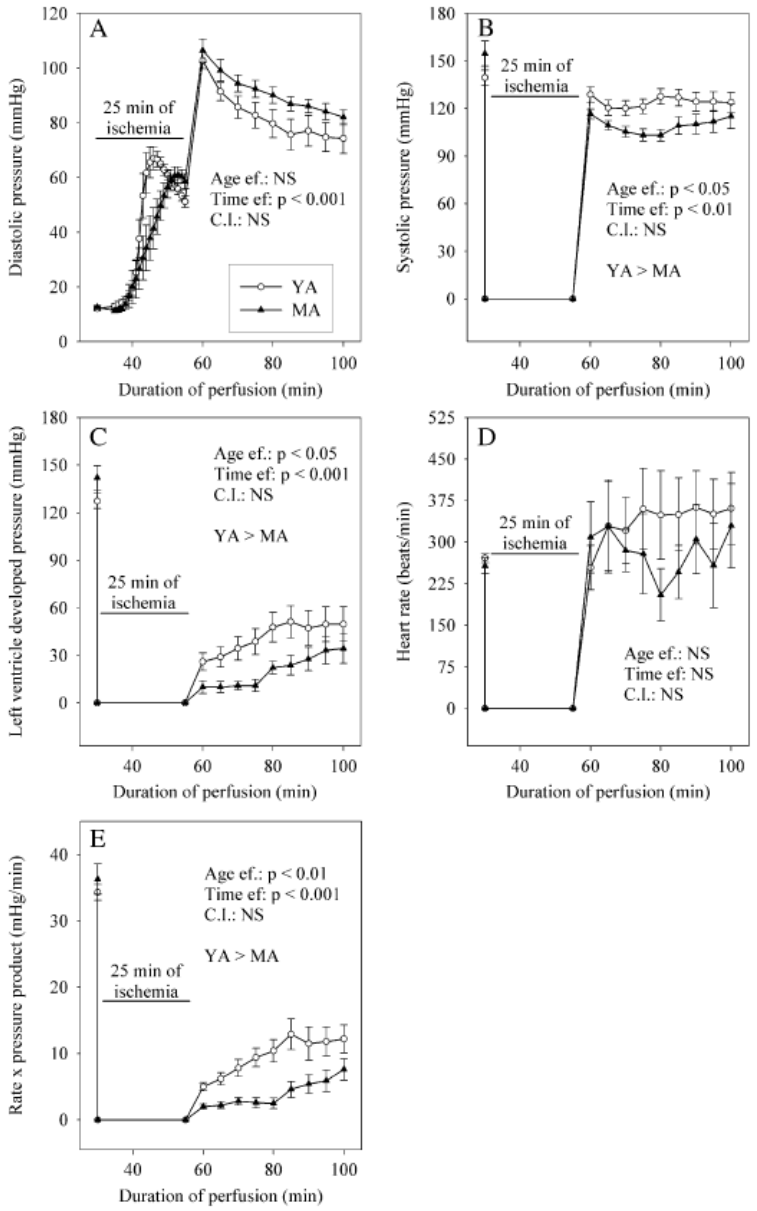

Fig. 2 Effects of aging on cardiac mechanical function during post-ischemic reperfusion. **a** Diastolic pressure; **b** systolic pressure; **c** left ventricle developed pressure; **d** heart rate; **e** rate×pressure product. The number of experiments was ten per group. *YA* young adult rats, *MA* middle-aged rats, *Age ef.* effect of the age, *Time ef.* effect of the duration of reperfusion

as $FADH_2$-linked substrate and glutamate/malate/succinate as NADH- and $FADH_2$-linked substrates). Whatever the substrate used, the parameters of mitochondrial respiration (Table 3) were similar between young adult and middle-aged animals. This was verified with only exception the RCR value with glutamate/malate as substrate. Indeed, this value was lower in the mitochondria of middle-aged rats in comparison with those of young adults (−33%).

Mitochondrial H_2O_2 release was also evaluated (Fig. 5). It was determined during the state II respiration rate. Under these conditions, H_2O_2 release was low with glutamate/malate and high with succinate/rotenone or glutamate/succinate/malate. Inhibition of complex I by rotenone slightly augmented H_2O_2 release with glutamate/malate, but strongly reduced it with succinate/rotenone and glutamate/malate/succinate. Additional inhibition of complex III with antimycin A aggravated H_2O_2 release with glutamate/malate and succinate/rotenone, but not with glutamate/malate/succinate. Aging had no effect on H_2O_2 release with glutamate/malate and succinate/

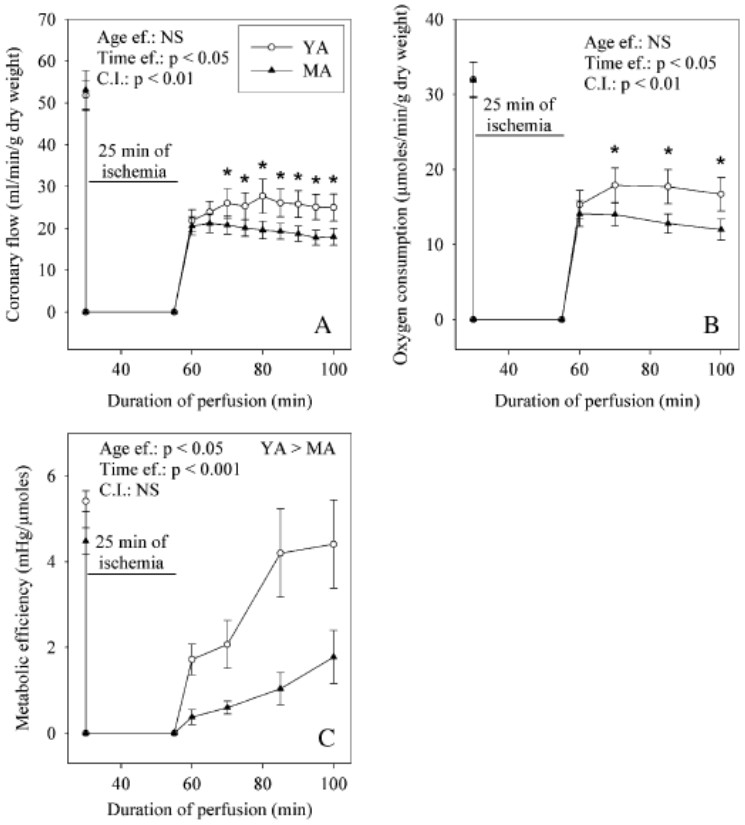

Fig. 3 Effects of aging on cardiac metabolism during post-ischemic reperfusion. **a** Coronary flow; **b** oxygen consumption; **c** metabolic efficiency. The number of experiments was ten per group. *YA* young adult rats, *MA* middle-aged rats, *Age ef.* effect of the age, *Time ef.* effect of the duration of reperfusion, *C.I.* cross-interaction; *asterisk* significantly different

rotenone, but enlarged the one measured with glutamate/malate/succinate when complexes I and III were simultaneously blocked.

Respiratory complex activities in myocardial biopsies

Citrate synthase activity (4.37±0.13 in the young adults vs. 3.87±0.28 mU/mg of proteins in the middle-aged hearts) was not modified by ischemia/reperfusion and by aging. In pre-ischemic myocardium, aging did not modify activities of the different respiratory complexes (Table 4), except that of cytochrome *c* oxidase which was slightly increased (+29%). The effect of ischemia/reperfusion was different in the adult and middle-aged hearts. In the younger hearts, the pathological event reduced the succinate-ubiquinone oxido-reductase (−27%) and NADH cytochrome *c* reductase (−43%) activities without sparing the ratio between NADH cytochrome *c* reductase and succinate cytochrome *c* reductase (−50%). In the middle-aged hearts, ischemia/reperfusion did not trigger any decrease in these parameters. Ubiquinol cytochrome *c* reductase tended to be lower (−23%), but this reduction was not significant.

Discussion

In this study, we verified that the well-known increase in ischemia/reperfusion-induced functional abnormalities occurring with aging also arises in middle-aged animals and we tried to evaluate the possible biochemical mechanisms involved in these changes. Fifty-two-week-old Wistar rats, considered as middle-aged animals with a life period approximating half of the longevity of this animal strain, were thus compared with 10-week-old animals, considered as young adults. Their hearts were collected, perfused according to the constant-pressure Langendorff mode and subjected to global zero-flow ischemia followed by reperfusion. Ischemic contracture was delayed in the middle-aged rats, suggesting better maintenance

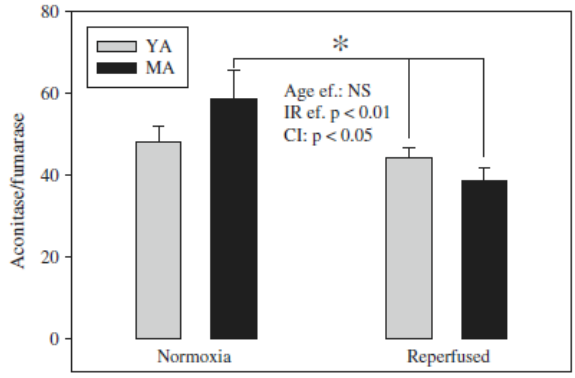

Fig. 4 Effects of aging and of ischemia/reperfusion on the aconitase to fumarase ratio. The measurements have been performed on the freeze-clamped hearts at the end of the stabilization and reperfusion periods. The number of experiments was eight and ten per group for the normoxic and reperfused hearts, respectively. *YA* young adult rats, *MA* ten middle-aged rats; *asterisk* significantly different

of ATP concentration in the older animals. In the literature, there is a study in apparent contradiction with this statement. Indeed, Headrick (1998) indicated that aging tended to increase ischemic- and hypoxic-contracture. Contrariwise, Ramani et al. (1996) showed a decelerated ischemic contracture. The two studies contrasted young or adult vs. aged animals. Our work supports the fact that middle age is associated with a delayed ischemic-related contracture. Rigor tension is explained by cellular ATP depletion due to arrest of the anaerobic glycolysis which results from proton-induced inhibition of the phosphofructokinase (PFK) reaction. This occurs in the diverse cells composing the myocardium at different times, depending on their localization (epi- vs. endocardium) and finally the intensity of their metabolism. The gap junction connexin 43 content has been tightly involved in the development of rigor tension, since it facilitates cell-to-cell communication and generalization of the behavior of a cell minority to the total cellular population of the heart. It is known to be decreased with aging, starting precisely at middle duration of the lifespan (Boengler et al. 2007). Since middle age reduces the gap junction connexin 43 content, excess proton accumulated in the most metabolically active cells should not be easily diffused in the less active cells, which should delay PFK inhibition in these last cells and allow the upholding of their metabolic activity. This decline in

Table 3 Mitochondrial oxidative capacities after 30 min of normoxic perfusion

	Respiratory state	Young adults	Middle aged	ANOVA
GM	Substrate	23±1	20±1	NS
	+ADP	153±6	131±15	NS
	+Oligomicine	26±3	33±6	NS
	+DNP	219±14	183±26	NS
	RCR	6.43±0.68	4.28±0.38	$p<0.05$
S	Substrate	70±4	78±4	NS
	+ADP	239±16	276±14	NS
	+Oligomicine	70±4	81±5	NS
	+DNP	214±15	246±11	NS
	RCR	3.46±0.04	3.45±0.19	NS
GMS	Substrate	59 ±4	67±3	NS
	+ADP	263±11	245±31	NS
	+Oligomicine	74±4	80±7	NS
	+DNP	259±21	279 ±13	NS
	RCR	3.33 ±0.13	3.57±0.27	NS

Except the RCR which is the ratio between the state III and the state IV respiration rates, the results are expressed in ng atoms of oxygen/min/mg of proteins. The number of experiments was eight per group

GM glutamate (5 mM)+malate (2.5 mM), *S* succinate (5 mM)+rotenone (2.5 µM), *GMS* glutamate (5 mM)+malate (2.5 mM)+succinate (5 mM), *substrate* state II respiration rate, *+ADP* state III respiration rate, *+oligomicine* state IV respiration rate, *+DNP* state uncoupled by dinitrophenol, *RCR* respiratory complex ratio

AGE

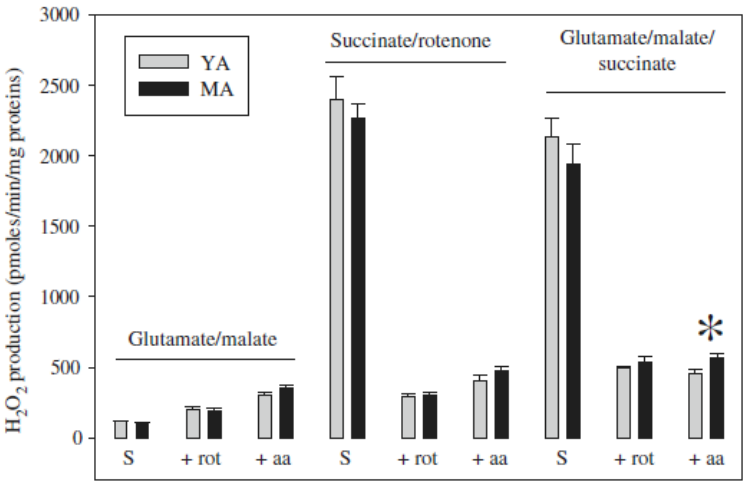

Fig. 5 Effect of the transition from youth to middle age on H_2O_2 release by isolated mitochondria from normoxic myocardium. The number of experiments was eight per group. *YA* young adults, *MA* middle-aged animals, *S* substrate alone (state II respiration rate), *+rot* substrate+rotenone, *+aa* substrate+rotenone+antimycine A, *asterisk* significantly different

the cell-to-cell communication should delay the development of the ischemic contracture in the middle-aged myocardium (Ruiz-Meana et al. 2008), but it should also augment the pH decrease in those cells mostly resistant to proton-induced metabolic inhibition.

In spite of this apparent beneficial effect on the ischemic contracture, recovery of the mechanical activity (left ventricular developed pressure and rate×pressure product) during post-ischemic reperfusion was hampered in the middle-aged animals. This is in agreement with numerous studies showing that middle-aged and senescent hearts (Azhar et al. 1999; Leichtweis et al. 2001; Xia et al. 2003; Willems et al. 2003; Willems et al. 2005) augment reperfusion-induced contraction disorders. Delayed ischemic

Table 4 Complexes of the respiratory chain at the end of reperfusion

	Young adults		Middle aged	
	Pre-ischemic[a]	Reperfused[b]	Pre-ischemic[a]	Reperfused[b]
CI[c]	1.49±0.17	1.65±0.20	1.86±0.23	1.50±0.25
CII[d]	0.86±0.04 a	0.63±0.05 b	0.92±0.05 a	0.86±0.10 a
CIII[e]	1.65±0.32	1.76±0.21	1.51±0.21	1.16±0.36
CIV[f]	0.21±0.01 a, d	0.26±0.01 b, c	0.27±0.01 b, c	0.24±0.02 c, d
CI+III[g]	0.054±0.009 a	0.031±0.005 b	0.045±0.001 a, b	0.044±0.006 a, b
CII+III[h]	0.031±0.001	0.039±0.004	0.042±0.003	0.041±0.005
CI+III/CII+III[i]	1.56±0.20 a	0.78±0.10 b	1.24±0.13 a, c	1.08±0.07 b, c

All the results are expressed in mU/mg of mitochondrial proteins. The number of experiments was eight and ten for the normoxic and reperfused groups. Lowercase letters (a, b, c, and d) are significantly different

[a] Hearts collected at the end of the stabilisation period

[b] Reperfused: hearts collected at the end of the reperfusion period

[c] NADH dehydrogenase

[d] Succinate dehydrogenase

[e] Ubiquinol cytochrome *c* reductase

[f] Cytochrome *c* oxidase

[g] NADH cytochrome *c* reductase

[h] Succinate cytochrome *c* reductase

[i] Ratio between the activities of NADH cytochrome *c* reductase and succinate cytochrome *c* reductase

contracture with preservation of residual metabolic activity might be responsible for these intensified abnormalities. Ischemia triggers acidosis that is likely redoubled by continuation of the metabolic activity. Intracellular protons are extruded from the cells by the Na^+/H^+ exchanger (NHE-1 in the heart) that favors firstly intracellular sodium accumulation and secondly cellular calcium entry through the Na^+/Ca^{2+} exchanger (Sniecinski and Liu 2004) when deprivation of ATP does not allow functioning of the Na^+/K^+-ATPase. Middle-aged and senescent hearts have been characterized by increased cellular sodium accumulation at the end of ischemia (Tani et al. 1997 and 1999) compared with young hearts. They are protected against reperfusion-induced cellular damage by either the NHE-1 inhibitor cariporide (Nakai et al. 2002; Besse et al. 2004; Simm et al. 2008) or the Na^+/Ca^{2+} exchanger (NCX) inhibitor KB-R7943 (Yamamura et al. 2001). This stresses the importance of ischemia-induced proton production and NHE-1/NCX axis in genesis of the ischemia/reperfusion-induced functional disturbances of the aged heart.

The lower salvage of the cardiac mechanical activity during reperfusion in the older animals was associated with a reduced recovery of the oxygen consumption (−28%). This reflects a depressed oxidative metabolism leading to reduced energy production. The impairment of this low oxygen consumption-related energy production was further amplified by a powerless restoration of the metabolic efficiency that never exceeded 37±13% of the pre-ischemic value in the middle-aged group versus 80±19% in the young adult group. Reduced cardiac metabolic efficiency during reperfusion is due to several processes involving decreased mitochondrial energy production (mitochondrial calcium loading, bulge of ROS production, opening of the permeability transition pore and mitochondrial uncoupling) and augmented energy wasting (elimination of excess sodium and calcium via the Na^+/K^+-ATPase and Ca^{2+}-ATPase). If and when these abnormalities disappear, the cardiac metabolic efficiency is restored. In the middle-aged hearts, restoration of this parameter during reperfusion was strongly delayed, which could be explained by a higher proton production, increased sodium, and calcium loadings and resulting abnormalities of energy production and utilization. Contraction was thus more depressed in the older animals compared with the younger ones and this accounted for the lower recovery of the rate×pressure product in the middle-aged rats. The decreased energy availability of the reperfused aged hearts might be explained by a distortion of the cellular functioning as well as by an abnormality of the coronary perfusion leading to insufficient oxygen supply. We observed lower recovery of the coronary flow of the middle-aged hearts compared with that of the young adults. This has been already mentioned by Willems et al. (2005) who showed that impaired salvage of the ventricular contractility in reperfused hearts of senescent animals correlates with recovery of the coronary flow. Furthermore, Besse et al. (2006) have shown that the post-ischemic coronary flow of the aged heart can be improved by treatment with superoxide dismutase and catalase, highlighting the prominent role of superoxide anions. This enhancement of the coronary perfusion was accompanied with a considerable improvement of the contractile function. This strongly suggests that insufficient coronary perfusion is rate-limiting during reperfusion of aged hearts with a major role of the abnormal vascular tone and the vascular cell dysfunction.

Insufficient coronary perfusion is thus probably related to the oxidative stress (Besse et al. 2006). ROS production has been reported to be associated with reduced nitric oxide (NO) bioavailability through scavenging by superoxide anions (Wei et al. 2006) and/or endothelial NO synthase uncoupling (Crabtree et al. 2009). In the present study, we evaluated the instant mitochondrial ROS impregnation at two moments of the perfusion: just before ischemia and at the end of reperfusion. It was performed by measuring the aconitase to fumarase ratio in cardiac homogenates (Gardner et al. 1994). Transition from normoxia to end of reperfusion triggered a significant decrease in the aconitase to fumarase ratio in the middle-aged hearts, whereas it did not alter this parameter in the hearts of young adult animals. This strongly suggests an increased oxidative stress in the oldest animals. This was reinforced by the measurement of hydrogen peroxide (H_2O_2) release by mitochondria isolated from normoxic hearts. Indeed, this H_2O_2 release was either unaltered or amplified by aging, depending on the conditions of substrate supply and of respiratory chain complex inhibition. The ampler reduction of the aconitase to fumarase ratio in the older hearts reflected thus necessarily a higher ex vivo mitochondrial ROS release. Such an

aging-related increase in the mitochondrial ROS release can partly explain the lower recovery of the coronary flow during reperfusion. However, other phenomena also probably intervene. Indeed, aging has been associated with augmented expression of NADPH oxidase in the vascular wall (Oudot et al. 2006). In any case, the low coronary perfusion reduced the oxygen supply and energy production, leading to delayed restoration of the mechanical function.

An argument issued from our results suggests the importance of the ROS release during reperfusion on the restoration of the coronary flow. Young adult myocardium, but not middle-aged hearts, had an ischemia/reperfusion-induced reduction of complex II activity. This decrease is known to be related to the oxidative stress (Chen et al. 2007). Indeed, at the beginning of reperfusion, calcium invades the mitochondrial matrix (Miyata et al. 1992) and opens the permeability transition pore, leading to release of NADH from the mitochondrial matrix (Batandier et al. 2004). Furthermore, it activates the α-ketoglutarate dehydrogenase, which triggers succinate accumulation in the mitochondrial environment (Sentex et al. 1999). Both phenomena favor oxidation of the $FADH_2$-linked substrate succinate that is known to trigger ROS over generation. In the present study, we ascertained that succinate augments considerably H_2O_2 release by isolated cardiac mitochondria in comparison with the NADH-linked substrate glutamate plus malate. As indicated by the inhibitory effect of rotenone, this occurs at complex I level by reverse electron flux. The high-ROS release occurring during the first 3 min of reperfusion (Demaison et al. 2001) oxidizes the complex II portion of the respiratory chain (Chen et al. 2007). ROS-induced inhibition of complex II at restoration of the coronary flow has a huge effect on subsequent mitochondrial ROS production, since it provokes its inhibition. Utilization of complex II inhibitors such as 3-nitro-*N-methyl*-salicylamide, malonate, or 3-nitropropionic acid indeed protects the myocardium against reperfusion-induced contractile dysfunction by reducing the burst of ROS occurring ordinarily at the beginning of reperfusion (Zhang et al. 2006; Turan et al. 2006; Wojtovich and Brookes 2008). In our work, ischemia/reperfusion-induced inhibition of the complex II activity in young adults related to the burst of ROS occurring at early reperfusion tempered ROS release during the remaining duration of reperfusion as it was indicated by the unchanged aconitase to fumarase ratio before and after ischemia. This was associated with a better recovery of the coronary flow. On the contrary, complex II activity was maintained in the middle-aged heart and this was associated with a decreased aconitase to fumarase ratio. As a consequence of the higher ROS production, recovery of the coronary flow during reperfusion was worsened.

Complex II activity might be modulated by its lipid environment and its preservation after ischemia/reperfusion in middle-aged hearts suggests membrane protection against the huge oxidative stress occurring under these circumstances. In our study, such a protection was also observed for complex I+III whose activity was reduced by ischemia/reperfusion in the young adult hearts, but not in the middle-aged myocardium. This suggests that biochemical composition of the lipid environment surrounding the respiratory complexes was different in young adult and middle-aged hearts. According to Pepe et al. (1999), aged hearts displays less n-3 polyunsaturated fatty acids (PUFAs) than young ones. This ascertainment has also been verified in skeletal muscle (Martin et al. 2007). Yet, n-3 PUFAs are extremely sensitive to the oxidative stress, more than n-6 PUFAs. The lower content of n-3 PUFAs for the benefit of n-6 PUFAs in the aged myocardium could protect activity of the complexes II and I+III against ROS deleterious effect during ischemia/reperfusion. Such a membrane lipid-related protection has been already observed in the middle-aged rat myocardium (Kakarla et al. 2005) in which the antioxidant defense (SOD, catalase, glutathione reductase) and the lipid peroxidation are reduced, although the oxidative stress evaluated by the drop of the reduced glutathione content is increased.

A reduction of the activity of the complex I+III in young adult hearts was observed whereas activities of the complexes I and III were not altered, suggesting the involvement of the quinone pool. Coenzyme Q treatment has been shown to be cardioprotective during ischemia/reperfusion (Maulik et al. 2000; Crestanello et al. 2002; Lakomkin et al. 2002; Timoshin et al. 2003; Verma et al. 2007; Sahach et al. 2007). The protective effect is associated with a shift of the redox equilibrium between the semi-reduced forms of ubiquinone and flavine coenzymes to a higher output of ubisemiquinone (Timoshin et al.

2003). This contributes to lower succinate-related ROS release (Lakomkin et al. 2002), lipid peroxidation, and thiol oxidation (Maulik et al. 2000) during reperfusion. The mitochondrial function is hence preserved (Crestanello et al. 2002; Lakomkin et al. 2002) with a reduced capacity of opening the permeability transition pore (Sahach et al. 2007). The coronary perfusion is also protected (Lakomkin et al. 2002). Ischemia/reperfusion is thus accompanied with disturbances of the quinone metabolism that can be responsible for the associated perfusion and mechanical dysfunctions. In the aged rat heart, although complex I+III is not damaged in our study, cardioprotective effect of the CoQ is also observed (Timoshchuk et al. 2009) with better restorations of contractile dysfunction, coronary flow, and metabolic efficiency. This further confirms that ROS release is more important in the aged heart, although the membrane environment and respiratory complex activities are less damaged probably through reduction of the n-3 PUFAs to n-6 PUFAs ratio. Conversely, other important cellular targets of the oxidative stress such as proteins (thiol oxidation, tyrosine nitration, protein oxidation, ROS-induced uncoupling of eNOS, etc.) can be involved in the lower resistance of the aged myocardium to ischemia/reperfusion. As it was shown by Gao et al. (2000), the aged myocardium seems to have a reduced capacity of nitric oxide production.

In conclusion, middle age augmented reperfusion mechanical dysfunction via a lower recovery of the coronary flow and insufficient oxygen supply. Due to preservation of the respiratory complex II activity, reperfusion-induced mitochondrial ROS release was enlarged, which explained the lower restoration of coronary perfusion probably through decreased NO bioavailability.

Acknowledgments This work was supported by the National Institute of Agronomical Research (INRA, France) and the Université Joseph Fourier.

References

Amrani M, Chester AH, Jayakumar J, Yacoub MH (1996) Aging reduces postischemic recovery of coronary endothelial function. J Thorac Cardiovasc Surg 111:238–245

Azhar G, Gao W, Liu L, Wei JY (1999) Ischemia-reperfusion in the adult mouse heart: influence of age. Exp Gerontol 34:699–714

Batandier C, Leverve X, Fontaine E (2004) Opening of the mitochondrial permeability transition pore induces reactive oxygen species production at the level of the respiratory chain complex I. J Biol Chem 279:17197–17204

Besse S, Tanguy S, Riou B, Boucher F, Bulteau AL, Le Page C, Swynghedauw B, de Liris J (2001) Coronary and aortic vasoreactivity protection with endothelin receptor antagonist, bosentan, after ischemia and hypoxia in aged rats. Eur J Pharmacol 432:167–175

Besse S, Tanguy S, Boucher F, Le Page C, Rozenberg S, Riou B, Liris J, Swynghedaw B (2004) Cardioprotection with cariporide, a sodium-proton exchanger inhibitor, after prolonged ischemia and reperfusion in senescent rats. Exp Gerontol 39:1307–1314

Besse S, Bulteau AL, Boucher F, Riou B, Swynghedauw B, de Liris J (2006) Antioxidant treatment prevents cardiac protein oxidation after ischemia-reperfusion and improves myocardial function and coronary perfusion in senescent hearts. J Physiol Pharmacol 57:541–552

Boengler K, Konietzka I, Buechert A, Heinen Y, Garcia-Dorado D, Heusch G, Schulz R (2007) Loss of ischemic preconditioning's cardioprotection in aged mouse hearts is associated with reduced gap junctional and mitochondrial levels of connexin 43. Am J Physiol Heart Circ Physiol 292:H1764–H1769

Capel F, Rimbert V, Lioger D, Diot A, Rousset P, Mirand PP, Boirie Y, Morio B, Mosoni L (2005) Due to reverse electron transfer, mitochondrial H_2O_2 release increases with age in human vastus lateralis muscle although oxidative capacity is preserved. Mech Ageing Dev 126:505–511

Chen YR, Chen CL, Pfeiffer DR, Zweier JL (2007) Mitochondrial complex II in the post-ischemic heart: oxidative injury and the role of protein S-glutathionylation. J Biol Chem 282:32640–32654

Chen CL, Chen J, Rawale S, Varadharaj S, Kaumaya PP, Zweier JL, Chen YR (2008) Protein tyrosine nitration of the flavin subunit is associated with oxidative modification of mitochondrial complex II in the post-ischemic myocardium. J Biol Chem 283:27991–28003

Crabtree MJ, Tatham AL, Al-Wakeel Y, Warrick N, Hale AB, Cai S, Channon KM, Alp NJ (2009) Quantitative regulation of intracellular endothelial nitric-oxide synthase (eNOS) coupling by both tetrahydrobiopterin-eNOS stoichiometry and biopterin redox status: insights from cells with tet-regulated GTP cyclohydrolase I expression. J Biol Chem 284:1136–1144

Crestanello JA, Doliba NM, Doliba NM, Babsky AM, Niborii K, Osbakken MD, Whitman GJ (2002) Effect of coenzyme Q10 supplementation on mitochondrial function after myocardial ischemia reperfusion. J Surg Res 102:221–228

Demaison L, Moreau D, Vergely-Vandriesse C, Grégoire S, Degois M, Rochette L (2001) Effects of dietary polyunsaturated fatty acids and hepatic steatosis on the functioning of isolated working rat heart under normoxic conditions and during post-ischemic reperfusion. Mol Cell Biochem 224:103–116

Faloona GR, Srere PA (1969) Escherichia coli citrate synthase. Purification and the effect of potassium on some properties. Biochemistry 8:4497–4503

Fannin SW, Lesnefsky EJ, Slabe TJ, Hassan MO, Hoppel CL (1999) Aging selectively decreases oxidative capacity in rat heart interfibrillar mitochondria. Arch Biochem Biophys 372:399–407

Gao F, Christopher TA, Lopez BL, Friedman E, Cai G, Ma XL (2000) Mechanism of decreased adenosine protection in reperfusion injury of aging rats. Am J Physiol Heart Circ Physiol 279:H329–H338

Gardner PR, Nguyen DD, White CW (1994) Aconitase is a sensitive and critical target of oxygen poisoning in cultured mammalian cells and in rat lungs. Proc Natl Acad Sci USA 91:12248–12252

Gnaiger E (2001) Oxygen solubility in experimental media. Oroboros Bioenergetics Newsletter 6(3):1–6

Goodwin AT, Amrani M, Marchbank AJ, Gray CC, Jayakumar J, Yacoub MH (1999) Coronary vasoconstriction to endothelin-1 increases with age before and after ischaemia and reperfusion. Cardiovasc Res 41:554–562

Hansford RG, Tsuchiya N, Pepe S (1999) Mitochondria in heart ischaemia and aging. Biochem Soc Symp 66:141–147

Headrick JP (1998) Aging impairs functional, metabolic and ionic recovery from ischemia-reperfusion and hypoxia-reoxygenation. J Mol Cell Cardiol 30:1415–1430

Hoppel CL, Moghaddas S, Lesnefsky EJ (2002) Interfibrillar cardiac mitochondrial complex III defects in the aging rat heart. Biogerontology 3:41–44

Hu A, Jiao X, Gao E, Li Y, Sharifi-Azad S, Grunwald Z, Ma XL, Sun JZ (2008) Tonic beta-adrenergic drive provokes proinflammatory and proapoptotic changes in aging mouse heart. Rejuvenation Res 11:215–226

Jahangir A, Ozcan C, Holmuhamedov EL, Terzic A (2001) Increased calcium vulnerability of senescent cardiac mitochondria: protective role for a mitochondrial potassium channel opener. Mech Ageing Dev 122:1073–1086

Juhaszova M, Rabuel C, Zorov DB, Lakatta EG, Sollott SJ (2005) Protection in the aged heart: preventing the heat-break of old age? Cardiovasc Res 66:233–244

Kakarla P, Vadluri G, Reddy KS, Leeuwenburgh C (2005) Vulnerability of the mid aged rat myocardium to the age-induced oxidative stress: influence of exercise training on antioxidant defense system. Free Radic Res 39:1211–1217

Krähenbühl S, Talos C, Wiesmann U, Hoppel CL (1994) Development and evaluation of a spectrophotometric assay for complex III in isolated mitochondria, tissues and fibroblasts: application to mitochondrial encephalomyopathies. Clin Chim Acta 230:177–187

Kramer KA, Oglesbee D, Hartman SJ, Huey J, Anderson B, Magera MJ, Matern D, Rinaldo P, Robinson BH, Cameron JM, Hahn SH (2005) Automated spectrophotometric analysis of mitochondrial respiratory chain complex enzyme activities in cultured skin fibroblasts. Clin Chem 51:2110–2116

Lacraz G, Couturier K, Taleux N, Servais S, Sibille B, Letexier D, Guigas B, Dubouchaud H, Leverve X, Favier R (2008) Liver mitochondrial properties from the obesity-resistant Lou/C rat. Int J Obes (Lond) 32:629–638

Lakatta EG, Sollott SJ, Pepe S (2001) The old heart: operating on the edge. Novartis Found Symp 235:172–196

Lakomkin VL, Korkina OV, Tsyplenkova VG, Timoshin AA, Ruuge EK, Kapel'ko VI (2002) The protective action of ubiquinone at ischemia and reperfusion. Kardiologiia 42:51–55

Leichtweis S, Leeuwenburgh C, Bejma J, Ji LL (2001) Aged rat hearts are not more susceptible to ischemia-reperfusion injury in vivo: role of glutathione. Mech Ageing Dev 122:503–518

Lesfnefsky EJ, Hoppel CL (2003) Ischemia-reperfusion injury in the aged heart: role of mitochondria. Arch Biochem Biophys 420:287–297

Lesnefsky EJ, Hoppel CL (2008) Cardiolipin as an oxidative target in cardiac mitochondria in the aged heart. Biochim Biophys Acta 1777:1020–1027

Lesnefsky EJ, Gudz TI, Moghaddas S, Migita CT, Ikeda-Saito M, Turkaly PJ, Hoppel CL (2001a) Aging decreases electron transport complex III activity in heart interfibrillar mitochondria by alteration of the cytochrome *c* binding site. J Mol Cell Cardiol 33:37–47

Lesnefsky EJ, Gudz TI, Migita CT, Ikeda-Saito M, Hassan MO, Turkaly PJ, Hoppel CL (2001b) Ischemic injury to mitochondrial electron transport in the aging heart: damage to the iron-sulfur protein subunit of electron transport complex III. Arch Biochem Biophys 385:117–128

Lesnefsky EJ, Minkler P, Hoppel CL (2009) Enhanced modification of cardiolipin during ischemia in the aged heart. J Mol Cell Cardiol 46:1008–1015

Martin C, Dubouchaud H, Mosoni L, Chardigny JM, Oudot A, Fontaine E, Vergely C, Keriel C, Rochette L, Leverve X, Demaison L (2007) Abnormalities of mitochondrial functioning can partly explain the metabolic disorders encountered in sarcopenic gastrocnemius. Aging Cell 6:165–177

Maulik N, Yoshida T, Engelman RM, Bagchi D, Otani H, Das DK (2000) Dietary coenzyme Q(10) supplement renders swine hearts resistant to ischemia-reperfusion injury. Am J Physiol Heart Circ Physiol 278:H1084–H1090

Miro O, Barrientos A, Alonso JR, Casademont J, Jarreta D, Urbano-Marquez A, Cardellach F (1999) Effects of general anaesthetic procedures on mitochondrial function of human skeletal muscle. Eur J Pharmacol 55:35–41

Miyata H, Lakatta EG, Stern MD, Silverman HS (1992) Relation of mitochondrial and cytosolic free calcium to cardiac myocyte recovery after exposure to anoxia. Circ Res 71:605–613

Nagy K, Takacs IE, Pankucsi C (1996) Age-dependence of free radical-induced oxidative damage in ischemic-reperfused rat heart. Arch Gerontol Geriatr 22:297–309

Nakai Y, Horimoto H, Mieno S, Sasaki S (2002) $Na^{(+)}/H^{(+)}$ exchanger inhibitor HOE642 offers myoprotection in senescent myocardium independent of ischemic preconditioning mechanisms. Eur Surg Res 34:244–250

Nakamura K, Al-Ruzzeh S, Chester AH, Dewar A, Rothery S, Severs NJ, Yacoub MH, Amrani M (2003) Age-related changes in the protective effect of chronic administration of L-arginine on post-ischemic recovery of endothelial function. Eur J Cardiothorac Surg 23:626–632

Oudot A, Martin C, Busseuil D, Vergely C, Demaison L, Rochette L (2006) NADPH oxydases are in part responsible for increased cardiovascular superoxide production during aging. Free Radic Biol Med 40:2214–2222

Paradies G, Petrosillo G, Pistolese M, Di Venosa N, Federici A, Ruggiero FM (2004) Decrease in mitochondrial complex I activity in ischemic/reperfused rat heart: involvement of reactive oxygen species and cardiolipin. Circ Res 94:53–59

Pasdois P, Beauvoit B, Tariosse L, Vinassa B, Bonoron-Adèle S, Santos PD (2006) MitoK(ATP)-dependent changes in mitochondrial volume and in complex II activity during ischemic and pharmacological preconditioning of Langendorff-perfused rat heart. J Bioenerg Biomembr 38:101–112

Pepe S, Tsuchiya N, Lakatta EG, Hansford RG (1999) PUFA and aging modulate cardiac mitochondrial membrane lipid composition and Ca2+ activation of PDH. Am J Physiol 276:H149–H158

Polewczyk A, Janion M, Gasior M, Gierlotka M (2008) Myocardial infarction in the elderly. Clinical and therapeutic differences. Kardiol Pol 66:166–172

Ramani K, Lust WD, Wittingham TS, Lesnefsky EJ (1996) ATP catabolism and adenosine generation during ischemia in the aging heart. Mech Ageing Dev 89:113–124

Ruiz-Meana M, Rodriguez-Sinovas A, Cabestrero A, Boengler K, Heusch G, Garcia-Dorado D (2008) Mitochondrial connexin 43 as a new player in the pathophysiology of myocardial ischaemia-reperfusion injury. Cardiovasc Res 77:325–333

Sahach VF, Vavilova HL, Rudyk OV, Dobrovol's'kyĭ FV, Shymans'ka TV, Miedviediev OS (2007) Inhibition of mitochondrial permeability transition pore is one of the mechanisms of cardioprotective effect of coenzyme Q10. Fiziol Zh 53:35–42

Sentex E, Laurent A, Martine L, Grégoire S, Rochette L, Demaison L (1999) Calcium- and ADP-magnesium-induced respiratory uncoupling in isolated cardiac mitochondria: influence of cyclosporine A. Mol Cell Biochem 202:73–84

Simm A, Friedrich I, Scheubel RJ, Gursinsky T, Silber RE, Bartling B (2008) Age dependency of the cariporide-mediated cardio-protection after simulated ischemia in isolated human atrial heart muscles. Exp Gerontol 43:691–699

Sniecinski R, Liu H (2004) Reduced efficacy of volatile anesthetic preconditioning with advanced age in isolated rat myocardium. Anesthesiology 100:589–597

Tani M, Suganuma Y, Hasegawa H, Shinmura K, Ebihara Y, Hayashi Y, Guo X, Takayama M (1997) Decrease in ischemic tolerance with aging in isolated perfused Fisher 344 rat hearts: relation to increases in intracellular Na^+ after ischemia. J Mol Cell Cardiol 29:3081–3089

Tani M, Honma Y, Takayama M, Hasegawa H, Shinmura K, Ebihara Y, Tamaki K (1999) Loss of protection by hypoxic preconditioning in aging Fisher 344 rat hearts related to myocardial glycogen content and Na^+ imbalance. Cardiovasc Res 41:594–602

Timoshchuk SV, Vavilova HL, Strutyns'ka NA, Talanov SA, Petukhov DM, Kuchmenko OB, Donchenko HV, Sahach VF (2009) Cardioprotective action of coenzyme Q in conditions of its endogenous synthesis activation in cardiac ischemia-reperfusion in old rats. Fiziol Zh 55:58–63

Timoshin AA, Lakomkin VL, Gubkin AA, Ruuge EK (2003) Effect of coenzyme Q10 on free radical centers in isolated rat myocardium tissue. Biofizika 48:717–721

Tsukube T, McCully JD, Federman M, Krukenkamp IB, Levitsky S (1996) Developmental differences in cytosolic calcium accumulation associated with surgically induced global ischemia: optimization of cardioplegic protection and mechanism of action. J Thorac Cardiovasc Surg 112:175–184

Turan N, Csonka C, Csont T, Giricz Z, Fodor G, Bencsik P, Gyongyosi M, Cakici I, Ferdinandy P (2006) The role of peroxynitrite in chemical preconditioning with 3-nitropropionic acid in rat hearts. Cardiovasc Res 70:384–390

Veitch K, Hue L (1994) Flunarizine and cinnarizine inhibit complexes I and II: possible implication for Parkinsonism. Mol Pharmacol 45:158–163

Verma DD, Hartner WC, Thakkar V, Levchenko TS, Torchilin VP (2007) Protective effect of coenzyme Q10-loaded liposomes on the myocardium in rabbits with an acute experimental myocardial infarction. Pharm Res 24:2131–2137

Wei Y, Sowers JR, Nistala R, Gong H, Uptergrove GM, Clark SE, Morris EM, Szary N, Manrique C, Stump CS (2006) Angiotensin II-induced NADPH oxidase activation impairs insulin signaling in skeletal muscle cells. J Biol Chem 281:35137–35146

Willems L, Garnham B, Headrick JP (2003) Aging-related changes in myocardial purine metabolism and ischemic tolerance. Exp Gerontol 38:1169–1177

Willems L, Zatta A, Holmgren K, Ashton KJ, Headrick JP (2005) Age-related changes in ischemic tolerance in male and female mouse hearts. J Mol Cell Cardiol 38:245–256

Wojtovich AP, Brookes PS (2008) The endogenous mitochondrial complex II inhibitor malonate regulates mitochondrial ATP-sensitive potassium channels: implications for ischemic preconditioning. Biochim Biophys Acta 1777:882–889

Xia Z, Godin DV, Ansley DM (2003) Propofol enhances ischemic tolerance of middle-aged rat hearts: effects on 15-F(2t)-isoprostane formation and tissue antioxidant capacity. Cardiovasc Res 59:113–121

Yamamura K, Tani M, Hasegawa H, Gen W (2001) Very low dose of the $Na^{(+)}/Ca^{(2+)}$ exchange inhibitor, KB-R7943, protects ischemic reperfused aged Fischer 344 rat hearts: considerable strain difference in the sensitivity to KB-R7943. Cardiovasc Res 52:397–406

Zhang S, Yang JH, Yu F, Zhao J, Jiang P, Chang L, Tang C, Xu J (2006) Protective role of 3-nitro-N-methyl-salicylamide on isolated rat heart during 4 hours of cold storage and reperfusion. Transplant Proc 38:1247–1252

Zorov DB, Juhaszova M, Sollott SJ (2006) Mitochondrial ROS-induced ROS release: an update and review. Biochim Biophys Acta 1757:509–517

3.2 ARTICLE II

"Functional development of the coronary microvasculature with aging as regard the energy metabolism and oxidative stress"

This work is submitted for publish to the journal "Aging Cell".

Date of sublission: 12 Septembre 2012

Functional development of the coronary microvasculature with aging as regard the energy metabolism and oxidative stress

Evangelia Mourmoura,[1,2] Karine Couturier,[1,2] Isabelle Hininger [1,2] and Luc Demaison[1,2,3]

(1) Laboratoire de Bioénergétique Fondamentale et Appliquée, INSERM U1055, BP 53, 38041 Grenoble cedex 09, France ;

(2) Université Joseph Fourier, Laboratoire de Bioénergétique Fondamentale et Appliquée, BP 53, 38041 Grenoble cedex 09, France ;

(3) INRA, Clermont Université, Université d'Auvergne, Unité de Nutrition Humaine, BP 10448, F-63000 Clermont-Ferrand, France.

Correspondence to L. Demaison, Laboratoire de Bioénergétique Fondamentale et Appliquée, INSERM U1055, Université Joseph Fourier, BP 53, 38041 Grenoble cedex 09, France. Tel. (+33) 476 63 56 00; Fax (+33) 476 51 42 18; e-mail: luc.demaison@ujf-grenoble.fr

Summary

This study was aimed at characterizing the functional progression of the coronary microvasculature endothelial and smooth muscle cells (ECs and SMCs) between youth and middle age as well as at determining the mechanisms of the observed changes on the basis of the mitochondrial energy metabolism and oxidative stress. Male rats were divided into 3 age groups (3, 6 and 11 months for the young (Y), young adult (YA) and middle-aged (MA) animals). The cardiac mechanical function, endothelial-dependent dilatation (EDD) and endothelial-independent dilatation (EID) of the coronary microvasculature were determined in a Langendorff preparation. The mitochondrial respiration and H_2O_2 production were evaluated and completed with *ex vivo* measurements of the oxidative stress. Although the cardiac mechanical function was unchanged, the EDD was progressively decreased between youth and middle age. The relaxation properties of the SMCs, although high in the Y rats, decreased drastically between youth and young adulthood to stabilize thereafter, paralleling a reduction of the mitochondrial oxidative phosphorylation. The ECs dilatation activity, low at youth, was stimulated in YA animals and returned to their initial level at middle age. The reduction occurring between young adulthood and middle age could be due to problems of energy metabolism related to the plasma oxidative stress. In conclusion, the progressive decrease in EDD occurring with aging is due to different functional behaviours of the ECs and SMCs which appear to be related to the energy metabolism and oxidative stress. The decline in EDD could progressively reduce the welfare of individuals.

Introduction

Vascular aging has been extensively studied with a particular focus on the large conduit arteries such as the aorta. Indeed, normal aging is characterized by intima-media thickness (Liviakis *et al.*, 2010), aortic dilatation (Sawabe *et al.*, 2011), calcification of the aortic smooth muscle cells (SMCs)

(Takemura *et al.*, 2010; Burton *et al.*, 2010), disruption of elastin fibers (Sawabe *et al.*, 2010), stiffness of the vascular wall (Lee & Oh, 2010) and development of hypertension (Shirwany *et al.*, 2010; Safar, 2010). Associated with other lifestyle-related abnormalities (lack of physical training, smoking, insulin resistance, diabetes, dyslipidemia, etc.), aging progressively contributes to the occurrence of cardiovascular diseases including stroke, renal failure, myocardial ischemia, arrhythmias and cardiac failure (Takemura *et al.*, 2010).

Aging is also characterized by a progressive reduction of the physical capacities (Charansonney, 2011) of individuals which is partly due to a decline in cardiac function (Froehlich *et al.*, 1978; Capasso *et al.*, 1983; Effron *et al.*, 1987). Aside from the pathological events such as atherosclerosis and wall thickening (Scott *et al.*, 2011) of the large and medium coronary conductance arteries, this can be related to the coronary microvasculature. Indeed, the resistance arteries of the coronary network (arterioles and capillaries) finely regulate the blood flow of the heart and thus the maximal capacity of that organ to pump blood through the body of the organism. The effect of aging on that microvasculature is poorly described in the literature. A morphological study performed in the senescent beagle (Tomanek *et al.*, 1991) indicates lower capillary length density and capillary numerical density without change in volume density due to the enlargement of the capillary diameter. Two physiological studies in humans (Egashira *et al.*, 1993; Chauhan *et al.*, 1996) and one in guinea-pigs (Toma *et al.*, 1985) emphasize the gradual decrease of the endothelial-dependent dilation (EDD) from youth to senescence. However, the relative contributions of ECs and SMCs in that phenomenon have not been well documented. The aging-induced decrease in EDD is completely reversed by L-arginine infusion in the coronary network (Chauhan *et al.*, 1996), highlighting the importance of the bioavailability of the endothelial nitric oxide synthase (eNOS) substrate in the age-related disturbance of the coronary microvasculature.

After L-arginine utilisation by the eNOS enzyme, replenishment of its EC pool depends on two pathways. The first one is based on the uptake of circulating L-arginine through the system y+ transporter (Wyatt *et al.*, 2004), whereas the second one is a rescue pathway which regenerates L-arginine from citrulline, the product of the eNOS reaction, through an energy-dependent process

(Wijnands *et al.*, 2012). This emphasizes the importance of the energy metabolism when L-arginine transport is poorly functioning. Yet, the energy metabolism appears profoundly affected by aging. Some research teams have described a decline in oxygen consumption (Delaval *et al.*, 2004) or oxidation phosphorylation rates (Fannin *et al.*, 1999) in aged cardiac mitochondria. These alterations have been related to age-induced modifications of the respiratory chain complex activities with complex I appearing to be the most susceptible to age related declines (Sugiyama *et al.*, 1993; Castellucio *et al.*, 1994; Lenaz *et al.*, 1997). Age-associated decreases in the activities of complexes III (Castellucio *et al.*, 1994; Lesnefsky *et al.*, 2001; Yan *et al.*, 2004) and IV (Castellucio *et al.*, 1994; Sugiyama *et al.*, 1993) have also been reported. In contrast, complex II activity appears maintained (Sugiyama *et al.*, 1993) or even increased. A possible explanation for these modifications could be the attack of the mitochondrial DNA (mtDNA) by reactive oxygen species, since mtDNA encodes for some of the subunits of Complexes I, III and IV but not for those of complex II (Ozawa, 1997). The oxidative stress known to be increased by aging (Labunskyy & Gladyshev, 2012) can also influence the energy metabolism, mainly through inhibition of the energy transfer. Indeed, the creatine kinase system is sensitive to the redox potential and its activity is reduced by the oxidative stress (Venkataraman *et al.*, 2009).

This study was aimed at determining the influence of aging from youth to middle age on the functional behavior of ECs and SMCs as well as at explaining the mechanism(s) by which the observed modifications occurred. The effect of aging on the ECs and SMCs functions was studied in the *ex vivo* Langendorff perfused heart derived from 3 batches of Wistar rats displaying different ages (3, 6 and 11 months for youth, young adulthood and middle age). The results were compared to the state of oxidative stress of various biological compartments (*in vivo* plasma and *ex vivo* cardiac cytosol and mitochondria) as well as the mitochondrial function (oxidative phosphorylation and H_2O_2 production). Furthermore, oral glucose tolerance tests were performed and the cardiac mechanical activity was also determined.

Results

General data

As shown in table 1, the body weight followed a progressive increase with age. The YA rats had a 15.3% increase in their body weight which was followed by a further increase of 13.3% for the MA animals. This was not the case for the adipose tissue which did not follow the same pattern. More specifically, all types of adipose tissue were significantly increased between 3 and 6 months of age (+90, +114 and +73% for the epididymal, visceral and retroperitoneal adipose tissues) and stabilized thereafter. Consequently, the abdominal adipose tissue estimated as the sum of the retroperitoneal and visceral adipose tissues was similarly increased (+88% between 3 and 6 months of age). Triglycerides and cholesterol concentrations in the plasma at the moment of the sacrifice were not modified by aging.

There was a significant impact of aging on the basal glycemia. Compared to the values measured in the two youngest groups, the ones measured at 11 months of age were lower (Fig. 1.A.). The results of the oral glucose tolerance test indicated no difference between the groups as evidenced by the total area under the curve (Fig. 1.B.). However, we considered as a valuable measure the delta 180 (glycemia between time zero and time 180 minutes) in order to evaluate the glucose response. According to figure 1.D., there was a significant effect of aging with the middle-aged group having slower glucose elimination.

Cardiac function studied *ex vivo*

The mechanical function of the perfused isolated hearts was monitored before the infusion of U46619 (Table 2). Aging had no significant effects on the heart rate, LVDP and RPP. Furthermore, no change was observed in the heart rate and coronary pressure before and after the infusion of U46619. However, the infusion of U46619 raised the coronary pressure from 80 mmHg to a value close to 125 mmHg in all groups.

Coronary Reactivity

The responses to Ach of the coronary microvasculature were significantly affected by aging as shown in figure 2.A. Indeed, aging triggered a progressive decrease in the EDD, first between 3 and 6 months of age (-23% at 60 pmoles of injected Ach) and then between 6 and 11 months (-38.5% at 60 pmoles of injected Ach). Figure 2.B. depicts the SNP-induced vasodilatation in the three age groups. Interestingly, the EID strongly decreased from youth to young adulthood (-56.7% at 600 pmoles of injected SNP) and slightly increased afterwards at middle age (+18.9% compared to the YA group at 600 pmoles of injected SNP). The calculated vasodilatation activities of the endothelial cells are presented in figure 2.C. That parameter was increased between 3 and 6 months (+280% at 60 pmoles of injected Ach) but was decreased thereafter reaching the initial level observed at the young age.

eNOS expression and phosphorylation

No changes were observed between age groups in the levels of total eNOS, phosphorylated eNOS and the ratio of phosphorylated to total eNOS (Fig. 3).

Oxidative stress

The mitochondrial-derived oxidative stress was estimated in cardiac homogenates by the aconitase-to-fumarase ratio. As shown in figure 4.A., this ratio was never significantly decreased by aging, indicating no significant mitochondrial oxidative stress. Similarly, no difference was observed in the cytosolic oxidative stress as estimated by the lactate-to-pyruvate ratio in the coronary effluents (Fig. 4.B.). In the plasma, even though the antioxidant enzyme GPx was not modified (Fig. 4.C.), the global antioxidant power as estimated by the FRAP assay was progressively decreased by aging (Fig. 4.D.), reaching a significant difference at the age of 11 months (-21% for the MA group compared to the Y group). Similarly, the plasma oxidative stress (Fig. 4.E.) measured as the reduction of the plasma thiol groups was only decreased in the oldest animals (-15% for the MA group compared to the Y group).

Mitochondrial H_2O_2 production

The effect of aging on basal glutamate/malate-related mitochondrial H_2O_2 production (Figure 5.A.) was biphasic. After a significant increase between 3 and 6 months of age (+73%), this parameter was than reduced between 6 and 11 months (-23%). These differences were erased when rotenone alone and in association with antimycine A were added, emphasizing the involvement of the respiratory chain complex I in the age effects.

A similar biphasic pattern was observed for basal succinate-related mitochondrial H_2O_2 production (Figure 5.B.). However, this pattern evolved in the opposite direction. Indeed, the production was decreased between 3 and 6 months (-33%) and increased thereafter (+117% at 11 months compared to the value measured at 6 months) in order to reach a higher value (+46%) than that measured in the youngest animals. The aging-related decrease occurring between 3 and 6 months was inversed by the addition of rotenone alone and in association with antimycin A, suggesting that complex I was involved in that phenomenon probably through reverse electron flux. However, the maximal H_2O_2 production occurring at the level of complex III appeared to be higher in the 6-month old animals. The age-related increase observed between 6 and 11 months was erased by the addition of rotenone alone, which showed the involvement of complex I by reverse electron flux. It was inversed by antimycin A, indicating a return of the complex III-related maximal H_2O_2 production capacities close to that observed at 3 months.

When glutamate/malate/succinate where used as substrates, the pattern for the basal H_2O_2 production (Figure 5.C.) was different. This parameter was similar in 3- and 6-month old rats and increased only in the 11-month animals (+47% compared to the Y group). Although no difference was observed between 3 and 6 months, addition of rotenone rendered the 6-month value higher, a difference which was erased by antimycin A. Thus, complex I through inverse electron flux and also complex III were involved in that production. Furthermore, the increase in basal H_2O_2 production occurring between 6 and 11 month was erased and even inversed by rotenone and can thus be attributable to the activity of complex I, although a participation of complex III was also likely given the effect of antimycin A.

Mitochondrial respiration

As shown in figure 6, whatever the substrate(s) used (glutamate/malate, succinate/rotenone, glutamate/malate/succinate) and the respiration state studied (state 3 or ADP-stimulated respiration and state 4 or rotenone-related respiration), the respiration was reduced between 3 and 6 months (i.e. -29% for the state 3 of glutamate/malate/succinate) and stabilized thereafter until middle age.

Mitochondrial enzymatic activity

Aging altered neither the activities of the respiratory chain complexes measured in isolated mitochondria nor the mitochondrial density as evidenced by the activity of citrate synthase of cardiac homogenates (data not shown).

Discussion

This study was aimed at determining the effects of aging between youth and middle-age on the function of the coronary microvasculature by evaluating the contribution of each cellular type (endothelial and smooth muscle cells) in relation to the oxidative stress and mitochondrial energy metabolism. The main results were that the EDD and EID were progressively reduced by aging whereas the vasodilatation activity of the endothelial cells was decreased between adulthood and middle-age after having been noticeably increased from youth to adulthood.

Aging, coronary flow, cardiac mechanical function and mitochondrial energy metabolism

In the present study, we were not able to obtain a satisfying evaluation of the coronary flow, since we used part of the fresh myocardium to prepare mitochondria. We were thus unable to determine the heart weight, a parameter which is essential to estimate the coronary flow. Yet, the heart weight is known to increase with age in the rat. One of our recent study (Mourmoura *et al.*, 2011) performed with the same batch of animals revealed that the heart weight increased by 28% between the ages of

2.5 and 12 months. However, the coronary flow expressed as ml/min/g of dry weight was unchanged, suggesting that the coronary bed adapted in parallel with the gain of heart weight in normal aging. This confirms the study of Tomanek et *al.* (1991) which indicates remodeling of the coronary vessels with age. This morphological study performed in young and senescent beagles showed that aging reduces the capillary numerical density, but maintains their volume density through a compensatory increase in capillary diameter. Thus, aging could not modify the coronary flow. We do not know if this vessel remodeling occurred in our rats, since species difference could occur and the animals used in the present study were not senescent but only middle-aged, but the supposed maintenance of their coronary flow with age allows the gratifying estimation of the coronary reserve. It could also be responsible for a maintained cardiac mechanical activity in the middle aged animals.

The results of our study confirmed the age-related maintenance of the cardiac mechanical activity as the rate pressure products, left ventricle developed pressures and heart rates were similar in all age groups studied. Furthermore, the study that we recently published (Mourmoura *et al.*, 2011) permitted to demonstrate that the cardiac mechanical efficiency estimated as the ratio between rate pressure product and heart dry weight was the same in young and middle aged animals. This observation is in striking contrast with the results of the mitochondrial oxidative phosphorylation observed in our study. Indeed, we saw that the transition from youth to young adulthood reduced the oxidative phosphorylation whatever the substrate used and the respiration conditions, but stabilized thereafter until middle age. These changes were not correlated with modifications of the body weight, but paralleled those of the abdominal fat mass, suggesting the involvement of adipocytokines. They agree well with the results published in the literature (Fannin *et al.*, 1999; Delaval *et al.*, 2004) which report an age-related decline in mitochondrial oxidative phosphorylation, but they are in disagreement with results previously obtained in our laboratory, which did not show any modification of the respiration between youth and middle age (Mourmoura *et al.*, 2011). However, in this previous study, the oxidative phosphorylation was estimated in the absence of calcium, whereas calcium was present in this study. Calcium is known to activate several Krebs cycle dehydrogenases (Cox & Matlib 1993). This leads to maximally stimulated mitochondrial respirations in states II, III and IV, allowing the

emphasis of differences which does not exist in the absence of the divalent cation. Similar were the results of the cardiac mechanical function which can also be explained by a low cardiac activity in our Langendorff's mode perfusion at low extracellular calcium concentration. Aging could have reduced the cardiac mechanical work if the hearts had been maximally stimulated (working mode with high preload and perfusate calcium concentration) as also evidenced by the observation that the decreased mitochondrial function was associated with a progressive decline in EDD as the animals got older.

Oxidative stress

Advanced aging is known to increase the oxidative stress (Labunskyy & Gladyshev, 2012) notably in the mitochondrial fraction at the level of the respiratory chain complex III due to an inhibition of this electron transfer system (Fannin *et al.*, 1999; Lesnefsky *et al.*, 2001; Hoppel *et al.*, 2002). In the present study, we also evaluated the H_2O_2 production by isolated cardiac mitochondria derived from young, young adult and middle-aged rats in order to detect the initial changes in reactive oxygen species (ROS) generation and their localization in the respiration chain. Glutamate/malate, a complex I-related substrate, increased the H_2O_2 generation as soon as the 6^{th} month of life and the phenomenon seemed to occur mainly at the level of complex I. In contrast, succinate, a complex II-related substrate, increased the H_2O_2 generation only at the 11^{th} month of life through a production occurring by reverse electron flux at the level of complex I. A similar pattern was observed when glutamate/malate and succinate were used together. Transition from youth to young adulthood did not favor H_2O_2 production, but that occurring from young adulthood to middle age increased it at the level of complex I. These results indicate that the increase in mitochondrial H_2O_2 generation occurs mainly from middle age and that the complex III-related overproduction occurring with advanced aging was not observed at this period of life. That was confirmed by the results of the respiratory chain complex activities which were not affected by age. Finally, it is interesting to emphasize that the increased H_2O_2 production observed at middle age paralleled the decreased glucose tolerance measured after glucose loading in the animals.

The impact of these changes in mitochondrial oxidative stress was estimated *ex vivo* by evaluating the aconitase to fumarase and lactate to pyruvate ratios in the whole perfused hearts. The aconitase to fumarase and lactate to pyruvate ratios reflecting the *ex vivo* mitochondrial and cytosolic oxidative stress were not affected by aging. Thus, although producing more H_2O_2 at the mitochondrial level, the middle-aged hearts contained sufficient anti-oxidant reserves to scavenge these toxic molecules. The only increase in oxidative stress was noticed in middle-aged animals in the plasma compartment. It could result from the activation of NADPH oxidase occurring at this age in the large conduit arteries (Oudot *et al.*, 2006) or in the adipose tissue (Furukawa *et al.*, 2004) when its mass augments. Since the endothelial and smooth muscle cells contain phosphocreatine (Sterin *et al.*, 2008) and creatine kinases, the plasma oxidative stress observed at middle age in our study could depress the energy transfer into the vascular cells.

Aging and coronary reserve

Our study showed that aging triggered a progressive decrease in EDD, which began as soon as youth. That phenomenon is well recognized now with studies in humans (Chauhan *et al.*, 1996; Egashira *et al.*, 1993) and laboratory animals (Toma *et al.*, 1985) agreeing well with this age-related decline. However, the contribution of each vascular cellular type is not known. Our study allows the description of that contribution. The function of the vascular smooth muscle cells of the coronary microvasculature was easily depicted in our study through the measurement of the EID, since the nitric oxide donor nitroprusside permits the relaxation of those cells. That parameter was high in young hearts and drastically decreased as soon as the young adulthood to values which were very close to those observed at the middle age. Those results perfectly fit with the observations made by Toma *et al.* (1985) in the isolated guinea pig hearts. Energy is necessary for the relaxation of muscular cells and the low oxidative phosphorylation detected in the isolated mitochondria derived from young adult and middle age hearts can perfectly explain the age-related decline observed for EID. That decrease contributed to the progressive age-related loss of EDD.

The function of endothelial cells is more difficult to evaluate. In the present study, we mathematically extract from the EDD and EID curves a parameter that depicted the vasodilatation activity of endothelial cells. Although that parameter is expressed in picomoles of nitroprusside, it does not reflect the vasodilatation activity resulting only from NO production, but it also takes into account all the vasodilatation agents emitted by the endothelial cells. Interestingly, the endothelial cell vasodilatation activity (ECVA) was strongly increased from youth to young adulthood. As shown by the unchanged Western Blot analysis of the total and phosphorylated eNOS forms, the difference in ECVA was not due to that enzyme, although the analysis was performed under basal conditions when the endothelial cells were not stimulated by acetylcholine. It could be due to an increase in muscarinic receptor density or to an increase in acetylcholine-induced calcium influx, since calcium is known to stimulate eNOS activity (Haines *et al.*, 2012). It could also result from production of a rescue vasodilatation agent different than nitric oxide, in example the endothelium-derived hyperpolarizing factor (EDHF) which is known to play an important role in the regulation of the coronary microvasculature (Oltman *et al.*, 2001). The reduction of the production of a constrictor factor could also intervene. With the transition from young adulthood to middle age, an important decrease in ECVA occurred which paralleled the increased plasma oxidative stress observed during this phase. The decreased EDD occurring with age with the contribution of the reduced ECVA is known to be reversed by L-arginine infusion in the coronary network (Chauhan *et al.*, 1996). Yet, citrulline, the degradation product of L-arginine during the production of nitric oxide, is regenerated in L-arginine through an energy-dependent process (Wu & Meininger, 1993). The age-induced decrease in mitochondrial energy production observed in our study in isolated mitochondria could be related to problems of energy transfer due to the plasma oxidative stress and thus contribute to a reduction of the L-arginine bioavailability in endothelial cells and the eventual decrease in ECVA occurring between young adulthood and middle age.

Conclusion

These data indicate that aging from youth to middle age triggered a decline in EDD which was due to functional modifications of both ECs and SMCs. Between youth and young adulthood the EDD decrease was due to a strong reduction of the SMCs function, but ECs tried to compensate by augmenting their dilatation activity. Thereafter, between young adulthood and middle age, relaxation of SMCs stabilized, but EC dilatation activity significantly decreased. These aging-induced alterations of the vascular cell function could be explained by abnormalities of the energy metabolism, namely a reduction of the mitochondrial oxidative phosphorylation occurring as soon as the young adulthood, and a possible systemic oxidative stress-related inhibition of the energy transfer occurring at middle age.

Experimental procedures

Experimental Animals and Diet

All experiments followed the European Union recommendations concerning the care and use of laboratory animals for experimental and scientific purposes. All animal work was approved by the local board of ethics for animal experimentation (Cometh, authorization number: 380537).

Twenty-one male Wistar rats from an inbred colony were housed two per cage in our animal facility at 3 months of age. Afterwards, they were divided in three age groups of 7 animals; the young (Y), young adult (YA) and middle-aged (MA) rats sacrificed at the age of 3, 6 and 11 months, respectively. They were fed a standard carbohydrate diet (A04, Safe, France) *ad libitum*, had free access to water and their body weight was recorded twice per week. On the day of the experiment, the rats were weighed and heparinized via the saphenous vein (1000 I.U./kg) before their sacrifice. Blood samples were collected for further biochemical analysis and their adipose tissue was quantified for determination of the abdominal fat mass.

Oral Glucose Tolerance Test (OGTT)

An OGTT was performed two weeks before the sacrifice. Food was removed from rats 18 h before they were given orally a glucose dose (1 g glucose/kg body weight, between 08.00 and 10.00 am). Blood samples were collected from the tail vein in heparinized tubes immediately before and at 5, 25, 40, 60 and 180 min after glucose administration to determine the plasma glucose concentrations. Glucose concentrations were determined with a glucose analyzer (ACCU-CHECK Active, Softclix). The area under the plasma glucose curve (AUC) as well as the difference between the initial glucose concentration and that determined at times 25 (delta 25) and 180 min (delta 180) post-administration were then calculated in order to evaluate the glucose tolerance as previously used by Cortez *et al.* (1991).

Heart perfusion

A rapid thoracotomy was performed and the heart was immediately collected in Krebs-Heinselet solution maintained at 4°C. It was then rapidly (during the first min following thorax opening) perfused at constant pressure (59 mmHg) according to the Langendorff mode. The Krebs–Heinselett buffer used contained (in mM) NaCl 119, $MgSO_4$ 1.2, KCl 4.8, $NaHCO_3$ 25, KH_2PO_4 1.2, $CaCl_2$ 1.2 and glucose 11 mM as sole energy substrate. It was maintained at 37°C and continuously oxygenated with carbogen (95% O_2/5% CO_2). A latex balloon connected to a pressure probe was inserted into the left ventricle and filled until the diastolic pressure reached a value of 7–8 mmHg. It allowed the evaluation of heart rate, systolic, diastolic and left ventricle developed pressures throughout the perfusion protocol. The heart was perfused at constant pressure for 30 minutes with a pressure gauge inserted into the perfusion circuit just upstream the aortic cannula. This allowed the estimation of the coronary flow for each heart which was evaluated by weight determination of 1-min collected samples at the 25th min of perfusion. After the 30-min perfusion at constant pressure, the heart was perfused with a peristaltic pump (Gilson, Villiers-Le-Bel, France) at the coronary flow previously determined during the perfusion at constant pressure. The systolic, diastolic and left ventricle developed pressures

as well as the heart rates were determined after 10 min of perfusion at forced flow in order to allow the heart a satisfying stabilization. The left ventricle developed pressure was calculated by subtracting the diastolic pressure to the systolic pressure. The rate pressure product (RPP) was defined as the product between the left ventricle developed pressure and heart rate. It was used as indicator of the cardiac mechanical work (Gobel *et al.*, 1978). All the parameters were recorded and analyzed with a computer using the HSE IsoHeart software (Hugo Sachs Elektronik). The perfusion at constant flow was continued until the end of the measurement of the coronary reactivity.

Coronary Reactivity

After the 10-min equilibration period at constant flow, the coronary tone was raised via the constant infusion of the thromboxane analog U46619 (30 nM) that was continuously infused into the perfusion system near the aortic cannula at a rate never exceeding 1.5% of the coronary flow. This allowed the obtainment of a coronary pressure between 110 and 130 mmHg. In our model of perfusion at forced flow, the aortic pressure equaled the coronary pressure and changes in the coronary tone triggered modifications of this pressure. Changes in aortic perfusion pressure were thus used to monitor changes in coronary tone. Relaxation responses to acetylcholine (Ach, 4, 10, 20, 40, 60, 80 and 100 pmoles) and sodium nitroprusside (SNP, 100, 200, 400, 600, 800 and 1000 pmoles) injections were then determined reflecting the endothelial-dependent vasodilatation (EDD) and endothelium-independent vasodilatation (EID) respectively.

The dilatation amplitude was calculated as the ratio between the maximal decrease in the coronary pressure and the coronary pressure just before the injection of the dilatation agents. Since the heart weight and coronary volume were subjected to intra- and inter-group variations, a correction was performed to normalise the input-function of the vasodilatation agents according to the coronary flow. The dose-response curve between the amount of vasodilatation agent injected and the maximal vasodilatation was then fitted to a logarithm function for each heart which allowed the fulfillment of statistical analyses. Moreover, the vasodilatation activities of the endothelial cells were also estimated

from the corrected EDD and EID curves. For each heart and each injected Ach dose, the amount of SNP (reflecting the amount of dilatation agent) necessary to obtain the same percentage of Ach-induced vasodilatation was extracted from the EID curve according to the formula: endothelial cell vasodilatation activity (ECVA) = $e^{[(\%\ \text{Ach-induced dilatation} - b) / a]}$, where a and b are the coefficients of the theoretical EID curve. The results were expressed in pmoles-equivalents of SNP. At the end of the perfusion protocol, a piece of myocardium (about 200 mg) from the apex of the heart was immediately freeze-clamped and stored at −80°C for further analysis. The other part of the myocardium was immediately used for isolated mitochondria preparation.

Mitochondria preparation

After the perfusion, atria and the remaining aorta were cut off from the heart. Myocardium was minced with scissors in a cold isolation buffer composed of (in mM) sucrose (150), KCl (75), Tris–Base (50), KH_2PO_4 (1), $MgCl_2$ (5), and EGTA (1), pH 7.4, fatty acid-free serum albumin 0.2%. The pieces of myocardium were rinsed several times on a filter and put in an Elvehjem potter containing 15 ml of isolation buffer. A protease (subtilisin 0.02%) was added for 1 min to digest myofibrils at ice temperature, and the totality was then homogenized with the potter (300 rpm, 5 to 6 transitions). Subtilisin action was stopped by addition of the isolation buffer (30 ml). The homogenate was then centrifuged (800 x g, 10 min, 4°C), and the resulting supernatant was collected and filtered. Mitochondria were then washed through two series of centrifugation (8,000 × g, 10 min, 4°C). The last pellet of mitochondria was re-suspended in sucrose 250 mM, Tris–Base 10 mM, EGTA 1 mM, pH 7.4 at a concentration of approximately 10 mg/ml.

Respiration measurements

The rate of mitochondrial oxygen consumption was measured at 30°C in an incubation chamber with a Clarke-type O_2 electrode filled with 1 ml of incubation medium (KCl 125 mM, Tris–Base 20 mM,

EDTA 5 μM, $CaCl_2$ 10 μM, KH_2PO_4 3 mM, pH 7.2, fatty acid-free bovine serum albumin 0.15%). A low amount of $CaCl_2$ was added to the medium in order to stimulate the oxidative phosphorylation. All measurements were performed using mitochondria (0.2 mg mitochondrial protein/ml) incubated with the following substrates: i) glutamate (5.5 mM)/malate (2.5 mM); ii) succinate (5.5 mM) plus rotenone (2.5 μM); iii) glutamate (5.5 mM)/malate (2.5 mM)/succinate (5.5 mM) in the presence of ADP 1 mM (state 3) and after addition of oligomycin (0.5 μg/ml). The incubation medium was constantly stirred with a built-in electromagnetic stirrer and bar flea. Coupling of the mitochondrial oxidative phosphorylation was assessed by the state 3/state 4 ratio (respiratory control ratio or RCR). When glutamate/malate was used as a substrate, the RCR averaged 6.5 ± 0.3, 6.6 ± 0.9 and 7.3 ± 0.5 in the Y, YA and MA groups, indicating a satisfying integrity of our mitochondrial preparations.

Mitochondrial reactive oxygen species release

The rate of mitochondrial H_2O_2 production was measured at 30°C on a F-2500 Hitachi spectrofluorimeter. It followed the linear increase in fluorescence (excitation at 560 nm and emission at 584 nm) due to enzymatic oxidation of amplex red by H_2O_2 in presence of horseradish peroxidase. Reaction conditions were 0.25 mg of mitochondrial protein/ml, 5 U/ml of horseradish peroxidase, 1 μM of amplex red, with either glutamate/malate, succinate without rotenone, or glutamate/malate/succinate (in the same concentrations as in the respiration measurements). They were added in order to start the reaction in the same incubation buffer with that used for measurements of mitochondrial oxygen consumption. Mitochondrial ROS were measured in the absence of ADP. Rotenone (1 μM) and antimycin A (0.5 μM) were sequentially added to determine, respectively, the maximum rate of H_2O_2 production of complexes I and III of the respiratory chain.

Oxidative stress measurements

Plasma oxidative stress

Protein oxidation in the plasma was evaluated by the disappearance of protein thiol groups (Favier, 1995).

The antioxidant status of the plasma was evaluated using ferric reducing antioxidant power (FRAP) assay as a global marker of the antioxidant power. The FRAP assay uses antioxidants as reductants in a redox-linked colorimetric method. In this assay, at low pH, a ferric-tripyridyltriazine (Fe^{III}-TPTZ) complex is reduced to the ferrous form, which is blue and monitored by measuring the change in absorption at 593 nm. The change in absorbance is directly proportional to the reducing power of the electron-donating antioxidants present in the plasma. The absorbance change is translated into a FRAP value (in μmol/l) by relating the change of absorbance at 593 nm of test sample to that of a standard solution of known FRAP value.

GPx activity was evaluated by the modified method of Gunzler *et al.*(1974) using terbutyl hydroperoxide (Sigma Chemical Co, Via Coger, Paris, France) as a substrate.

Cytosolic Oxidative stress

Lactate and pyruvate released in the coronary effluents were spectrophotometrically assayed according to Bergmeyer (1974). The lactate to pyruvate ratio was calculated to estimate the cytosolic redox potential (Nuutinen, 1984).

Mitochondrial oxidative stress

The ratio between the activities of aconitase and fumarase of the myocardium was calculated as an indicator of *ex vivo* mitochondrial ROS production. Aconitase and fumarase activities were determined according to Gardner *et al.* (1994).

Activities of the respiratory chain complexes and citrate synthase

Activities of the NADH-ubiquinone oxydo-reductase (complex I), succinate-ubiquinone oxydo-reductase (complex II), ubiquinol cytochrome c reductase (complex III) and cytochrome c oxidase (complex IV) were determined as previously described (Mourmoura *et al.*, 2011) in isolated mitochondria. The citrate synthase activity was determined in cardiac homogenates according to Faloona and Srere (1969).

Western blot

The expression of total endothelial NOS (eNOS) and phosphorylated eNOS Ser1177 was evaluated by Western blot. Frozen samples were homogenized in ice-cold lysis buffer containing 20 mM Tris (pH 7.8), 137 mM NaCl, 2.7 mM KCl, 1 mM MgCl2, 1% Triton X-100, 10% (w/v) glycerol, 10 mM NaF, 1 mM ethylenediaminetetraacetic acid, 5 mM Na pyrophosphate, 0.5 mM Na_3VO_4, 1 µg/ml leupeptin, 0.2 mM phenylmethylsulfonyl fluoride and 1 mM benzamidine. The homogenates were centrifuged at 5,000 *g* for 20 min at 4°C, and the protein concentration in the supernatant was determined in each aliquot. Protein extracts (50 µg/lane) were loaded onto a 10% SDS gel and separated by electrophoresis. Extracts from the control group were loaded on both gels, and the amount of protein was accordingly compared pairwise. Proteins were transferred to nitrocellulose membranes. The membranes were incubated overnight at 4°C with rabbit antibodies against total eNOS (1:150, Thermoscientific, Illkirch, France) and phosphospecific mouse antibodies against eNOS Ser1177 (1:1,000, BD Biosciences Pharmingen, Le Pont de Claix, France). After being washed in TBS-Tween, the membranes were incubated with horseradish peroxidase-conjugated anti-mouse IgG for eNOS Ser1177 (1:3000, Jackson Immunoresearch, *Montluçon*, France) and anti-rabbit IgG for total eNOS (1:20000, Jackson Immunoresearch, *Montluçon*, France) for 1h at room temperature, followed by additional washing. Proteins were visualized by enhanced chemiluminescence with ECL advanced Western blotting detection kit (Amersham Biosciences, Brumath, France) and quantified using

densitometry and Image J software. PAN-Actin (1:1000, Cell Signaling Technology, *St-Quentin-en-Yvelines*, France) was used as a loading control.

Other biochemical determinations

Proteins were measured using the bicinchoninic acid method with a commercially available kit (Thermo Scientific, Rockford, IL).

Statistical analysis

Results are presented as mean ± S.E.M. Animal weight, glycemia, activity of respiratory chain complexes and data describing the oxidative stress, the mitochondrial function, the cardiac mechanical and vascular function (developed pressure, heart rate, rate pressure product, coronary pressure) were contrasted across the three groups by one-way analysis of variance (ANOVA). Measures related to the action of the vasodilatation agents were treated with repeated-measures ANOVA to test the effect of the age (external factor), that of the amount of dilatation agent (internal factor) and their interactions. When required, group means were contrasted with a Fisher's LSD test. A probability (p) less than 0.05 was considered significant. Statistical analysis was performed using the NCSS 2004 software.

Acknowledgements

We would like to thank M. Christophe Cottet for carefully editing the manuscript, Cindy Tellier for animal care, Joëlle Demaison for the determination of the respiratory chain complex activities, and Mireille Osman for the measurements of GPx activity, FRAP assay and thiol groups in the plasma. This work was supported by the French National Institute of Agronomical Research (INRA), the French National Institute of Health and Medical Research (INSERM) and Joseph Fourier University, Grenoble, France.

References

Bergmeyer HU (1974) Methods of enzymatic analysis. New-York, London: Verlag Chemie, Weinheim

Castelluccio C, Baracca A, Fato R, Pallotti F, Maranesi M, Barzanti V, Gorini A, Villa RF, Parenti Castelli G, Marchetti M (1994) Mitochondrial activities of rat heart during ageing. Mech Ageing Dev. **76**, 73-88

Charansonney OL (2011) Physical activity and aging: a life-long story. Discov Med. **12**, 177-185

Chauhan A, More RS, Mullins PA, Taylor G, Petch C, Schofield PM (1996) Aging-associated endothelial dysfunction in humans is reversed by L-arginine. J Am Coll Cardiol. **28**, 1796-1804

Cortez MY, Torgan CE, Brozinick JT Jr, Ivy JL (1991) Insulin resistance of obese Zucker rats exercise trained at two different intensities. Am J Physiol. **261**, E613-E619

Cox DA, Matlib MA (1993) A role for the mitochondrial $Na^{(+)}$-Ca^{2+} exchanger in the regulation of oxidative phosphorylation in isolated heart mitochondria. J Biol Chem. **268**, 938-947

Delaval E, Perichon M, Friguet B (2004) Age-related impairment of mitochondrial matrix aconitase and ATP-stimulated protease in rat liver and heart. Eur J Biochem. **271**, 4559-4564

Effron MB, Bhatnagar GM, Spurgeon HA, Ruaño-Arroyo G, Lakatta EG (1987) Changes in myosin isoenzymes, ATPase activity, and contraction duration in rat cardiac muscle with aging can be modulated by thyroxine. Circ Res. **60**, 238-245

Egashira K, Inou T, Hirooka Y, Kai H, Sugimachi M, Suzuki S, Kuga T, Urabe Y, Takeshita A (1993) Effects of age on endothelium-dependent vasodilation of resistance coronary artery by acetylcholine in humans. Circulation. **88**, 77-81

Faloona GR, Srere PA (1969) Escherichia coli citrate synthase. Purification and the effect of potassium on some properties. Biochemistry. **8**, 4497-4503

Fannin SW, Lesnefsky EJ, Slabe TJ, Hassan MO, Hoppel CL (1999) Aging selectively decreases oxidative capacity in rat heart interfibrillar mitochondria. Arch Biochem Biophys. **372**, 399-407

Favier AE (1995) Analysis of free radicals in biological systems. Basel: Birkhauser Verlag

Furukawa S, Fujita T, Shimabukuro M, Iwaki M, Yamada Y, Nakajima Y, Nakayama O, Makishima M, Matsuda M, Shimomura I (2004) Increased oxidative stress in obesity and its impact on metabolic syndrome. J Clin Invest. **114**, 1752-1761

Gardner PR, Nguyen DD, White CW (1994) Aconitase is a sensitive and critical target of oxygen poisoning in cultured mammalian cells and in rat lungs. Proc Natl Acad Sci USA. **91**, 12248-12252

Gobel FL, Norstrom LA, Nelson RR, Jorgensen CR, Wang Y (1978) The rate-pressure product as an index of myocardial oxygen consumption during exercise in patients with angina pectoris. Circulation. **57**, 549-556

Günzler WA, Kremers H, Flohé L (1974) An improved coupled test procedure for glutathione peroxidase (EC 1-11-1-9-) in blood. Z Klin Chem Klin Biochem. **12**, 444-448

Haines RJ, Corbin KD, Pendleton LC, Eichler DC (2012) Protein Kinase Cα Phosphorylates a Novel Argininosuccinate Synthase Site at Serine 328 during Calcium-dependent Stimulation of Endothelial Nitric-oxide Synthase in Vascular Endothelial Cells. J Biol Chem. **287**, 26168-26176

Hoppel CL, Moghaddas S, Lesnefsky EJ (2002) Interfibrillar cardiac mitochondrial complex III defects in the aging rat heart. Biogerontology. **3**, 41-44

Labunskyy VM, Gladyshev VN (2012) Role of Reactive Oxygen Species-mediated Signaling in Aging. Antioxid Redox Signal. [Epub ahead of print]

Lee HY, Oh BH (2010) Aging and arterial stiffness. Circ J. **74**, 2257-2262

Liviakis L, Pogue B, Paramsothy P, Bourne A, Gill EA (2010) Carotid intima-media thickness for the practicing lipidologist. J Clin Lipidol. **4**, 24-35

Mourmoura E, Leguen M, Dubouchaud H, Couturier K, Vitiello D, Lafond JL, Richardson M, Leverve X, Demaison L (2011) Middle age aggravates myocardial ischemia through surprising upholding of complex II activity, oxidative stress, and reduced coronary perfusion. Age (Dordr). **33**, 321-336

Nuutinen EM (1984) Subcellular origin of the surface fluorescence of reduced nicotinamide nucleotides in the isolated perfused rat heart. Basic Res Cardiol. **79**, 49-58

Oltman CL, Kane NL, Fudge JL, Weintraub NL, Dellsperger KC (2001) Endothelium-derived hyperpolarizing factor in coronary microcirculation: responses to arachidonic acid. Am J Physiol. **281**, H1553-H1560

Oudot A, Martin C, Busseuil D, Vergely C, Demaison L, Rochette L (2006) NADPH oxidases are in part responsible for increased cardiovascular superoxide production during aging. Free Radic Biol Med. **40**, 2214-2222

Ozawa T (1997) Genetic and functional changes in mitochondria associated with aging. Physiol Rev. **77**, 425-464

Sawabe M (2010) Vascular aging: from molecular mechanism to clinical significance. Geriatr Gerontol Int. **10**, S213-S220

Sawabe M, Hamamatsu A, Chida K, Mieno MN, Ozawa T (2011) Age is a major pathobiological determinant of aortic dilatation: a large autopsy study of community deaths. J Atheroscler Thromb. **18**, 157-165

Scott AD, Keegan J, Mohiaddin RH, Firmin DN (2011) Noninvasive detection of coronary artery wall thickening with age in healthy subjects using high resolution MRI with beat-to-beat respiratory motion correction. J Magn Reson Imaging. **34**, 824-830

Shirwany NA, Zou MH (2010) Arterial stiffness: a brief review. Acta Pharmacol Sin. **31**, 1267-1276

Sterin M, Ringel I, Lecht S, Lelkes PI, Lazarovici P (2008) 31P magnetic resonance spectroscopy of endothelial cells grown in three-dimensional matrigel construct as an enabling platform technology: I. The effect of glial cells and valproic acid on phosphometabolite levels. Endothelium. **15**, 288-298

Sugiyama S, Takasawa M, Hayakawa M, Ozawa T (1993) Changes in skeletal muscle, heart and liver mitochondrial electron transport activities in rats and dogs of various ages. Biochem Mol Biol Int. **30**, 937-944

Takemura A, Iijima K, Ouchi Y (2010) Molecular mechanism of vascular aging: impact of vascular smooth muscle cell calcification via cellular senescence. Clin Calcium. **20**, 1646-1655

Toma BS, Wangler RD, DeWitt DF, Sparks HV Jr (1985) Effect of development on coronary vasodilator reserve in the isolated guinea pig heart. Circ Res. **57**, 538-544

Tomanek RJ, Aydelotte MR, Torry RJ (1991) Remodeling of coronary vessels during aging in purebred beagles. Circ Res. **69**, 1068-1074

Venkataraman P, Krishnamoorthy G, Selvakumar K, Arunakaran J (2009) Oxidative stress alters creatine kinase system in serum and brain regions of polychlorinated biphenyl (Aroclor 1254)-exposed rats: protective role of melatonin. Basic Clin Pharmacol Toxicol. **105**, 92-97

Wijnands KA, Vink H, Briedé JJ, van Faassen EE, Lamers WH, Buurman WA, Poeze M (2012) Citrulline a more suitable substrate than arginine to restore NO production and the microcirculation during endotoxemia. PLoS One. **7**, e37439

Wu G, Meininger CJ (1993) Regulation of L-arginine synthesis from L-citrulline by L-glutamine in endothelial cells. Am J Physiol. **265**, H1965-H1971

Wyatt AW, Steinert JR, Mann GE (2004) Modulation of the L-arginine/nitric oxide signalling pathway in vascular endothelial cells. Biochem Soc Symp. **71**, 143-156

Table 1 Basic characteristics of the animals

	Y	YA	MA
Body weight (g)	386 ± 5^{a}	445 ± 8^{b}	503 ± 15^{c}
Epididymal AT (g)	7.1 ± 0.5^{a}	13.5 ± 1.3^{b}	15.4 ± 1.1^{b}
Visceral AT (g)	4.4 ± 0.4^{a}	9.4 ± 1^{b}	10.7 ± 0.6^{b}
Retroperitoneal AT (g)	7.4 ± 0.6^{a}	12.8 ± 1.4^{b}	12.7 ± 1^{b}
Abdominal AT (g)	11.8 ± 0.8^{a}	22.2 ± 2.2^{b}	23.3 ± 21.3^{b}
Abdominal AT/BW	0.03 ± 0.002^{a}	0.05 ± 0.005^{b}	0.05 ± 0.002^{b}
Triglycerides (g/l)	1.2 ± 0.1	1.3 ± 0.1	0.9 ± 0.2
Cholesterol (g/l)	0.52 ± 0.02	0.56 ± 0.02	0.63 ± 0.01

The number of experiments was 7 per group. The abdominal adipose tissue weight normalized to the body weight is expressed in g of wet weight per g of body weight. AT: adipose tissue; BW: body weight; a, b, c: the absence of a common letter indicates a significant difference.

Table 2 *Ex vivo* cardiac function

	Y	YA	MA
HR (beats/min)	279 ± 20	264 ± 13	249 ± 16
LVDP (mmHg)	113 ± 11	92.4 ± 9	109 ± 9
RPP (mHg/min)	31.2 ± 3	23.6 ± 1	26.9 ± 2
CP before U46619 (mmHg)	68.2 ± 8	73.6 ± 5	81.5 ± 3
CP after U46619 (mmHg)	110 ± 15	123 ± 8	132 ± 9

The number of experiments was 7 per group. HR: heart rate; LVDP: left ventricle developed pressure; RPP: rate pressure product; CP: coronary pressure

Figure captions

Fig. 1 Basal glycaemia (panel A), area under the curve after a glucose loading (panel B), difference between the basal glycaemia and those measured 25 min (delta25, panel C) and 180 min (delta180, panel D) after the glucose loading. The number of experiments was 7 per group. Y: young animals; YA: young adult animals; MA: middle-aged animals; AUC total: total area under the curve; a,b: significantly different.

Fig. 2 Coronary reactivity in Y (young) YA (young adult) and MA (middle-aged) rats. The number of experiments was 7 per group. EDD (panel A): endothelial-dependant vasodilatation; EID (panel B): endothelia-independent vasodilatation; ECVA (panel C): endothelial cell vasodilatation activity; SNP: sodium nitroprusside; a,b,c: the absence of a common letter indicates a significant difference.

Fig. 3 Western Blotting of the total endothelial nitric oxide synthase (eNOS), eNOS phosphorylated at serine 1177 (peNOS) and actin. p-eNOS/eNOS: ratio between the phosphorylated and total eNOS. Panel A: representative immunoblots; panel B: quantification. The number of experiments was 7 per group. Y, YA, MA: young, young adult and middle-aged animals.

Fig. 4 Influence of aging on the oxidative stress. Panel A: plasma thiol groups; panel B: antioxidant status of the plasma (FRAP); panel C: plasma glutathione peroxidase activity; panel D: lactate to pyruvate ratio in the coronary effluents reflecting the cytosolic oxidative stress; panel E: cardiac aconitase to fumarase ratio reflecting the mitochondrial oxidative stress. The number of experiments was 7 per group. Y, YA, MA: young, young adult and middle-aged rats; a,b: the absence of a common letter indicates a significant difference.

Fig. 5 Influence of aging on the mitochondrial H_2O_2 production under basal conditions (absence of rotenone and antimycin A), after inhibition of complex I (rotenone alone) and after inhibition of complexes I and III (rotenone in association with antimycin A) in the presence of glutamate/malate (panel A), succinate (panel B) and glutamate/malate/succinate (panel C) as substrates. The number of experiments was 7 per group. Y, YA, MA: young, young adult and middle-aged rats; a,b,c: the absence of a common letter indicates a significant difference.

Fig. 6 Influence of aging on the state 3 and state 4 respiration rates of mitochondria oxidizing glutamate/malate (panel A), succinate/rotenone (panel B) and glutamate/malate/succinate (panel C). The number of experiments was 7 per group. Y, YA, MA: young, young adult and middle-aged rats; G/M/S: glutamate/malate/succinate; a,b: the absence of a common letter indicates a significant difference.

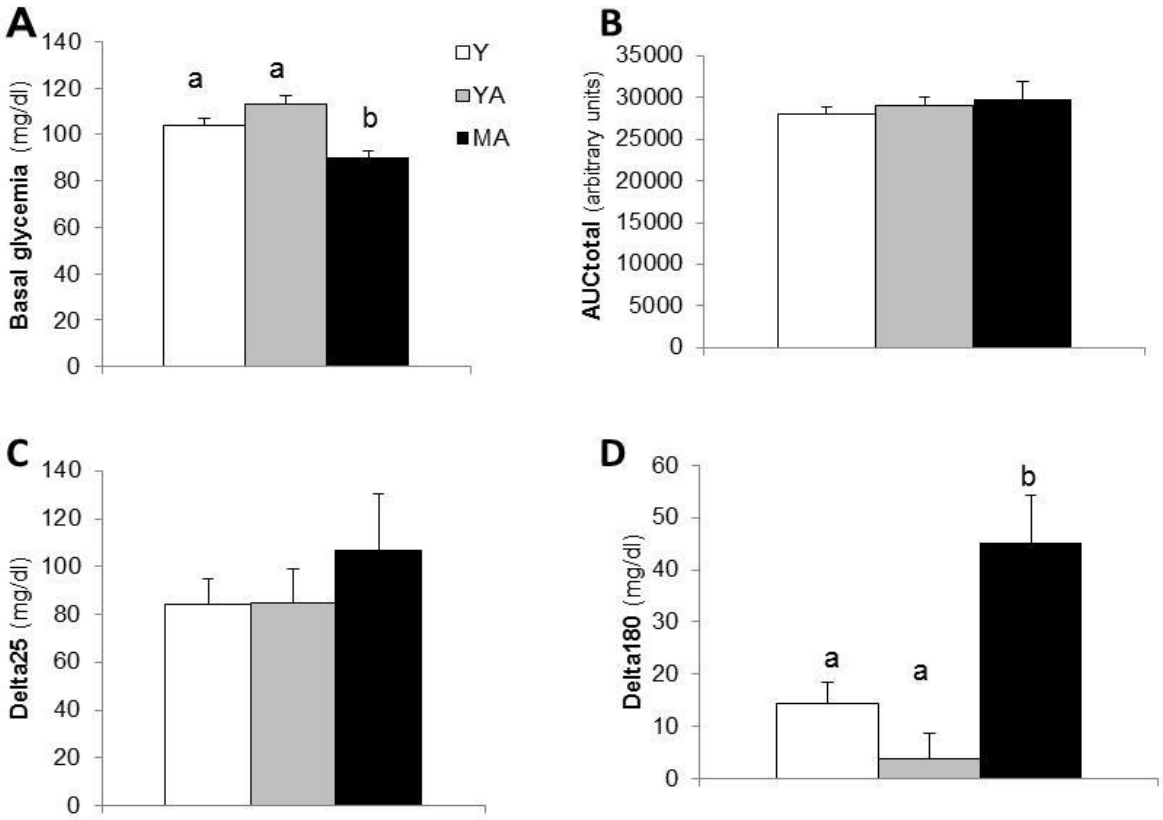
A
Basal glycemia (mg/dl)
140
120
100
80
60
40
20
0
a
a
b
Y
YA
MA
B
AUCtotal (arbitrary units)
35000
30000
25000
20000
15000
10000
5000
0
C
Delta25 (mg/dl)
140
120
100
80
60
40
20
0
D
Delta180 (mg/dl)
60
50
40
30
20
10
0
a
a
b

Figure 1

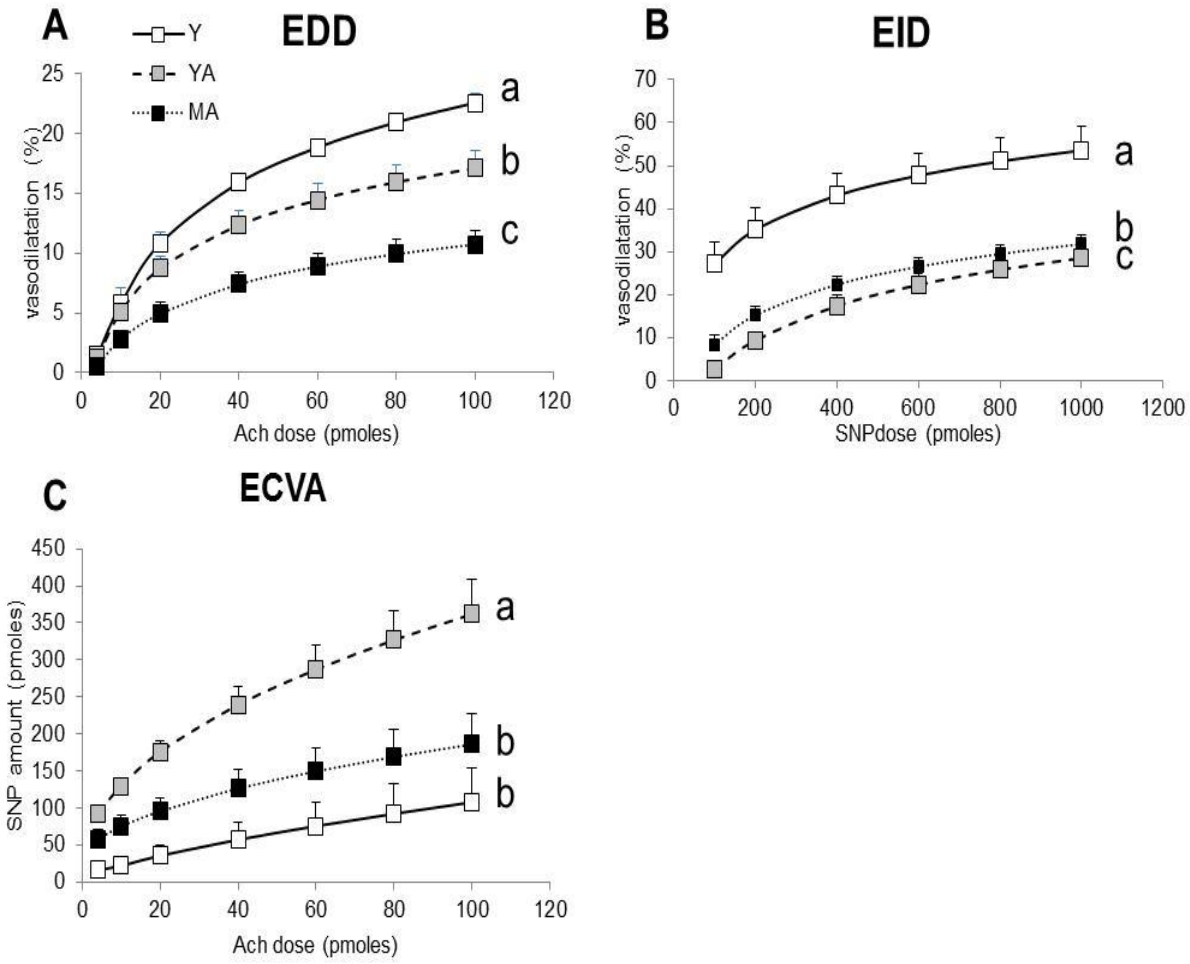
A
EDD
Y
YA
MA
vasodilatation (%)
Ach dose (pmoles)
a
b
c
B
EID
vasodilatation (%)
SNPdose (pmoles)
a
b
c
C
ECVA
SNP amount (pmoles)
Ach dose (pmoles)
a
b
b

Figure 2

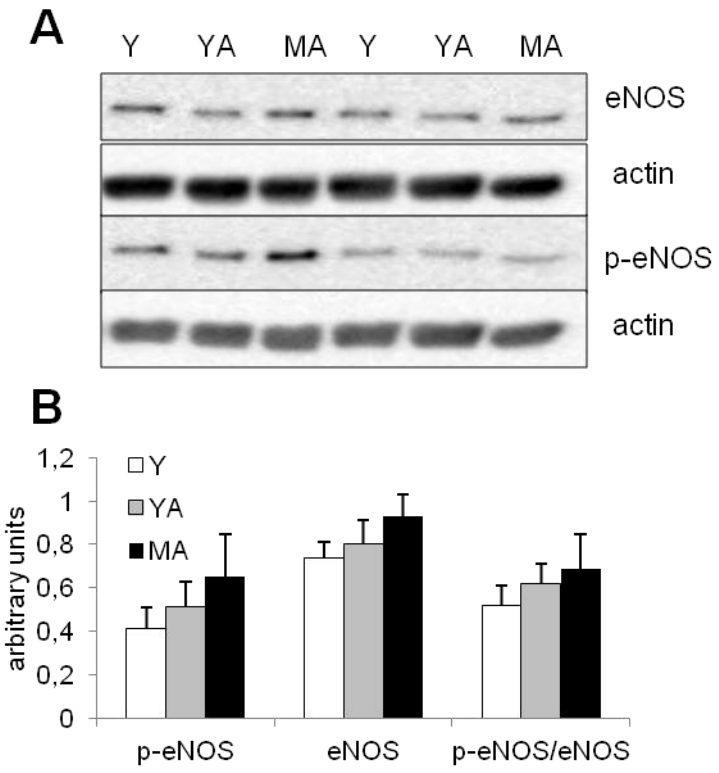
A
Y
YA
MA
Y
YA
MA
eNOS
actin
p-eNOS
actin
B
arbitrary units
1,2
1
0,8
0,6
0,4
0,2
0
Y
YA
MA
p-eNOS
eNOS
p-eNOS/eNOS

Figure 3

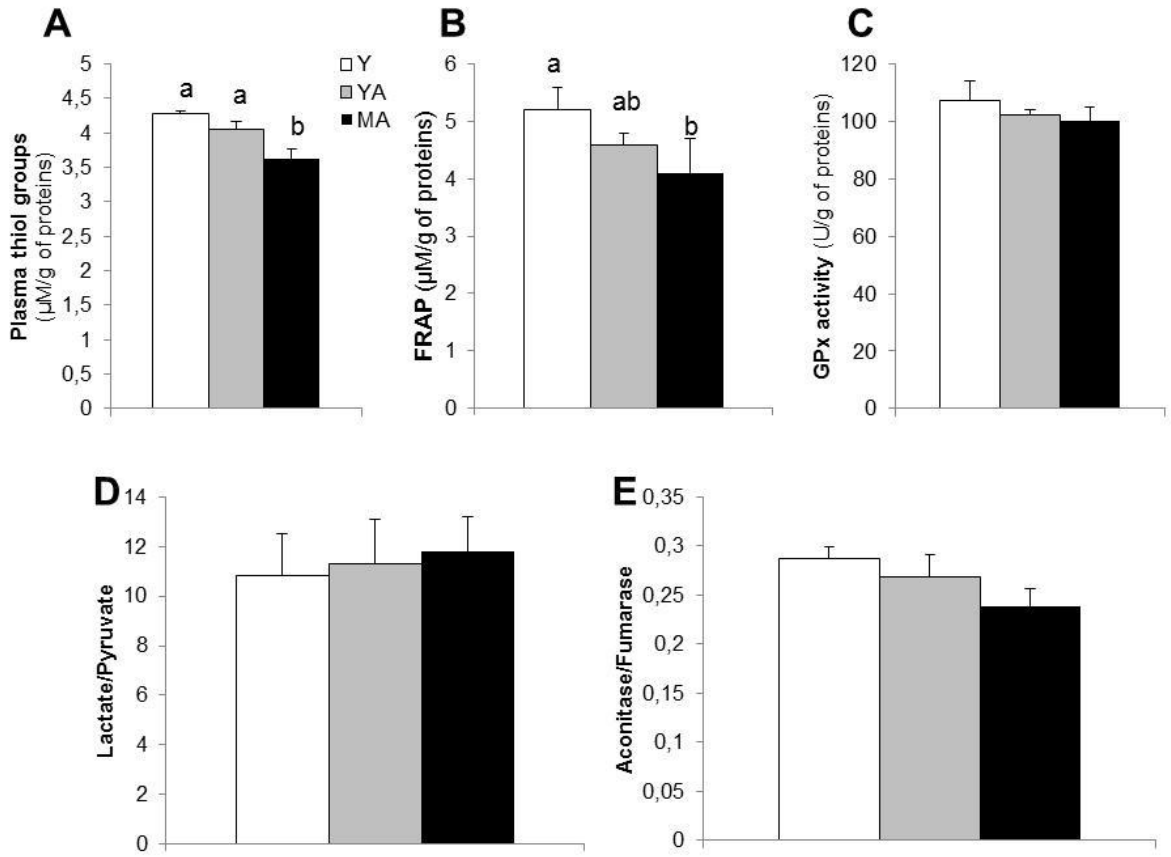
A
B
C
D
E
Y
YA
MA
Plasma thiol groups (µM/g of proteins)
FRAP (µM/g of proteins)
GPx activity (U/g of proteins)
Lactate/Pyruvate
Aconitase/Fumarase
a
a
b
a
ab
b

Figure 4

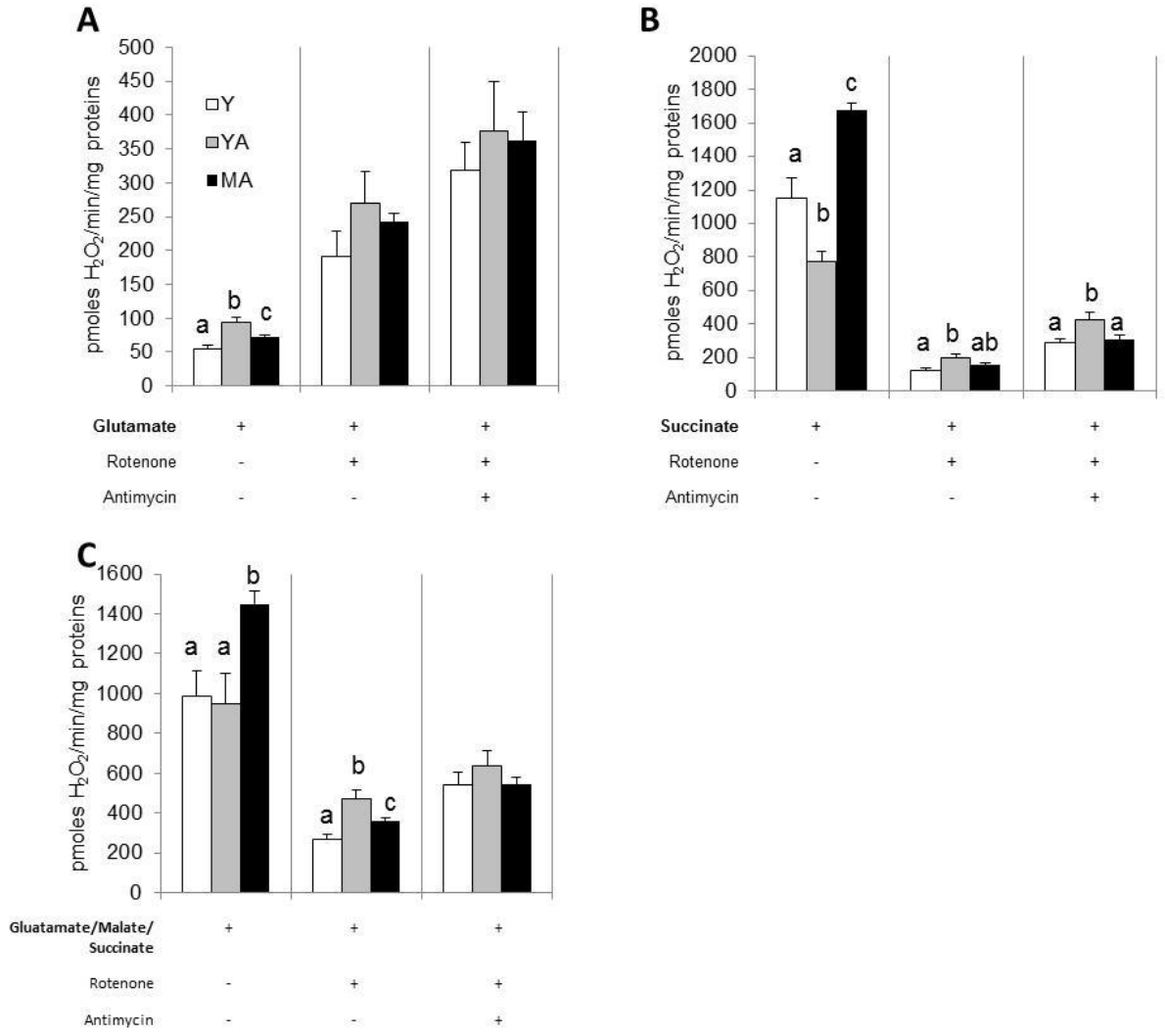
A
pmoles H_2O_2/min/mg proteins
Y
YA
MA
Glutamate
Rotenone
Antimycin
B
pmoles H_2O_2/min/mg proteins
Succinate
Rotenone
Antimycin
C
pmoles H_2O_2/min/mg proteins
Gluatamate/Malate/ Succinate
Rotenone
Antimycin

Figure 5

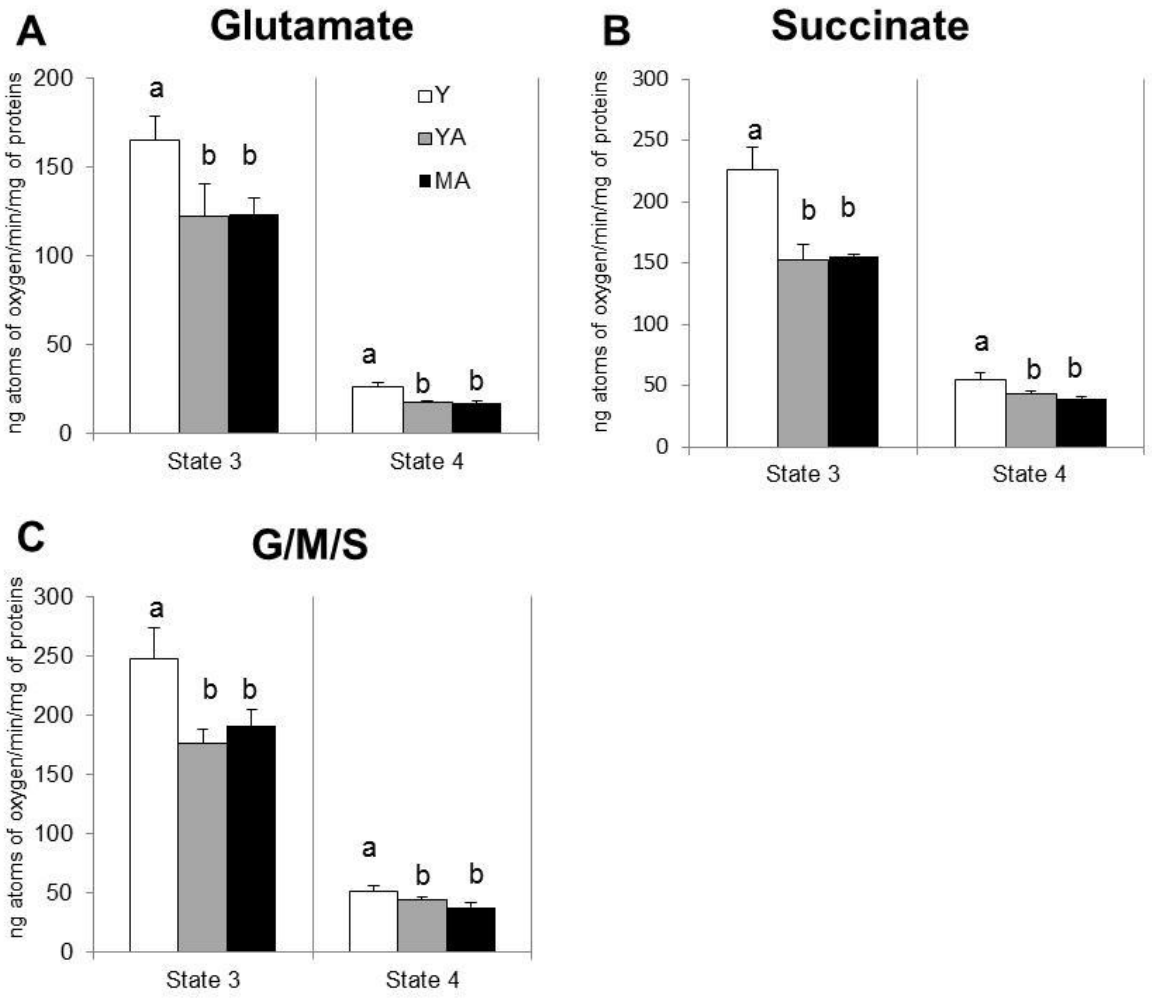
A
Glutamate
ng atoms of oxygen/min/mg of proteins
200
150
100
50
0
a
b
b
a
b
b
State 3
State 4
Y
YA
MA
B
Succinate
ng atoms of oxygen/min/mg of proteins
300
250
200
150
100
50
0
a
b
b
a
b
b
State 3
State 4
C
G/M/S
ng atoms of oxygen/min/mg of proteins
300
250
200
150
100
50
0
a
b
b
a
b
b
State 3
State 4

Figure 6

3.3 ARTICLE III

"Effects of a short- and long-term high-fat feeding protocol on the *ex vivo* cardiac function and reactivity of the coronary microvasculature in association with oxidative stress and mitochondrial function"

This work will be submitted to the journal "Biochimica et Biophysica Acta: Bioenergetics".

Effects of a short- and long-term high-fat feeding protocol on the *ex vivo* cardiac function and reactivity of the coronary microvasculature in association with oxidative stress and mitochondrial function.

Evangelia Mourmoura[1,2,*], Karine Couturier[1,2], Isabelle Hininger[1,2], Luc Demaison[(1,2,3)]

[(1)] Laboratoire de Bioénergétique Fondamentale et Appliquée, INSERM U1055, Grenoble cedex 09, F-38041, France;

[(2)] Université Joseph Fourier, Laboratoire de Bioénergétique Fondamentale et Appliquée, INSERM U1055, Grenoble cedex 09, F-38041, France;

[(3)] INRA, Clermont Université, Université d'Auvergne, Unité de Nutrition Humaine, BP 10448, F-63000 Clermont-Ferrand, France;

E-mail adresses :

Evangelia Mourmoura : evangelia.mourmoura@ujf-grenoble.fr

Karine Couturier : karine.couturier@ujf-grenoble.fr

Isabelle Hininger : isabelle.hininger@ujf-grenoble.fr

Luc Demaison : luc.demaison@ujf-grenoble.fr

*Corresponding author at : Laboratoire de Bioénergétique Fondamentale et Appliquée, INSERM U1055, Université Joseph Fourier, BP 53, 38041 Grenoble cedex 09, France. Tel. (+33) 476 63 56 25; Fax (+33) 476 51 42 18; e-mail: evangelia.mourmoura@ujf-grenoble.fr

Highlights

- The effects of high-fat diet for 3 and 7 months are studied.
- Increased oxidative stress and *ex vivo* contractile dysfunction are revealed.
- Mitochondrial and coronary system adaptations are suggested.
- These adaptations reflect an effort for the heart to maintain adequate perfusion.

Abstract

Diet-induced obesity is characterized by an imbalance between myocardial substrate uptake and fatty acid oxidation. The high-fat (HF) diet has been related to the development of cardiac as well as endothelial dysfunction mostly in large vessels. We aimed at characterizing the changes in cardiovascular and mitochondrial function during a short- and long-term HF feeding protocol. Rats followed a standard or HF diet for 3 or 7 months. Mitochondrial function was determined in isolated mitochondria whereas biochemical analyses allowed the evaluation of the oxidative stress. Cardiac function and coronary microvessels reactivity were determined using an *ex vivo* heart perfusion model. After 3 months of HF diet, adiposity was increased in the animals, whose hearts exhibited increased mitochondrial and cytosolic oxidative stress and decreased cardiac activity *ex vivo*. Mitochondrial respiration was not affected while a role for electron transfer flavoprotein (ETF) in the mitochondrial ROS production was suggested. Interestingly, the responses to acetylcholine (Ach) of the coronary microvasculature were enhanced. These changes were established and remained constant until the end of the long-term HF protocol where a diminished complex I activity was revealed. The age affected significantly the Ach-responses, which were reduced in middle-aged animals. The age under HF diet revealed also a diminished mitochondrial H_2O_2 formation at the level of complex I. Thus, our study shows a temporal pattern of changes occurring during a HF diet and an adaptation of the coronary circulation and mitochondrial function in order to maintain the cardiac metabolism and an adequate heart perfusion.

Keywords: high-fat diet, mitochondrial function, cardiac function, coronary dilatation, oxidative stress

Abbreviations

Ach, acetylcholine; ANT, adenine nucleotide translocator; CI/II/III/IV, complexes I/II/III/IV; EC, endothelial cells; ECVA, endothelial cell vasodilatation activity; EDD, endothelium-dependent dilatation; EID, endothelium-independent dilatation; eNOS, endothelial nitric oxide synthase; ETC, electron transport chain; ETF, electron transfer flavoprotein; FRAP, ferric reducing antioxidant power; HF, high fat; LDH, lactate dehydrogenase; LVDP, left ventricle developed pressure; MUFAs, monounsaturated fatty acids; OGTT, oral glucose tolerance test; PUFAs, Polyunsaturated fatty acids; RCR, prespiratory control ratio; ROS, reactive oxygen species; RPP, rate pressure product; SFAs, saturated fatty acids; SNP, sodium nitroprusside; RCC, recpiratory chain complexes; PC, palmitoylcarnitine.

1. Introduction

The prevalence of obesity is increasing worldwide at an alarming rate counting 2.8 million deaths each year (World Health Organization). The "obesogenic" environment of our societies [1] promotes sedentariness and excessive food intake (especially high fat foods) that are strongly associated with obesity and higher body weight [2]. Obesity is related to metabolic abnormalities such as disturbed glucose homeostasis and impaired insulin secretion [3, 4], which are mostly attributed to increases in visceral adipose tissue with an associated increase in portal vein free fatty acid levels [5]. These changes may result eventually in the development of metabolic syndrome, diabetes mellitus and cardiovascular diseases.

Diet–induced obesity is characterized by increases in circulating plasma non-esterifed fatty acids and an imbalance between myocardial substrate uptake and fatty acid oxidative capacity that may induce enhanced lipid accumulation and a futile cycle in the heart [6, 7]. A chronic exposure of the heart to this excess supply of substrates and the increased reliance of the heart in β-oxidation of fatty acids may cause the formation of harmful reactive oxygen species (ROS) [6]. ROS could further result in lipid peroxidation that could alter the mitochondrial function, structure and metabolism [6, 8].

Obese or type 2 diabetic patients have increased myocardial triglycerides content [8] and impaired cardiac energy phosphate metabolism that may arise from abnormal mitochondrial respiration impairing the ATP synthesis [9]. These changes have been shown to precede changes in contractile function [9] and have been related to decrease left ventricular function [8]. In rodent heart, it has been demonstrated that an increased lipid influx [10, 11], a decreased mobilization of triacylglycerol reserves [12] and an increased fatty acid metabolism [13, 14] are associated with cardiac hypertrophy and contractile dysfunction [8, 15, 16] probably through alterations of mitochondrial function [15]. However, most of these rodent models were genetically modified for cardiac lipotoxicity. Energy production of the heart is

almost entirely dependent on oxidative phosphorylation for contraction in relation to ventricular wall tension, myocyte shortening, heart rate and contractility [17]. Since the heart maintains a very high rate of oxygen extraction at rest, increases in myocardial energy production must be met by parallel increases in myocardial oxygen delivery [18, 19]. However, it has been recently demonstrated that a HF diet increases mitochondrial fatty acid oxidation and uncoupled respiration in the rat heart, and that was related to decreased cardiac metabolic efficiency [9].

States of hyperglycemia and insulin resistance found in obese individuals have been also shown to affect the peripheral and coronary vascular function especially that of large conduit arteries [20, 21] via reduced nitric oxide production, increased ROS production and inflammation. However, the impact of obesity on the coronary microcirculation remains controversial. The primary function of the coronary microcirculation is to optimize nutrient and oxygen supply to the heart in response to any metabolic demand by coordinating the resistances within different microvascular domains, each governed by distinct regulatory mechanisms [22]. Resistance to blood flow rises as the vessels diameter decreases; thus, the large conduit coronary arteries exert small, if any, resistance. These observations raise the need for direct examination of the function of coronary resistance arteries to understand how their vasomotor behavior changes and how it relates to coronary blood flow alterations in obese individuals. In uncomplicated obesity (absence of comorbid conditions) morphological changes in microvessels are quite rare [23]. Furthermore, recent studies on isolated coronary arterioles have shown that the endothelium-dependent dilation (EDD) in obese, young diabetic or high-fat fed rats are maintained or even enhanced [24-26].

However, most of these studies either have studied short-term feeding protocols [27, 28] or have investigated the effects of high-fat diets on cardiac metabolism and function in rodents of a modified genetic background [15, 29, 30]. It should also be noted that data collected from

this type of rodents exaggerate lipid disorders far beyond what is usually observed in patients suffering from obesity or diabetes [8]. Furthermore, there are studies that have shown that dietary fat can either be neutral or even protective for the heart [27, 31].

Another point is that most of the research until now has been focused on the identification of risk factors and their consequences at adulthood [32]. However, it has been suggested that dietary habits during early life (childhood or adolescence) may affect the risk of developing obesity or diabetes mellitus later in life. It has been demonstrated that dietary patterns during adolescence increases the risk of type 2 diabetes in middle aged women [32]. Findings from the Bogalusa Heart study indicate that risk factors such as high blood pressure, hyperinsulinemia and dyslipidemia that begin to cluster during childhood due to unhealthy dietary habits can predict adult cardiovascular factors [33]. This clustering of risk factor has been linked to unhealthy dietary habits during childhood [34].

Thus, the aim of our study was to characterize and follow the effects induced by a HF diet applied from youth to middle age adulthood on the i) state of oxidative stress of the organism, ii) cardiac mitochondrial function and iii) cardiovascular function *ex vivo*. For this reason, we applied a short- and long-term HF feeding protocol on Wistar rats from young to middle aged adulthood. HF diet is an excellent model for excess caloric intake, which contributes to the development of obesity and metabolic syndrome. We evaluated the levels of oxidative stress in their organisms and the cardiac mitochondrial function in terms of respiration, ROS release and respiratory complex activities. The cardiac function and reactivity of coronary microvessels in terms of endothelium-dependent and endothelium-independent dilatations were evaluated *ex vivo* in a Langendorff model of isolated heart perfusion. The age-matched rats fed on a standard rodent chow for the time points examined helped us discriminate diet- and age-induced changes. Furthermore, this life-course approach could help our knowledge concerning the changes and etiology of obesity and its comorbidities.

2. Materials and Methods

2.1.Experimental Animals and Diet

All experiments followed the European Union recommendations concerning the care and use of laboratory animals for experimental and scientific purposes. All animal work was approved by the local board of ethics for animal experimentation (Cometh) and notified to the research animal facility of our laboratory (authorization n° 38 07 23).

32 male Wistar rats from an inbred colony were housed two per cage in our animal facility at 3 months of age. Rats were randomly assigned to be maintained on standard carbohydrate (C: 16.1% proteins, 3.1% lipids, 60% cellulose; A04, Safe, France) or high-fat (HF: 31.5% proteins, 54% lipids (50% lard, 4% soya-bean oil w/w), 7% cellulose) diet over a twelve- or thirty-two-week period. This defined 4 groups of rats: the young adults control (YAC), the young adults high-fat (YAF), the middle-aged adults control (MAC) and the middle-aged adults high-fat (MAF). After analysis of the fatty acid composition of the diets chosen we found that the standard diet contained approximately 24% of saturated fatty acids (SFAs), 23% of monounsaturated fatty acids (MUFAs), 48% of n-6 polyunsaturated fatty acids (PUFAs) and 4.5% of n-3 PUFAs while the HF diet contained 37% of SFAs, 46% of MUFAs, 15% of n-6 PUFAs and 1.2% of n-3 PUFAs. All groups were fed *ad libitum* with free access to water and their body weight was recorded twice per week. The food intake for the rats fed a HF diet was measured at the beginning and at the end of the experimental diet period in order to assure that there was no caloric restriction due to the type of the diet. It should be noted that the protein content of the HF-diet was 2-fold higher because of the lower food intake (g/day) in these rats due to the higher energy density. This allowed a similar daily protein intake in all rat groups. On the day of the experiment, the rats were weighed and heparinized (1000 I.U./kg) via the saphenous vein before their sacrifice. Blood samples were collected for

further biochemical analysis and their adipose tissue was quantified for determination of the abdominal fat mass.

2.2.*Oral Glucose Tolerance Test (OGTT)*

An OGTT was performed 2 wks before the sacrifice. Food was removed from rats 18 h before they were given orally a glucose dose (1 g glucose/kg body weight, between 08.00 and 10.00 am). Blood samples were collected from the tail vein in heparinized tubes immediately before glucose administration to determine the basal glucose and insulin values and 5, 25, 40, 60 and 180 min after. Glucose values were determined with a glucose analyzer (ACCU-CHECK Active, Softclix). After centrifugation (3000 × g, 7 min, 4^{o}C) plasma samples were stored at −20°C until insulin determination using a radioimmunoassay kit (SRI-13K, Miilipore, Molheim, France). However, the samples of the middle-aged groups had an important degree of hemolysis, which made the detection of their insulin levels impossible. The area under the curve (AUC) for glucose was then calculated in order to evaluate the glucose tolerance as previously used by Cortez et al. [35].

2.3.Heart perfusion

A rapid thoracotomy was performed and the heart was immediately collected in Krebs-Heinselet solution maintained at 4^{o}C. It was then rapidly (less than 1 minute from the chest opening to avoid problem of cellular damages and preconditioning) perfused at constant pressure according to the Langendorff mode with a Krebs–Heinselett buffer containing (in mM) NaCl 119, $MgSO_4$ 1.2, KCl 4.8, $NaHCO_3$ 25, KH_2PO_4 1.2, $CaCl_2$ 1.2 and glucose 11 mM as sole energy substrate. The buffer was maintained at 37^{o}C and continuously oxygenated with carbogen (95% O_2/5% CO_2). A latex balloon connected to a pressure probe was inserted into the left ventricle and filled until the diastolic pressure reached a value of 7–8

mmHg. It allowed the evaluation of systolic, diastolic and left ventricle developed pressures as well as heart rate throughout the perfusion protocol. The heart was perfused at constant pressure (59 mmHg) for 30 minutes with a pressure gauge inserted into the perfusion circuit just upstream the aortic cannula. The coronary flow for each heart was estimated by weight determination of 1-min collected samples at the 25^{th} min of perfusion. After the 30-min perfusion at constant pressure, the heart was perfused with a peristaltic pump (Gilson, Villiers-Le-Bel, France) at the coronary flow previously determined during the perfusion at constant pressure. The systolic, diastolic and left ventricle developed pressures as well as the heart rates were determined after 10 min of perfusion at forced flow in order to allow the heart a satisfying stabilization. The left ventricle developed pressure was calculated by subtracting the diastolic pressure to the systolic pressure. The rate pressure product (RPP) was defined as the product between the left ventricle developed pressure and heart rate. It was used as indicator of the cardiac mechanical work [36]. All the parameters were recorded and analyzed with a computer using the HSE IsoHeart software (Hugo Sachs Elektronik, March-Hugstetten, Germany). The perfusion at constant flow was continued until the end of the measurement of the coronary reactivity.

2.4.Coronary Reactivity

After the 10-min equilibration period at constant flow, the coronary tone was raised via the constant infusion of the thromboxane analog U46619 (30nM) which was continuously infused into the perfusion system near the aortic cannula at a rate never exceeding 1.5% of the coronary flow. This allowed the obtainment of a coronary pressure between 100 and 130 mmHg. In our model of perfusion at forced flow, the aortic pressure equaled the coronary pressure and changes in the coronary tone triggered modifications of the aortic pressure. Changes in aortic perfusion pressure were thus used to monitor changes in coronary tone.

Relaxation responses to Ach (4, 10, 20, 40, 60, 80 and 100 pmoles) and sodium nitroprusside (SNP, 100, 200, 400, 600, 800 and 1000 pmoles) injections were then determined reflecting the EDD and endothelium-independent vasodilatation (EID) respectively.

The dilatation amplitude was calculated as the ratio between the maximal decrease in the coronary pressure and the coronary pressure just before the injection of the dilatation agents. Since the heart weight and coronary volume were subjected to intra- and inter-group variations, a correction was performed to normalise the input-function of the vasodilatation agents according to the coronary flow. The dose-response curve between the amount of vasodilatation agent injected and the maximal vasodilatation was then fitted to a logarithm function for each heart which allowed the fulfillment of statistical analyses. Moreover, the endothelial cell vasodilatation activity was also estimated from the corrected endothelium-dependent-dilatation and endothelium-independent-dilatation curves. For each heart and each injected Ach dose, the amount of SNP (reflecting the amount of dilatation agents) necessary to obtain the same percentage of Ach-induced vasodilatation was extracted from the EID curve according to the formula: endothelial cell vasodilatation activity (ECVA) = $e^{[(\%\ \text{Ach-induced dilatation} - b) / a]}$, where a and b are the coefficients of the theoretical EID curve. The results were expressed in pmole equivalents of nitroprusside. At the end of the perfusion protocol, a piece of myocardium (about 200 mg) from the apex of the heart was immediately freeze-clamped and stored at −80°C for further analysis. The other part of the myocardium was immediately used for isolated mitochondria preparation.

2.5.Mitochondria preparation

After the perfusion, atria and the remaining aorta were cut off from the heart. Myocardium was minced with scissors in a cold isolation buffer composed of (in mM) sucrose (150), KCl (75), Tris–Base (50), KH_2PO_4 (1), $MgCl_2$ (5), and EGTA (1), pH 7.4, fatty acid-free serum

albumin 0.2%. The pieces of myocardium were rinsed several times on a filter and put in an Elvehjem potter containing 15 ml of isolation buffer. A protease (subtilisin 0.02%) was added for 1 min to digest myofibrils at ice temperature, and the totality was then homogenized with the potter (300 rpm, 5 to 6 transitions). Subtilisin action was stopped by addition of the isolation buffer (30 ml). The homogenate was then centrifuged (800 g, 10 min, 4°C), and the resulting supernatant was collected and filtered. Mitochondria were then washed through two series of centrifugation (8,000×g, 10 min, 4°C). The last pellet of mitochondria was re-suspended in sucrose 250 mM, Tris–Base 10 mM, EGTA 1 mM, pH 7.4 at a concentration of approximately 10 mg/ml.

2.6.Respiration measurements

The rate of mitochondrial oxygen consumption was measured at 30°C in an incubation chamber with a Clarke-type O_2 electrode filled with 1 ml of incubation medium (KCl 125 mM, Tris–Base 20 mM, EDTA 5 µM, $CaCl_2$ 10 µM, KH_2PO_4 3 mM, pH 7.2, fatty acid-free bovine serum albumin 0.15%). A low amount of $CaCl_2$ was added to the medium in order to stimulate the oxidative phosphorylation. All measurements were performed using mitochondria (0.2 mg mitochondrial protein/ml) incubated with the following substrates (at final concentrations): i. DL-palmitoylcarnitine (0.05 mM)/ malate (2.5 mM) ii. glutamate (5.5 mM)/ malate (2.5 mM) iii. succinate (5.5 mM) + rotenone (2.5 µM) iv. glutamate (5.5 mM)/ malate (2.5 mM)/succinate (5.5 mM) in the presence (state 3) of ADP 1 mM and after addition of oligomycin (0.5 µg/ml) (state 4). The incubation medium was constantly stirred with a built-in electromagnetic stirrer and bar flea. Coupling of the mitochondrial oxidative phosphorylation was evaluated by the values of the respiratory control ratio (RCR), which was calculated by the state 3/state 4 ratio. When glutamate/malate were used as substrates, the RCR averaged 6.6 ± 0.9, 8.2 ± 0.7, 7.3 ± 0.5 and 8.1 ± 0.7 in the YAC, YAF, MAC and MAF

groups respectively, indicating a satisfying integrity of our mitochondrial preparations. However, the efficiency of the mitochondrial respiration was not measured in this study.

2.7.Mitochondrial reactive oxygen species release

The rate of mitochondrial H_2O_2 production was measured at 30°C on a F-2500 Hitachi spectrofluorometer and followed linear increase in fluorescence (excitation at 560 nm and emission at 584 nm). This was due to enzymatic oxidation of amplex red by H_2O_2 in presence of horseradish peroxidase, modified to follow kinetically the rate of H_2O_2 production by isolated mitochondria. Reaction conditions were 0.25 mg of mitochondrial protein/ml, 5 U/ml of horseradish peroxidase, 1 μM of amplex red, with i. DL-palmitoylcarnitine / malate ii. glutamate/ malate iii. succinate without rotenone (in the same concentrations as in respiration measurements). They were added in order to start the reaction in the same incubation buffer with that used for measurements of mitochondrial oxygen consumption. Mitochondrial ROS was measured in the absence of ADP (state 2 respiration rate). Rotenone (1 μM) and antimycin A (0.5 μM) were sequentially added to determine the maximum rate of H_2O_2 production of complexes I and III of the respiratory chain respectively.

2.8.Oxidative stress measurements

2.8.1. Plasma oxidative stress

Protein oxidation in the plasma was evaluated by the disappearance of protein thiol groups [37]. Plasma thiols were assayed in 20 μl of plasma, using 5,5'-dithiobis(2-nitrobenzoic acid (DTNB)) for derivating the thiol groups. The calibration curve was obtained by mixing two stock solutions of N-acetyl cystein (NAC) in the range of 0.125–0.6 mmol/l. Standards and plasma samples were measured spectrophotometrically at 415 nm (Hitachi 912, B Braun

Science Tec, France) in the presence of a phosphate buffer 50 mM, EDTA 100 mM, pH 8 and bis-5,5'-dithio-bis(2-nitrobenzoic acid) 10 mM.

The antioxidant status of the plasma was evaluated using ferric reducing antioxidant power (FRAP) assay as a global marker of the antioxidant power. The FRAP assay uses antioxidants as reductants in a redox-linked colorimetric method. In this assay, at low pH, a ferric-tripyridyltriazine (Fe^{III}-TPTZ) complex is reduced to the ferrous form, which is blue and monitored by measuring the change in absorption at 593 nm. The change in absorbance is directly proportional to the reducing power of the electron-donating antioxidants present in plasma. The absorbance change is translated into a FRAP value (in μmol/l) by relating the change of absorbance at 593 nm of test sample to that of a standard solution of known FRAP value.

Glutathione peroxidase (GPx) activity, which is a seleno-enzyme involved in protection against hydrogen peroxide was evaluated by the modified method of Gunzler [38] using terbutyl hydroperoxide (Sigma Chemical Co, Via Coger, Paris, France) as a substrate instead of hydrogen peroxide.

2.8.2. Cytosolic Oxidative stress

Lactate and pyruvate released in the coronary effluents were spectrophotometrically assayed according to Bergmeyer [39]. The lactate to pyruvate ratio was calculated to estimate the cytosolic redox potential [40]. This is a highly specific assay using the enzyme lactate dehydrogenase (LDH) to catalyze the reversible reaction of pyruvate and NADH to lactate and NAD^+. The catalytic action of LDH permits spectrophotometric measurement at 340 nm (spectrophotometer ULTROSPEC^{TM} 2100 pro, Amersham Biosciences, Uppsala, Sweden) of lactate production in terms of the generation of NADH in the reaction shown above. To measure lactate, the reaction is carried out from right to left with excess NAD^+. To force the

reaction to completion in this direction, it is necessary to trap formed pyruvate with hydrazine. The increased absorbance at 340 nm due to NADH formation becomes a mole-to-mole measure of the lactate originally present in the sample.

2.8.3. Mitochondrial oxidative stress

The ratio between the activities of aconitase and fumarase of the myocardium was calculated as an indicator of mitochondrial ROS production. Aconitase and fumarase activities were determined according to Gardner *et al.* [41], but were measured after extraction with a medium supplemented with citrate sodium (1M) in order to stabilize the *in vitro* aconitase activity. Values of aconitase and fumarase activities were determined on the same extract for each biological sample.

2.9.Activities of the respiratory chain complexes and citrate synthase

Activities of the NADH-ubiquinone oxydo-reductase (complex I), succinate-ubiquinone oxydo-reductase (complex II), ubiquinol cytochrome c reductase (complex III) and cytochrome c oxidase (complex IV) were determined as previously described [42] in isolated mitochondria. Heart samples (100 mg) were homogenized at 4°C with 0.9 ml of a potassium phosphate buffer 100 mM, pH 7.4. The homogenates were centrifuged (1,500×g, 5 min, 4°C), and the resulting supernatants were stored at −80°C until the determination of the citrate synthase activity according to Faloona and Srere [43]. The activities of the respiratory chain complexes and citrate synthase were expressed in units per mg of proteins.

2.10. Western blot

The expressions of total endothelial NOS (eNOS) and phosphorylated eNOS at Ser1177 were evaluated by Western blot. Frozen samples were homogenized in ice-cold lysis buffer

containing 20 mM Tris (pH 7.8), 137 mM NaCl, 2.7 mM KCl, 1 mM MgCl2, 1% Triton X-100, 10% (w/v) glycerol, 10 mM NaF, 1 mM ethylenediaminetetraacetic acid, 5 mM Na pyrophosphate, 0.5 mM Na_3VO_4, 1 μg/ml leupeptin, 0.2 mM phenylmethylsulfonyl fluoride and 1 mM benzamidine. The homogenates were centrifuged at 5,000 *g* for 20 min at 4°C, and the protein concentration in the supernatant was determined in each aliquot. Protein extracts (50 μg/lane) were loaded onto a 10% SDS gel and separated by electrophoresis. Extracts from the control group were loaded on both gels, and the amount of protein was accordingly compared pairwise. Proteins were transferred to nitrocellulose membranes. The membranes were incubated overnight at 4°C with rabbit antibodies against total eNOS (1:150, Thermoscientific, Illkirch, France) and phosphospecific mouse antibodies against eNOS Ser1177 (1:1,000, BD Biosciences Pharmingen, Le Pont de Claix, France). After being washed in TBS-Tween, the membranes were incubated with horseradish peroxidase-conjugated anti-mouse IgG for eNOS Ser1177 (1:3000, Jackson Immunoresearch, *Montluçon*, France) and anti-rabbit IgG for total eNOS (1:20000, Jackson Immunoresearch, *Montluçon*, France) for 1h at room temperature, followed by additional washing. Proteins were visualized by enhanced chemiluminescence with ECL advanced Western blotting detection kit (Amersham Biosciences, Brumath, France) and quantified using densitometry and Image J software. PAN-Actin (1:1000, Cell Signaling Technology, *St-Quentin-en-Yvelines*, France) was used as a loading control.

2.11. Other biochemical determinations

Proteins were measured using the bicinchoninic acid method with a commercially available kit (Thermo Scientific, Rockford, IL).

2.12. Statistical analysis

Results are presented as mean ± S.E.M. Animal weight, glycemia, activity of enzymes and data describing the oxidative stress, the cardiac function (developed pressure, heart rate, rate pressure product, coronary pressure, coronary flow) were contrasted across the two groups by one-way analysis of variance (ANOVA). Measures related to the action of the vasodilatation agents were treated with repeated-measures ANOVA to test the effects of age and obesity of high-fat fed rats (external factors), that of the amount of dilatation agent (internal factor) and their interactions. When required, group means were contrasted with a Fisher's LSD test. A probability (p) less than 0.05 was considered significant. Statistical analysis was performed using the NCSS 2004 software.

3. Results

3.1.General data

We verified that the type of the HF diet chosen did not induce any caloric restriction to the HF fed rats by measuring the food consumption at the beginning and the end of the experimental protocol for the HF groups. Their food consumption was slightly decreased for the MAF group but not significantly (in g/day/cage: YAF: 24.6 ± 2.2, MAF: 20.5 ± 2.8, data not shown). As shown in table 1, neither the short-term nor the long-term HF protocol had any effect on the body weight of the animals, since no difference was observed between the YAC and YAF groups and between MAC and MAF groups respectively. The age for the control groups increased the body weight of the animals (+14% for the MAC group compared to the YAC one) while the age under the HF diet did not alter this parameter as no difference was observed between YAF and MAF groups. The abdominal adipose tissue content of the rats was calculated as the sum of the retroperitoneal and visceral adipose tissue. The short-term HF protocol significantly increased the adipose tissue content of the YAF animals compared to the YAC ones as estimated by the weights of retroperitoneal (+112%), epididymal (+68%), visceral (+55%) and abdominal (+87%) adipose tissues. Similar were the results for the long-term HF diet (+160%, +56%, +58% and +112% of the retroperitoneal, epididymal, visceral and abdominal adipose tissue weights respectively for the MAF group compared to the MAC one). The age for the control groups did not modify these parameters and neither did the age under HF conditions. Triglycerides concentration in the plasma at the moment of sacrifice was modified neither by the HF diet protocols nor by the age. Cholesterol levels though were significantly increased by the short-term HF diet (+75% for the YAF compared to the YAC group) and by the long-term one (+88% for the MAF compared to the MAC group). The age for the control groups or for the HF ones did not alter this parameter.

Regarding the glucose metabolism, there was a significant increase after the short-term HF diet on the basal fasting glycemia (+11% for the YAF compared to the YAC group) (Fig. 1A). No effect was observed on the basal fasting glycemia after the long-term HF protocol. The age decreased the basal glycemia for the control groups (-20% for the MAC animals compared to the YAC ones) and for the HF ones (-18% for the MAF compared to the YAF group). According to the results of the oral glucose tolerance test there was no difference in the glucose response or the total area under the curve (AUC_{total}) concerning any of the manipulations (Fig. 1B and 1C). However, statistical analysis only for the young adult groups revealed a significant impact of the short-term HF diet on the AUC_{total} (Fig. 1C) with the YAF group having higher values that the YAC one (+15%, p=0.016). This difference disappeared with the long-term HF protocol. However, since the basal glycemia was not the same for all the groups we considered as a valuable measure the delta180 (glycemia between time zero and time 180 minutes) in order to evaluate the glucose elimination from the circulation. According to Fig. 1E, the short-term or long-term HF diet do not modify this parameter, while the age either under control (+540% for the MAC compared to the YAC animals) or HF (+166% for the MAF compared to the YAF animals) conditions significantly increased this parameter indicating a slower rate of glucose elimination from the circulation in the middle-aged animals.

3.2.Cardiac function studied ex vivo

The mechanical function of the perfused isolated hearts was monitored before the infusion of U46619 (Table 2). The short-term HF protocol induced a significant decrease in the left ventricle developed pressure (LVDP) and RPP (-28 and -34% respectively for the YAF group compared to the YAC one). Similar were the results for the long-term HF protocol (-37 and -25% of LVDP and RPP values respectively for the MAF group compared to the MAC one).

The decrease in the RPP was due to the decreased LVDP as the heart rate did not change for any group. The age either under control or HF conditions had no effect on these functions monitored *ex vivo*. No changes were observed in the heart rate and coronary pressure before and after the infusion of U46619. The infusion of U46619 raised the coronary pressure from 75 mmHg to a value close to 120 mmHg in all groups.

3.3.Coronary Reactivity

The responses to Ach of the coronary microvasculature are shown in Fig. 2A. Interestingly, it was observed an enhanced response to Ach after the short-term HF protocol (+18% for the YAF group compared to the YAC one at 60 pmoles of injected Ach) but also after the long-term one (+55% for the MAF group compared to the MAC one at 60 pmoles of injected Ach). A decrease in the EDD was observed with age under control (-39% for the MAC compared to the YAC group at 60 pmoles of injected Ach) but also under HF conditions (-19% for the MAF compared to the YAF group at 60 pmoles of injected Ach).

Fig. 2B depicts the EID, which reached 25% of dilatation as soon as 600 pmoles of SNP were injected. The SNP-responses were not affected by any of the diet or age conditions. Fig. 2C represents the endothelial cells vasodilatation activity. The short-term HF protocol tended to increase this parameter but not significantly for the YAF compared to the YAC group. Similar were the results regarding the long period of HF diet. The age significantly reduced the ECVA under both control (-48% for the MAC compared to the YAC group at 60 pmoles of injected Ach) or HF conditions (-42% for the MAF compared to the YAF group at 60 pmoles of injected Ach).

3.4.eNOS expression and phosphorylation

No changes were induced in the levels of total eNOS, phosphorylated eNOS or the ratio phosphorylated eNOS/total eNOS, which was used as an indicator of its activity, by any of the diet of age conditions (Fig. 3). It has to be noted though that these results concern the basal expression levels of the protein and not upon stimulation of the vasculature with the vasodilator agents.

3.5.Oxidative stress

In the plasma the thiol group concentration, which is inversely correlated to circulating oxidative stress, was significantly decreased after the short-term HF protocol (-8% for the YAF compared to the YAC group) (Fig. 4A) but it was not modified by the long-term one. The presence of plasma thiol groups was also decreased by the age either under control (-15% for the MAC compared to the YAC group) or HF (-11% for the MAF compared to the YAF group) conditions. The short-term HF protocol, however, increased the total antioxidant power (+28% for the YAF compared to the YAC group) (Fig. 4B). Similar were the results for the long-term HF diet (+78% for the MAF compared to the MAC group). The age affected this parameter neither under control nor under HF conditions. The activity of the antioxidant enzyme GPx in the plasma was not modified by any of the diet or age conditions (Fig. 4C).

The lactate-to-pyruvate ratio of the coronary effluents (Fig. 4d), inversely correlated with the cytosolic oxidative stress, was significantly reduced by the short-term HF period (-77% for the YAF compared to the YAC group) and by the long one (-87% for the MAF compared to the MAC group). The age under control or HF diet did not change its levels. The results for aconitase-to-fumarase ratio in cardiac homogenates (Fig. 4E), inversely correlated with the mitochondrial-derived oxidative stress, followed the same pattern. More specifically, a decrease in this ratio was observed after the short-term HF protocol (-41% for the YAF group

compared to the YAC one) and after the long one (-44% for the MAF group compared to the MAC one) while the age did not affect it under any diet condition.

3.6.Mitochondrial H_2O_2 production

With palmitoylcarnitine, a substrate largely present in the HF diet, no change in the basal mitochondrial H_2O_2 production or after the addition of rotenone in the respiration milieu was observed after the short-term HF protocol (Fig. 5A). The addition of antimycin A though revealed an increase in H_2O_2 production (+68% for the YAF compared to the YAC group) happening between CI and CIII. The long-term HF protocol followed the same pattern as the short one (+78% for the MAF compared to the MAC group when antimycin A was added to the respiration milieu). The age under control conditions affected neither the basal H_2O_2 production nor that at the levels of CI and CIII. However, the age under HF diet, even though it did not modify the basal H_2O_2 production, decreased it at the level of CI as evidenced with the addition of rotenone (-32% for the MAF compared to the YAF group) while the addition of antimycin A erased that difference.

In the presence of glutamate/malate, a CI-related substrate, the short-term HF diet did not affect H_2O_2 production neither under basal conditions nor after adding rotenone alone or in association with antimycin A (Fig. 5b). Similar were the results for the long-term HF diet. However, the age under control conditions decreased the basal production of H_2O_2 (-23% for the MAC compared to the YAC group). This difference was erased after adding rotenone alone or with antimycin A, indicating that CI is implicated at the age-related decrease in basal H_2O_2 production for the control animals. The age under HF diet also decreased the basal H_2O_2 production (-21% for the MAF compared to the YAF group). This difference persisted in the presence of rotenone (-41% for the MAF compared to the YAF group) while it disappeared

with the addition of antimycin A, suggesting that the decreased H_2O_2 production occurred at the level of CIII for the aging under HF conditions.

When succinate, a CII-related substrate, was used as a source of reduced equivalents the results were not the same (Fig. 5C). The short-term HF diet increased the basal H_2O_2 production (+66% for the YAF compared to the YAC group) but the addition of rotenone alone or in association with antimycin A erased the difference. This could imply a role of reverse electron flux to the H_2O_2 production during the short-term HF diet. However, the long-term HF diet did not modify the H_2O_2 production even after the addition of rotenone alone or in association with antimycin A. The age under control conditions induced an increase in the basal H_2O_2 production (+117% for the MAC compared to the YAC group), which was erased with the addition of rotenone alone or in association with antimycin A, indicating a role of reverse electron flux to this process. The age under HF conditions also induced an increase in the basal H_2O_2 production (+55% for the MAF compared to the YAF group). This result was inversed with the addition of rotenone (-16% for the MAF compared to the YAF group) and erased with further addition of antimycin A revealing a role of the reverse electron flux to this decreased production of H_2O_2.

When glutamate/ malate and succinate were used together as sources of reduced equivalents the results were different (Fig. 5C). Both the short- and long-term HF diets did not affect H_2O_2 production neither under basal conditions nor after adding rotenone alone or in association with antimycin A (Fig. 5d). The age under control conditions induced an increase in the basal H_2O_2 production (+53% for the MAC compared to the YAC group), which was inversed with the addition of rotenone alone (-23% for the MAC compared to the YAC group) and erased with further addition of antimycin A. These results could imply a major role of reverse electron flux to the age-related increase of the basal H_2O_2 production or even an adaptation of the CI to diminish the CI-related ROS release. The age under HF conditions also

induced an increase in the basal H_2O_2 production (+44% for the MAF compared to the YAF group). This result was inversed with the addition of rotenone alone (-22% for the MAF compared to the YAF group) or in association with antimycin A (-12% for the MAF compared to the YAF group) indicating an important role of the reverse electron flux to the basal H_2O_2 production or a diminished maximal capacity of CI and CIII to produce ROS.

3.7.Mitochondrial respiration

In isolated mitochondria oxidizing PC, all states of the respiration rate were not affected by the short-term HF protocol (Fig. 6A). However, the long-term HF diet increased the state 2 of the respiration rate (+66% for the MAF compared to the MAC group) but the states 3 and 4 were unaffected. The age under control conditions did not modify these parameters while the age under HF conditions significantly increased the state 2 of the respiration rate (+33% for the MAF compared to the YAF group). The yield of mitochondrial H_2O_2 production (Table 3), calculated as the ratio of basal mitochondrial H_2O_2 production divided by the state 2 respiration rate for each substrate, was not affected by the short-term HF protocol but only by the long term one, which decreased it (-23% for the MAF compared to the MAC group). This parameter was not altered by the age under control conditions but only by the age under HF conditions resulting to decreased values in the MAF group (-38% compared to the YAF group).

In the presence of glutamate/malate, all states of the respiration rate were not affected by the short-term HF protocol (Fig. 6B). The long-term HF diet increased the states 2 and 3 of the respiration rate (+51 and +46% respectively for the MAF compared to the MAC group) while the state 4 was unaffected. The age under control diet did not change these parameters but the age under HF conditions increased the states 2 and 3 of the respiration rate (+38 and +20% respectively for the MAF compared to the YAF group) while the state 4 was unaffected. The

yield of mitochondrial H_2O_2 production (Table 3) was not affected by the short-term HF protocol but only by the long term one, which decreased it (-28% for the MAF compared to the MAC group). This parameter was not altered by the age under control conditions but only by the age under HF conditions resulting to decreased values in the MAF group (-40% compared to the YAF group).

With succinate as respiration substrate, all states of the respiration rate were not affected by the short-term HF protocol (Fig. 6C). The long-term HF diet increased the state 2 of the respiration rate (+17% for the MAF compared to the MAC group) while the states 3 and 4 were unaffected. The age under control or HF conditions did not affect the states of the respiration rate. The yield of mitochondrial H_2O_2 production (Table 3) was significantly increased by the short-term HF protocol (+84% for the YAF compared to the YAC group) but not by the long one. The age under control conditions significantly increased this parameter (+157% for the MAC compared to the YAC group) but this did not occur with age under HF conditions.

Finally, when glutamate/malate and succinate were used together as substrates all states of the respiration rate were not affected by the short-term HF protocol (Fig. 6D). The long-term HF diet did not modify the state 2 of the respiration rate but significantly increased the states 3 and 4 (+38 and +29% respectively for the MAF compared to the MAC group). The age under control conditions did not affect the states of the respiration rate but under HF conditions it significantly affected only the states 3 and 4 (+38 and +23% respectively for the MAF compared to the YAF group). The yield of mitochondrial H_2O_2 production (Table 3) was not affected by the HF diet protocols. However, it was significantly increased by the age under control conditions (+67% for the MAC compared to the YAC group) but not affected by the age under HF diet.

3.8.Mitochondrial enzymatic activity

We measured the activity of citrate synthase in cardiac homogenates and the activities of the respiratory chain complexes (RCC) in isolated mitochondria (Table 4). Mitochondrial density as evidenced by the activity of citrate synthase was modified neither by the diet nor by the age conditions. The short-term HF diet did not affect the activities of the RCC but the long-term induced a decrease in the CI activity (-41%for the MAF compared to the MAC group). The age under control conditions did not affect the RCC activities while the age under HF conditions decreased the CIV activity (-34% for the MAF compared to the YAF group).

4. Discussion

This study aimed at investigating and monitoring the *ex vivo* cardiovascular function, the oxidative stress status and the cardiac mitochondrial function from youth to middle age adulthood in a rat model of high-fat diet-induced obesity, in order to better understand the consequences of obesity in the absence of overt diabetes. This study used two types of HF feeding protocols; short-term of 3 months and long-term of 7 months in order to evaluate the progression of changes caused by the diet between youth and middle-age adulthood. The use of age-matched control helped in distinguishing between diet and age effects. Our study yielded a number of novel observations.

4.1.Effect of short-term HF feeding protocol

In our rat model of obesity, the short-term HF feeding protocol did not affect the body weight or the plasma triglycerides levels but significantly increased the adipose tissue content and the circulating cholesterol levels which is consistent with previous findings [9]. It also induced a fasting hyperglycemia in the animals, indicating certain glucose intolerance. However, since the basal glycemia was not similar between YAC and MAF and delta 25 the same, we considered as more valuable measurement for the glucose elimination the delta180 than the AUC_{total}. This parameter was not modified indicating a similar rate of glucose elimination from the circulation for the YAC and YAF groups. This could happen through an increase in the insulin secretion as a response to the early development of glucose intolerance as previously described in HF-fed rodent models [44, 45]. These metabolic changes accompanied modifications in the cardiac mechanical activity measured *ex vivo,* which was also negatively affected as evidenced by the decrease in the rate-pressure product. This was mainly due to the decreased left ventricle pressure as the heart rate remained unchanged. A limitation of this study is the perfusion of the hearts with glucose as only substrate while it would be interesting to perfuse the hearts with glucose together with a lipid substrate,

especially in working mode so that the cardiac mechanical activity can be maximal. Contractile dysfunction has already been described after as soon as 7 weeks of high-fat diet [46]. No changes were found in the coronary pressure. The depressed *ex vivo* cardiac mechanical activity observed in this study could be related to changes in the cardiac metabolism, since a decreased cardiac metabolic efficiency has been already shown in high-fat fed rat hearts [9], or to increased oxidative stress, as previously reported [47].

However, the cardiac mitochondrial function did not seem to be affected by the short-term HF diet in this study. This was evidenced by measurements of mitochondrial respiration in isolated organelles where the states 2, 3 and 4 of the respiration rate were not affected by this protocol independently of substrate used. Moreover, the mitochondrial content, as shown by the citrate synthase activity, and the RCC activities were not altered. However, it could be assumed a reduced activity of ATP synthase or an altered ATP transfer resulting in inefficient ATP utilization by the cardiomyocytes eventually leading to decreased mechanical function. This could have been related to the status of the oxidative stress found in all cellular compartment of the animals after the short-term HF protocol. An increased circulating, cytosolic and mitochondrial oxidative stress was present in the YAF animals despite the increase in the antioxidant capacity of the plasma. These data imply that ROS defenses were not sufficiently increased to circumvent the increased oxidant burden. Thus, these conditions could have helped in the development of the observed *ex vivo* cardiac dysfunction. This mechanism could occur via the impairment in the ratio phosphocreatine/ATP [48] as already described in obesity-related states. It has been reported that a H_2O_2 overload may lead eventually to de-energization upon total ATP and phosphocreatine depletion in cardiomyocytes [49]. The increased oxidative stress could have also affected cardiolipin [50] and consequently the adenine nucleotide transporter (ANT).

The assessment of H_2O_2 released from the mitochondrial respiratory chain was helpful to understand the origin of mitochondrial oxidative stress. Palmitoylcarnitine (PC) was used as a substrate for the electron transport chain (ETC) as it is abundant in high-fat diets. PC is a lipid substrate used to assess the ability of the mitochondria to oxidize long-chain lipids. Its oxidation yields both NADH and $FADH_2$ stimulating both CI and CII of the electron transport chain. In addition, the dehydrogenases of β-oxidation can transfer electrons to the ETF, which then reduces ETF-ubiquinone oxidoreductase (ETF-QO) passing electrons to CIII. During this process, there is the possibility of electron leakage [51]. The basal mitochondrial H_2O_2 release with this substrate was not affected by the short term HF protocol despite the increased H_2O_2 release between CI and CIII as evidenced by the addition of rotenone and antimycin A combined. The glutamate/malate-induced basal H_2O_2 production was not affected whereas the succinate-induced H_2O_2 production was increased due to increased reverse electron flow at CI. However, glutamate/malate and succinate together, which were used to stimulate both CI and CII of the ETC did not reveal any difference in the H_2O_2 production between YAC and YAF animals. This result was not observed with PC as substrate, even though it feeds also the ETC at the levels of CI and CII. This may be due to the fact that PC gives also electrons to ETF. Thus, a role of ETF in the ROS formation with the HF diet could be suggested.

Interestingly, the short-term high-fat feeding protocol induced an increase in the Ach-responses of the intact coronary microvasculature. Maintained or enhanced responses have already been described in the vasculature of rodent models of obesity [25, 26]. In our study, this enhanced response to Ach was not due to smooth muscle cells function, since the response to SNP did not differ among groups. Thus, a role of endothelial cells, as evidenced also by the increase in the ECVA even though it did not reach significance. The activity of eNOS, the main enzyme responsible for the production of nitric oxide, seemed unaltered as evaluated indirectly by the ratio of phosphorylated eNOS to total eNOS. However, its

expression was measured under basal conditions and not upon stimulation by the vasodilator agents, thus it is unknown if this parameter was affected under these last conditions. Furthermore, the presence of other EC-derived factors contributing in the coronary microvessels Ach-responses could be possible. It has already been shown that the endothelium-derived hyperpolarizing factor (EDHF) could contribute to EDD of microvessels especially as a mechanism of compensation in order for the heart to keep an adequate perfusion in states of obesity [52]. Thus, these vascular alterations may reflect an adaptation of the coronary microvasculature in order to adjust organ perfusion during physiological processes such as exercise, otherwise the heart would not be able to respond to increased metabolic demands and lead eventually to ischemic incidents.

4.2.Effect of long-term HF feeding protocol

The long-term HF feeding affected the basic body and metabolic characteristics of the animals in a similar way as the short-term HF protocol. More specifically, the body weight or the plasma triglycerides levels were unaltered but the adipose tissue content and the circulating cholesterol levels were significantly increased. However, the basal fasting glycemia was not modified between MAC and MAF animals in contrast to the short-term protocol effect. The rate of the glucose elimination from the circulation was also unchanged by the long-term protocol, as evidenced from the AUC_{total} and delta180. Interestingly, the fact that the difference found in basal glycemia between the young dietary groups disappeard with middle age paralleled the disappearance of the circulating oxidative stress. Increased glucose levels have been correlated to the production of certain form of oxidative stress [53]; thus, an adaptation of the glucose metabolism observed after the long-term diet could explain the disappearance of the circulating oxidative stress. The fact that the high-fat fed animals did not gain body weight but had increased adiposity after both HF feeding protocols could represent

a case of the normal weight obesity syndrome. This syndrome has been described recently and is defined as a normal body mass index associated with increased body fat [54, 55].

The cardiac *ex vivo* mechanical activity was negatively affected as it did by the short-term HF protocol. The RPP was decreased due to the decreased left ventricle pressure as the heart rate remained unchanged, while no changes were observed in the coronary pressure. Diets with increased content of lipids (45%) have been related to cardiac dysfunction in rats [56]. Interestingly, the mitochondrial function studied in vitro by respiration measurements indicated an enhancement in this parameter by the long period of the diet. State 2 of the respiration rate was increased with PC, glutamate/malate or succinate as substrates. State 3 in the presence of glutamate/malate or glutamate/malate plus succinate was also increased while state 4 was increased only in the presence of glutamate/malate plus succinate. The rest of the conditions did not affect the mitochondrial respiration. This observed enhanced mitochondrial respiration occurred despite an unchanged mitochondrial density, as shown by the activity of the citrate synthase, and a decrease in the CI activity. Thus, it could be argued that a mechanism of adaptation is taking place with the long-term feeding protocol in order for the mitochondria to provide adequate energy to the myocardium to meet the higher metabolic demands due to adiposity. However, it seems that this mitochondrial adaptation was not sufficient enough to restore the cardiac mechanical activity. The increased cytosolic and mitochondrial oxidative stress found after the long-term HF protocol could have an important role in the development of the observed *ex vivo* cardiac dysfunction via the mechanism already described for the short-term HF diet. Interestingly, the circulating oxidative stress seems to disappear due probably to further increase of the antioxidant plasma capacity.

The assessment of hydrogen peroxide released form the mitochondrial respiratory chain revealed interesting information concerning the ETC function. The basal mitochondrial H_2O_2 release with PC had the same results as the short term HF protocol revealing an increased

H_2O_2 release between CI and CIII as evidenced by the addition of rotenone and antimycin A combined. The glutamate/malate-induced basal H_2O_2 production was not affected as well as the succinate-induced production. Similar were the results for the glutamate/malate and succinate together. The result of glutamate/malate plus succinate was not observed with PC as substrate revealing a possible role of ETF in the observed ROS formation. Furthermore, the increased succinate-induced H_2O_2 production via reverse electron flux observed with the short term diet disappeared with the longer period which could be associated with the decreased CI activity. This could be due to the increase in β-oxidation in HF fed animals, since β-oxidation depends less on CI than does the oxidation of glucose.

The enhanced Ach responses of the coronary microvasculature observed after the short-term protocol were also observed after the long-term one. In the literature, it has been described an enhanced vascular reactivity at 20 or 32 weeks of age in rodent models of obesity [57]. Interestingly, the difference between MAC and MAF groups was amplified compared to the one between YAC and YAF groups. However, the role of endothelial cells, the functional coupling between endothelial and smooth muscle cells and the contribution of other factors in the enhanced EDD, as already described for the short-term HF diet, are implied.

These data suggest that, aside the vascular adaptations observed already after the short-term protocol, an adaptation taking place at the level of the mitochondrial respiration, including the decreased CI activity, is revealed with the long-term HF diet. Moreover, the circulating oxidative stress seems to return to the normal levels probably through increase of the antioxidant defenses.

4.3.Effect of age under control conditions

The period between young and middle aged adulthood under a control diet increased only the body weight of the animals while adiposity, circulating triglycerides and cholesterol levels

stayed unaffected. However, there was a decrease in the basal fasting glycemia accompanied though by a decrease in the glucose elimination rate from the circulation. No changes were observed in the measured parameters of the cardiac function studied *ex vivo* or in the mitochondrial respiration independently of substrate used. Mitochondrial density or RCC activities were also unchanged. The age induced an increase in the circulating oxidative stress occurring probably because of the lack of sufficient antioxidant defenses. However, no cytosolic or mitochondrial oxidative stress was developed. These data suggest that the maintained mitochondrial respiration was accompanied by a satisfying energy transfer or utilization by the heart since no cellular oxidative stress was observed to inhibit it.

Despite the fact that no mitochondrial oxidative stress was found by the aconitase-to-fumarase ratio, the mitochondrial H_2O_2 release by the electron transport chain was modified by the age. More specifically, when PC was used as substrate the H_2O_2 release was not affected but when GM was used the basal H_2O_2 release was significantly decreased probably due to CI. The increased basal succinate-induced H_2O_2 release seemed to occur mainly via reverse electron flow at complex I. The combination of the last two substrates indicated a decrease in the H_2O_2 production at the level of CI together with an increase reverse electron flux. The decrease CI activity could have contributed to this decreased CI-related H_2O_2 production.

Moreover, even though the cardiac function was not changed, age induced a decrease in the Ach-responses of the coronary microvasculature, which could be related to the increased circulating oxidative stress found in the middle-aged animals. This result occurred mostly at the level of endothelial cells since the SNP responses were not affected and the vasodilatation activity of the endothelial cells was reduced with age. It has been previously demonstrated that vascular NADPH oxidases are in part responsible for increased superoxide production during aging [58]. A decreased nitric oxide bioavailability caused by the increased circulating presence of ROS could result to the reduced Ach-response. Thus, we may conclude that this

aging period affected the glucose metabolism associated with the circulating oxidative status leading eventually to a reduced reactivity of the coronary microvasculature while the cardiac and mitochondrial functions were less affected.

4.4.Effect of age under HF conditions

The effects of the age under a HF diet did not induce any changes in the body weight, adiposity and circulating triglycerides and cholesterol levels. However, there was a decrease in the basal fasting glycemia accompanied by a decrease in the glucose elimination rate from the circulation as found also during aging under control conditions. Similarly, no changes were observed in the cardiac function studied *ex vivo.* The mitochondrial respiration, however, was increased by the age under HF conditions as evidenced by the state 2 with PC, the states 2 and 3 with glutamate/malate and state 3 and 4 with glutamate/malate plus succinate. This enhanced mitochondrial respiration was not accompanied by an increase in the mitochondrial density or in the RCC activities. In contrast, the CIV activity was found decreased by the age under HF conditions. This result in association with the presence of oxidative stress could interfere with the production, transfer or utilization of the energy by the heart. CIV could be itself a ROS target, since some of its subunits are encoded by mitochondrial DNA [59] and would be more susceptible in ROS-induced damages. Thus, the age under HF conditions induced an enhanced mitochondrial respiration, which was not though reflected to the cardiac mechanical function.

The age under HF conditions modified the oxidative stress of the organism in a similar way as the age under control conditions (increased circulating ROS but unchanged cytosolic and mitochondrial oxidative stress). The basal H_2O_2 released from the mitochondrial respiratory chain in the presence of PC was not altered but a decrease production at the level of CI was observed. In the presence of glutamate/malate, a decreased basal H_2O_2 production was

observed occurring at the level of CI. When succinate was used as substrate, the basal H_2O_2 production was increased occurring via the electron reverse flow at CI while the glutamate/malate and succinate together increased the basal H_2O_2 production despite its decreased production at the level of CI and CIII. These data suggest an adaptation of CI in order to decrease the ETC-derived ROS formation with the age under HF conditions. However, the CIV activity was significantly decreased. These data suggest that the mitochondria try to produce more energy to meet the increased cardiac demands of the heart due to obesity.

The Ach-responses of the coronary microvasculature were reduced under these conditions but not to the same amplitude as under control conditions. The SNP responses were not affected while the vasodilatation activity of the endothelial cells was also reduced. This reduction might take place via the same mechanism as already described for the control conditions.

5. Conclusions

Our study reveals important new information regarding the changes that take place during a high-fat feeding protocol providing evidence for the existence of a temporal pattern for changes that are contingent on the progression of the diet. Furthermore, it is the first study that tries to evaluate the overall image of the heart function in terms of oxidative stress, mitochondrial and cardiac function, and coronary reactivity. Despite these changes, the mitochondria maintained at first and enhanced later the oxidative phosphorylation in an effort to supply the heart with energy. However, the presence of increased oxidative stress in all cellular compartments established at the beginning of the diet could have affected the system of phosphocreatine or even induced an increased calcium content [60] and consequent opening of the permeability transition pore (PTP) resulting to inefficient transfer or utilization of the produced energy by the heart. A possible role of ETF in the process of ROS formation at the beginning of the diet is also suggested. A major finding of our study is the adaptation of the coronary microvasculature that took place with the beginning of the HF diet resulting to increased Ach-responses which remained until end of the protocol. This phenomenon together with the preserved mitochondrial respiration could participate to the better recuperation after ischemia-reperfusion found in diet-induced obese rats [61, 62]. This mechanism could also be related to the obesity paradox concerning the better survival rates of obese individuals after cardiovascular incidents [63]. Whether the detrimental effects of a high-fat diet would predominate following a longer duration of HF feeding is unknown. An understanding of the mechanism of the enhanced EDD would be helpful in order to understand the factors that are implied and could thus be potential therapeutic targets.

References

[1] B. Swinburn, G. Egger, F. Raza, Dissecting obesogenic environments: the development and application of a framework for identifying and prioritizing environmental interventions for obesity, Prev Med 29 (1999) 563-570.

[2] M.A. Martinez-Gonzalez, J.A. Martinez, F.B. Hu, M.J. Gibney, J. Kearney, Physical inactivity, sedentary lifestyle and obesity in the European Union, Int J Obes Relat Metab Disord 23 (1999) 1192-1201.

[3] J. Vague, Sexual differentiation. A determinant factor of the forms of obesity. 1947, Obes Res 4 (1996) 201-203.

[4] J. Vague, The degree of masculine differentiation of obesities: a factor determining predisposition to diabetes, atherosclerosis, gout, and uric calculous disease. 1956, Nutrition 15 (1999) 89-90; discussion 91.

[5] P. Bjorntorp, "Portal" adipose tissue as a generator of risk factors for cardiovascular disease and diabetes, Arteriosclerosis 10 (1990) 493-496.

[6] K. Ballal, C.R. Wilson, R. Harmancey, H. Taegtmeyer, Obesogenic high fat western diet induces oxidative stress and apoptosis in rat heart, Mol Cell Biochem 344 (2010) 221-230.

[7] J.H. Rennison, T.A. McElfresh, X. Chen, V.R. Anand, B.D. Hoit, C.L. Hoppel, M.P. Chandler, Prolonged exposure to high dietary lipids is not associated with lipotoxicity in heart failure, J Mol Cell Cardiol 46 (2009) 883-890.

[8] R. Harmancey, C.R. Wilson, N.R. Wright, H. Taegtmeyer, Western diet changes cardiac acyl-CoA composition in obese rats: a potential role for hepatic lipogenesis, J Lipid Res 51 (2010) 1380-1393.

[9] M.A. Cole, A.J. Murray, L.E. Cochlin, L.C. Heather, S. McAleese, N.S. Knight, E. Sutton, A.A. Jamil, N. Parassol, K. Clarke, A high fat diet increases mitochondrial fatty acid oxidation and uncoupling to decrease efficiency in rat heart, Basic Res Cardiol 106 (2011) 447-457.

[10] H.C. Chiu, A. Kovacs, R.M. Blanton, X. Han, M. Courtois, C.J. Weinheimer, K.A. Yamada, S. Brunet, H. Xu, J.M. Nerbonne, M.J. Welch, N.M. Fettig, T.L. Sharp, N. Sambandam, K.M. Olson, D.S. Ory, J.E. Schaffer, Transgenic expression of fatty acid transport protein 1 in the heart causes lipotoxic cardiomyopathy, Circ Res 96 (2005) 225-233.

[11] H. Yagyu, G. Chen, M. Yokoyama, K. Hirata, A. Augustus, Y. Kako, T. Seo, Y. Hu, E.P. Lutz, M. Merkel, A. Bensadoun, S. Homma, I.J. Goldberg, Lipoprotein lipase (LpL) on the surface of cardiomyocytes increases lipid uptake and produces a cardiomyopathy, J Clin Invest 111 (2003) 419-426.

[12] G. Haemmerle, A. Lass, R. Zimmermann, G. Gorkiewicz, C. Meyer, J. Rozman, G. Heldmaier, R. Maier, C. Theussl, S. Eder, D. Kratky, E.F. Wagner, M. Klingenspor, G. Hoefler, R. Zechner, Defective lipolysis and altered energy metabolism in mice lacking adipose triglyceride lipase, Science 312 (2006) 734-737.

[13] H.C. Chiu, A. Kovacs, D.A. Ford, F.F. Hsu, R. Garcia, P. Herrero, J.E. Saffitz, J.E. Schaffer, A novel mouse model of lipotoxic cardiomyopathy, J Clin Invest 107 (2001) 813-822.

[14] B.N. Finck, J.J. Lehman, T.C. Leone, M.J. Welch, M.J. Bennett, A. Kovacs, X. Han, R.W. Gross, R. Kozak, G.D. Lopaschuk, D.P. Kelly, The cardiac phenotype induced by PPARalpha overexpression mimics that caused by diabetes mellitus, J Clin Invest 109 (2002) 121-130.

[15] S. Boudina, S. Sena, H. Theobald, X. Sheng, J.J. Wright, X.X. Hu, S. Aziz, J.I. Johnson, H. Bugger, V.G. Zaha, E.D. Abel, Mitochondrial energetics in the heart in obesity-related diabetes: direct evidence for increased uncoupled respiration and activation of uncoupling proteins, Diabetes 56 (2007) 2457-2466.

[16] G.D. Lopaschuk, C.D. Folmes, W.C. Stanley, Cardiac energy metabolism in obesity, Circ Res 101 (2007) 335-347.

[17] D.J. Duncker, R.J. Bache, Regulation of coronary blood flow during exercise, Physiol Rev 88 (2008) 1009-1086.

[18] E.O. Feigl, Coronary physiology, Physiol Rev 63 (1983) 1-205.

[19] J.D. Tune, M.W. Gorman, E.O. Feigl, Matching coronary blood flow to myocardial oxygen consumption, J Appl Physiol 97 (2004) 404-415.

[20] M. Hashimoto, M. Akishita, M. Eto, K. Kozaki, J. Ako, N. Sugimoto, M. Yoshizumi, K. Toba, Y. Ouchi, The impairment of flow-mediated vasodilatation in obese men with visceral fat accumulation, Int J Obes Relat Metab Disord 22 (1998) 477-484.

[21] S. Kapiotis, G. Holzer, G. Schaller, M. Haumer, H. Widhalm, D. Weghuber, B. Jilma, G. Roggla, M. Wolzt, K. Widhalm, O.F. Wagner, A proinflammatory state is detectable in obese children and is accompanied by functional and morphological vascular changes, Arterioscler Thromb Vasc Biol 26 (2006) 2541-2546.

[22] W.M. Chilian, Coronary microcirculation in health and disease. Summary of an NHLBI workshop, Circulation 95 (1997) 522-528.

[23] Z. Bagi, A. Feher, J. Cassuto, Microvascular responsiveness in obesity: implications for therapeutic intervention, Br J Pharmacol 165 (2012) 544-560.

[24] C.L. Oltman, L.L. Richou, E.P. Davidson, L.J. Coppey, D.D. Lund, M.A. Yorek, Progression of coronary and mesenteric vascular dysfunction in Zucker obese and Zucker diabetic fatty rats, Am J Physiol Heart Circ Physiol 291 (2006) H1780-1787.

[25] R. Prakash, J.D. Mintz, D.W. Stepp, Impact of obesity on coronary microvascular function in the Zucker rat, Microcirculation 13 (2006) 389-396.

[26] E. Jebelovszki, C. Kiraly, N. Erdei, A. Feher, E.T. Pasztor, I. Rutkai, T. Forster, I. Edes, A. Koller, Z. Bagi, High-fat diet-induced obesity leads to increased NO sensitivity of rat coronary arterioles: role of soluble guanylate cyclase activation, Am J Physiol Heart Circ Physiol 294 (2008) H2558-2564.

[27] I.C. Okere, M.P. Chandler, T.A. McElfresh, J.H. Rennison, V. Sharov, H.N. Sabbah, K.Y. Tserng, B.D. Hoit, P. Ernsberger, M.E. Young, W.C. Stanley, Differential effects of saturated and unsaturated fatty acid diets on cardiomyocyte apoptosis, adipose distribution, and serum leptin, Am J Physiol Heart Circ Physiol 291 (2006) H38-44.

[28] D.P. Relling, L.B. Esberg, C.X. Fang, W.T. Johnson, E.J. Murphy, E.C. Carlson, J.T. Saari, J. Ren, High-fat diet-induced juvenile obesity leads to cardiomyocyte dysfunction and upregulation of Foxo3a transcription factor independent of lipotoxicity and apoptosis, J Hypertens 24 (2006) 549-561.

[29] J. Cao, K. Sodhi, N. Puri, S.R. Monu, R. Rezzani, N.G. Abraham, High fat diet enhances cardiac abnormalities in SHR rats: Protective role of heme oxygenase-adiponectin axis, Diabetol Metab Syndr 3 (2011) 37.

[30] W. Hsueh, E.D. Abel, J.L. Breslow, N. Maeda, R.C. Davis, E.A. Fisher, H. Dansky, D.A. McClain, R. McIndoe, M.K. Wassef, C. Rabadan-Diehl, I.J. Goldberg, Recipes for creating animal models of diabetic cardiovascular disease, Circ Res 100 (2007) 1415-1427.

[31] J.F. Carroll, W.J. Zenebe, T.B. Strange, Cardiovascular function in a rat model of diet-induced obesity, Hypertension 48 (2006) 65-72.

[32] V.S. Malik, T.T. Fung, R.M. van Dam, E.B. Rimm, B. Rosner, F.B. Hu, Dietary patterns during adolescence and risk of type 2 diabetes in middle-aged women, Diabetes care 35 (2012) 12-18.

[33] W. Bao, S.R. Srinivasan, W.A. Wattigney, G.S. Berenson, Persistence of multiple cardiovascular risk clustering related to syndrome X from childhood to young adulthood. The Bogalusa Heart Study, Arch Intern Med 154 (1994) 1842-1847.

[34] G.S. Berenson, S.R. Srinivasan, T.A. Nicklas, Atherosclerosis: a nutritional disease of childhood, Am J Cardiol 82 (1998) 22T-29T.

[35] M.Y. Cortez, C.E. Torgan, J.T. Brozinick, Jr., J.L. Ivy, Insulin resistance of obese Zucker rats exercise trained at two different intensities, Am J Physiol 261 (1991) E613-619.

[36] F.L. Gobel, L.A. Norstrom, R.R. Nelson, C.R. Jorgensen, Y. Wang, The rate-pressure product as an index of myocardial oxygen consumption during exercise in patients with angina pectoris, Circulation 57 (1978) 549-556.

[37] A.E. Favier, Analysis of free radicals in biological systems, Birkhauuser Verl., Basel, 1995.

[38] W.A. Gunzler, H. Kremers, L. Flohe, An improved coupled test procedure for glutathione peroxidase (EC 1-11-1-9-) in blood, Z Klin Chem Klin Biochem 12 (1974) 444-448.

[39] H.-U. Bergmeyer, K. Gawehn, D.H. Williamson, P. Lund, Methods of enzymatic analysis, second English ed, Verlag Chemie ; Academic Press, Weinheim New York ; London, 1974.

[40] E.M. Nuutinen, Subcellular origin of the surface fluorescence of reduced nicotinamide nucleotides in the isolated perfused rat heart, Basic Res Cardiol 79 (1984) 49-58.

[41] P.R. Gardner, D.D. Nguyen, C.W. White, Aconitase is a sensitive and critical target of oxygen poisoning in cultured mammalian cells and in rat lungs, Proc Natl Acad Sci U S A 91 (1994) 12248-12252.

[42] E. Mourmoura, M. Leguen, H. Dubouchaud, K. Couturier, D. Vitiello, J.L. Lafond, M. Richardson, X. Leverve, L. Demaison, Middle age aggravates myocardial ischemia through surprising upholding of complex II activity, oxidative stress, and reduced coronary perfusion, Age 33 (2011) 321-336.

[43] G.R. Faloona, P.A. Srere, Escherichia coli citrate synthase. Purification and the effect of potassium on some properties, Biochemistry 8 (1969) 4497-4503.

[44] M.S. Winzell, B. Ahren, The high-fat diet-fed mouse: a model for studying mechanisms and treatment of impaired glucose tolerance and type 2 diabetes, Diabetes 53 Suppl 3 (2004) S215-219.

[45] C. Cruciani-Guglielmacci, M. Vincent-Lamon, C. Rouch, M. Orosco, A. Ktorza, C. Magnan, Early changes in insulin secretion and action induced by high-fat diet are related to a decreased sympathetic tone, Am J Physiol Endocrinol Metabol 288 (2005) E148-154.

[46] D.M. Ouwens, C. Boer, M. Fodor, P. de Galan, R.J. Heine, J.A. Maassen, M. Diamant, Cardiac dysfunction induced by high-fat diet is associated with altered myocardial insulin signalling in rats, Diabetologia 48 (2005) 1229-1237.

[47] S. Furukawa, T. Fujita, M. Shimabukuro, M. Iwaki, Y. Yamada, Y. Nakajima, O. Nakayama, M. Makishima, M. Matsuda, I. Shimomura, Increased oxidative stress in obesity and its impact on metabolic syndrome, J Clin Invest 114 (2004) 1752-1761.

[48] C.J. Holloway, L.E. Cochlin, Y. Emmanuel, A. Murray, I. Codreanu, L.M. Edwards, C. Szmigielski, D.J. Tyler, N.S. Knight, B.K. Saxby, B. Lambert, C. Thompson, S. Neubauer, K. Clarke, A high-fat diet impairs cardiac high-energy phosphate

metabolism and cognitive function in healthy human subjects, Am J Clin Nutr 93 (2011) 748-755.

[49] D.R. Janero, D. Hreniuk, H.M. Sharif, Hydrogen peroxide-induced oxidative stress to the mammalian heart-muscle cell (cardiomyocyte): nonperoxidative purine and pyrimidine nucleotide depletion, J Cell Physiol 155 (1993) 494-504.

[50] F.L. Hoch, Cardiolipins and biomembrane function, Biochim Biophys Acta 1113 (1992) 71-133.

[51] J. St-Pierre, J.A. Buckingham, S.J. Roebuck, M.D. Brand, Topology of superoxide production from different sites in the mitochondrial electron transport chain, J Biol Chem 277 (2002) 44784-44790.

[52] Z. Bagi, Mechanisms of coronary microvascular adaptation to obesity, Am J Physiol 297 (2009) R556-567.

[53] A. Ceriello, L. Quagliaro, B. Catone, R. Pascon, M. Piazzola, B. Bais, G. Marra, L. Tonutti, C. Taboga, E. Motz, Role of hyperglycemia in nitrotyrosine postprandial generation, Diabetes care 25 (2002) 1439-1443.

[54] A. Romero-Corral, V.K. Somers, J. Sierra-Johnson, Y. Korenfeld, S. Boarin, J. Korinek, M.D. Jensen, G. Parati, F. Lopez-Jimenez, Normal weight obesity: a risk factor for cardiometabolic dysregulation and cardiovascular mortality, Eur Heart J 31 (2010) 737-746.

[55] P. Marques-Vidal, A. Pecoud, D. Hayoz, F. Paccaud, V. Mooser, G. Waeber, P. Vollenweider, Normal weight obesity: relationship with lipids, glycaemic status, liver enzymes and inflammation, Nutr Metab Cardiovasc Dis 20 (2010) 669-675.

[56] C.R. Wilson, M.K. Tran, K.L. Salazar, M.E. Young, H. Taegtmeyer, Western diet, but not high fat diet, causes derangements of fatty acid metabolism and contractile dysfunction in the heart of Wistar rats, Biochem J 406 (2007) 457-467.

[57] R. Subramanian, K.M. MacLeod, Age-dependent changes in blood pressure and arterial reactivity in obese Zucker rats, Eur J Pharmacol 477 (2003) 143-152.

[58] A. Oudot, C. Martin, D. Busseuil, C. Vergely, L. Demaison, L. Rochette, NADPH oxidases are in part responsible for increased cardiovascular superoxide production during aging, Free Radic Biol Med 40 (2006) 2214-2222.

[59] G. Lenaz, M.L. Genova, Structure and organization of mitochondrial respiratory complexes: a new understanding of an old subject, Antioxid Redox Signal 12 (2010) 961-1008.

[60] G. Ermak, K.J. Davies, Calcium and oxidative stress: from cell signaling to cell death, Mol Immunol 38 (2002) 713-721.

[61] M.J. Kruger, A.M. Engelbrecht, J. Esterhuyse, E.F. du Toit, J. van Rooyen, Dietary red palm oil reduces ischaemia-reperfusion injury in rats fed a hypercholesterolaemic diet, Br J Nutr 97 (2007) 653-660.

[62] P. Wang, J.C. Chatham, Onset of diabetes in Zucker diabetic fatty (ZDF) rats leads to improved recovery of function after ischemia in the isolated perfused heart, Am J Physiol Endocrinol Metab 286 (2004) E725-736.

[63] P.A. McAuley, S.N. Blair, Obesity paradoxes, J Sports Sci 29 773-782.

Acknowledgements

We would like to thank Mr. Cristophe Cottet for carefully editing the manuscript, Cindy Tellier for animal care, Joelle Demaison for the determination of respiratory complex chain activities and Mireille Osman for the plasma thiol, FRAP assay and GPx activity determination. This work was supported by the French National Institute of Agronomical Research (INRA), the French National Institute of Health and Medical Research (INSERM) and Joseph Fourier University, Grenoble, France.

Figure Captions

Fig. 1. Glucose metabolism. A: Basal glycemia for the four groups two weeks before sacrifice; B: Glucose response of the animals two weeks before sacrifice; C: Total area under the curve for the glucose response two weeks before sacrifice; D: Difference between glycemia at timepoints zero and 25 derived from the glucose response diagram; E: Difference between glycemia at timepoints zero and 180 derived from the glucose response diagram. YAC: young adult control group; YAF: young adult HF-fed group; MAC: middle-aged adult control group and MAF: middle-aged adult HF-fed group. The number of experiments was 8 for each group. a, b, c: significantly different; a common letter between two values indicates no significant difference

Fig. 2. Effets of age and high-fat diet on the endothelial-dependent dilatation (EDD, panel A), endothelial-independent dilatation (EID, panel B) and endothelial cell vasodilatation activity (ECVA, panel C) of the coronary microvascular network of the perfused hearts. YAC: young adult control group; YAF: young adult HF-fed group; MAC: middle-aged adult control group and MAF: middle-aged adult HF-fed group. The number of experiments was 8 for each group. a, b, c: significantly different; a common letter between two values indicates no significance

Fig. 3. Protein expression of total eNOS and phosphorylated eNOS at Ser1177 in cardiac homogenates. A: representative immunoblots of total eNOS, phosphorylated eNOS at Ser1177 (p-eNOS) and actin; B: quantified total eNOS and phosphorylated eNOS and ratio between the phosphorylated and total eNOS. YAC: young adult control group; YAF: young adult HF-fed group; MAC: middle-aged adult control group and MAF: middle-aged adult HF-fed group. The number of experiments was 6 for each group

Fig. 4. Oxidative stress measurements. A: plasma oxidative stress estimated by the disappearance of the plasma thiol groups; B: antioxidant power of the plasma estimated by the

FRAP assay; C: enzymatic activity of GPx in the plasma; D: cytosolic oxidative stress estimated by the lactate-to-pyruvate ratio; E: mitochondrial oxidative stress estimated by the aconitase-to-fumarase ratio. YAC: young adult control group; YAF: young adult HF-fed group; MAC: middle-aged adult control group and MAF: middle-aged adult HF-fed group. The number of experiments was 8 for each group. a, b, c: significantly different; a common letter between two values indicates no significance

Fig. 5. H_2O_2 release from cardiac isolated mitochondria. H_2O_2 production was measured in the presence of substrate, rotenone and antimycin A: palmitoylcarnitine as substrate; B glutamate/malate as substrates; C succinate as substrate; D: glutamate/malate plus succinate (G/M/S) as substrates. YAC: young adult control group; YAF: young adult HF-fed group; MAC: middle-aged adult control group and MAF: middle-aged adult HF-fed group. The number of experiments was 8 for each group. a, b, c: significantly different; a common letter between two values indicates no significance

Fig. 6. Mitochondrial respiration studied in cardiac isolated mitochondria. State 2 corresponds to respiration in the presence of substrate, state 3 is the respiration in the presence of substrate plus exogenous ADP and state 4 corresponds to respiration in the absence of ATP synthesis using exogenous oligomycin to inhibit ATP synthase. A: palmitoylcarnitine respiration; B glutamate/malate respiration; C succinate respiration ; D : glutamate/malate plus succinate (G/M/S) respiration. YAC: young adult control group; YAF: young adult HF-fed group; MAC: middle-aged adult control group and MAF: middle-aged adult HF-fed group. The number of experiments was 8 for each group. a, b: significantly different; a common letter between two values indicates no significance

Table 1. Basic characteristics of the animals

	YAC	YAF	MAC	MAF
Body weight	443 ± 4^{a}	473 ± 11^{ab}	503 ± 15^{b}	487 ± 30^{ab}
Epididymal AT	13.5 ± 1.3^{a}	22.7 ± 1.9^{b}	15.4 ± 1.1^{a}	24.0 ± 3.3^{b}
Visceral AT	9.4 ± 1^{a}	14.6 ± 1.4^{b}	10.7 ± 0.6^{a}	16.9 ± 2.2^{b}
Retroperitoneal AT	12.8 ± 1.4^{a}	27.1 ± 2.4^{b}	12.6 ± 0.9^{a}	32.5 ± 4.4^{b}
Abdominal AT	22.2 ± 2.2^{a}	41.6 ± 3.6^{b}	23.3 ± 1.3^{a}	49.4 ± 6.5^{b}
Abdominal AT/BW	0.050 ± 0.005^{a}	0.086 ± 0.006^{b}	0.046 ± 0.002^{a}	0.099 ± 0.009^{b}
Triglycerides	1.3 ± 0.1	1 ± 0.08	1.2 ± 0.30	1.2 ± 0.10
Cholesterol	0.56 ± 0.02^{a}	0.98 ± 0.06^{b}	0.59 ± 0.11^{a}	1.11 ± 0.05^{b}

Body weight, epididymal, visceral, retroperitoneal and abdominal adipose tissues weights are expressed in g of wet weight. The abdominal adipose tissue weight normalized to the body weight is expressed in g of wet weight per g of body weight. Triglycerides and cholesterol are expressed in g/l. AT: adipose tissue; BW: body weight; YAC: young adult control group; YAF: young adult high-fat fed group; MAC: middle-aged adult control group and MAF: middle-aged adult high-fat-fed group. The number of experiments was 8 for each group. a, b: significantly different; a common letter between two values indicates no significant difference.

Table 2. *Ex vivo* cardiac function

	YAC	YAF	MAC	MAF
HR (beats/min)	272 ± 11	270 ± 8	253 ± 17	278 ± 17
LVDP (mmHg)	90.1 ± 4[a]	64.8 ± 6.9[b]	104 ± 9[a]	66 ± 5[b]
RPP (mHg/min)	23.2 ± 1[a]	15.2 ± 1.6[b]	24.7 ± 2.6[a]	18.5 ± 2.2[b]
CP before U46619 (mmHg)	74 ± 5	77 ± 4	82 ± 3	64 ± 4
CP after U46619 (mmHg)	123 ± 8	129 ± 7	132 ± 9	101 ± 15

HR: heart rate; LVDP: left ventricle developed pressure; RPP: rate pressure product; CP: coronary pressure; YAC: young adult control group; YAF: young adult high-fat fed group; MAC: middle-aged adult control group and MAF: middle-aged adult high-fat fed group. The number of experiments was 8 for each group. a, b: significantly different; a common letter between two values indicates no significant difference

Table 3. Yield of mitochondrial H_2O_2 production

		YAC	YAF	MAC	MAF
yield of H_2O_2 production	Palmitoylcarnitine	8.0 ± 1.0^{a}	7.4 ± 0.9^{a}	6 ± 0.3^{a}	4.6 ± 0.5^{b}
	Glutamate/Malate	5.0 ± 0.7^{a}	5.2 ± 0.5^{a}	4.3 ± 0.2^{a}	3.1 ± 0.4^{b}
	Succinate	14.7 ± 0.5^{a}	27.1 ± 3.3^{b}	37.8 ± 2.7^{c}	36.9 ± 5.5^{bc}
	G/M/S	19.5 ± 3.4^{a}	25.2 ± 3.5^{ab}	32.5 ± 2.3^{b}	31.6 ± 3.9^{b}

The yield of H_2O_2 production is expressed in pmoles of H_2O_2/ng atom of oxygen. G/M/S: glutamate/malate/succinate; YAC: young adult control group; YAF: young adult high-fat fed group; MAC: middle-aged adult control group and MAF: middle-aged adult high-fat fed group. The number of experiments was 8 for each group. a, b, c: significantly different; a common letter between two values indicates no significant difference

Table 4. Activities of mitochondrial enzymes

	YAC	YAF	MAC	MAF
CS	4.75 ± 0.1	5.43 ± 0.15	4.44 ± 0.14	6.1 ± 1.5
CI	2.39 ± 0.14^{ab}	1.82 ± 0.3^{a}	2.7 ± 0.06^{b}	1.6 ± 0.32^{a}
CII	0.86 ± 0.09	0.79 ± 0.04	0.72 ± 0.05	0.75 ± 0.1
CIII	2.19 ± 0.09	1.75 ± 0.13	1.87 ± 0.21	1.53 ± 0.53
CIV	3.59 ± 0.21^{ab}	4 ± 0.33^{a}	3.51 ± 0.22^{ab}	2.64 ± 0.38^{b}

The results are expressed in mU/mg of proteins. CS: citrate synthase; CI: NADH:ubiquinone oxidoreductase; CII: succinate-ubiquinone oxydo-reductase; CIII: ubiquinol-cytochrome-c reductase; CIV: cytochrome c oxidase; YAC: young adult control group; YAF: young adult high-fat fed group; MAC: middle-aged adult control group and MAF: middle-aged adult high-fat fed group. The number of experiments was 8 for each group. a, b: significantly different; a common letter between two values indicates no significant difference

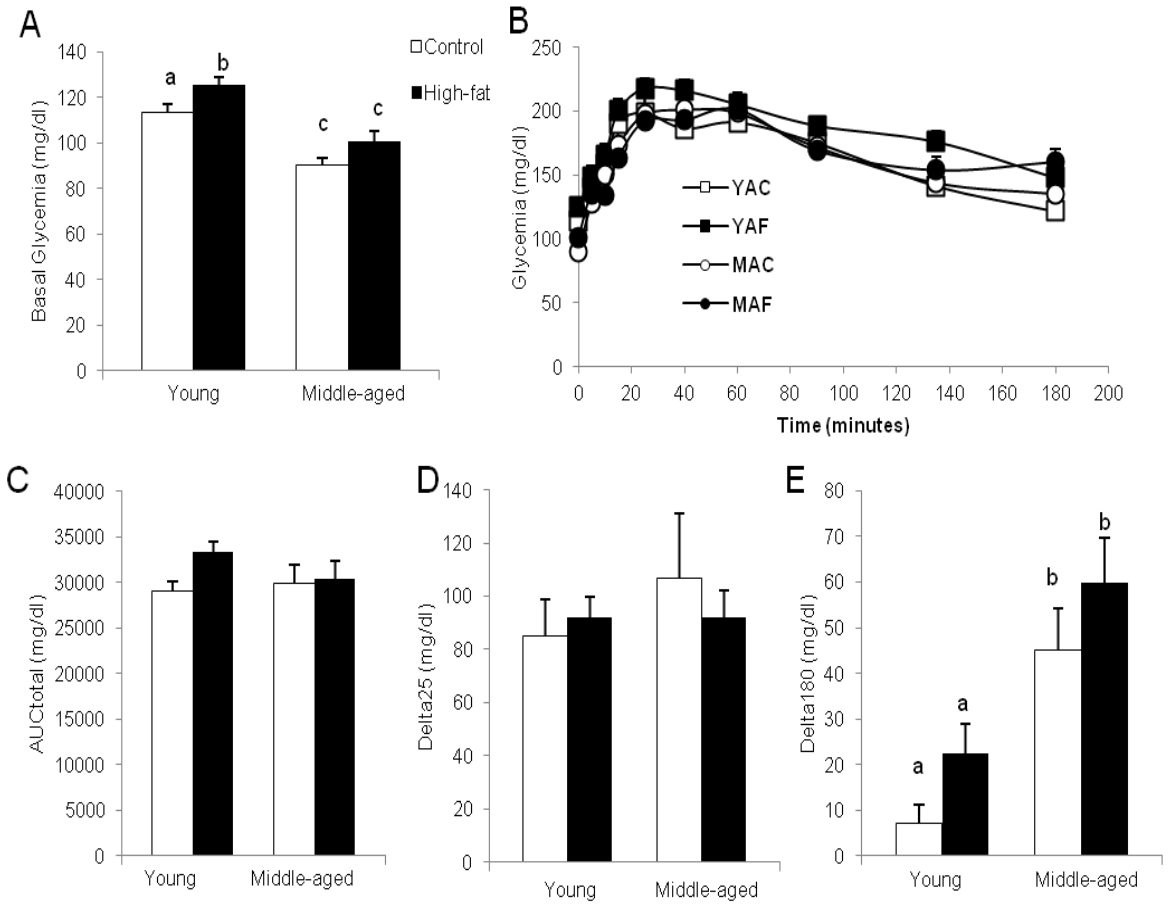
A
Basal Glycemia (mg/dl)
Control
High-fat
a
b
c
c
Young
Middle-aged
B
Glycemia (mg/dl)
YAC
YAF
MAC
MAF
Time (minutes)
C
AUCtotal (mg/dl)
Young
Middle-aged
D
Delta25 (mg/dl)
Young
Middle-aged
E
Delta180 (mg/dl)
a
a
b
b
Young
Middle-aged

Figure 1

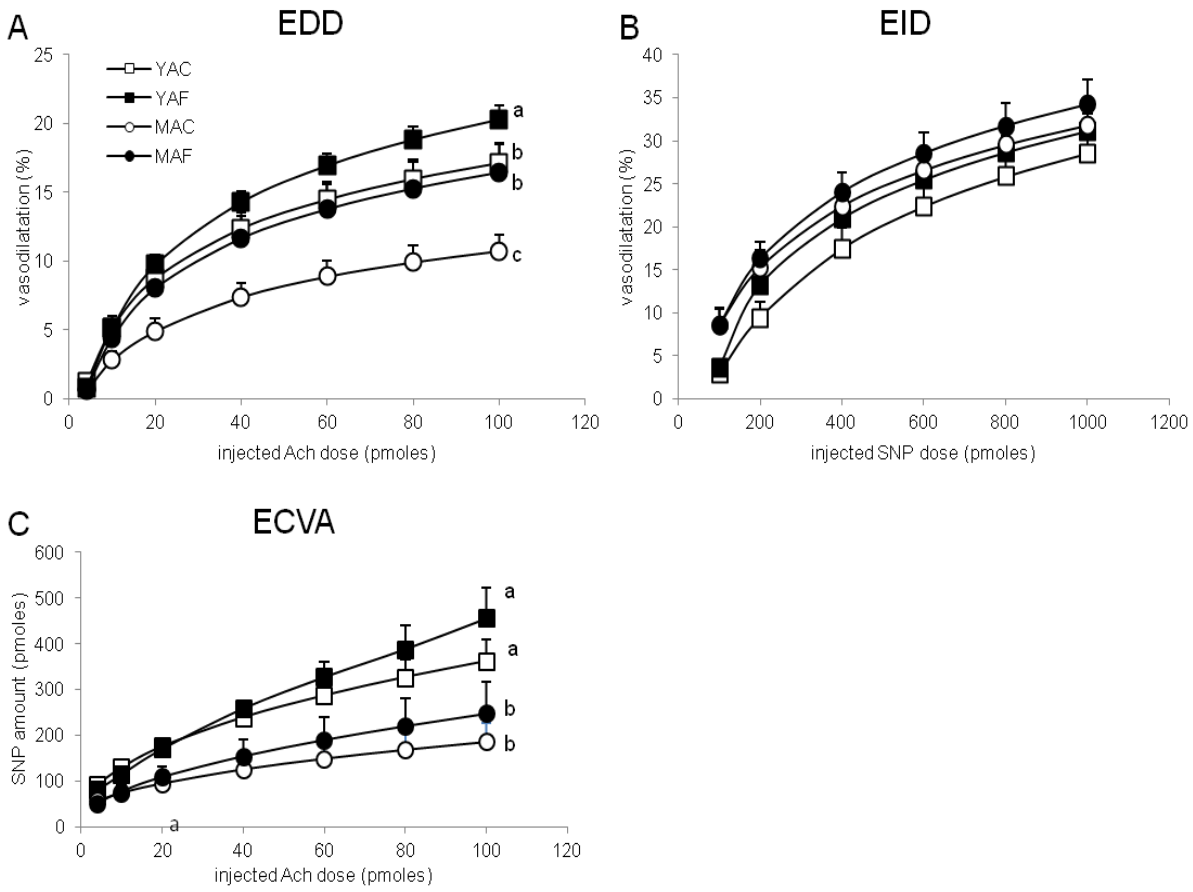
A
EDD
YAC
YAF
MAC
MAF
vasodilatation (%)
injected Ach dose (pmoles)
a
b
b
c
B
EID
vasodilatation (%)
injected SNP dose (pmoles)
C
ECVA
SNP amount (pmoles)
injected Ach dose (pmoles)
a
a
b
b
a

Figure 2

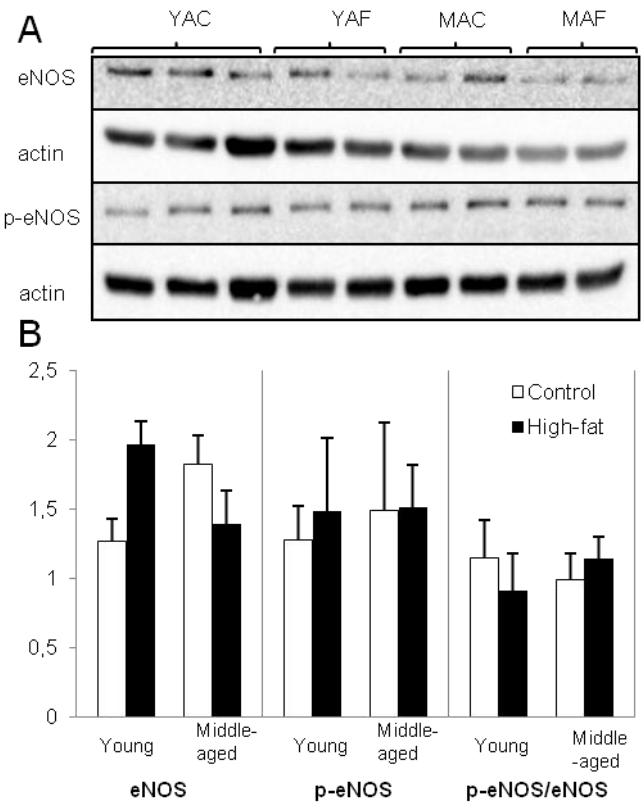
A
YAC
YAF
MAC
MAF
eNOS
actin
p-eNOS
actin
B
2,5
2
1,5
1
0,5
0
Control
High-fat
Young
Middle-aged
Young
Middle-aged
Young
Middle-aged
eNOS
p-eNOS
p-eNOS/eNOS

Figure 3

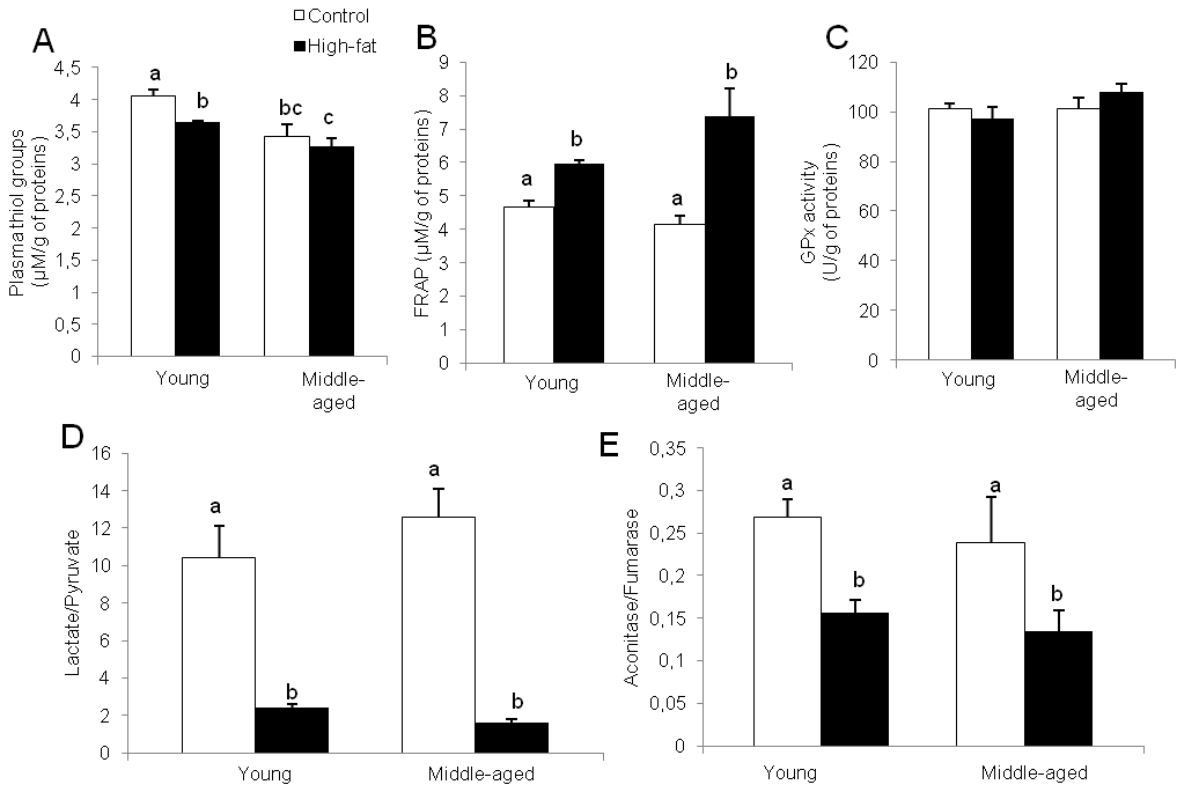
A
Control
High-fat
Plasma thiol groups (µM/g of proteins)
4,5
4
3,5
3
2,5
2
1,5
1
0,5
0
a
b
bc
c
Young
Middle-aged
B
FRAP (µM/g of proteins)
9
8
7
6
5
4
3
2
1
0
a
b
a
b
Young
Middle-aged
C
GPx activity (U/g of proteins)
120
100
80
60
40
20
0
Young
Middle-aged
D
Lactate/Pyruvate
16
14
12
10
8
6
4
2
0
a
b
a
b
Young
Middle-aged
E
Aconitase/Fumarase
0,35
0,3
0,25
0,2
0,15
0,1
0,05
0
a
b
a
b
Young
Middle-aged

Figure 4

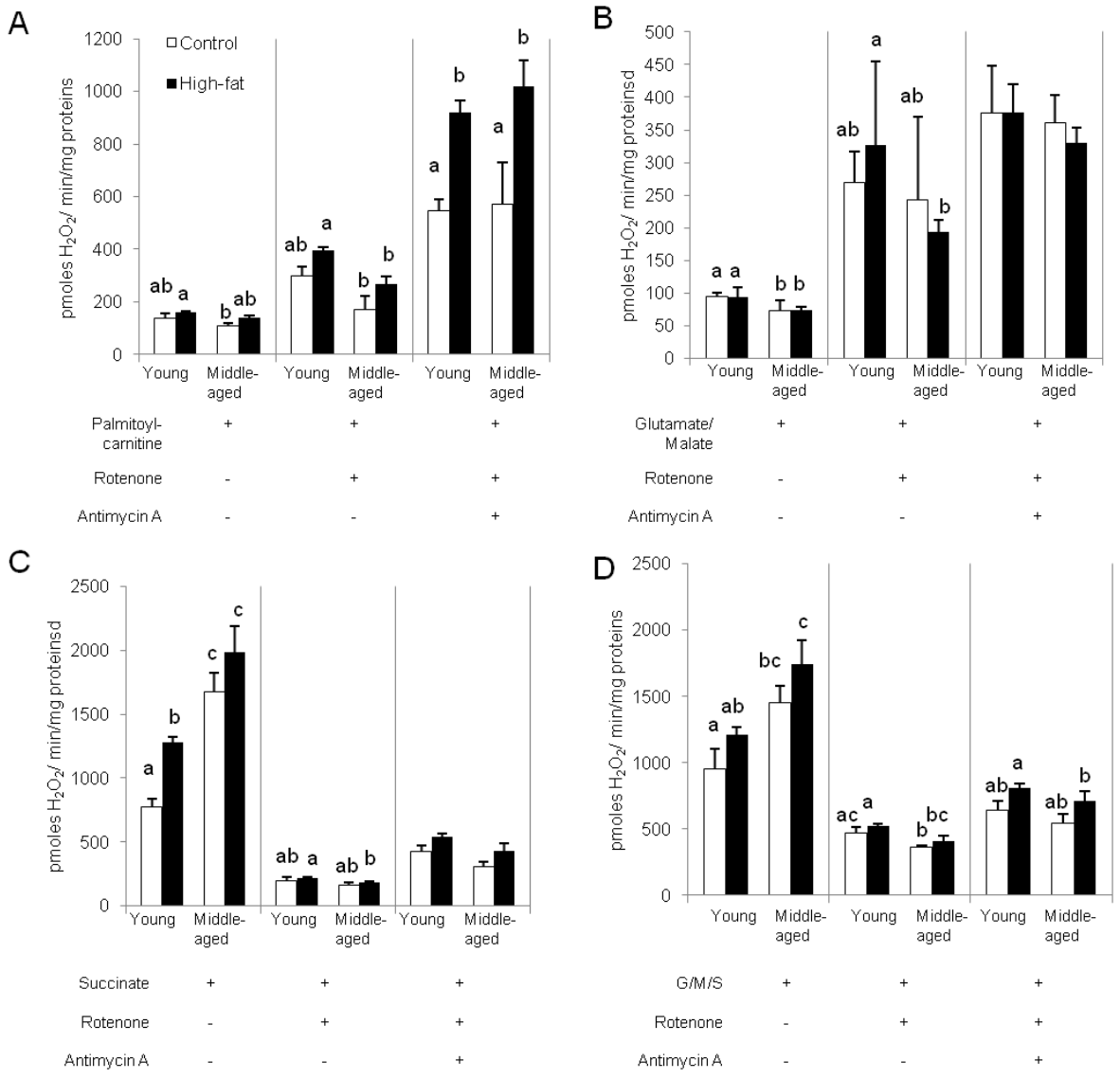
A
Control
High-fat
pmoles H_2O_2/ min/mg proteins
Young
Middle-aged
Palmitoyl-carnitine
Rotenone
Antimycin A
B
pmoles H_2O_2/ min/mg proteinsd
Glutamate/ Malate
Rotenone
Antimycin A
C
pmoles H_2O_2/ min/mg proteinsd
Succinate
Rotenone
Antimycin A
D
pmoles H_2O_2/ min/mg proteins
G/M/S
Rotenone
Antimycin A

Figure 5

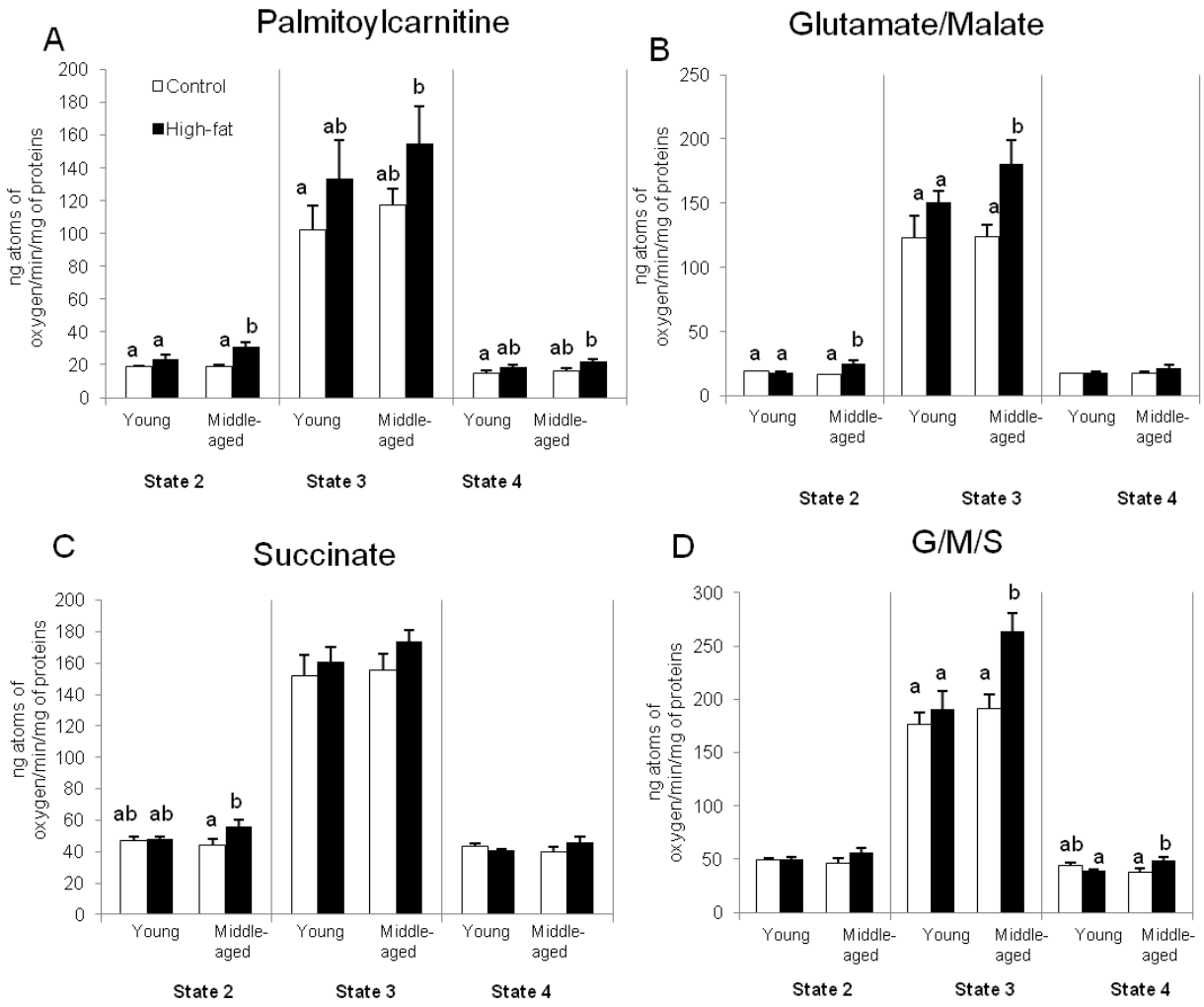
A
Palmitoylcarnitine
Control
High-fat
ng atoms of oxygen/min/mg of proteins
Young
Middle-aged
State 2
State 3
State 4
B
Glutamate/Malate
C
Succinate
D
G/M/S

Figure 6

3.4 ARTICLE IV

"Enhanced ACh-response of the coronary microvasculature in high-fat fed rats: relative contribution of nitric oxide, cyclooxygenase and K^+ channels"

This work will be submitted to the "Journal of Physiology".

Enhanced ACh-response of the coronary microvasculature in high-fat fed rats: relative contribution of nitric oxide, cyclooxygenase and K^+ channels

Evangelia Mourmoura[1,2], Guillaume Vial[1,2], Brigitte Laillet[3], Jean-Paul Rigaudière[3], Beatrice Morio[3], Luc Demaison[1,2,3]

[1]Laboratoire de Bioénergétique Fondamentale et Appliquée, INSERM U1055, Grenoble cedex 09, F-38041, France;

[2]Université Joseph Fourier, Laboratoire de Bioénergétique Fondamentale et Appliquée, INSERM U1055, Grenoble cedex 09, F-38041, France;

[3]INRA, Clermont Université, Université d'Auvergne, Unité de Nutrition Humaine, BP 10448, F-63000 Clermont-Ferrand, France;

Running title : High-fat diet induces coronary microvascular adaptation

Key words : obesity, microvasculature, vasodilation

Total number of words: 6701

Correspondence to L. Demaison, Laboratoire de Bioénergétique Fondamentale et Appliquée, INSERM U1055, Université Joseph Fourier, BP 53, 38041 Grenoble cedex 09, France. Tel. (+33) 476 63 56 00; Fax (+33) 476 51 42 18; e-mail: luc.demaison@ujf-grenoble.fr

Key points summary

- Previous studies on coronary vessels have led to controversial results concerning the effects of obesity on the microvascular reactivity.
- In this study we focused on the impact of high-fat diet induced obesity on the cardiac function and the reactivity of the intact coronary microvasculature perfused *ex vivo*.
- We show that the chosen high-fat diet in this study induced enhanced responses to ACh of the coronary microvessels despite the depressed cardiac mechanical activity *ex vivo*.
- The presence of various inhibitors during the heart perfusion revealed an important role of nitric oxide and cyclooxygenase in this response.
- These results suggest that coronary microvessels adapt to maintain correct coronary reserve when needed in order to avoid insufficient oxygen supply to the heart.

Word count: 124

Abstract

Despite the accumulating evidence associating obesity and vascular dysfunction, the impact of obesity on the coronary microvessels is controversial. This study aimed at characterizing the effects of DIO on the function of the intact coronary microvasculature. 3 month-old rats were randomly assigned to follow a standard or a HF diet (54% of fat) protocol for 3 months. The *ex vivo* perfusion of their hearts revealed a decreased cardiac mechanical activity but a maintained mechanical efficiency whereas the responses to ACh of the coronary microvasculature were enhanced. Inhibition of NOS in the presence of L-NAME reduced the response in both dietary groups whereas COX inhibition by indomethacin reduced it significantly only in the HF fed group. A synergistic action between NO and COX-derived mediators in the ACh-response was revealed with the use of both inhibitors. Blockage of K^+ channels with TEA erased almost totally the response indicating a major role of these channels in coronary microvessel dilatation and a possible role for EDHF. The cardiac membrane phospholipid fatty acid composition demonstrated an increase in the AA content that could be related to the results of EDD observed in the presence of indomethacin. Thus, these findings suggest that the coronary microvasculature adapts in response to HF diet by modulating the NOS and COX pathways. This adaptation may counteract for the decreased cardiac mechanical activity observed in the present study in order for the heart to maintain a satisfying myocardial pumping activity in physiological processes with increased metabolic demand such as exercise.

Abbreviations

AA, arachidonic acid; COX, cyclooxygenase; DHA, docosahexaenoic acid; ECs, endothelial cells; EDD, endothelium-dependent dilatation; EID, endothelium-independent dilatation; EDHF, endothelium-derived hyperpolarizing factor; eNOS, endothelial nitric oxide synthase; EPA, eicosapentanoic acid; HF, high-fat; LVDP, left ventricle developed pressure; MUFA, monounsaturated fatty acid; NO, nitric oxide; NOS, nitric oxide synthase; PUFA, polyunsaturated fatty acid; RPP, rate pressure product; SNP, sodium nitroprusside; SFA, saturated fatty acid.

Introduction

In Western societies, the prevalence of obesity has increased dramatically in the past decade (Flegal *et al.*, 2010). Obesity, and especially central or abdominal obesity, is strongly associated with the development of metabolic syndrome and type 2 diabetes mellitus conferring increased risk for developing cardiovascular disease and its complications. States of hyperglycemia and insulin resistance that may characterize obese individuals are associated with increased oxidative stress and inflammation in the organism (Bagi, 2009). These metabolic changes affect eventually the peripheral and coronary vascular function especially of large conduit arteries (Hashimoto *et al.*, 1998; Kapiotis *et al.*, 2006). A key feature in this process is the reduced production of NO, a compound that mediates endothelium-dependent vasorelaxation and inhibits inflammation.

However, the impact of obesity on the coronary microcirculation remains controversial. The primary function of the coronary microcirculation is to optimize nutrient and oxygen supply to the heart in response to any metabolic demand by coordinating the resistances within different microvascular domains, each governed by distinct regulatory mechanisms (Jones *et al.*, 1995; Chilian, 1997). The large conduit coronary arteries exert small, if any, resistance since resistance to blood flow rises as the vessel diameter decreases. These observations underline the need for direct examination of the function of coronary resistance arteries to understand how their vasomotor behavior changes and how it relates to coronary blood flow alterations in obese individuals.

One of the early alterations in obesity is considered to be the vasomotor dysfunction of the coronary vessels, which leads to the disturbed regulation of tissue perfusion and predisposes patients to myocardial ischemia (Caballero, 2003). However, in states of uncomplicated obesity, when no comorbid conditions such as hypertension or diabetes exist, morphological changes in microvessels are quite rare (Hall *et al.*, 1999; Bagi *et al.*, 2012). Furthermore,

recent studies on isolated coronary arterioles have shown that the EDD in obese, young diabetic or HF fed rats are maintained or even enhanced (Oltman *et al.*, 2006; Prakash *et al.*, 2006; Jebelovszki *et al.*, 2008). In the coronary circulation where oxygen extraction is near maximal, changes in EDD can have significant consequence if other mediators fail to compensate. An increased sensitivity of the soluble guanylate cyclase to NO (Brandes *et al.*, 2000) and upregulation of COX-2 (Sanchez *et al.*, 2010) have been described in situations of obesity and diabetes.

Moreover, in patients with coronary artery disease, the primary mediator of flow-induced dilation in the coronary circulation of healthy patients shifts from NO to an EDHF, which acts via Ca^{2+}-activated potassium channels (Miura *et al.*, 2001). This shift in mediator balance to endothelial-dependent hyperpolarizing factor could be a compensation for the loss of NO. Molecules such as the H_2O_2 (Liu *et al.*, 2011) or AA derived products of cytochrome P-450 (CYP-450) (Fisslthaler *et al.*, 1999) have been proposed to act as EDHF in different vascular beds and species.

Thus, the aim of this study was to determine the effects of a HF diet on the cardiac function and to assess the endothelial function of the intact coronary microvasculature in terms of endothelium-dependent and -independent vasodilatations in an *ex vivo* heart perfusion model. We also evaluated the contribution of the main vasodilator pathways in the observed EDD by using inhibitors that block NO production, cyclooxygenases or potassium channels during the perfusion protocol. Finally, the fatty acid profile of cardiac membrane phospholipids was estimated.

Materials and Methods

Ethical approval

All experiments followed the European Union recommendations concerning the care and use of laboratory animals for experimental and scientific purposes. All animal work was approved by the local board of ethics for animal experimentation (Cometh) and notified to the research animal facility of our laboratory (authorization n° 38 07 23).

Experimental Animals and Diet

Male Wistar rats from an inbred colony were housed two per cage in our animal facility at 3 months of age. They were randomly assigned to be maintained on standard carbohydrate (C: 16.1% proteins, 3.1% lipids, 60% cellulose; A04, Safe, France) or high-fat (HF: 31.5% proteins, 54% lipids (50% lard, 4% soya-bean oil w/w), 7% cellulose) diet over a twelve-week period. The energy from fat in this diet typically represents more than 50% of total calories (Wilkes *et al.*, 1998; Dobrian *et al.*, 2000) as in an average Western diet. After analysis of the fatty acid composition of the diets chosen we found that the standard diet contained approximately 24% of SFAs, 23% of MUFAs, 48% of n-6 PUFAs and 4.5% of n-3 PUFAs while the HF diet contained 37% of SFAs, 46% of MUFAs, 15% of n-6 PUFAs and 1.2% of n-3 PUFAs. All groups were fed *ad libitum* with free access to water and their body weight and food intake were recorded twice weekly as previously described (Vial *et al.*). It should be noted that the protein content of the HF-diet was 2-fold higher because of the lower food intake (g/day) in these rats due to the higher energy density. This allowed a similar daily protein intake in all rat groups.

On the day of the experiment, the rats were weighed and heparinized (1,000 I.U./kg) via the saphenous vein before their sacrifice. Blood samples were collected for further biochemical analysis and their adipose tissue was quantified for determination of the abdominal fat mass.

Cardiac function study

All rats underwent *ex vivo* Langendorff assessment of their cardiac function. For this reason, a rapid thoracotomy was performed and the heart was immediately collected in Krebs-Heinselet solution maintained at 4^{o}C. It was then rapidly (less than 1 minute from the chest opening to avoid problem of cellular damages and preconditioning) perfused at constant pressure according to the Langendorff mode with a Krebs–Heinselett buffer containing (in mM) NaCl 119, $MgSO_4$ 1.2, KCl 4.8, $NaHCO_3$ 25, KH_2PO_4 1.2, $CaCl_2$ 1.2 and glucose 11 mM as sole energy substrate. The buffer was maintained at 37^{o}C and continuously oxygenated with carbogen (95% O2/5% CO2). A latex balloon connected to a pressure probe was inserted into the left ventricle and filled until the diastolic pressure reached a value of 7–8 mmHg. This allowed the monitoring of heart rate, systolic, diastolic and left ventricle developed pressures throughout the perfusion protocol. A pressure gauge inserted into the perfusion circuit just upstream the aortic cannula allowed the evaluation of the coronary pressure. The heart was perfused at constant pressure of 59 mmHg for 30 minutes and the coronary flow for each heart was evaluated by weight determination of 1-min collected samples at the 25th min of perfusion. After this period, the heart was perfused at constant flow conditions, for which the flow rate was adjusted in order to obtain the same coronary flow as in the preparation at constant pressure. The systolic, diastolic and left ventricle developed pressures as well as the heart rates were determined after 10 min of perfusion at forced flow in order to allow a satisfying stabilization of the heart. The left ventricle developed pressure was calculated by subtracting the diastolic pressure to the systolic pressure. The rate-pressure product (RPP) was defined as the product of left ventricle developed pressure and heart rate. All the parameters were recorded and analyzed with a computer using the HSE IsoHeart software (Hugo Sachs Elektronik, March-Hugstetten, Germany).

Coronary Reactivity

After the evaluation of the cardiac function at constant flow, we assessed the effects of the HF diet on the coronary reactivity. After the 10-min equilibration period at constant flow, the coronary tone was raised by using the thromboxane analog U46619 (30nM), which was constantly infused into the perfusion system near the aortic cannula at a rate never exceeding 1.5% of the coronary flow. This allowed the obtainment of a coronary pressure between 90 and 110 mmHg. In our model of perfusion at forced flow, the aortic pressure equaled the coronary pressure and changes in the coronary tone triggered modifications of the aortic pressure. Changes in aortic perfusion pressure were thus used to monitor changes in coronary tone. Furthermore, this experimental model permitted the evaluation of the coronary microvasculature reactivity since the coronary resistance vessels determine the overall coronary pressure. Relaxation responses to ACh (4, 10, 20, 40, 60, 80 and 100 pmoles) and sodium nitroprusside (SNP, 100, 200, 400, 600, 800 and 1000 pmoles) injections were determined reflecting the endothelial-dependent vasodilatation (EDD) and endothelium-independent vasodilatation (EID) respectively.

The dilatation amplitude was calculated as the ratio between the maximal decrease in the coronary pressure and the coronary pressure just before the injection of the dilatation agents. Since the heart weight and coronary volume were subjected to intra- and inter-group variations, a correction was performed to normalise the input-function of the vasodilatation agents according to the coronary flow. The dose-response curve between the amount of vasodilatation agent injected and the maximal vasodilatation was then fitted to a logarithm function for each heart, which allowed the fulfillment of statistical analyses. Moreover, the vasodilatation activity of the ECs was also estimated from the corrected EDD and EID curves. For each heart and each injected ACh dose, the amount of SNP (reflecting the amount of vasodilator agents) necessary to obtain the same percentage of ACh-induced vasodilatation

was extracted from the EID curve according to the formula: endothelial cell vasodilatation activity (ECVA) = $e^{[(\%\ \text{ACh-induced dilatation} - b) / a]}$, where a and b are the coefficients of the theoretical EID curve. The results were expressed in pmole equivalents of nitroprusside. At the end of the perfusion protocol, the hearts were freeze-clamped and stored at -80°C until the biochemical analyses were performed.

Fatty acid composition of cardiac phospholipids

The phospholipid fatty acid composition was determined in cardiac homogenates as previously described (Demaison *et al.*, 2001). The lipids were extracted according to Folch *et al*. (Folch *et al.*, 1957). The phospholipids were separated from non-phosphorus lipids using a Sep-pack cartridge (Juaneda *et al.*, 1990). After transmethylation, the fatty acid methyl esters were separated and analyzed by gas chromatography.

Other biochemical determinations

All biochemical measures (total cholesterol, triglycerides, glucose) were done in plasma samples by using an automated analyser (HITACHI 912, Roche Diagnostics). Chemicals were obtained from Roche, (Meylan, France) Proteins were measured using the bicinchoninic acid method with a commercially available kit (Thermo Scientific, Rockford, IL).

Perfusion protocols with inhibitors

A second series of experiments was conducted to further examine the contribution of the main vasorelaxant molecules to the EDD. For this reason, we performed the experiments of the coronary reactivity in the presence of inhibitors in order to evaluate the contribution of NO, COX and potassium channels in the ACh-induced dilatation for both control and HF fed rats. To examine the involvement of NO, L-NAME, an inhibitor of NO synthesis, was added

extemporaneously to the Krebs solution at a concentration of 0.1 mM and was allowed to circulate during the whole perfusion. In separate experiments, indomethacin, a COX inhibitor, was added to the bath at a concentration of 2.5 µM and the coronary reactivity of control and HF rats was assessed in order to evaluate the role of prostaglandins released by the COX pathway. The indomethacin was prepared and diluted in 2% Na_2CO_3 immediately before use. Experiments were also conducted in the presence of both L-NAME (0.1 mM) and indomethacin (2.5 µM) in order to evaluate the contribution of other mediators in the EDD. Finally, the role of potassium channels was investigated by adding extemporaneously TEA, a non-selective K^+ channel blocker, in the Krebs solution at a concentration of 10 mM. ACh- and SNP- responses were then performed as described previously.

Statistical analysis

Results are presented as mean ± S.E.M. Animal weight, metabolic parameters and data describing the cardiac mechanical and vascular function (developed pressure, heart rate, rate pressure product, coronary pressure, and coronary flow) were contrasted across the two groups by one-way analysis of variance (ANOVA). Measures related to the action of the vasodilatation agents were treated with repeated-measures ANOVA to test the effect of the diet (external factor), that of the amount of dilatation agent (internal factor) and their interactions. To compare the effect of each inhibitor in each dietary group we used one-way repeated measures ANOVA. To determine the effect of each inhibitor in the different dietary groups, two-way repeated measures ANOVA with two factors (inhibitor and diet) were performed. When required, group means were contrasted with a Fisher's LSD test. A probability (p) less than 0.05 was considered significant. Statistical analysis was performed using the NCSS 2004 software.

Results

General data

As shown in Table 1, the body weight of the rats fed the HF diet was not significantly changed. However, the abdominal adipose tissue of the HF rats was significantly increased compared to the control group (+113%). This was responsible for the increase in the ratio of abdominal adipose tissue-to-body weight in the HF group (+96%) indicating a change of fat and muscle distribution in their bodies. The heart weight of the control rats did not differ of that of the HF animals but the ratio heart-to-body weight was significantly decreased in the HF group (-18%). Plasma glucose and insulin concentration was not modified by the HF diet. However, a significant increase in the concentration of cholesterol and triglycerides was observed in the plasma of the HF rats (+48 and +20% respectively).

Fatty acid composition of cardiac phospholipids

The fatty acid composition of cardiac phospholipids was modulated by the HF diet (Table 2). The SFAs were significantly increased in the HF group (+8%). This increase partly occurred at the detriment of the total content of MUFAs (-16%). Indeed, apart from the C18:1n-9 which was increased (+35%), the others MUFAs were significantly reduced (-52 and -43% for the C16:1n-7, and C18:1n-7, respectively). The n-6 polyunsaturated fatty acids (PUFAs) were also reduced, not only in their totality (-5%) but also regarding the 18:2n-6 (-22%). However, all the other n-6 PUFAs were significantly increased (+128, +130, +17, +94 and +109% for C20:2n-6, C20:3n-6, C20:4n-6, C22:4n-6 and C22:5n-6 respectively). The total n-3 PUFAs were not modified by the diet despite the modifications of C20:5n-3 and C22:5n-3 (-68 and +117% respectively). Finally, the n-6 to n-3 PUFA ratio of cardiac phospholipids was not affected by the HF diet.

Cardiac function study

The results of the *ex vivo* cardiac function are shown in Table 3. The measured parameters were recorded when the heart was perfused at constant flow before the infusion of U46619. In the HF group, the developed pressure (LVDP) and the RPP were significantly reduced (-32 and -27% respectively) compared to the control group. However, the significance disappeared when these two parameters were divided by the dry heart weight indicating a maintained cardiac mechanical efficiency. No changes were observed in the heart rate and coronary flow. The coronary pressures at baseline conditions and after the infusion of U46619 were also unaffected.

Coronary reactivity at baseline conditions

In the absence of inhibitors, ACh produced a dose-dependent vasodilatation (Fig. 1A) for both dietary groups. The EDD was significantly greater in the HF compared to the control group (+41% at 60 pmoles of ACh). The EID was not modified by the HF diet and reached approximately 23% of vasodilatation for both groups as soon as the SNP dose of 600 picomoles was injected (Fig. 1B). Finally, the calculated ECVA was not significantly modified by the HF diet (Fig. 1B), but it tended to be higher in this group.

Coronary reactivity in presence of inhibitors

We examined the potential contribution of NOS, cyclooxygenase and K^+ channels to the reactivity of the intact coronary microvasculature *ex vivo* in the control and HF groups in terms of EDD (Fig. 2), EID (Fig. 3) and ECVA (Fig. 4).

- *Effects of L-NAME*

In the presence of L-NAME (Fig. 2A), dilatation to ACh was significantly reduced in both groups (-35% for the control and -42% for the HF group at 60 pmoles of injected ACh). The ACh-responses in the presence of L-NAME were similar among groups and were not influenced by the diet. The difference that was observed in the EDD between control and HF groups in the absence of inhibitors was attenuated in the presence of L-NAME, even though it was not totally erased. We also examined the response of the smooth muscle cells of the coronary microvasculature to increased doses of SNP in order to determine the maximal dilatation response. In the presence of L-NAME (Fig. 3A), the responses to SNP were significantly increased in both groups (+165% for the control and +120% for the HF group at 600 pmoles of injected SNP). Finally, we calculated the potential contribution of L-NAME to ECVA (Fig. 4). In its presence, ECVA was significantly reduced in both groups (Fig. 4A) and almost reached null values (-91% for the control and -89% for the HF group at 60 pmoles of injected ACh).

- *Effects of indomethacin*

As shown in Fig. 2B, indomethacin did not alter the EDD in the control group but this parameter was significantly reduced in the HF group (-33% at 60 pmoles of injected ACh). In the presence of indomethacin, the difference observed in the ACh responses between control and HF groups in the absence of inhibitors was attenuated (from +41% to +14% at 60 pmoles of injected ACh) but it remained significant. The presence of indomethacin did not induce modifications of the EID (Fig. 3B) in the control and HF groups. Interestingly, in the presence of indomethacin, endothelial cells demonstrated an enhanced ECVA (Fig. 4B) in the control group (+50% at 60 pmoles of injected ACh) even though it did not reach significance

revealing the inhibition of vasoconstrictors deriving from this pathway. In the HF group, the ECVA was not modified by the presence of indomethacin.

- *Effects of L-NAME+indomethacin*

In the presence of both L-NAME+Indomethacin, ACh-induced dilatation (Fig. 2C) was reduced in both groups (-26 and -48% for the control and HF groups respectively at 60 pmoles of injected ACh). The association between the two inhibitors erased totally diet-induced difference of EDD observed in the absence of inhibitors. However, no one of these inhibitors, even when used together, erased completely the EDD. The responses to SNP (Fig. 3C) were significantly increased in both groups (+183 and +84% for the control and HF groups respectively at 600 pmoles of injected SNP). However, this parameter was less increased in the HF group compared to the control one resulting in lower SNP-induced responses for the doses ranging from 600 to 1000 pmoles of SNP (-26% for the HF group at 800 pmoles of injected SNP). The ECVA (Fig. 4C) was attenuated in the control group but this difference did not reach significance (-69% at 60 pmoles of injected ACh) while it was reduced significantly in the HF group (-71% at 60 pmoles of injected ACh).

- *Effects of TEA*

TEA reduced dramatically the responses to ACh in both groups as depicted in Fig. 2D (-89 and -85% for control and HF group respectively at 60 pmoles of injected ACh) reaching values close to zero signifying a role of K^+ channels for both groups. The difference that was observed in the EDD between control and HF groups in the absence of inhibitors was attenuated in the presence of TEA. The presence of TEA did not affect the EID (Fig. 3D) in the control group but tended to reduce it (-40% at 600 pm of SNP) while decreased it significantly in the HF group (-43% at 60 pmoles of injected ACh). The presence of TEA

reduced the ECVA (Fig. 4D) in the control group even though it did not reach significance (-56% at 60 pmoles of injected ACh). In the HF group, ECVA was significantly reduced by the presence of TEA (-57% at 60 pmoles of injected ACh).

Discussion

In this study, we aimed at characterizing the impact of HF diet-induced obesity on both the cardiac function and the intact coronary reactivity of the microvasculature *ex vivo*. Previous studies have already examined the effects of HF diets on the reactivity of isolated vessels, especially that of large arteries (Henderson *et al.*, 2004; Turk *et al.*, 2005; Mundy *et al.*, 2007). This is the first one that focuses on the function of the intact coronary microvasculature. Resistance arteries are of a great physiological importance in the control of vascular resistance and organ perfusion and consequently they intervene in the welfare of individuals. Findings from previous studies suggest that various mediator factors contribute to the regulation of vascular tone and their relative contribution differ among vascular beds and size (Chadha *et al.*; Holzer *et al.*, 1994; Urakami-Harasawa *et al.*, 1997). Thus, since the findings obtained in large arteries cannot be generalized there is the need to study the effects of a HF diet specifically on microvessels. Furthermore, the isolated heart perfusion model used in this study allows the evaluation of the coupling of cardiac mechanical and coronary functions that is not feasible in isolated vessels.

It has been shown that obesity is related to increase incidence of cardiovascular diseases (Poirier *et al.*, 2006). HF containing diets can lead to Western diet-associated obesity related to changes in the organism such as hyperglycemia, insulin resistance and hypercholesterolemia, which are associated with alterations in the endothelial function. In this study, obesity was induced by a HF diet containing 54% of fat. This model of diet-induced obesity is likely the result of the content of the diet and not of the increased caloric intake as happens with the Zucker rats, which are models of overfeeding-induced Type 2 diabetes (Clark *et al.*, 1983). After 3 months of diet, the body weight of the animals did not change whereas the abdominal adiposity of the HF rats was significantly elevated. This was associated with increased circulating cholesterol and triglyceride levels while glucose and

insulin were not affected. The high values of plasma glucose observed in our animals could be a result of a possible meal since the rats were not fasted before sacrifice. The fact that no hyperglycemia was observed after 3 months of HF diet may be due to the type of the dietary fat. The fat content of the HF diet was 37% SFAs, 46% MUFAs, 15% n-6 PUFAs and 1% n-3 PUFAs while for the standard diet was 24% SFAs, 23% MUFAs, 48% n-6 PUFAs and 4% n-3 PUFAs. The fact that the fat content of the HF diet chosen was not consisted entirely by saturated fat might explain the state of obesity that we found in our rats. It could also explain any differences concerning the basic characteristics from previous studies (Jebelovszki *et al.*, 2008). Recently, a new syndrome has been described in humans as normal weight obesity (Marques-Vidal *et al.*, 2010; Romero-Corral *et al.*, 2010). This state is defined as an excessive body fat associated with normal body mass index. This could be the case for the HF fed rats in this study since they do have an increased adiposity but no alteration in their body weight.

In our isolated heart perfusion model, we found that the HF rats exhibited a decreased cardiac mechanical activity *ex vivo*. Contractile dysfunction has already been described after as soon as 7 weeks of HF diet (Ouwens *et al.*, 2005). More specifically, the RPP was decreased in our HF rat hearts and that was mainly due to the decreased LVDP as the heart rate remained unchanged. This result could be due to decreased cardiac metabolic efficiency that has already been shown in HF fed rat hearts (Cole *et al.*, 2011). However, when these parameters were normalized to heart weight, these differences disappeared indicating a maintained cardiac mechanical efficiency. Taken together these data though, we may hypothesize that the HF-fed rat hearts demonstrated a diminished capacity for pumping activity and blood expulsion through the body of the organism. Moreover, no changes were observed in the coronary flow and pressure. Blood pressure *in vivo* has been found to be elevated or normal in HF fed rats that could have been influenced by intrinsic vasoregulatory mechanisms of the peripheral resistance arteries (Wilde *et al.*, 2000; Barnes *et al.*, 2003).

The observed cardiac function *ex vivo* in the HF rats could be related to the fatty acid profile of the cardiac membrane phospholipids that may influence lipid-protein interactions, inflammation and related metabolic processes (Hunte & Richers, 2008). The HF diet induced an increase in the SFAs in cardiac membranes at the detriment of MUFAs. This increased degree of saturation could negatively affect the membrane fluidity and increase its rigidity. Similarly, n-6 PUFAs were reduced despite the increase of the polyunsaturated fatty acids downstream of the linoleic acid (C18:2n-6) suggesting a stimulation of the desaturase enzymes in the HF fed rats. n-3 PUFAs were unaltered in their totality despite the reduced amount of EPA (C20:5n-3). Also, an increase in the amount of C22:5n-3 was observed indicating a stimulation of the elongation enzymes in this dietary group. The low ratio EPA/AA in the HF hearts predisposed to a balance of eicosanoids favoring platelet aggregation and inflammatory signaling (Abeywardena *et al.*, 1991; Rupp *et al.*, 2004). Furthermore, low levels of EPA+DHA (DHA, C22:6n-3) have been related to increased risk for sudden cardiac death (Rupp *et al.*, 2004). This was not the case for our HF rats since this value was not different between dietary groups. Thus, it seems that the high fat diet favored a pro-inflammatory environment in the heart that could be associated with the decreased *ex vivo* cardiac function. Furthermore, this could be associated with a state of increased oxidative stress in the plasma, cytosol and mitochondria of the high-fat rats as it was shown by previous work in our laboratory (unpublished data).

Interestingly, in the present study we did not observe endothelial dysfunction of the coronary microvessels *ex vivo*. In contrast, the coronary microvessels of the HF rats demonstrated an enhanced endothelium-dependent dilation compared with the control vessels, which could reflect an adaptation of the coronary system to protect the heart from ischemic incidents related to insufficient oxygen supply. Dilatations to SNP though did not differ among groups. The ECVA was not significantly different between groups even though it tended to be

increased in the HF rats. These data suggest that mechanisms derived from the ECs or mechanisms that mediate the coupling between endothelial and smooth muscle cells could be implicated in this increased response to ACh. Previous studies suggest that obesity may reduce NO levels mostly through increased oxidative stress (Cai & Harrison, 2000) and that when NO bioavailability is reduced a compensatory mechanism takes place in order to maintain a normal coronary function (Bagi, 2009). Adaptation of coronary vessels is particularly important, as in the coronary circulation oxygen extraction is near maximal and any mismatch between blood supply and metabolic demand would deteriorate myocardial contractile function (Tune *et al.*, 2004). Furthermore, the increase in body mass, either muscular or adipose, requires higher cardiac output and expanded intravascular volume to meet the elevated metabolic requirements (Lavie & Messerli, 1986). Thus, the vascular alterations observed in our study could help the coronary microvasculature to adjust the organ perfusion during physiological processes such as exercise. Otherwise the heart would not be able to respond to increased metabolic demands and lead eventually to ischemic incidents.

The results of the pharmacology experiments with the use of inhibitors in the perfusate revealed a number of novel observations concerning both the control and HF groups. L-NAME, an inhibitor of NOS, reduced the EDD in both groups. However, the percentage of the reduction was greater in the HF group suggesting that the effect of L-NAME was more important. An activation of NO biosynthesis elements such as the L-arginine transport has been reported in mice fed unsaturated (mono- or poly-unsaturated fat) HF diets (Martins *et al.*, 2010) that could be also the case for our animals given the high percentage of monounsaturated fat in our HF diet. The significant EDD difference between dietary groups in the absence of inhibitors was thus disappeared with L-NAME but not totally erased. This was also evident by the results of ECVA, where in the presence of L-NAME no difference was found between dietary groups. Interestingly, despite the dramatic reduction of the ECVA

the EDD was not totally blocked revealing the existence of other mediators in the ACh-response. The sensitivity to SNP was also similarly altered in both dietary groups confirming that the HF diet induced alterations occuring mostly at the level of ECs. Thus, these findings suggest that NOS pathway is implicated in the enhanced ACh response in the HF group, but other factors are also involved.

Interestingly, the presence of indomethacin did not significantly alter the ACh response in the control group but only in the HF one indicating an important role of the COX pathway in the EDD of the HF animals. However, the EDD difference between dietary groups in the absence of inhibitors remained in the presence of indomethacin indicating the important role of NO pathway in this phenomenon. The sensitivity to SNP in the presence of indomethacin was the same between groups. This was also reflected in the ECVA results. In the control group, the inhibition of COX-derived mediators enhanced this parameter suggesting the inhibition of the vasoconstrictors (endothelial prostanoids) produced from this pathway (Antman *et al.*, 2005). This was not the case for the HF group whose endothelial-dependent dilatation was not changed. This could imply an altered balance between COX-derived vasodilators and vasoconstrictors in the HF group. The HF diet seems to reduce the availability of vasoconstrictor mediators and maintain or even enhance that of vasodilators contributing eventually to the enhanced EDD. The analysis of the fatty acid content of the cardiac phospholipids also revealed that the AA (C20:4n-6) was increased in the HF rat hearts which could lead eventually to an increase in the COX-vasoactive agents (Baber *et al.*, 2005). However, no data was obtained concerning the availability of these molecules, which consists a limitation of this study.

The inhibition of both NOS and COX significantly reduced the Ach response in both groups but for the HF group their impact was greater than in the control group. This reflected the fact that in the HF group the L-NAME or indomethacin alone had greater impact on the ACh

response than they had in the control group. This resulted to the complete disappearance of the EDD difference between the dietary groups that was observed in the absence of inhibitors. The ECVA was also reduced in the presence of these two inhibitors for both dietary groups even though it did not reach significance in the control animals. This could be due to an important variability of this parameter between control individuals since the reduction percentage was almost the same for the two groups. These results suggest a synergistic effect of NOS and COX pathways (Cuzzocrea & Salvemini, 2007). It is known that many of the same signals such as calcium (Ledoux *et al.*, 2006) that stimulate COX production of endothelium-derived prostacyclin also stimulate endothelial NO synthase (eNOS) while the similar dilator properties of NO and prostacyclin suggest some degree of interaction (Beierwaltes, 2002) as already reported (Cheng *et al.*, 2006). However, a role of smooth muscle cells is also revealed for the HF group as shown by the significant EID difference between groups in the presence of L-NAME + indomethacin. Moreover, these results revealed the existence of other vasoactive agents contributing to the coronary microvessel vasodilatation since the action of L-NAME + indomethacin did not abolish the response to ACh. This response became almost null with the inhibition of the potassium channels with TEA in the dietary groups revealing the major role of the potassium channels in this response. TEA also reduced the SNP-responses of both dietary groups even though it did not reach significance in the control animals. Similar were the results for the ECVA. This could be due to an important variability of this parameter between control individuals since the reduction percentage was almost the same for the two dietary groups. Thus, these data indicate a major role of potassium channels of endothelial and smooth muscle cells in the coronary microvascular reactivity. It has already been described that the relative contribution of vasodilating mediators change according to the vessel size and that EDHF is more important in small size vessels (Urakami-Harasawa *et al.*, 1997). EDHF acts via activation of K^+

channels (Murphy & Brayden, 1995) and our findings support an important contribution of EDHF in the regulation of coronary microvascular tone. It should be noted thought that NO may also act via K^+ channels (Bolotina *et al.*, 1994), which could explain also the fact that EDD was almost totally suppressed with the inhibition of these channels.

Thus, our observations confirm the importance of potassium channels in the ACh response of the coronary microvasculature and the synergistic role of NO and COX-derived vasodilators. The findings of the present study suggest that this type of HF diet creates a proinflammatory environment in the heart that could be related to the decreased *ex vivo* cardiac mechanical activity. Despite all these alterations, the coronary microvasculature of HF fed obese rats adapts resulting to enhanced ACh responses in order to maintain an adequate tissue perfusion in cases of physiological processes of enhanced metabolic demand such as exercise. The HF diet appears to induce alterations at the level of NOS and COX pathway, which contribute together to the enhanced ACh response of the HF coronary microvessels. The HF-induced increase in coronary reserve favors the upholding of tissue perfusion and welfare of obese individuals.

References

Abeywardena MY, McLennan PL & Charnock JS. (1991). Differential effects of dietary fish oil on myocardial prostaglandin I2 and thromboxane A2 production. *Am J Physiol* **260,** H379-385.

Antman EM, DeMets D & Loscalzo J. (2005). Cyclooxygenase inhibition and cardiovascular risk. *Circulation* **112,** 759-770.

Baber SR, Deng W, Rodriguez J, Master RG, Bivalacqua TJ, Hyman AL & Kadowitz PJ. (2005). Vasoactive prostanoids are generated from arachidonic acid by COX-1 and COX-2 in the mouse. *Am J Physiol Heart Circ Physiol* **289,** H1476-1487.

Bagi Z. (2009). Mechanisms of coronary microvascular adaptation to obesity. *Am J Physiol Regul Integr Comp Physiol* **297,** R556-567.

Bagi Z, Feher A & Cassuto J. (2012). Microvascular responsiveness in obesity: implications for therapeutic intervention. *Br J Pharmacol* **165,** 544-560.

Barnes MJ, Lapanowski K, Conley A, Rafols JA, Jen KL & Dunbar JC. (2003). High fat feeding is associated with increased blood pressure, sympathetic nerve activity and hypothalamic mu opioid receptors. *Brain Res Bull* **61,** 511-519.

Beierwaltes WH. (2002). Cyclooxygenase-2 products compensate for inhibition of nitric oxide regulation of renal perfusion. *Am J Physiol Renal Physiol* **283,** F68-72.

Bolotina VM, Najibi S, Palacino JJ, Pagano PJ & Cohen RA. (1994). Nitric oxide directly activates calcium-dependent potassium channels in vascular smooth muscle. *Nature* **368,** 850-853.

Brandes RP, Kim D, Schmitz-Winnenthal FH, Amidi M, Godecke A, Mulsch A & Busse R. (2000). Increased nitrovasodilator sensitivity in endothelial nitric oxide synthase knockout mice: role of soluble guanylyl cyclase. *Hypertension* **35,** 231-236.

Caballero AE. (2003). Endothelial dysfunction in obesity and insulin resistance: a road to diabetes and heart disease. *Obes Res* **11,** 1278-1289.

Cai H & Harrison DG. (2000). Endothelial dysfunction in cardiovascular diseases: the role of oxidant stress. *Circ Res* **87,** 840-844.

Chadha PS, Liu L, Rikard-Bell M, Senadheera S, Howitt L, Bertrand RL, Grayson TH, Murphy TV & Sandow SL. Endothelium-dependent vasodilation in human mesenteric artery is primarily mediated by myoendothelial gap junctions intermediate conductance calcium-activated K+ channel and nitric oxide. *J Pharmacol Exp Ther* **336,** 701-708.

Cheng HF, Zhang MZ & Harris RC. (2006). Nitric oxide stimulates cyclooxygenase-2 in cultured cTAL cells through a p38-dependent pathway. *Am J Physiol Renal Physiol* **290,** F1391-1397.

Chilian WM. (1997). Coronary microcirculation in health and disease. Summary of an NHLBI workshop. *Circulation* **95,** 522-528.

Clark JB, Palmer CJ & Shaw WN. (1983). The diabetic Zucker fatty rat. *Proc Soc Exp Biol Med* **173,** 68-75.

Cole MA, Murray AJ, Cochlin LE, Heather LC, McAleese S, Knight NS, Sutton E, Jamil AA, Parassol N & Clarke K. (2011). A high fat diet increases mitochondrial fatty acid oxidation and uncoupling to decrease efficiency in rat heart. *Basic Res Cardiol* **106,** 447-457.

Cuzzocrea S & Salvemini D. (2007). Molecular mechanisms involved in the reciprocal regulation of cyclooxygenase and nitric oxide synthase enzymes. *Kidney Int* **71,** 290-297.

Demaison L, Moreau D, Vergely-Vandriesse C, Gregoire S, Degois M & Rochette L. (2001). Effects of dietary polyunsaturated fatty acids and hepatic steatosis on the functioning of isolated working rat heart under normoxic conditions and during post-ischemic reperfusion. *Mol Cell Biochem* **224,** 103-116.

Dobrian AD, Davies MJ, Prewitt RL & Lauterio TJ. (2000). Development of hypertension in a rat model of diet-induced obesity. *Hypertension* **35,** 1009-1015.

Fisslthaler B, Popp R, Kiss L, Potente M, Harder DR, Fleming I & Busse R. (1999). Cytochrome P450 2C is an EDHF synthase in coronary arteries. *Nature* **401,** 493-497.

Flegal KM, Carroll MD, Ogden CL & Curtin LR. (2010). Prevalence and trends in obesity among US adults, 1999-2008. *JAMA* **303,** 235-241.

Folch J, Lees M & Sloane Stanley GH. (1957). A simple method for the isolation and purification of total lipides from animal tissues. *J Biol Chem* **226,** 497-509.

Hall JE, Brands MW & Henegar JR. (1999). Mechanisms of hypertension and kidney disease in obesity. *Ann N Y Acad Sci* **892,** 91-107.

Hashimoto M, Akishita M, Eto M, Kozaki K, Ako J, Sugimoto N, Yoshizumi M, Toba K & Ouchi Y. (1998). The impairment of flow-mediated vasodilatation in obese men with visceral fat accumulation. *Int J Obes Relat Metab Disord* **22,** 477-484.

Henderson KK, Turk JR, Rush JW & Laughlin MH. (2004). Endothelial function in coronary arterioles from pigs with early-stage coronary disease induced by high-fat, high-cholesterol diet: effect of exercise. *J Appl Physiol* **97,** 1159-1168.

Holzer P, Wachter C, Jocic M & Heinemann A. (1994). Vascular bed-dependent roles of the peptide CGRP and nitric oxide in acid-evoked hyperaemia of the rat stomach. *J Physiol* **480 (Pt 3),** 575-585.

Hunte C & Richers S. (2008). Lipids and membrane protein structures. *Curr Opin Struct Biol* **18,** 406-411.

Jebelovszki E, Kiraly C, Erdei N, Feher A, Pasztor ET, Rutkai I, Forster T, Edes I, Koller A & Bagi Z. (2008). High-fat diet-induced obesity leads to increased NO sensitivity of rat coronary arterioles: role of soluble guanylate cyclase activation. *Am J Physiol Heart Circ Physiol* **294,** H2558-2564.

Jones CJ, Kuo L, Davis MJ & Chilian WM. (1995). Regulation of coronary blood flow: coordination of heterogeneous control mechanisms in vascular microdomains. *Cardiovasc Res* **29,** 585-596.

Juaneda P, Rocquelin G & Astorg PO. (1990). Separation and quantification of heart and liver phospholipid classes by high-performance liquid chromatography using a new light-scattering detector. *Lipids* **25,** 756-759.

Kapiotis S, Holzer G, Schaller G, Haumer M, Widhalm H, Weghuber D, Jilma B, Roggla G, Wolzt M, Widhalm K & Wagner OF. (2006). A proinflammatory state is detectable in obese children and is accompanied by functional and morphological vascular changes. *Arterioscler Tthromb Vasc Biol* **26,** 2541-2546.

Lavie CJ & Messerli FH. (1986). Cardiovascular adaptation to obesity and hypertension. *Chest* **90,** 275-279.

Ledoux J, Werner ME, Brayden JE & Nelson MT. (2006). Calcium-activated potassium channels and the regulation of vascular tone. *Physiology (Bethesda)* **21,** 69-78.

Liu Y, Bubolz AH, Mendoza S, Zhang DX & Gutterman DD. (2011). H2O2 is the transferrable factor mediating flow-induced dilation in human coronary arterioles. *Circ Res* **108,** 566-573.

Marques-Vidal P, Pecoud A, Hayoz D, Paccaud F, Mooser V, Waeber G & Vollenweider P. (2010). Normal weight obesity: relationship with lipids, glycaemic status, liver enzymes and inflammation. *Nutr Metab Cardiovasc Dis* **20,** 669-675.

Martins MA, Catta-Preta M, Mandarim-de-Lacerda CA, Aguila MB, Brunini TC & Mendes-Ribeiro AC. (2010). High fat diets modulate nitric oxide biosynthesis and antioxidant defence in red blood cells from C57BL/6 mice. *Arch Biochem Biophys* **499,** 56-61.

Miura H, Wachtel RE, Liu Y, Loberiza FR, Jr., Saito T, Miura M & Gutterman DD. (2001). Flow-induced dilation of human coronary arterioles: important role of Ca(2+)-activated K(+) channels. *Circulation* **103,** 1992-1998.

Mundy AL, Haas E, Bhattacharya I, Widmer CC, Kretz M, Hofmann-Lehmann R, Minotti R & Barton M. (2007). Fat intake modifies vascular responsiveness and receptor expression of vasoconstrictors: implications for diet-induced obesity. *Cardiovasc Res* **73,** 368-375.

Murphy ME & Brayden JE. (1995). Apamin-sensitive K+ channels mediate an endothelium-dependent hyperpolarization in rabbit mesenteric arteries. *J Physiol* **489 (Pt 3),** 723-734.

Oltman CL, Richou LL, Davidson EP, Coppey LJ, Lund DD & Yorek MA. (2006). Progression of coronary and mesenteric vascular dysfunction in Zucker obese and Zucker diabetic fatty rats. *Am J Physiol Heart Circ Physiol* **291,** H1780-1787.

Ouwens DM, Boer C, Fodor M, de Galan P, Heine RJ, Maassen JA & Diamant M. (2005). Cardiac dysfunction induced by high-fat diet is associated with altered myocardial insulin signalling in rats. *Diabetologia* **48,** 1229-1237.

Poirier P, Giles TD, Bray GA, Hong Y, Stern JS, Pi-Sunyer FX & Eckel RH. (2006). Obesity and cardiovascular disease: pathophysiology, evaluation, and effect of weight loss: an update of the 1997 American Heart Association Scientific Statement on Obesity and Heart Disease from the Obesity Committee of the Council on Nutrition, Physical Activity, and Metabolism. *Circulation* **113,** 898-918.

Prakash R, Mintz JD & Stepp DW. (2006). Impact of obesity on coronary microvascular function in the Zucker rat. *Microcirculation* **13,** 389-396.

Romero-Corral A, Somers VK, Sierra-Johnson J, Korenfeld Y, Boarin S, Korinek J, Jensen MD, Parati G & Lopez-Jimenez F. (2010). Normal weight obesity: a risk factor for cardiometabolic dysregulation and cardiovascular mortality. *Eur Heart J* **31,** 737-746.

Rupp H, Wagner D, Rupp T, Schulte LM & Maisch B. (2004). Risk stratification by the "EPA+DHA level" and the "EPA/AA ratio" focus on anti-inflammatory and antiarrhythmogenic effects of long-chain omega-3 fatty acids. *Herz* **29,** 673-685.

Sanchez A, Contreras C, Martinez P, Villalba N, Benedito S, Garcia-Sacristan A, Salaices M, Hernandez M & Prieto D. (2010). Enhanced cyclooxygenase 2-mediated vasorelaxation in coronary arteries from insulin-resistant obese Zucker rats. *Atherosclerosis* **213,** 392-399.

Tune JD, Gorman MW & Feigl EO. (2004). Matching coronary blood flow to myocardial oxygen consumption. *J Appl Physiol* **97,** 404-415.

Turk JR, Henderson KK, Vanvickle GD, Watkins J & Laughlin MH. (2005). Arterial endothelial function in a porcine model of early stage atherosclerotic vascular disease. *Int J Exp Pathol* **86,** 335-345.

Urakami-Harasawa L, Shimokawa H, Nakashima M, Egashira K & Takeshita A. (1997). Importance of endothelium-derived hyperpolarizing factor in human arteries. *J Clin Invest* **100,** 2793-2799.

Vial G, Dubouchaud H, Couturier K, Cottet-Rousselle C, Taleux N, Athias A, Galinier A, Casteilla L & Leverve XM. Effects of a high-fat diet on energy metabolism and ROS production in rat liver. *J Hepatol* **54,** 348-356.

Wilde DW, Massey KD, Walker GK, Vollmer A & Grekin RJ. (2000). High-fat diet elevates blood pressure and cerebrovascular muscle Ca(2+) current. *Hypertension* **35,** 832-837.

Wilkes JJ, Bonen A & Bell RC. (1998). A modified high-fat diet induces insulin resistance in rat skeletal muscle but not adipocytes. *Am J Physiol* **275,** E679-686.

Author Contributions

Experiments on animals and *ex vivo* experiments were conducted at the Laboratory of Fundamental and Applied Bioenergetics, Joseph Fourier University of Grenoble, France. The experiments concerning the fatty acid profile of cardiac phospholipids were conducted at Unité de Nutrition Humaine, Institut National de la Recherche Agronomique, Clermont-Ferrand, France. E.M. conducted the experiments and contributed to the study implementation, statistical analysis, interpretation, and the preparation of the manuscript. G.V. conducted a part of biochemical experiments and participated in the animal care. B.L., J-P.R. and B.M. helped to conduct the experiments and acquire data. L.D. supervised the study conduction and contributed to the study conception and design, implementation, statistical interpretation, the preparation and finalization of the manuscript. All authors approved the final version of the manuscript for publication. The authors declare no conflicts of interest.

Acknowledgements

We would like to thank Mr. Cristophe Cottet for carefully editing the manuscript and Cindy Tellier for animal care. This work was supported by the French National Institute of Agronomical Research (INRA), the French National Institute of Health and Medical Research (INSERM) and Joseph Fourier University, Grenoble, France.

Figure Legends

Figure 1. Effect of the high-fat diet on the endothelial-dependent dilatation (EDD, panel A), endothelial-independent dilatation (EID, panel B) and endothelial cell vasodilatation activity (ECVA, panel C) of the coronary microvascular network of the perfused hearts. The number of experiments was 8 for each group. HF: high-fat group; ACh: acetylcholine; SNP: sodium nitroprusside. *: significantly different.

Figure 2. Effects of diet and L-NAME (panel A), indomethacin (panel B), L-NAME plus indomethacin (panel C) and tetraetylammonium (panel D) on the endothelial-dependent dilatation (EDD) of the coronary microvasculature. The number of experiments was 8 for each group. HF: high-fat group; Indo: indomethacin; TEA: tetraethylammonium; ACh: acetylcholine; SNP: sodium nitroprusside. *: significant difference between control and HF groups in the absence of inhibitors; #: significant difference between control and HF in the presence of inhibitors; $: significant difference between control groups in the absence and presence of inhibitors; †: significant difference between HF groups in the absence and presence of inhibitors.

Figure 3. Effects of diet and L-NAME (panel A), indomethacin (panel B), L-NAME plus indomethacin (panel C) and tetraetylammonium (panel D) on the endothelial-independent dilatation (EID) of the coronary microvasculature. The number of experiments was 8 for each group. HF: high-fat group; Indo: indomethacin; TEA: tetraethylammonium; ACh: acetylcholine; SNP: sodium nitroprusside. #: significant difference between control and HF in the presence of inhibitors; $: significant difference between control groups in the absence and presence of inhibitors; †: significant difference between HF groups in the absence and presence of inhibitors.

Figure 4. Effects of diet and L-NAME (panel A), indomethacin (panel B), L-NAME plus indomethacin (panel C) and tetraetylammonium (panel D) on the endothelial cell

vasodilatation activity (ECVA) of the coronary microvasculature. The number of experiments was 8 for each group. HF: high-fat group; Indo: indomethacin; TEA: tetraethylammonium; ACh: acetylcholine; SNP: sodium nitroprusside. $: significant difference between control groups in the absence and presence of inhibitors; †: significant difference between HF groups in the absence and presence of inhibitors.

Table 1. Basic characteristics of the animals

	C	HF
BW (g of ww)	438 ± 7	472 ± 19
Abdominal adipose tissue (g of ww)	11.9 ± 1.4	25.3 ± 3.3*
AAT/BW (g of ww/g of BW)	0.027 ± 0.003	0.053 ± 0.006*
Heart weight (mg of dw)	251 ± 7	222 ± 16
HW/BW (mg of dw/g of BW)	0.57 ± 0.01	0.47 ± 0.03*
Glucose (mM)	8.5 ±0.6	9.1 ± 0.1
Insulin (ng/ml)	1.53 ± 0.17	2.09 ± 0.87
Triglycerides (g/l)	1.00 ± 0.04	1.20 ± 0.10*
Cholesterol (g/l)	0.59 ± 0.06	0.88 ± 0.05*

The number of experiments was 8 for each group. ww: wet weight; dw: dry weight; AAT: abdominal adipose tissue; BW: body weight; HW: heart weight; C: control group; HF: high-fat fed group. *: significantly different.

Table 2. Fatty acid composition of cardiac membrane phospholipids

Fatty acids (%)	C	HF
14:0	0.10 ± 0.01	0.05±0.01*
DMA16:0	3.19 ± 0.18	3.27 ± 0.20
16:0	14.01 ± 0.73	10.69 ± 0.49*
DMA18:0	1.09 ± 0.06	2.54 ± 0.11*
18:0	21.50 ± 0.37	26.68 ± 0.47*
SFA	39.90 ± 1.3	43.20 ± 0.80*
16:1n-7	0.33 ± 0.03	0.16 ± 0.01*
18:1n-9	3.08 ± 0.15	4.15 ± 0.17*
18:1n-7	5.25 ± 0.18	2.98 ± 0.06*
MUFA	8.67 ± 0.20	7.29 ± 0.19*
18:2n-6	26.59 ± 1.36	20.77 ± 0.95*
20:2n-6	0.09 ± 0.01	0.20 ± 0.01*
20:3n-6	0.27 ± 0.03	0.59 ± 0.03*
20:4n-6	17.14 ± 0.36	19.98 ± 0.82*
22:4n-6	0.25 ± 0.01	0.48 ± 0.03*
22:5n-6	0.22 ± 0.02	0.47 ± 0.03*
n-6 PUFA	44.54 ± 1.20	42.48 ± 0.61*
20:5n-3	0.14 ± 0.01	0.05 ± 0.01*
22:5n-3	0.80 ± 0.06	1.74 ± 0.11*
22:6n-3	5.95 ± 0.45	5.21 ± 0.38
n-3 PUFA	6.90 ± 0.51	7.00 ± 0.45
PUFA	51.40 ± 1.42	49.5 ± 0.83
n-6/n-3	6.57 ± 0.40	6.26 ± 0.42
Total 16:0	17.20 ± 0.87	13.96 ± 0.62*
Total 18:0	22.60 ± 0.40	29.2 ± 0.50*
Total 18:1	8.34 ± 0.20	7.13 ± 0.19*
EPA/AA	0.008 ± 0.001	0.002 ± 0.001*
EPA+DHA	6.09 ± 0.46	5.26 ± 0.38

The number of experiments was 5 for each group. Values are expressed as relative amounts of the total fatty acid content. DMA: dimethylacetal; SFA: saturated fatty acids; MUFA: monounsaturated fatty acids; PUFA: polyunsaturated fatty acids; EPA: eicosapentaenoic acid; AA: arachidonic acid; DHA: docosahexaenoic acid; C: control group; HF: high-fat fed group. *: significantly different.

Table 3. ***Ex vivo*** **cardiac function**

	C	HF
HR (beats/min)	288 ± 29	267 ± 16
LVDP (mmHg)	92 ± 10	63 ± 3*
LVDP/HW (mmHg/g dw)	370 ± 42	304 ± 33
RPP (mHg/min)	22.9 ± 3.1	16.7 ± 1.2*
RPP/HW (mHg/g dw)	92 ± 9	80 ± 10
CF (ml/min/g dry weight)	40 ± 5	41 ± 6
CP before U46619 (mmHg)	65.6 ± 4.9	67.9 ± 3.7
CP after U46619 (mmHg)	94 ± 3	112 ± 6.

The number of experiments was 8 for each group. HR: heart rate; LVDP: left ventricle developed pressure; RPP: rate pressure product; CF: coronary flow; CP: coronary pressure; C: control group; HF: high-fat fed group. *: significantly different.

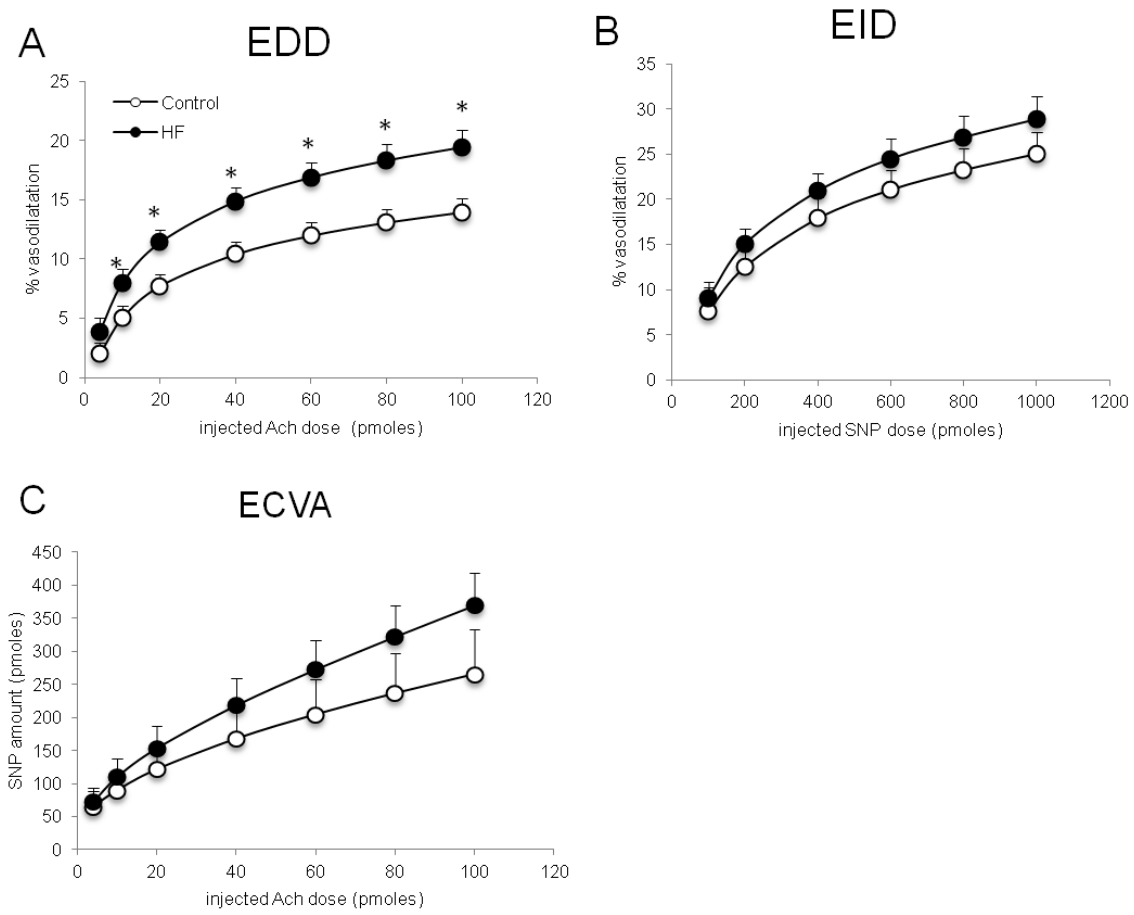
A
EDD
Control
HF
% vasodilatation
injected Ach dose (pmoles)
B
EID
% vasodilatation
injected SNP dose (pmoles)
C
ECVA
SNP amount (pmoles)
injected Ach dose (pmoles)

Figure 1

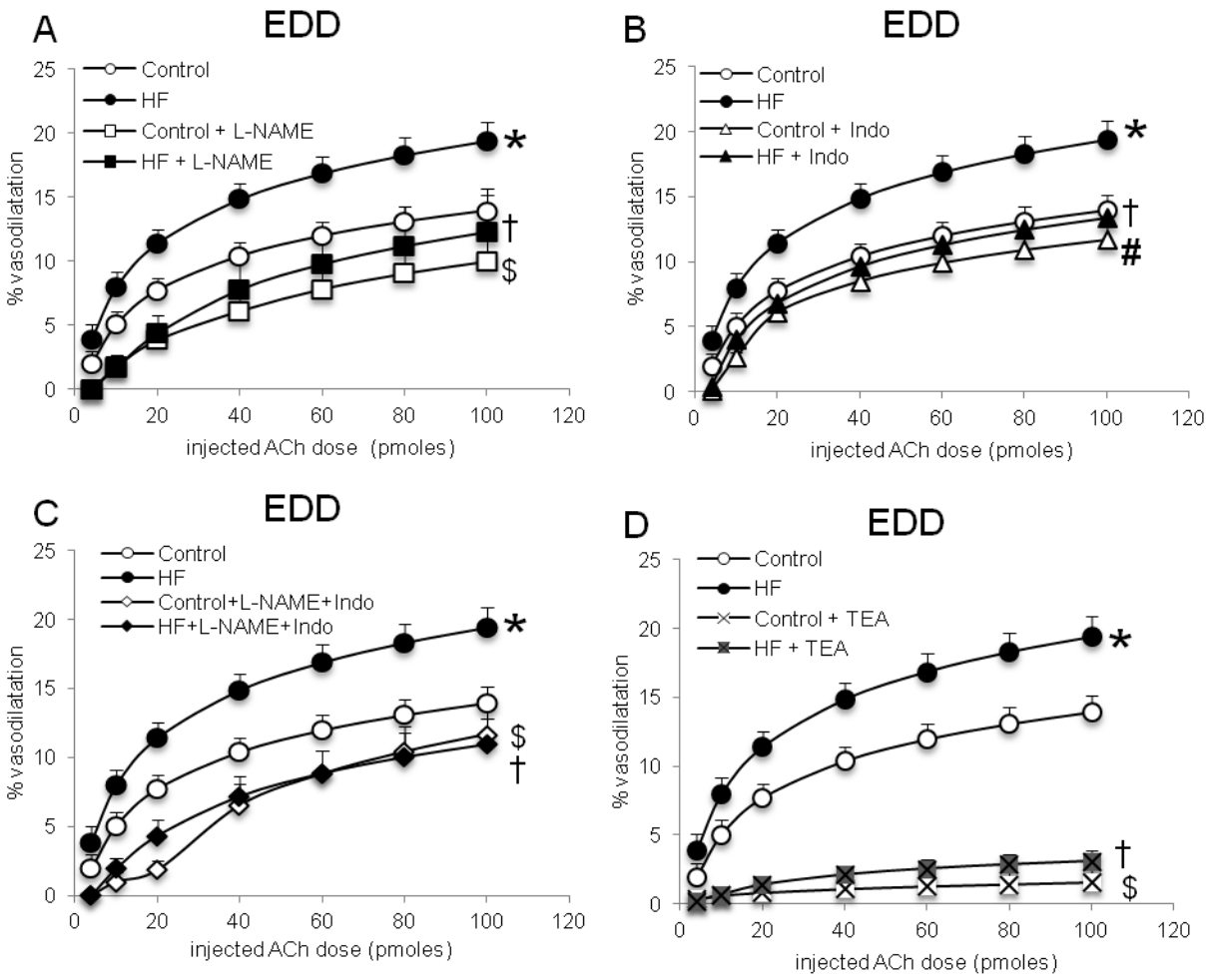
A
EDD
Control
HF
Control + L-NAME
HF + L-NAME
% vasodilatation
injected ACh dose (pmoles)
B
EDD
Control
HF
Control + Indo
HF + Indo
% vasodilatation
injected ACh dose (pmoles)
C
EDD
Control
HF
Control+L-NAME+Indo
HF+L-NAME+Indo
% vasodilatation
injected ACh dose (pmoles)
D
EDD
Control
HF
Control + TEA
HF + TEA
% vasodilatation
injected ACh dose (pmoles)

Figure 2

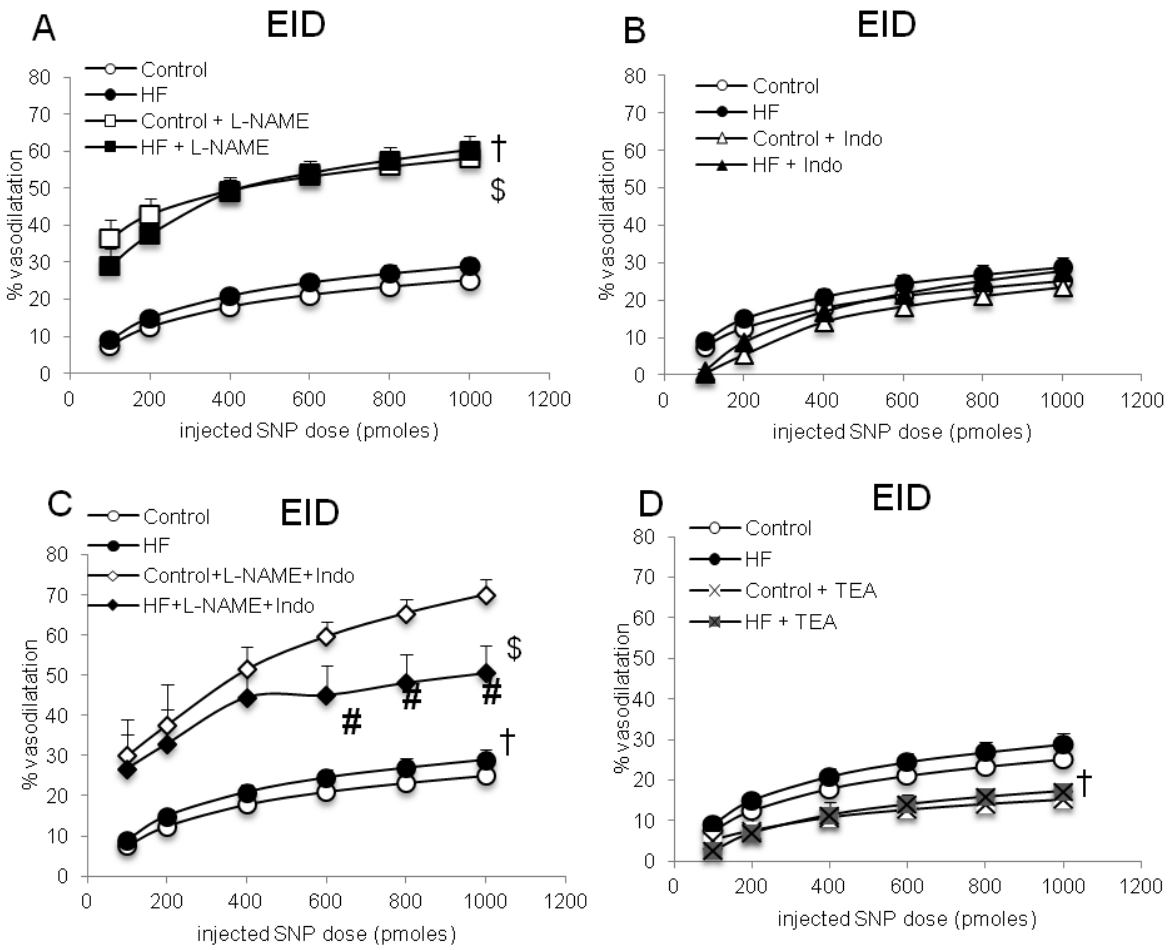
A
EID
Control
HF
Control + L-NAME
HF + L-NAME
% vasodilatation
injected SNP dose (pmoles)
†
$
B
EID
Control
HF
Control + Indo
HF + Indo
% vasodilatation
injected SNP dose (pmoles)
C
EID
Control
HF
Control+L-NAME+Indo
HF+L-NAME+Indo
% vasodilatation
injected SNP dose (pmoles)
$
#
#
#
†
D
EID
Control
HF
Control + TEA
HF + TEA
% vasodilatation
injected SNP dose (pmoles)
†

Figure 3

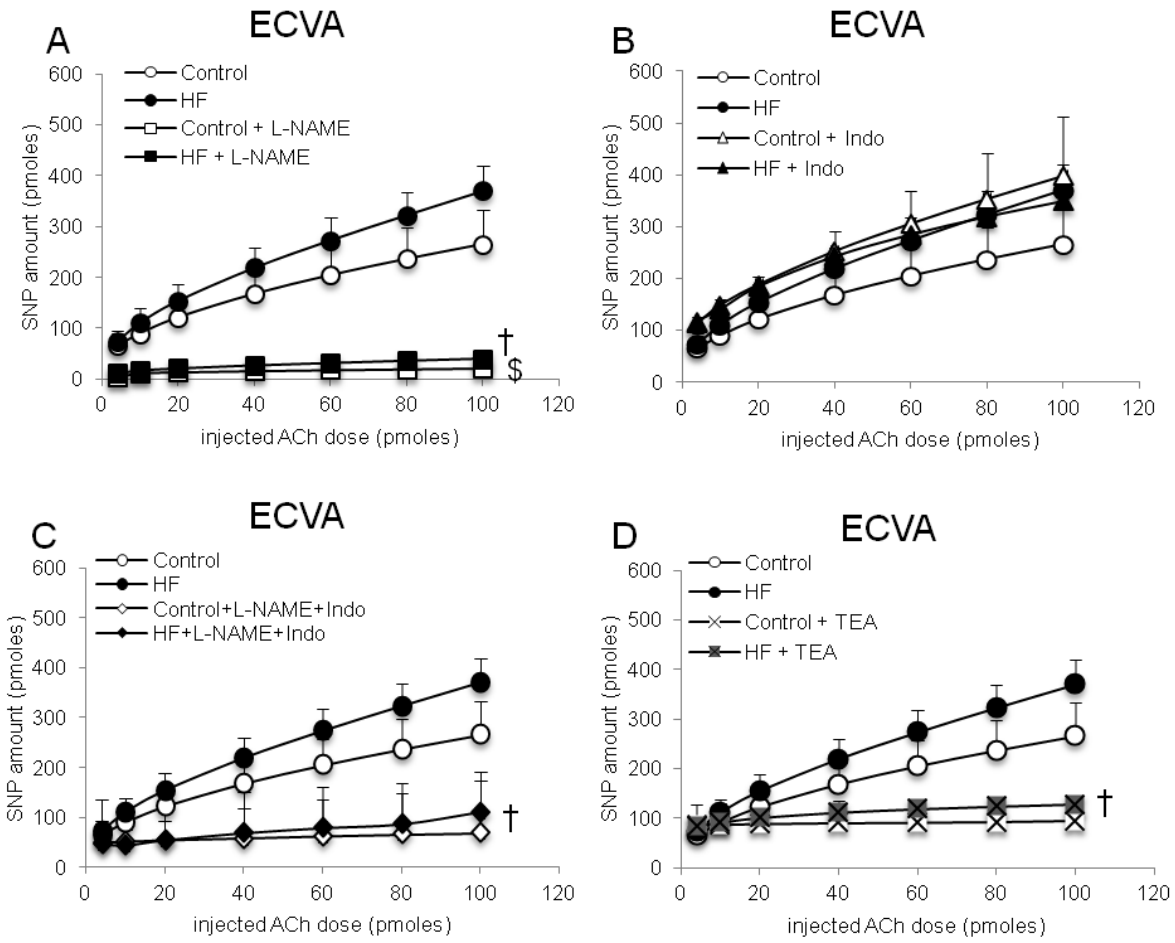
A
ECVA
Control
HF
Control + L-NAME
HF + L-NAME
SNP amount (pmoles)
injected ACh dose (pmoles)
†
$
B
ECVA
Control
HF
Control + Indo
HF + Indo
SNP amount (pmoles)
injected ACh dose (pmoles)
C
ECVA
Control
HF
Control+L-NAME+Indo
HF+L-NAME+Indo
SNP amount (pmoles)
injected ACh dose (pmoles)
†
D
ECVA
Control
HF
Control + TEA
HF + TEA
SNP amount (pmoles)
injected ACh dose (pmoles)
†

Figure 4

3.6 ARTICLE V

"Preserved endothelium-dependent dilatation of the coronary microvasculature at the early phase of diabetes mellitus despite the increased oxidative stress and depressed cardiac mechanical function *ex vivo*"

This work will be submitted to the journal "Cardiovascular Diabetology".

Preserved endothelium-dependent dilatation of the coronary microvasculature at the early phase of diabetes mellitus despite the increased oxidative stress and depressed cardiac mechanical function *ex vivo*

Evangelia Mourmoura[1,2*], Guillaume Vial[1,2], Brigitte Laillet[3], Jean-Paul Rigaudière[3], Isabelle Hininger[1,2], Hervé Dubouchaud[1,2], Beatrice Morio[3], Luc Demaison[1,2,3]

[1]Laboratoire de Bioénergétique Fondamentale et Appliquée, INSERM U1055, Grenoble cedex 09, F-38041, France;

[2]Université Joseph Fourier, Laboratoire de Bioénergétique Fondamentale et Appliquée, INSERM U1055, Grenoble cedex 09, F-38041, France;

[3]INRA, Clermont Université, Université d'Auvergne, Unité de Nutrition Humaine, BP 10448, F-63000 Clermont-Ferrand, France;

*Corresponding author at: Laboratoire de Bioénergétique Fondamentale et Appliquée, INSERM U1055, Université Joseph Fourier, BP 53, 38041 Grenoble cedex 09, France. Tel. (+33) 476 63 56 25; Fax (+33) 476 51 42 18; e-mail: evangelia.mourmoura@ujf-grenoble.fr

E-mail adresses :

Evangelia Mourmoura : evangelia.mourmoura@ujf-grenoble.fr

Guillaume Vial : guillaume.vial@ujf-grenoble.fr

Brigite Laillet : brigitte.laillet@clermont.inra.fr

Jean-Paul Rigaudière : jean-paul.rigaudiere@clermont.inra.fr

Isabelle Hininger : isabelle.hininger@ujf-grenoble.fr

Hervé Dubouchaud : herve.dubouchaud@ujf-grenoble.fr

Beatrice Morio : beatrice.morio@clermont.inra.fr

Luc Demaison : luc.demaison@ujf-grenoble.fr

Abstract

Background

There has been accumulating evidence associating diabetes mellitus and vascular dysfunctions. However, most of the studies are focused on the late stages of diabetes and on the function of large arteries. This study aimed at characterizing the effects of the early phase of diabetes mellitus on the function of the intact coronary microvasculature.

Materials and methods

Zucker diabetic fatty rats and their lean littermates fed with standard diet A04 (Safe) were studied at the 11th week of age. Biochemical parameters such as glucose, insulin and triglycerides levels as well as their oxidative stress status were measured. Their hearts were perfused *ex vivo* according to Langendorff and their cardiac activity and coronary microvascular reactivity were evaluated.

Results

Zucker fatty rats already exhibited a diabetic state at this age as demonstrated by the elevated levels of plasma glucose, insulin, glycated hemoglobin and triglycerides. The *ex vivo* perfusion of their hearts revealed a decreased cardiac mechanical function and coronary flow. This was accompanied by an increase in the overall oxidative stress of the organism. However, estimation of the active form of endothelial nitric oxide synthase and coronary reactivity indicated a preserved function of the coronary microvessels at this phase of the disease. Diabetes affected also the cardiac membrane phospholipid fatty acid composition by increasing the arachidonic acid and n-3 polyunsaturated fatty acids levels.

Conclusions: The presence of diabetes, even at its beginning, significantly increased the overall oxidative stress of the organism resulting to decreased cardiac mechanical activity *ex vivo*. However, a number of adaptations were adopted at this early phase of the disease regarding the cardiac phospholipid composition and the preserved coronary microvascular reactivity in order to provide a certain protection to the heart and support the increased cardiac work.

Key Words: diabetes mellitus, insulin resistance, coronary reactivity, microvasculature, mechanical function, oxidative stress

Background

The prevalence of Type 2 Diabetes (T2D) is increasing at an alarming rate assuming epidemic dimensions in industrialized societies [1]. Individuals with T2D have increased risk for developing cardiovascular diseases (CVDs), which is the main cause of early mortality and morbidity in the Western world [2]. Insulin resistance and T2D usually result from excess intake of deleterious nutrients such as saturated and trans fatty acids [3]. Consequent metabolic changes such as hyperinsulinemia and hyperglycemia [4] can provoke vascular lesions and endothelial dysfunctions at both micro- and macro-circulations [5-8]. The vulnerability of the coronary circulation to the diabetic milieu can lead to endothelial dysfunction at this bed, which consists a significant biomarker of early coronary artery disease independently of atherosclerosis [9].

An accurate experimental model in order to clarify the mechanisms responsible for the pathophysiology of diabetes evolution and its complications is the inbred Zucker diabetic fatty (ZDF) rat. The homozygous fa/fa Zucker rat exhibits hyperphagia caused by a non-functioning leptin receptor. This leads to the development of obesity, hyperglycemia, hyperinsulinemia and finally diabetes at a young age [10, 11]. Previous studies on these rats in the later stages of diabetes have demonstrated that chronic hyperglycemia and hyperlipidemia can result to inflammation [12, 13], increased oxidative stress and vascular dysfunction [14, 15]. Coppey *et al.* [16] have shown that the endothelium-mediated responses to acetylcholine (Ach) are attenuated in epineurial arterioles of the sciatic nerve in diabetic ZDF rats. A key feature is the reduced production of nitric oxide (NO), a compound which mediates endothelium-dependent vasorelaxation and inhibits inflammation. In T2D, its bioavailability can be diminished either by the impaired insulin signaling either by the action of reactive oxygen species (ROS) [17].

Although the consequences of the later stages of T2D on the cardiac and endothelial function are well characterized, less is known concerning the early period of the disease where an interventional treatment may be more effective. Furthermore, most studies are focused on the endothelial function and perfusion of large arteries [18-20] and few on the coronary function of resistance vessels. The primary function of the coronary microcirculation is to optimize

nutrient and oxygen supply to the heart in response to any metabolic demand by coordinating the resistances within different microvascular domains, each governed by distinct regulatory mechanisms [21]. Coronary resistance arteries are capable of adapting to acute or chronic increases in blood flow leading to an increased NO-mediated relaxation and a consequent enlargement of their diameter. Furthermore, endothelial dysfunction in resistance arteries seems to precede that of large arteries [22]. Although there is strong evidence indicating that T2D is associated with impaired vasodilator responses of both peripheral and coronary vessels, Oltman *et al*. [22] have demonstrated that in diabetic young (8- to 12 wk old) ZDF rats the coronary arteriolar dilation to Ach of isolated microvessels is preserved. However, these in *vitro* studies isolate the coronary system from the cardiac environment and its influences.

Thus, the aim of this study was to characterize the diabetic state of young ZDF rats, the levels of the oxidative stress in their organisms and the *ex vivo* cardiac function. We also evaluated the fatty acid profile of cardiac membrane phospholipids since any modification at this level leads to functional changes in lipid-protein interactions and related signalling pathways. Finally, we assessed the endothelial function of the intact coronary microvasculature in terms of endothelium-dependent and -independent vasodilatations in an *ex vivo* heart perfusion model at this phase of T2D. The NO production in aortas and hearts was evaluated indirectly by estimating the degree of phosphorylation of the endothelial NO-synthase (eNOS) at serine 1177.

Methods

Animals and experimental design

All experiments followed the European Union recommendations concerning the care and use of laboratory animals for experimental and scientific purposes. All animal work was approved by the local board of ethics for animal experimentation (Cometh) and notified to the research animal facility of our laboratory (authorization n° 38 07 23).

Ten ZDF rats and eleven Zucker lean (ZL) rats were obtained from Charles Rivers (L'Arbresle, France) at 7 weeks (wk) of age. The two groups were fed *ad libitum* with a standard carbohydrate diet (A04, Safe, Augy, France), they had free access to water and their

body weight and food intake were recorded twice weekly. The composition of the chosen diet by weight is 60% assimilable glucides (52% mainly starch and cellulose), 16% proteins and 3% fat. After analysis of the fatty acid composition of our diet we found a formula with approximately 24% of saturated fatty acids (SFAs), 23% of monounsaturated fatty acids (MUFAs), 48% of n-6 polyunsaturated fatty acids (PUFAs) and 4.5% of n-3 PUFAs.

Plasma glucose and glycated hemoglobin (HbA1c) concentrations were also measured weekly via the tail vein. On the day of the experiment, the rats were weighed and heparinized (1500 I.U./kg) intraperitoneally 30 minutes (min) before their decapitation. Blood samples were collected for further biochemical analysis and their adipose tissue was quantified for determination of the abdominal fat mass.

Cardiac function study

All rats underwent *ex vivo* Langendorff assessment of their cardiac function. For this reason, a rapid thoracotomy was performed and the heart was immediately collected in Krebs-Heinselet solution maintained at 4^{o}C. It was then rapidly (less than one minute to avoid problems of cellular damages or preconditioning) perfused at constant pressure according to the Langendorff mode with a Krebs–Heinselett buffer containing (in mM) NaCl 119, $MgSO_4$ 1.2, KCl 4.8, $NaHCO_3$ 25, KH_2PO_4 1.2, $CaCl_2$ 1.2 and glucose 11 mM as sole energy substrate. The buffer was maintained at 37^{o}C and continuously oxygenated with carbogen (95% O_2/5% CO_2). A latex balloon connected to a pressure probe was inserted into the left ventricle and filled until the diastolic pressure reached a value of 7–8 mmHg. This allowed the monitoring of heart rate, systolic, diastolic and left ventricle developed pressures throughout the perfusion protocol. A pressure gauge inserted into the perfusion circuit just upstream the aortic cannula allowed the evaluation of the coronary pressure. The heart was perfused at constant pressure of 59 mmHg for 30 minutes and the coronary flow for each heart was evaluated by weight

determination of 1-min collected samples at the 25th min of perfusion. After this period, the heart was perfused at constant flow conditions, for which the flow rate was adjusted in order to obtain the same coronary flow as in the preparation at constant pressure. The systolic, diastolic and left ventricle developed pressures as well as the heart rate were determined after 10 min of perfusion at forced flow in order to allow a satisfying stabilization of the heart. The left ventricle developed pressure was calculating by subtracting the diastolic pressure to the systolic pressure. The rate-pressure product (RPP) was defined as the product of left ventricle developed pressure and heart rate and was used as indicator of the cardiac mechanical work [23]. All the parameters were recorded and analyzed with a computer using the HSE IsoHeart software (Hugo Sachs Elektronik, March-Hugstetten, Germany).

Coronary Reactivity

After the evaluation of the cardiac function at constant flow, we assessed the effects of diabetes on the coronary reactivity. After the 10-min equilibration period at constant flow, the coronary tone was raised by using the thromboxane analog U46619 (30nM), which was constantly infused into the perfusion system near the aortic cannula at a rate never exceeding 1.5% of the coronary flow. This allowed the obtainment of a coronary pressure between 120 and 130 mmHg. In our model of perfusion at forced flow, the aortic pressure equaled the coronary pressure and changes in the coronary tone triggered modifications of the aortic pressure. Changes in aortic perfusion pressure were thus used to monitor changes in coronary tone. Furthermore, this experimental model allows the evaluation of the coronary microvasculature reactivity since the coronary resistance vessels determine the overall coronary pressure. Relaxation responses to Ach (4, 10, 20, 40, 60, 80 and 100 pmoles) and sodium nitroprusside (SNP, 100, 200, 400, 600, 800 and 1000 pmoles) injections were

determined reflecting the endothelial-dependent vasodilatation (EDD) and endothelium-independent vasodilatation (EID) respectively.

The dilatation amplitude was calculated as the ratio between the maximal decrease in the coronary pressure and the coronary pressure just before the injection of the dilatation agents. Since the heart weight and coronary volume were subjected to intra- and inter-group variations, a correction was performed to normalise the input-function of the vasodilatation agents according to the coronary flow. The dose-response curve between the amount of vasodilatation agent injected and the maximal vasodilatation was then fitted to a logarithm function for each heart which allowed the fulfillment of statistical analyses. Moreover, the vasodilatation activity of the endothelial cells was also estimated from the corrected EDD and EID curves. For each heart and each injected Ach dose, the amount of SNP (reflecting the amount of vasodilator agents) necessary to obtain the same percentage of Ach-induced vasodilatation was extracted from the EID curve according to the formula: endothelial cell vasodilatation activity (ECVA) = $e^{[(\%\ \text{Ach-induced dilatation} - b) / a]}$, where a and b are the coefficients of the theoretical EID curve. The results were expressed in pmole equivalents of nitroprusside. At the end of the perfusion protocol, the hearts were freeze-clamped and stored at -80°C until the biochemical analyses were performed.

Oxidative stress measurements

i. Plasma oxidative stress

Protein oxidation in the plasma was evaluated by the disappearance of protein thiol groups [24]. Plasma thiols were assayed in 20 µl of plasma, using 5,5'-dithiobis(2-nitrobenzoic acid (DTNB)) for deriving the thiol groups. The calibration curve was obtained by mixing two stock solutions of N-acetyl cystein (NAC) in the range of 0.125–0.6 mmol/l. Standards and plasma samples were measured spectrophotometrically at 415 nm (Hitachi 912, B Braun

Science Tec, France) in the presence of a phosphate buffer 50 mM, EDTA 100 mM, pH 8 and bis-5,5'-dithio-bis(2-nitrobenzoic acid) 10 mM.

The antioxidant status of the plasma was evaluated using ferric reducing antioxidant power (FRAP) assay as a global marker of the antioxidant power. The FRAP assay uses antioxidants as reductants in a redox-linked colorimetric method. In this assay, at low pH, a ferric-tripyridyltriazine (Fe^{III}-TPTZ) complex is reduced to the ferrous form, which is blue and monitored by measuring the change in absorption at 593 nm. The change in absorbance is directly proportional to the reducing power of the electron-donating antioxidants present in plasma. The absorbance change is translated into a FRAP value (in μmol/l) by relating the change of absorbance at 593 nm of test sample to that of a standard solution of known FRAP value.

Glutathione peroxidase (GPx) activity, which is a seleno-enzyme involved in protection against hydrogen peroxide H_2O_2 was evaluated by the modified method of Gunzler [25] using terbutyl hydroperoxide (Sigma Chemical Co, Via Coger, Paris, France) as a substrate instead of hydrogen peroxide.

ii. Cytosolic Oxidative stress

Lactate and pyruvate released in the coronary effluents were spectrophotometrically assayed according to Bergmeyer [26]. The lactate to pyruvate ratio was calculated to estimate the cytosolic redox potential [27]. This is a highly specific assay using the enzyme lactate dehydrogenase (LDH) to catalyze the reversible reaction of pyruvate and NADH to lactate and NAD^+. The catalytic action of LDH permits spectrophotometric measurement at 340 nm (spectrophotometer ULTROSPEC^{TM} 2100 pro, Amersham Biosciences, Uppsala, Sweden) of lactate production in terms of the generation of NADH in the reaction shown above. To measure lactate, the reaction is carried out from right to left with excess NAD^+. To force the reaction to completion in this direction, it is necessary to trap formed pyruvate with

hydrazine. The increased absorbance at 340 nm due to NADH formation becomes a mole-to-mole measure of the lactate originally present in the sample.

iii. Mitochondrial oxidative stress

The ratio between the activities of aconitase and fumarase of the myocardium was calculated as an indicator of mitochondrial ROS production. Aconitase and fumarase activities were determined according to Gardner *et al.* [28], but were measured after extraction with a medium supplemented with citrate sodium (1M) in order to stabilize the aconitase activity *ex vivo*. Values of aconitase and fumarase activities were determined on the same extract for each biological sample.

Respiratory chain complexes and citrate synthase activities

Activities of the NADH-ubiquinone oxydo-reductase (complex I), succinate-ubiquinone oxydo-reductase (complex II), ubiquinol cytochrome c reductase (complex III), cytochrome c oxidase (complex IV), NADH cytochrome c reductase (activity of complex I+III) and succinate cytochrome c reductase (activity of complex II+III) were determined as previously described [29]. Heart samples (100 mg) were homogenized at 4°C with 0.9 ml of a potassium phosphate buffer 100 mM, pH 7.4. The homogenates were centrifuged (1,500×g, 5 min, 4°C), and the resulting supernatants were stored at −80°C until the determination of the various enzymatic activities. Activity of the citrate synthase was determined according to Faloona and Srere [30]. The activities of the respiratory chain complexes and citrate synthase were expressed in units per mg of proteins.

Western blot

The expressions of total eNOS and phosphorylated eNOS at Ser1177 was evaluated by Western blot. Frozen samples were homogenized in ice-cold lysis buffer containing 20 mM Tris (pH 7.8), 137 mM NaCl, 2.7 mM KCl, 1 mM MgCl2, 1% Triton X-100, 10% (w/v) glycerol, 10 mM NaF, 1 mM ethylenediaminetetraacetic acid, 5 mM Na pyrophosphate, 0.5 mM Na_3VO_4, 1 μg/ml leupeptin, 0.2 mM phenylmethylsulfonyl fluoride and 1 mM benzamidine. The homogenates were centrifuged at 5,000 *g* for 20 min at 4°C, and the protein concentration in the supernatant was determined in each aliquot. Protein extracts (50 μg/lane) were loaded onto a 10% SDS gel and separated by electrophoresis. Extracts from the control group were loaded on both gels, and the amount of protein was accordingly compared pairwise. Proteins were transferred to nitrocellulose membranes. The membranes were incubated overnight at 4°C with rabbit antibodies against total eNOS (1:150, Thermoscientific, Illkirch, France) and phosphospecific mouse antibodies against eNOS Ser1177 (1:1,000, BD Biosciences Pharmingen, Le Pont de Claix, France). After being washed in TBS-Tween, the membranes were incubated with horseradish peroxidase-conjugated anti-mouse IgG for eNOS Ser1177 (1:3000, Jackson Immunoresearch, Montluçon, France) and anti-rabbit IgG for total eNOS (1:20000, Jackson Immunoresearch, Montluçon, France) for 1h at room temperature, followed by additional washing. Proteins were visualized by enhanced chemiluminescence with ECL advanced Western blotting detection kit (Amersham Biosciences, Brumath, France) and quantified using densitometry and Image J software. PAN-Actin (1:1000, Cell Signaling Technology, St-Quentin-en-Yvelines, France) was used as a loading control.

Fatty acid composition of cardiac phospholipids

The phospholipid fatty acid composition was determined in cardiac homogenates as previously described [31]. The lipids were extracted according to Folch *et al*. [32]. The phospholipids were separated from non-phosphorus lipids using a Sep-pack cartridge [33]. After transmethylation, the fatty acid methyl esters were separated and analyzed by gas chromatography.

Other biochemical determinations

Blood glucose concentrations were determined with a glucose analyzer (ACCU-CHECK Active, Softclix). Plasma insulin concentrations were determined using a radioimmunoassay kit (ICN Pharmaceuticals, Orangeburg, SC). Plasma triglyceride and cholesterol levels were measured using commercially available kits from Biomérieux (Craponne, France) and Roche (Boulogne-Billancourt, France), respectively. HbA1c levels were evaluated with the kit Bayer Healthcare's analyser A1cNow® determined in blood samples (5 µl) drawn from the rat fingers. Proteins were measured using the bicinchoninic acid method with a commercially available kit (Thermo Scientific, Rockford, IL).

Statistical analysis

Results are presented as mean ± S.E.M. Animal weight, heart dry weight, glycemia, activity of respiratory chain complexes, aconitase-to-fumarase ratio and data describing the cardiac mechanical and vascular function (developed pressure, heart rate, rate pressure product, coronary pressure, and coronary flow) were contrasted across the two groups by one-way analysis of variance (ANOVA). Measures related to the action of the vasodilatation agents were treated with repeated-measures ANOVA to test the effect of the diabetes of ZDF rats (external factor), that of the amount of dilatation agent (internal factor) and their interaction.

When required, group means were contrasted with a Fisher's LSD test. A probability (p) less than 0.05 was considered significant. Statistical analysis was performed using the NCSS 2004 software.

Results

General data

As shown in Figure 1, the food intake was always higher in the ZDF compared to the ZL group (+85% at the 9th wk of age), which provoked their increased body weight (+21% at the day of the sacrifice). Consequently, based on the analysis of the diet ingredients, the ZDF group consumed greater amounts of fat than the lean group. The abdominal fat mass was partly responsible for the increased body weight since the mesenteric, retroperitoneal and visceral adipose tissues were significantly heavier as shown in table 1. However, the heart weight of the ZDF rats did not differ of that of the ZL animals (Table 1).

Figure 2 shows that the blood glucose concentration of the ZDF rats was increased as soon as the 7th wk of age and reached a value close to 5 g/l at the 9th wk (+276% compared to the ZL rats). The hyperglycemia triggered an increase in HbA1c already significant at the 9th wk (+56%) and a huge augmentation of the insulinemia (+244% at the moment of the sacrifice). The plasma triglyceride and cholesterol concentrations were also significantly higher for the ZDF rats at the moment of the sacrifice.

Oxidative stress

The mitochondrial-derived oxidative stress was estimated in cardiac homogenates by the aconitase-to-fumarase ratio. As shown in Figure 3A, the ratio was significantly reduced in the ZDF group (-41%), indicating an increase in the cardiac mitochondrial oxidative stress. The lactate-to-pyruvate ratio in the coronary effluents (Figure 3B) was also decreased in the ZDF group (-34%) indicating an increase in the cytosolic oxidative stress. In the plasma, even though the antioxidant enzyme GPx was significantly increased in the ZDF group (+21.5%, Figure 3C), the global antioxidant power as estimated by the FRAP assay was significantly

decreased (-15,6%, Fig. 3D). This was accompanied by a decrease in the plasma thiol groups (Figure 3E), which however did not reach significance.

Mitochondrial enzymatic activities

Citrate synthase was significantly increased (+4.5%) in the ZDF group as shown by the values for the ZL versus the ZDF rats in table 3. When normalized to the amount of myocardial proteins, the activity of the cytochrome oxidase was increased in the ZDF group (+20%). No modifications concerning the activities of the other respiratory chain complexes were observed.

Fatty acid composition of cardiac phospholipids

The fatty acid composition of cardiac membrane phospholipids was modulated by the development of diabetes (Table 2). The SFAs were significantly increased in the ZDF group (+24%), especially the 18:0 (+33%). This increase partly occurred at the detriment of the MUFAs. Indeed, all the MUFAs were reduced (-36, -27 and -42% for the 16:1n-7, 18:1n-9 and 18:1n-7, respectively). The n-6 PUFAs were also reduced, not only in their totality (-18%) but also regarding the 18:2n-6 (-52%). However, the 20:3 n-6 and 20:4 n-6 were significantly increased (+152 and +47%, respectively). The important reduction of the n-6 PUFAs was accompanied by an increase in n-3 PUFAs (+98%). This was particularly true for the 22:5 n-3 and 22:6 n-3 levels (+130 and + 97%, respectively). Finally, the n-6 to n-3 PUFA ratio of cardiac phospholipids was reduced by the occurence of diabetes (-60%).

Cardiac function study

The results of the *ex vivo* cardiac function are shown in table 4. The measured parameters were recorded when the heart was perfused at constant flow before the infusion of U46619. In the ZDF group, the RPP was reduced (-35%) compared to the ZL group. This was due to a reduction of the heart rate (-42%), since the left ventricle developed pressure was slightly increased (+18.2%). The changes in the RPP were consequently related to the observed decrease in coronary flow (-25%), but the coronary pressure was unaffected. The infusion of U46619 raised the coronary pressure from 80 mmHg to a value close to 125 mmHg in both groups.

Coronary reactivity

Figure 4A depicts an EDD, which was similar in the two groups, reaching 15% of dilatation as soon as 40 pmoles of Ach were injected. The EID was significantly increased in the ZDF group (Figure 4B) as soon as the SNP dose of 600 picomoles was injected (+14, +16 and +18% at the doses of 600, 800 and 1000 pmoles of SNP, respectively). Finally, the ECVA was not modified by the occurrence of diabetes (Figure 4C).

eNOS expression and phosphorylation

The eNOS expression and its phosphorylation at Ser1177 were evaluated in aortic and cardiac homogenates of both groups. No difference was observed between groups in the expression and phosphorylation of the enzyme neither in the aorta (Figures 5A and 5B) nor in the heart (Figures 5C and 5D).

Discussion

Even though several studies have examined the effects of diabetes on the vascular function, most of them used techniques of isolated vessels and most of them examined the late stages of diabetes [22, 34]. This is the first study that focuses on the effects of T2D on the intact coronary microvasculature at the early phase of the disease. This study addressed cardiac mechanical function in an isolated heart model that provided also the opportunity to study the vascular functionality in the intact coronary circulation. This allowed the analysis of the coupling of cardiac and coronary function, which is not feasible in isolated vessels.

The ZDF rat has been well characterized as experimental model of type 2 diabetes. The ZL rats in our study ate a normal amount of diet (approximately 20 g/day) and exhibited low blood glucose concentration (1 g/l) and proportion of HbA1c (approximately 4%) between the 7^{th} and 11^{th} wk of life. Their insulinemia was also low (1 μg/l) at the moment of sacrifice. In contrast, the ZDF animals consumed greater amounts of food (more than 30 g/day) that resulted to a higher body weight during the whole course of the experiment. Their blood analysis revealed a glycemia reaching 5 g/l at the 9^{th} wk of age and a proportion of HbA1c close to 9% representing an already established diabetic state. The insulinemia at the 11^{th} week was almost 4 times higher than that of the ZL control animals, indicating functional β cells in the Langerhans islets despite the high blood glucose concentration. Furthermore, their plasma triglycerides and cholesterol levels were approximately 2 times higher than those of the lean animals. All these characteristics associated with the fact that the visceral fat mass was abnormally high, clearly demonstrate that the ZDF animals displayed a severe insulin resistance responsible for the development of type-2 diabetes, which corresponds to a stage of early human type 2 diabetes.

In our study, the presence of diabetes provoked an enhanced cytosolic and mitochondrial oxidative stress in the hearts of the ZDF rats as observed by the lactate-to-pyruvate and

aconitase-to-fumarase ratios respectively. It seems though that the respiratory chain complexes (RCC) were not implicated in the development of this mitochondrial oxidative stress, especially since the CIV activity was increased in the ZDF animals. It has been previously proposed that an up-regulation of CIV activity without any other changes in the other RCC or citrate synthase activities may serve to reduce any production of oxidative stress by the electron transport chain and improve the electron flux [35]. However, it is probable that a lack of mitochondrial antioxidant defenses could result to the increased mitochondrial oxidative stress observed in this study. Furthermore, the plasma antioxidant capacity from ZDF rats was significantly decreased despite the increase of the GPx enzyme activity. This indicates an increased presence of ROS in their plasma as evidenced also by the disappearance of the plasma thiol groups, even though it did not reach absolute significance ($p=0.079$, ANOVA). Thus, an increased oxidative stress was already present in the cardiac tissue and plasma at the early phase of T2D despite the effort of the organism (CIV and GPx activities) to eliminate it.

The development of T2D also induced changes in the fatty acid profile of cardiac membrane phospholipids that may influence lipid-protein interactions, inflammation and related metabolic processes. In particular, an increase in the SFAs in cardiac membranes was observed to the detriment of MUFAs. This increased degree of saturation could negatively affect the membrane fluidity and increase its rigidity. However, an increase in the PUFAs content, in particular the C20:4 n-6 (arachidonic acid, AA), C22:5 n-3 (docosapentaenoic acid, DPA) and C22:6 n-3 (docosahexanoic acid, DHA) contents, was observed probably as an effort to maintain a proper membrane fluidity degree. Moreover, these increases seem to result from stimulation of the desaturation and elongation enzymes in the organism of the ZDF rats rather from an increase in the concentration of the initial phospholipids of the PUFAs metabolisms (e.g. C18:2 n-6 and C20:5 n-3 for n-6 and n-3 respectively). It has been

observed that tissues such as heart, kidney and liver from diabetic rats are characterized by a decrease in arachidonylated phospholipids and an increase in phospholipids containing linoleic acid (LA, C18:2 n-6). However, these modifications are mostly related to the later stages of diabetes. The n-3 and n-6 PUFAs of membrane phospholipids are also responsible for the production of anti- and pro-inflammatory molecules respectively. The low ratio EPA/AA found in our ZDF rats predisposes to a balance of eicosanoids favouring platelet aggregation and inflammatory mediator signalling [36]. The development of a compensatory mechanism might thus be in question as the levels of n-3 PUFAs were increased in the ZDF group. Low levels of EPA+DHA have been related to increased risk for sudden cardiac death [36] and hearts with high DHA content present very low *in vivo* and *in vitro* vulnerability to arrhythmia [37]. The ZDF hearts have high levels of EPA + DHA in order to reduce pro-inflammatory eicosanoids and cytokines. These modifications in the PUFAs levels of the cardiac membrane phospholipids probably help the heart to resist to any sudden cardiac damage at this early phase of diabetes [37].

In our study, we reported a strong decrease in the *ex vivo* cardiac function as already shown in pre-diabetic [38] and diabetic [39, 40] states. The RPP was significantly reduced, mainly because of the decreased heart rate. The T2D-induced reduction of the heart rate has already been commonly shown in the diabetic state [41] and it has been explained by an abnormal functioning of the cells involved in the generation and transfer of the electric influx triggering the cardiac contraction [42]. We also observed a noticeable diabetes-induced decrease in the coronary flow. This decrease could also be responsible for the reduction of the heart rate and cardiac mechanical work through insufficient oxygen supply. This could not be explained by an increase in the vascular tone triggering vasoconstriction and limitation of the oxygen and substrate supply since no abnormalities of the vascular function were observed according to the results of the vascular reactivity. Finally, the two phenomena could be synergistic and lead

to the decreased RPP. In contrast, the left ventricle developed pressure was increased, which could compensate for the decreased heart rate. Thus, our data confirm a decrease in the *ex vivo* cardiac function, and particularly in the heart rate, at this model of heart perfusion, which is a common characteristic of all types of diabetes.

The underlying mechanism, which could explain the observed decreased cardiac mechanical work, has been already characterized. Several metabolic modifications in our study suggest that the reduced *ex vivo* cardiac function was due to this mechanism. In this study, we found an increased plasma triglyceride concentration that could allow the excess free fatty acid uptake and stimulation of the peroxisome proliferator-activated receptor alpha (PPARα) [40]. This would lead to increased β-oxidation and mitochondrial oxygen consumption [43]. The resulting excessive mitochondria-related ROS production, as evidenced by the aconitase-to-fumarase ratio in our study, would favour the expression of protein 53 (p53). The observed increased activity of the cytochrome c oxidase suggests an increased expression of the cytochrome c oxidase 2 (SCO2). Consequently, ectopic lipid accumulation may occur in the cardiomyocytes through increased expression of the fatty acid translocase protein FAT/CD36. Lipotoxicity then contributes to cardiac cell damages and myocardial dysfunction. A severe intramyocardial lipid accumulation, even at 8 wk of age [44] and an increased fatty acid oxidation [39] have been observed in ZDF rats. Thus, the altered myocardial substrate utilization affecting the mitochondrial function and stimulating the above described mechanism could be one of the factors responsible for the development of the T2D-induced *ex vivo* cardiac mechanical dysfunction leading to reduction of oxygen demand and subsequent decrease in the coronary perfusion. In our study though we did not observe any decrease in the left ventricle developed pressure that could have resulted from this mechanism. Instead, the heart rate was the parameter mostly affected by the diabetes in our study. However, the conditions of the perfusion model did not allow us to evaluate correctly

the left ventricle developed pressure. A future study of heart perfusion at stable heart rate (pacing) in order to evaluate the cardiac contractility and relaxation by measuring the maximal rate of the ventricular pressure rise (dP/dt_{max}) and fall (dP/dt_{min}) respectively could enlighten our knowledge concerning this mechanism. Taken together, these observations suggest that the lipid accumulation and alterations of substrate utilization in ZDF rats may affect firstly the cells responsible for the cardiac contraction that are involved in the generation and transfer of the electric influx. Furthermore, hyperglycemia and insulin resistance, two states that characterized the ZDF rats in this study, have been related to damages in cardiac nodal cells and cardiac electrophysiological properties.

The effects of the T2D on the function of the coronary resistance arteries were also evaluated in this *ex vivo* model of isolated perfused heart through evaluation of the coronary reactivity. This parameter was estimated through changes in the global coronary tone which mainly reflects the function of the arteriole network, since atherosclerosis does not occur in the rat [45]. The effects of T2D on the heart can thus be evaluated independently of the development of coronary artery disease. We also evaluated indirectly the NO production through measurements of the expression and phosphorylation of the cardiac and aortic eNOS. In our study, diabetes did not modify the expression and phosphorylation of cardiac eNOS, which was also the case for the aortas. Furthermore, the coronary EDD was not reduced, but fully maintained. This was a surprising finding given the huge amount of studies associating T2D and dysfunctions of the coronary microcirculation [46-48]. Factors contributing to these discrepancies are the severity of the obesity and diabetic state studied as well as the experimental method used. Oltman *et al*. [22] have reported a preservation of the coronary arteriolar dilatation to Ach in isolated vessels of pre-diabetic young (8- to 12-wk old) ZDF rats. However, in the present study, the ZDF rats were not in a prediabetic state, but the T2D was already developed as indicated by the blood glucose concentration, which was already

high from the 8th wk of age. Thus, it seems that the endothelial function of the intact coronary microvasculature is not affected from the diabetes at this phase. An unaltered eNOS activity and high levels of AA and DHA despite the presence of oxidative stress found in the diabetic hearts could have contributed to this phenomenon. AA [49] and DHA [50] are known for their vasorelaxant effects via the production of prostacyclin (PGI2) and the reduction of calcium influx in vascular smooth muscle cells.

As shown by the calculated activity of endothelial cells to induce dilatation and the evaluation of eNOS expression the phenomenon of the maintained Ach-mediated vasodilatation was partly mediated by the activity of endothelial cells. However, the SNP responses were enhanced in the ZDF rats representing an enhanced function of the smooth muscle cells of the coronary system contributing to the maintained endothelium-dependent dilatation. This enhanced function may be due to a modified NO response, which could increase guanylate cyclase activity as already shown in cases of obesity and hypertension [51, 52].

These vascular alterations may reflect a compensatory adaptation of the cardiovascular system to support increased cardiac work since cardiac output and stroke volume are increased in obese and diabetic states [53, 54]. Taken also under consideration the decreased *ex vivo* cardiac mechanical function observed in this study, this adaptation seems to be essential to adjust organ perfusion during physiological processes such as exercise and pathological processes such as ischemic diseases [11]. Otherwise, the heart would not be able to respond to the increased metabolic demands.

Conclusions

Cardiovascular function was evaluated in young diabetic ZDF rats using an *ex vivo* heart perfusion model. Our data suggest that at the early phase of diabetes, increased oxidative stress in tissue and plasma is already present and probably responsible for the observed *ex*

vivo cardiac mechanical dysfunction. However, the heart tries to resist by developing a number of adaptations. These include the increased GPx and CIV activities, the increase in the n-3 PUFAs content of the myocardial membrane and the preserved EDD of the coronary microvasculature. This would help the heart to keep an adequate perfusion and respond to any acute cardiac incident at this phase. Thus, therapeutic interventions at this early phase of the disease aiming at increasing the heart rate and maintaining the observed adaptations could be an option for delaying or decreasing the late-stage complications of the diabetes.

Competing interests

The authors declare that they have no competing interests.

Authors' contributions

Evangelia Mourmoura conducted the experiments and contributed to the study implementation, statistical analysis, interpretation, and the preparation of the manuscript. Guillaume Vial conducted a part of biochemical experiments and participated in the animal care. Brigitte Laillet, Jean-Paul Rigaudière, Isabelle Hininger, Hervé Dubouchaud and Beatrice Morio helped to conduct the experiments and acquire data. Luc Demaison supervised the study conduction and contributed to the study conception and design, implementation, statistical interpretation, the preparation and finalization of the manuscript. All authors approved the final manuscript for publication.

Acknowledgements

We would like to thank Mr. Cristophe Cottet for carefully editing the manuscript, Cindy Tellier for animal care and Mireille Osman for the measurements of GPx activity, FRAP

assay and thiol groups in the plasma. This work was supported by the French National Institute of Agronomical Research (INRA), the French National Institute of Health and Medical Research (INSERM) and Joseph Fourier University, Grenoble, France.

References

1. Wild S, Roglic G, Green A, Sicree R, King H: **Global prevalence of diabetes: estimates for the year 2000 and projections for 2030**. *Diabetes care* 2004, **27**(5):1047-1053.
2. Mathers CD, Loncar D: **Projections of global mortality and burden of disease from 2002 to 2030**. *PLoS medicine* 2006, **3**(11):e442.
3. Funaki M: **Saturated fatty acids and insulin resistance**. *The journal of medical investigation : JMI* 2009, **56**(3-4):88-92.
4. Goldstein BJ: **Insulin resistance as the core defect in type 2 diabetes mellitus**. *The American journal of cardiology* 2002, **90**(5A):3G-10G.
5. Sowers JR, Epstein M, Frohlich ED: **Diabetes, hypertension, and cardiovascular disease: an update**. *Hypertension* 2001, **37**(4):1053-1059.
6. Chinen I, Shimabukuro M, Yamakawa K, Higa N, Matsuzaki T, Noguchi K, Ueda S, Sakanashi M, Takasu N: **Vascular lipotoxicity: endothelial dysfunction via fatty-acid-induced reactive oxygen species overproduction in obese Zucker diabetic fatty rats**. *Endocrinology* 2007, **148**(1):160-165.
7. Heitzer T, Schlinzig T, Krohn K, Meinertz T, Munzel T: **Endothelial dysfunction, oxidative stress, and risk of cardiovascular events in patients with coronary artery disease**. *Circulation* 2001, **104**(22):2673-2678.
8. Thuillez C, Richard V: **Targeting endothelial dysfunction in hypertensive subjects**. *J Hum Hypertens* 2005, **19 Suppl 1**:S21-25.
9. Nitenberg A, Valensi P, Sachs R, Dali M, Aptecar E, Attali JR: **Impairment of coronary vascular reserve and ACh-induced coronary vasodilation in diabetic patients with angiographically normal coronary arteries and normal left ventricular systolic function**. *Diabetes* 1993, **42**(7):1017-1025.

10. Clark JB, Palmer CJ, Shaw WN: **The diabetic Zucker fatty rat**. *Proceedings of the Society for Experimental Biology and Medicine Society for Experimental Biology and Medicine* 1983, **173**(1):68-75.

11. Wang P, Chatham JC: **Onset of diabetes in Zucker diabetic fatty (ZDF) rats leads to improved recovery of function after ischemia in the isolated perfused heart**. *Am J Physiol Endocrinol Metab* 2004, **286**(5):E725-736.

12. Greenberg AS, McDaniel ML: **Identifying the links between obesity, insulin resistance and beta-cell function: potential role of adipocyte-derived cytokines in the pathogenesis of type 2 diabetes**. *European journal of clinical investigation* 2002, **32 Suppl 3**:24-34.

13. Bastard JP, Maachi M, Van Nhieu JT, Jardel C, Bruckert E, Grimaldi A, Robert JJ, Capeau J, Hainque B: **Adipose tissue IL-6 content correlates with resistance to insulin activation of glucose uptake both in vivo and in vitro**. *The Journal of clinical endocrinology and metabolism* 2002, **87**(5):2084-2089.

14. Erdos B, Snipes JA, Miller AW, Busija DW: **Cerebrovascular dysfunction in Zucker obese rats is mediated by oxidative stress and protein kinase C**. *Diabetes* 2004, **53**(5):1352-1359.

15. Oltman CL, Coppey LJ, Gellett JS, Davidson EP, Lund DD, Yorek MA: **Progression of vascular and neural dysfunction in sciatic nerves of Zucker diabetic fatty and Zucker rats**. *American journal of physiology Endocrinology and metabolism* 2005, **289**(1):E113-122.

16. Coppey LJ, Gellett JS, Davidson EP, Dunlap JA, Yorek MA: **Changes in endoneurial blood flow, motor nerve conduction velocity and vascular relaxation of epineurial arterioles of the sciatic nerve in ZDF-obese diabetic rats**. *Diabetes/metabolism research and reviews* 2002, **18**(1):49-56.

17. Cai H, Harrison DG: **Endothelial dysfunction in cardiovascular diseases: the role of oxidant stress**. *Circulation research* 2000, **87**(10):840-844.

18. Pieper GM, Langenstroer P, Siebeneich W: **Diabetic-induced endothelial dysfunction in rat aorta: role of hydroxyl radicals**. *Cardiovascular research* 1997, **34**(1):145-156.

19. Winer N, Sowers JR: **Diabetes and arterial stiffening**. *Advances in cardiology* 2007, **44**:245-251.

20. Hattori Y, Kawasaki H, Abe K, Kanno M: **Superoxide dismutase recovers altered endothelium-dependent relaxation in diabetic rat aorta**. *Am J Physiol* 1991, **261**(4 Pt 2):H1086-1094.

21. Chilian WM: **Coronary microcirculation in health and disease. Summary of an NHLBI workshop**. *Circulation* 1997, **95**(2):522-528.

22. Oltman CL, Richou LL, Davidson EP, Coppey LJ, Lund DD, Yorek MA: **Progression of coronary and mesenteric vascular dysfunction in Zucker obese and Zucker diabetic fatty rats**. *American journal of physiology Heart and circulatory physiology* 2006, **291**(4):H1780-1787.

23. Gobel FL, Norstrom LA, Nelson RR, Jorgensen CR, Wang Y: **The rate-pressure product as an index of myocardial oxygen consumption during exercise in patients with angina pectoris**. *Circulation* 1978, **57**(3):549-556.

24. Faure P, Lafond J: **Measurement of plasma sulfhydryl and carbonyl groups as a possible indicatorof protein oxidation.** In *Analysis of Free Radicals in Biology Systems.* Edited by Favier A, Cadet J, Kalnyanaraman M, Fontecave M, Pierre J. Basel: Birkhauser; 1995:237-248.

25. Gunzler WA, Kremers H, Flohe L: **An improved coupled test procedure for glutathione peroxidase (EC 1-11-1-9-) in blood**. *Z Klin Chem Klin Biochem* 1974, **12**(10):444-448.

26. Bergmeyer H-U, Gawehn K, Williamson DH, Lund P: **Methods of enzymatic analysis**, 2nd English ed edn. Weinheim New York ; London: Verlag Chemie ; Academic Press; 1974.

27. Nuutinen EM: **Subcellular origin of the surface fluorescence of reduced nicotinamide nucleotides in the isolated perfused rat heart**. *Basic Res Cardiol* 1984, **79**(1):49-58.

28. Gardner PR, Nguyen DD, White CW: **Aconitase is a sensitive and critical target of oxygen poisoning in cultured mammalian cells and in rat lungs**. *Proceedings of the National Academy of Sciences of the United States of America* 1994, **91**(25):12248-12252.

29. Mourmoura E, Leguen M, Dubouchaud H, Couturier K, Vitiello D, Lafond JL, Richardson M, Leverve X, Demaison L: **Middle age aggravates myocardial ischemia through surprising upholding of complex II activity, oxidative stress, and reduced coronary perfusion**. *Age* 2011, **33**(3):321-336.

30. Faloona GR, Srere PA: **Escherichia coli citrate synthase. Purification and the effect of potassium on some properties**. *Biochemistry* 1969, **8**(11):4497-4503.

31. Demaison L, Moreau D, Vergely-Vandriesse C, Gregoire S, Degois M, Rochette L: **Effects of dietary polyunsaturated fatty acids and hepatic steatosis on the functioning of isolated working rat heart under normoxic conditions and during post-ischemic reperfusion**. *Molecular and cellular biochemistry* 2001, **224**(1-2):103-116.

32. Folch J, Lees M, Sloane Stanley GH: **A simple method for the isolation and purification of total lipides from animal tissues**. *J Biol Chem* 1957, **226**(1):497-509.

33. Juaneda P, Rocquelin G: **Rapid and convenient separation of phospholipids and non phosphorus lipids from rat heart using silica cartridges**. *Lipids* 1985, **20**(1):40-41.

34. Okon EB, Szado T, Laher I, McManus B, van Breemen C: **Augmented contractile response of vascular smooth muscle in a diabetic mouse model**. *Journal of vascular research* 2003, **40**(6):520-530.

35. Parise G, Brose AN, Tarnopolsky MA: **Resistance exercise training decreases oxidative damage to DNA and increases cytochrome oxidase activity in older adults**. *Exp Gerontol* 2005, **40**(3):173-180.

36. Rupp H, Wagner D, Rupp T, Schulte LM, Maisch B: **Risk stratification by the "EPA+DHA level" and the "EPA/AA ratio" focus on anti-inflammatory and antiarrhythmogenic effects of long-chain omega-3 fatty acids**. *Herz* 2004, **29**(7):673-685.

37. Pepe S, McLennan PL: **Cardiac membrane fatty acid composition modulates myocardial oxygen consumption and postischemic recovery of contractile function**. *Circulation* 2002, **105**(19):2303-2308.

38. Essop MF, Anna Chan WY, Valle A, Garcia-Palmer FJ, Du Toit EF: **Impaired contractile function and mitochondrial respiratory capacity in response to oxygen deprivation in a rat model of pre-diabetes**. *Acta Physiol (Oxf)* 2009, **197**(4):289-296.

39. Wang P, Lloyd SG, Zeng H, Bonen A, Chatham JC: **Impact of altered substrate utilization on cardiac function in isolated hearts from Zucker diabetic fatty rats**. *Am J Physiol Heart Circ Physiol* 2005, **288**(5):H2102-2110.

40. Finck BN, Han X, Courtois M, Aimond F, Nerbonne JM, Kovacs A, Gross RW, Kelly DP: **A critical role for PPARalpha-mediated lipotoxicity in the pathogenesis of diabetic cardiomyopathy: modulation by dietary fat content**. *Proc Natl Acad Sci U S A* 2003, **100**(3):1226-1231.

41. Semeniuk LM, Kryski AJ, Severson DL: **Echocardiographic assessment of cardiac function in diabetic db/db and transgenic db/db-hGLUT4 mice**. *American journal of physiology Heart and circulatory physiology* 2002, **283**(3):H976-982.

42. Barth AS, Tomaselli GF: **Cardiac metabolism and arrhythmias**. *Circulation Arrhythmia and electrophysiology* 2009, **2**(3):327-335.

43. Nakamura H, Matoba S, Iwai-Kanai E, Kimata M, Hoshino A, Nakaoka M, Katamura M, Okawa Y, Ariyoshi M, Mita Y *et al*: **p53 promotes cardiac dysfunction in diabetic mellitus caused by excessive mitochondrial respiration-mediated reactive oxygen species generation and lipid accumulation**. *Circ Heart Fail*, **5**(1):106-115.

44. Sharma S, Adrogue JV, Golfman L, Uray I, Lemm J, Youker K, Noon GP, Frazier OH, Taegtmeyer H: **Intramyocardial lipid accumulation in the failing human heart resembles the lipotoxic rat heart**. *FASEB J* 2004, **18**(14):1692-1700.

45. Wissler RW: **The production of atheromatous lesions in the albino rat**. *Proc Inst Med Chic* 1952, **19**(4):79-80.

46. Gao X, Picchi A, Zhang C: **Upregulation of TNF-alpha and Receptors Contribute to Endothelial Dysfunction in Zucker Diabetic Rats**. *Am J Biomed Sci*, **2**(1):1-12.

47. Oltman CL, Kleinschmidt TL, Davidson EP, Coppey LJ, Lund DD, Yorek MA: **Treatment of cardiovascular dysfunction associated with the metabolic syndrome and type 2 diabetes**. *Vascul Pharmacol* 2008, **48**(1):47-53.

48. Oniki H, Fujii K, Kansui Y, Goto K, Iida M: **Effects of angiotensin II receptor antagonist on impaired endothelium-dependent and endothelium-independent relaxations in type II diabetic rats**. *J Hypertens* 2006, **24**(2):331-338.

49. Spector AA, Hoak JC, Fry GL, Denning GM, Stoll LL, Smith JB: **Effect of fatty acid modification on prostacyclin production by cultured human endothelial cells**. *The Journal of clinical investigation* 1980, **65**(5):1003-1012.

50. Mori TA, Watts GF, Burke V, Hilme E, Puddey IB, Beilin LJ: **Differential effects of eicosapentaenoic acid and docosahexaenoic acid on vascular reactivity of the forearm microcirculation in hyperlipidemic, overweight men**. *Circulation* 2000, **102**(11):1264-1269.

51. Brandes RP, Kim D, Schmitz-Winnenthal FH, Amidi M, Godecke A, Mulsch A, Busse R: **Increased nitrovasodilator sensitivity in endothelial nitric oxide synthase knockout mice: role of soluble guanylyl cyclase**. *Hypertension* 2000, **35**(1 Pt 2):231-236.

52. Jebelovszki E, Kiraly C, Erdei N, Feher A, Pasztor ET, Rutkai I, Forster T, Edes I, Koller A, Bagi Z: **High-fat diet-induced obesity leads to increased NO sensitivity of rat coronary arterioles: role of soluble guanylate cyclase activation**. *American journal of physiology Heart and circulatory physiology* 2008, **294**(6):H2558-2564.

53. Radovits T, Korkmaz S, Loganathan S, Barnucz E, Bomicke T, Arif R, Karck M, Szabo G: **Comparative investigation of the left ventricular pressure-volume relationship in rat models of type 1 and type 2 diabetes mellitus**. *Am J Physiol Heart Circ Physiol* 2009, **297**(1):H125-133.

54. Crandall DL, Goldstein BM, Lizzo FH, Gabel RA, Cervoni P: **Hemodynamics of obesity: influence of pattern of adipose tissue cellularity**. *Am J Physiol* 1986, **251**(2 Pt 2):R314-319.

Figures

Figure 1 Evolution of the body weight and food intake of the animals. (A) Body weight and **(B)** Food intake of the animals between the 7th and 11th week of life. ZL: Zucker lean rats; ZDF: Zucker Diabetic Fatty rats. The number of experiments was 11 and 10 for the ZL and ZDF groups respectively. *: significantly different.

Figure 2 Evaluation of circulating biochemical parameters. (A) Evolution of blood glucose concentration and **(B)** proportion of glycated hemoglobin (HbA1c) between 7th and 11th wk of life. **(C)** Plasma levels of insulin, **(D)** triglycerides and **(E)** cholesterol at 11th wk of age. ZL: Zucker lean rats; ZDF: Zucker Diabetic Fatty rats. The number of experiments was 11 and 10 for the ZL and ZDF groups respectively. *: significantly different.

Figure 3 Oxidative stress measurements. (A) Mitochondrial oxidative stress estimated by aconitase-to-fumarase ratio. **(B)** Cytosolic oxidative stress estimated by lactate-to-pyruvate ratio. **(C)** Enzymatic activity of glutathione peroxidase (GPx) in the plasma. **(D)** Antioxidant power of the plasma estimated by the ferric reducing antioxidant power (FRAP) assay. **(E)** Systemic oxidative stress estimated by the disappearance of the plasma thiol (SH) groups. ZL: Zucker lean rats; ZDF: Zucker Diabetic Fatty rats. The number of experiments was 11 and 10 for the ZL and ZDF groups respectively. *: significantly different.

Figure 4 Coronary microvascular reactivity *ex vivo*. (A) Endothelial-dependent dilatation (EDD). (**B)** Endothelial-independent dilatation (EID). **(C)** Endothelial cell vasodilatation activity (ECVA). ZL: Zucker lean rats; ZDF: Zucker Diabetic Fatty rats; Ach: acetylcholine; SNP: sodium nitroprusside. The number of experiments was 11 and 10 for the ZL and ZDF groups respectively. *: significantly different.

Figure 5 Protein expressions of total eNOS and phosphorylated eNOS at Ser1177 in aortas and hearts. (A) Representative immunoblots of total eNOS, eNOS phosphorylated at Ser1177 and actin in aorta. Control is the common sample used for all Western blots. **(B)**

Quantified total eNOS and phosphorylated eNOS in the aortas and ratio between the phosphorylated and total eNOS in aorta. **(C)** Representative immunoblots of total eNOS, eNOS phosphorylated at Ser1177 and actin in heart. Control is the common sample used for all Western blots. (**D)** Quantified total eNOS and phosphorylated eNOS in the hearts and ratio between the phosphorylated and total eNOS. ZL: Zucker lean rats; ZDF: Zucker Diabetic Fatty rats. The number of experiments was 11 and 10 for the ZL and ZDF groups respectively. *: significantly different.

Table 1 Adipose tissue and heart weights

	ZL	ZDF
Mesenteric AT	1.77 ± 0.09	4.94 ± 0.22*
Retroperitoneal AT	1.04 ± 0.07	4.56 ± 0.13*
Visceral AT	2.81 ± 0.02	9.50 ± 0.32*
Abdominal AT	3.85 ± 0.22	14.06 ± 0.43*
Abdominal AT/BW	0.013 ± 0.001	0.039 ± 0.001*
Heart	203 ± 12	200 ± 6
Heart weight/BW (mg/g)	0.68 ± 0.03	0.55 ± 0.02*

The number of experiments was 11 and 10 for the ZL and ZDF groups respectively. The weight of mesenteric, retroperitoneal, visceral and abdominal adipose tissues is expressed in g of wet weight. The abdominal adipose tissue weight normalized to the body weight is expressed in g of wet weight per g of body weight. The heart weight is expressed in mg of dry weight. The heart-to-body weight ratio is expressed in mg of dry weight per g of body weight. ZL: Zucker lean rats; ZDF: Zucker diabetic fatty rats; AT: adipose tissue; BW: body weight; *: significantly different.

Table 2 Respiratory chain complex and citrate synthase activities

	ZL	ZDF
CI	1.06 ± 0.12	1.05 ± 0.08
CII	0.67 ± 0.04	0.68 ± 0.03
CIII	0.22 ± 0.03	0.23 ± 0.02
CIV	0.070 ± 0.006	0.084 ± 0.003*
CI+III	0.040 ± 0.003	0.040 ± 0.003
CII+III	0.022 ± 0.002	0.024 ± 0.002
CS	4.55 ± 0.01	4.75 ± 0.05*

The number of experiments was 11 and 10 for the ZL and ZDF groups respectively. ZL: Zucker lean rats; ZDF: Zucker Diabetic fatty rats; CI: NADH:ubiquinone oxidoreductase; CII: succinate-ubiquinone oxydo-reductase; CIII: ubiquinol-cytochrome-c reductase; CIV: cytochrome c oxidase; CI+III: NADH cytochrome c reductase; CII+III: succinate cytochrome c reductase; CS: citrate synthase. The results are expressed in mU/mg of proteins. *: significantly different.

Table 3 Fatty acid composition of cardiac phospholipids

Fatty acids (%)	ZL	ZDF
14:0	0.07 ± 0.01	0.05 ± 0.01*
DMA16:0	2.67 ± 0.15	4.39 ± 0.60*
16:0	12.63 ± 0.17	13.25 ± 0.58
DMA18:0	1.20 ± 0.06	1.29 ± 0.25
18:0	19.37 ± 0.50	25.70 ± 1.12*
SFA	35.94 ± 0.80	44.68 ± 1.07*
16:1n-7	0.56 ± 0.02	0.37 ± 0.02*
18:1n-9	3.49 ± 0.16	2.53 ± 0.08*
18:1n-7	5.77 ± 0.22	3.32 ± 0.10*
MUFA	9.81 ± 0.36	6.21 ± 0.16*
18:2n-6	32.94 ± 1.83	15.65 ± 2.57*
20:2n-6	0.17 ± 0.02	0.17 ± 0.01
20:3n-6	0.40 ± 0.05	1.01 ± 0.11*
20:4n-6	16.01 ± 0.83	23.62 ± 1.64*
22:4n-6	0.42 ± 0.04	0.38 ± 0.03
22:5n-6	0.31 ± 0.01	0.39 ± 0.04
n-6 PUFA	50.25 ± 0.94	41.23 ± 1.27*
20:5n-3	0.10 ± 0.01	0.08 ± 0.06
22:5n-3	0.55 ± 0.06	1.26 ± 0.11*
22:6n-3	3.31 ± 0.41	6.51 ± 0.55*
n-3 PUFA	3.95 ± 0.43	7.86 ± 0.64*
PUFA	54.20 ± 0.63	49.09 ± 1.17*
n-6/n-3	13.51 ± 1.70	5.40 ± 0.47*
Total 16:0	15.30 ± 0.28	17.63 ± 0.30*
Total 18:0	20.57 ± 0.54	26.00 ± 0.94*
Total 18:1	9.26 ± 0.35	5.87 ± 0.16*
EPA/AA	0.006 ± 0.001	0.004 ± 0.001*
EPA+DHA	3.4 ± 0.4	6.6 ± 0.6*

Values are expressed as relative amounts of the total fatty acid content. The analysis was performed on 5 samples randomly selected in each group. ZL: Zucker lean rats; ZDF: Zucker diabetic fatty rats; DMA: dimethylacetal; SFA: saturated fatty acids; MUFA: monounsaturated fatty acids; PUFA: polyunsaturated fatty acids; EPA: eicosapentanoic acid; AA: arachidonic acid; DHA: docosahexaenoic acid; *: significantly different.

Table 4 *Ex vivo* cardiac function

	ZL	ZDF
HR (beats/min)	294 ± 10	171 ± 23*
LVDP (mmHg)	99 ± 6	115 ± 6*
RPP (mHg/min)	29 ± 2	19 ± 2*
CF (ml/min)	14.1 ± 1.0	10.6 ± 0.8*
CP before U46619 (mmHg)	78 ± 8	78 ± 3
CP after U46619 (mmHg)	121 ± 9	130 ± 8

The number of experiments was 11 and 10 for the ZL and ZDF groups respectively. ZL: Zucker lean rats; ZDF: Zucker Diabetic fatty rats; HR: Heart Rate, LVDP: Left Ventricle Developed Pressure, RPP: Rate x Pressure Product, CF: Coronary Flow, CP: Coronary Pressure. * significantly different.

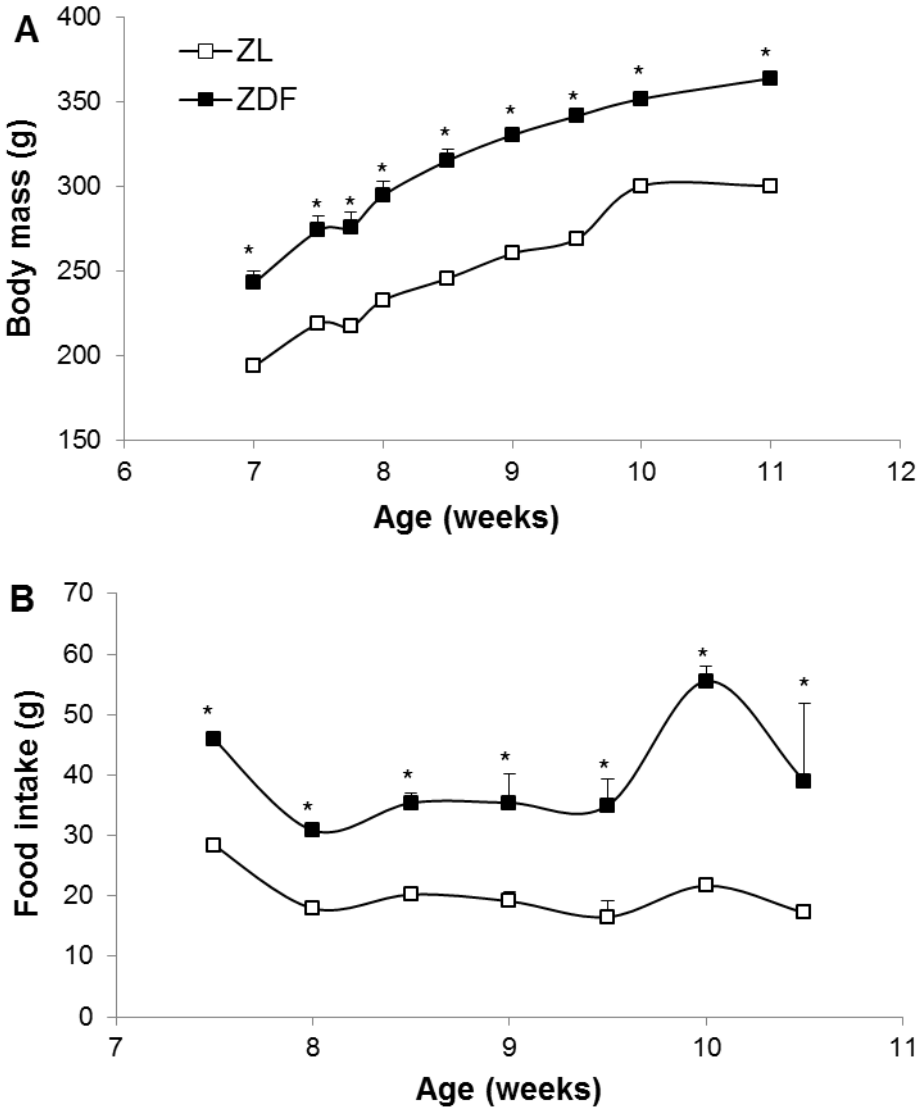
A
ZL
ZDF
Body mass (g)
400
350
300
250
200
150
6
7
8
9
10
11
12
Age (weeks)
B
Food intake (g)
70
60
50
40
30
20
10
0
7
8
9
10
11
Age (weeks)

Figure 1

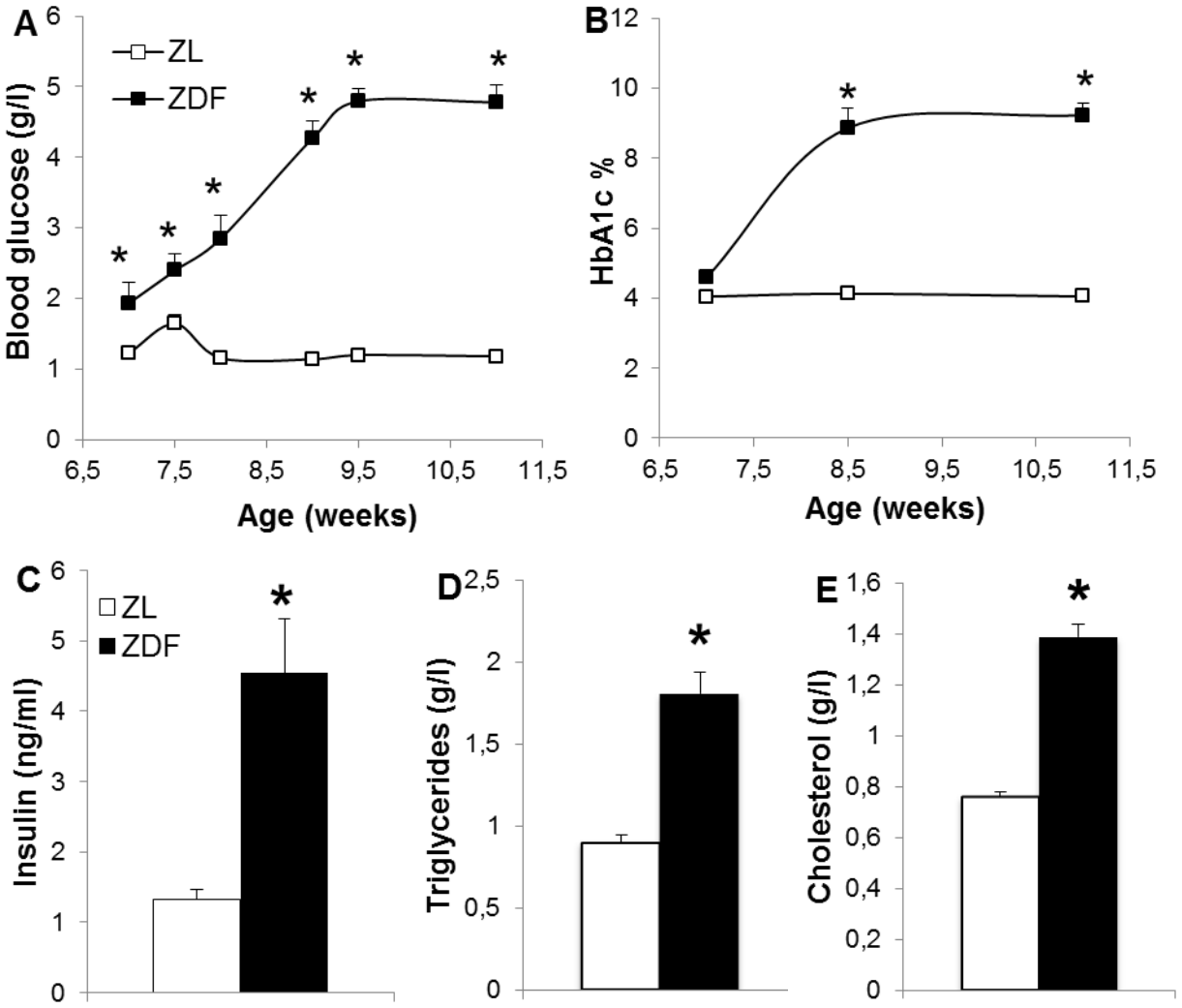
A
Blood glucose (g/l)
ZL
ZDF
Age (weeks)
B
HbA1c %
Age (weeks)
C
Insulin (ng/ml)
ZL
ZDF
D
Triglycerides (g/l)
E
Cholesterol (g/l)

Figure 2

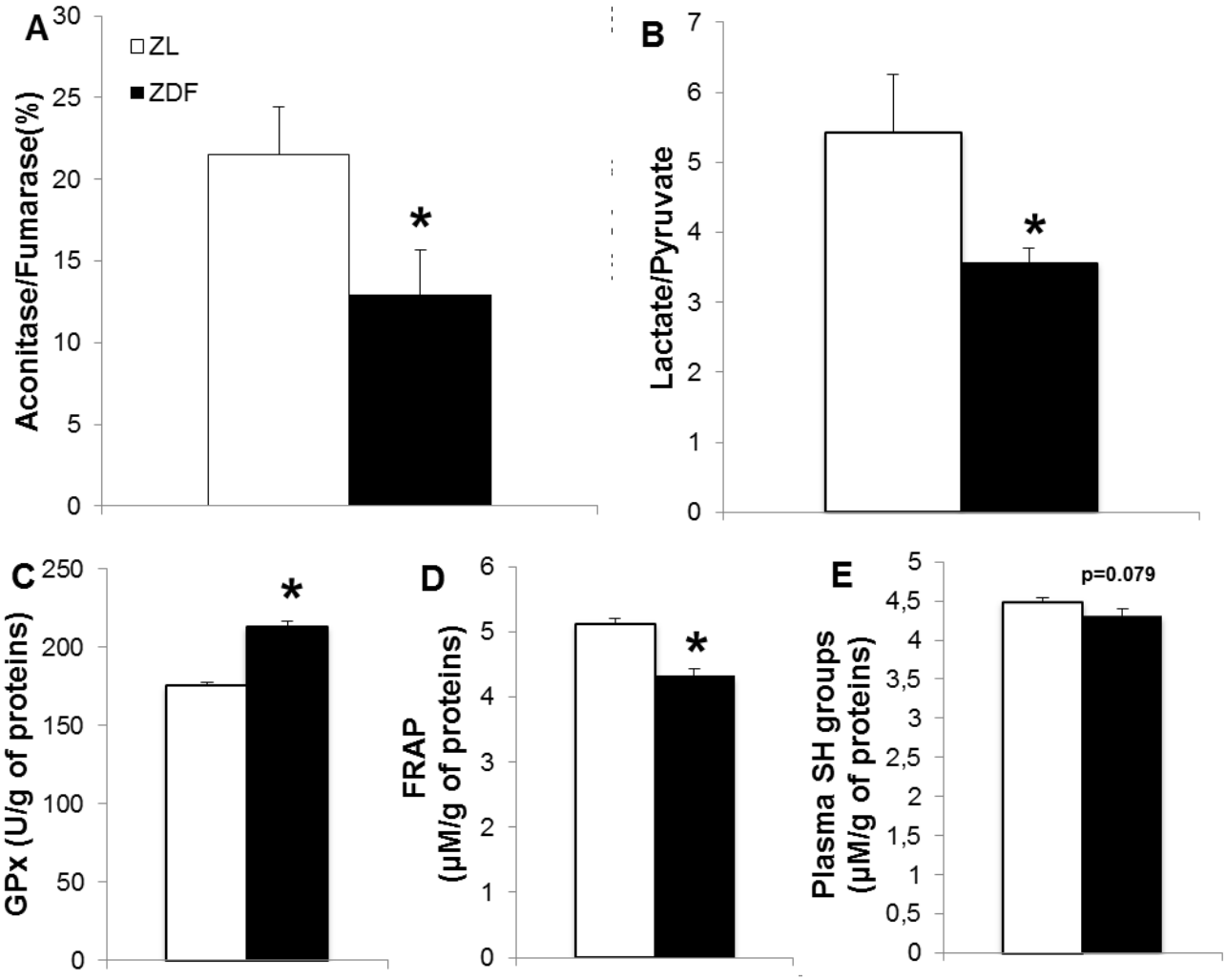
A
ZL
ZDF
Aconitase/Fumarase(%)
30
25
20
15
10
5
0
*
B
Lactate/Pyruvate
7
6
5
4
3
2
1
0
*
C
GPx (U/g of proteins)
250
200
150
100
50
0
*
D
FRAP (µM/g of proteins)
6
5
4
3
2
1
0
*
E
Plasma SH groups (µM/g of proteins)
5
4,5
4
3,5
3
2,5
2
1,5
1
0,5
0
p=0.079

Figure 3

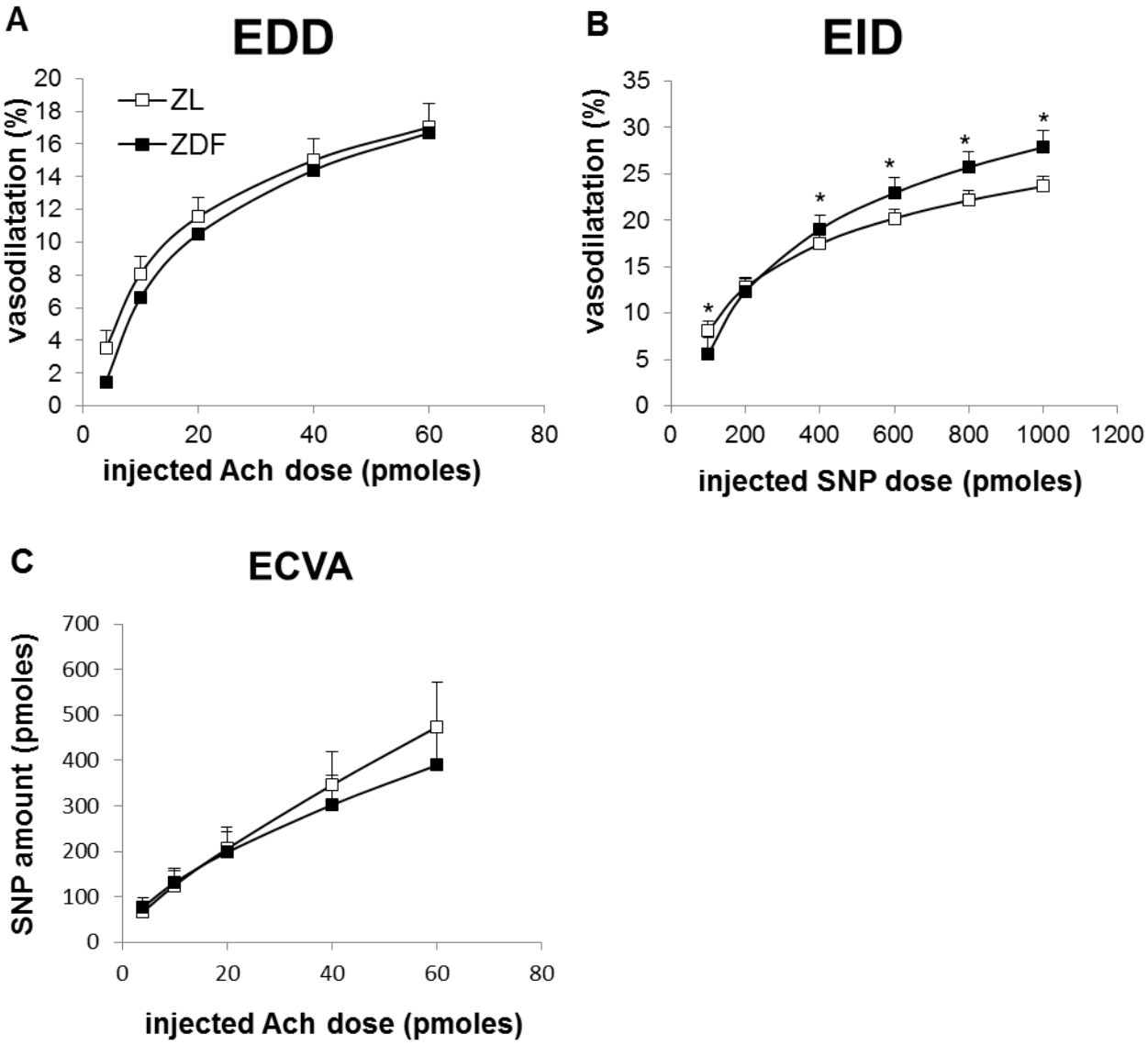
A
EDD
ZL
ZDF
vasodilatation (%)
injected Ach dose (pmoles)
B
EID
vasodilatation (%)
injected SNP dose (pmoles)
C
ECVA
SNP amount (pmoles)
injected Ach dose (pmoles)

Figure 4

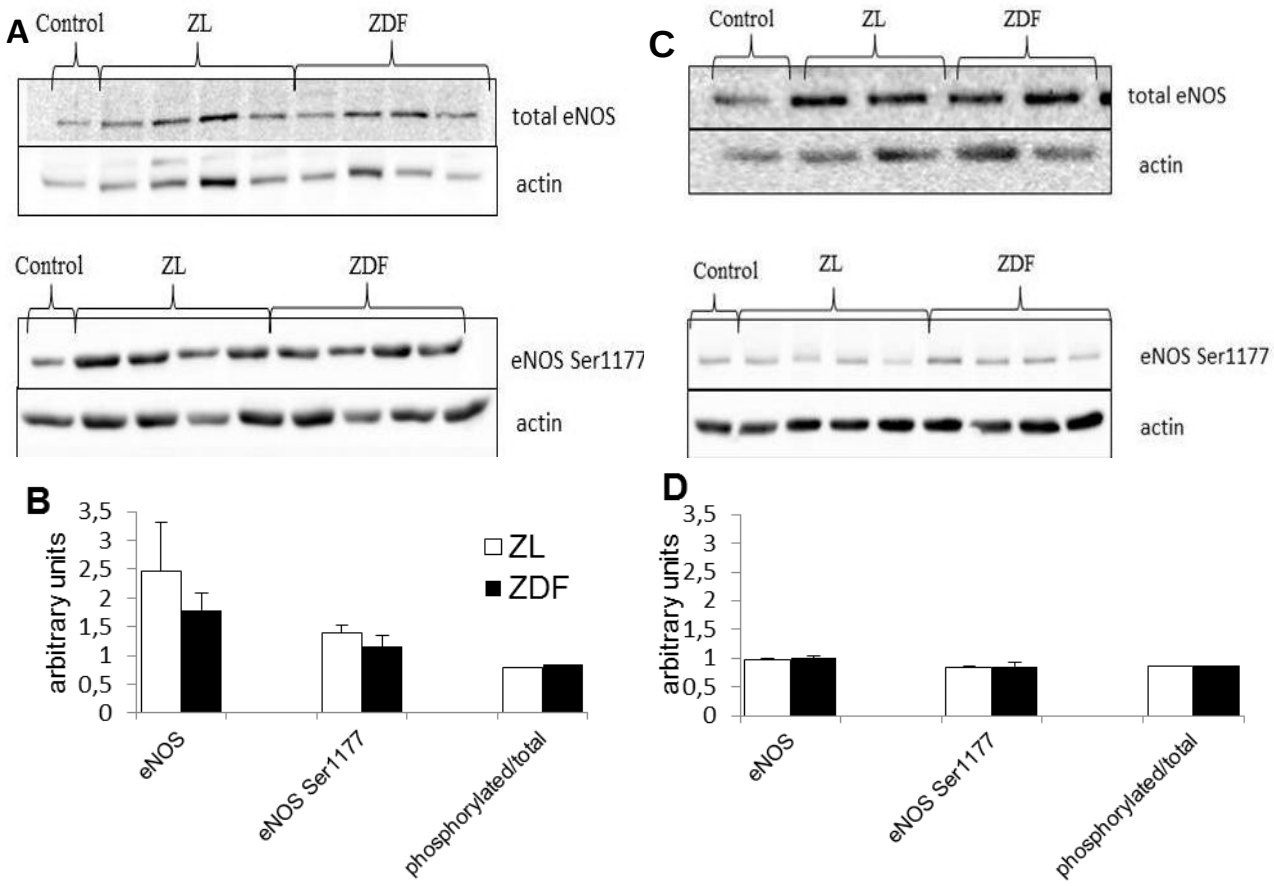
A
Control
ZL
ZDF
total eNOS
actin
Control
ZL
ZDF
eNOS Ser1177
actin
C
Control
ZL
ZDF
total eNOS
actin
Control
ZL
ZDF
eNOS Ser1177
actin
B
arbitrary units
3,5
3
2,5
2
1,5
1
0,5
0
ZL
ZDF
eNOS
eNOS Ser1177
phosphorylated/total
D
arbitrary units
3,5
3
2,5
2
1,5
1
0,5
0
eNOS
eNOS Ser1177
phosphorylated/total

Figure 5

PART III. GENERAL DISCUSSION

In conclusion, our work demonstrated that there is an age-related pattern of changes occurring from youth to middle age which is dramatically changed when a high-fat diet is applied during this period. The main findings of our work were:

- in normal aging, the EDD of the intact coronary microvasculature is progressively decreased, while the contribution of ECs and VSMCs in this phenomenon varies according to the age. Between youth and young adulthood, the decline in EDD is due mostly to a drastic decrease of the VSMCs function while the ECs tried to compensate by increasing their dilatation activity. Between young adulthood and middle age, the relaxation of VSMCs stabilizes, but ECs dilatation activity significantly decreases leading to further decline in EDD;

- middle-aged hearts are characterized from an impaired recovery of their function during reperfusion after ischemia related to reduced coronary perfusion and insufficient oxygen supply. The reduced coronary perfusion is related to an increased mitochondrial oxidative stress and maintenance of the CII activity;

- high-fat diet and T2D induce as soon as the beginning of the diet a state of oxidative stress in all compartments of the organism and an *ex vivo* cardiac mechanical dysfunction

- under high-fat conditions an adaptation occurs at the level of the mitochondria in an effort to produce more energy;

- in high-fat diet-induced obesity and T2D, an adaptation of the coronary microvasculature is taking place in order to meet the higher metabolic demands of the heart due to obesity and to react adequately in states of increased oxygen demand such as exercise or ischemic incidents.

As already described, aging manifests detrimental alterations in cardiovascular structure and function making age *per se* the major cardiovascular risk factor even in the absence of any underlying pathology. These alterations eventually lead to cardiovascular dysfunction and disease and are apparent even at middle age. However, nowadays, it is difficult to distinguish between normal aging and co-existing pathologies since the prevalence of obesity and obesity-related pathologies especially in industrialized societies is increasing exponentially [273]. This increase in body mass due to lifestyle habits such as obesogenic diets and sedentariness, appear to induce further alterations in the metabolism of the organism but also in the function of various organs with final result the development of the insulin resistance, MetS and T2D. Even though obesity has been recognized as a major risk factor for the annual increase in T2D prevalence [273, 274], it is estimated that the number of patients with type 2 diabetes will more than double by 2030, even if the prevalence of obesity remains constant [77] as a result of increased longevity. This kind of pathologies that accompany aging in modern world, affect even more negatively the cardiovascular system resulting to the early development of CVDs.

The aims of this investigation was thus to understand and characterize the progression of changes that happen from youth to middle-age adulthood in the body composition and its metabolic characteristics and how these changes could be related to the increased susceptibility of middle aged hearts to ischemic incidents. Furthermore, we were interested in examining the effects of a diet closed to the Western way of life (high-fat content diet) during this aging period in order to better understand the etiology and consequences of the obesity-related cardiovascular changes at middle-age.

Our work verified that a progressive gain of body weight accompanied aging under normal diet conditions from youth to middle age, which was related to an increase in the body adiposity of the animals established between youth and young adulthood. This gain of body weight was not observed when a high-fat diet containing 54% of fat was followed by the animals. However, the adipose tissue content of the high-fat fed rats was almost doubled as soon as 6 months of age and remained constant until middle age. Thus, aging both under normal and even more under HF conditions is characterized by the presence of increased adipose tissue.

The results of our study demonstrated a reduction in protein thiol groups, as a marker of oxidative stress, in the plasma of middle-aged animals. These data come in good agreement with studies suggesting that systemic oxidative stress correlates with BMI and waist circumference [275]. In our study, this increase in the oxidative stress was also related to a progressive decrease in the systemic antioxidant defenses. It is interesting though to note that our study demonstrated that the increase in the adipose tissue content preceded the development of systemic oxidative stress, which was apparent only at middle age. This state of increased oxidative stress may have resulted from the activation of NADPH oxidase occurring at this age when the adipose tissue mass augments [276]. However, no evident oxidative stress was found at the cardiac cytosolic level as already described in advanced aging [277, 278] or at the mitochondrial level, despite the increased ETC-derived H_2O_2 release when NAD- and FADH-linked respiration substrates were used.

As previously described, the high-fat diet induced a dramatic increase in the adiposity of the animals at the very beginning of the diet. This was directly reflected in the immediate increase in the systemic oxidative stress of the HF-fed rats enhancing the hypothesis that systemic oxidative stress is due to ROS production from accumulated fat [276]. This was also true for the ZDF animals of this work that were characterized from an increased adiposity and systemic oxidative stress at the early phase of T2D. In both models of diet-induced obesity, an increased oxidative stress was evident at the cytosolic and mitochondrial levels of the hearts of the animals. Thus, obesity seems to accelerate the processes of ROS production in the heart that would normally appear at advanced age under normal conditions.

The presence of the increased adipose tissue under all these conditions and the consequent systemic oxidative stress have been related to the dysregulation of adipokines production [276] involved in the pathogenesis of obesity-associated MetS, thrombosis [279] and atherosclerosis [280]. Increased production of TNF-α from accumulated fat is known to contribute to insulin resistance [281], while a decrease in plasma adiponectin has been inversely correlated with adiposity and insulin sensitivity [282]. Indeed, the glucose metabolism appeared to parallel the alterations of systemic oxidative stress occurring from young to middle age adulthood in our study that could reflect an alteration in the adipokines regulation. Under normal conditions, lower levels of fasting glycemia were observed in the middle-aged rats of our study. However, their lower rate of glucose elimination from the bloodstream indicated a degree of glucose intolerance, as found also in normal weight men with aging [283, 284]. Interestingly, the diminished glucose tolerance and increased

circulating oxidative stress observed at middle age under normal conditions, appeared earlier under the high-fat diet conditions as happened also for the oxidative stress status. Unfortunately, the lack of plasma insulin values does not allow us to have a more global estimation concerning the state of insulin sensitivity of our animals. Similar were the results of the oxidative stress and glucose metabolism in the ZDF rats. However, the presence of diabetes induced a severe insulin resistance in the animals despite the functional β cells in the Langerhans islets.

The enhanced oxidative stress occurring early in both models of diet-induced obesity (DIO) (HF-fed and ZDF rats) of our work, were related to a decreased *ex vivo* cardiac mechanical function, a parameter that stayed unaffected during normal aging. However, the reason underlying this result appeared to be different in the HF-fed and ZDF rats. Under the HF diet, the decreased RPP was due to a diminished LVDP while under the diabetic conditions it was due to a diminished heart rate despite the elevation of their LVDP. Thus, it seems that these two models of DIO affected differently the cellular types implicated in the mechanical activity of the heart. In the case of ZDF rats, a leptin-receptor deficient rat model, it appears that the cells first affected were those responsible for the cardiac contraction involved in the generation and transfer of the electric influx. These data could complement the results from a study in *ob/ob* leptin deficient mice suggesting that leptin deficiency contributes to cardiac contractile dysfunction, impaired intracellular Ca^{2+} homeostasis and ultrastructural derangement in ventricular myocytes [285]. Thus, a disturbance in the cells involved in the generation and transfer of the electric flux together with the impaired intracellular Ca^{2+} hemostasis of the cardiomyocytes could result to contractile dysfunction. Similar contractile dysfunction has been described in insulin-resistant rats fed a high-fat diet [286]. However, the fact that the HF-fed rats in our study demonstrated a hyperglycemia with glucose tolerance impairment only at 6 months of age while the ZDF were hyperglycemic and insulin-resistant could also explain the difference concerning the reason of the RPP decrease between HF and ZDF rats. Hyperglycemia is known to induce cell damage and apoptosis in neural [287] and cardiac cells [288] and it has been shown that in streptozotocin-induced diabetes there are alterations of the atrioventricular node properties and electric perturbations in the heart [289, 290]. Another interesting point is the fact that the HF-induced obesity in our study resulted from the content of the diet while the obesity of the ZDF rats from increased caloric intake. This could result to altered substrate utilization from the heart affecting differently the cardiac cellular types responsible for the cardiac activity. Thus, early development of DIO-related

oxidative stress was associated with a decreased *ex vivo* cardiac function due to different mechanisms depending on the severity of obesity and related conditions.

Despite all these negative changes, the mitochondrial oxidative phosphorylation was maintained under HF conditions. Thus, the mitochondria appeared to enhance their oxidative phosphorylation in an effort to supply the heart with adequate energy but as evidenced by the decrease *ex vivo* cardiac mechanical activity, this was not sufficient enough. However, all these observations describe situations occurring *ex vivo* (for the cardiac function) or *in vitro* (for the mitochondria) and may not reflect exactly what happens *in vivo* in the organism. It is probable that the increased cytosolic and mitochondrial oxidative stress developed at the beginning of the HF diet affected the transfer of the energy from mitochondria to intracellular sites of energy use or its utilization since no amelioration of the heart function was observed despite the normal respiration states. Interestingly, under a normal diet the changes seem to happen in a different way. The maintained *ex vivo* cardiac function seemed to be related to functional processes of energy synthesis, transfer and utilization in the myocardium despite the decrease in the mitochondrial respiration. This was also confirmed by the delayed ischemic contracture that the middle-aged hearts demonstrated which suggested a better maintenance of their ATP concentration. Aside from these results, myocardial oxygen consumption was found unaltered at middle age as shown in our first study. These maintained functions may be due to the absence of cytosolic or mitochondrial oxidative stress in middle-aged hearts.

However, aging could have reduced the cardiac mechanical work if the hearts had been maximally stimulated (working mode with high preload and perfusate calcium concentration) as also evidenced by the observation that the decreased mitochondrial function was associated with a progressive decline in EDD as the animals got older. Indeed, a main finding of our second study was the progressive decrease of the EDD of the coronary microvasculature with age, as already observed in other vascular beds in animals and humans [291, 292]. Since the endothelial and smooth muscle cells contain phosphocreatine and creatine kinases, the plasma oxidative stress observed at middle age in our study could depress the energy transfer into the vascular cells. Our study allowed also the description of the contribution of each vascular cellular type in the coronary vasodilatation from youth to middle age. The function of VSMCs was high in young hearts and drastically decreased as soon as the young adulthood to values, which were very close to those observed at the middle age. Energy is necessary for the relaxation of muscular cells and the low oxidative phosphorylation detected in the isolated

mitochondria derived from young adult and middle age hearts may explain the observed decline of EID with age. The EID decrease contributed to the progressive age-related loss of EDD. Interestingly, the endothelial cell vasodilatation activity was strongly increased from youth to young adulthood, which could be related to an increase in muscarinic receptor density, an increase in acetylcholine-induced calcium influx, since calcium is known to stimulate eNOS activity [293] or to a production of vasoactive agents other than NO such as the EDHF. However, from young to middle age adulthood this parameter was drastically decreased paralleling the increase in the plasma oxidative stress.

It appears that the progressive decline of EDD at middle age and the additional development of circulating oxidative stress limit the heart from the possibility to react adequately to ischemic incidents and/or properly recover from them. This was evident from the results of our first study. Indeed, in this work, we verified that the well-known increase in ischemia/reperfusion abnormalities occurring with advanced aging [294, 295] also arises in middle-aged animals. In this study, the impaired recovery of middle aged hearts during reperfusion was related to an impaired recovery of the coronary flow and insufficient oxygen supply during reperfusion despite the fact that no modification of the coronary flow was observed between the young and middle-age animals under pre-ischemic conditions. Tomanek *et al.* [296] have demonstrated that aging is characterized by a remodeling of the coronary vessels that includes a reduction in the capillary numerical density but a maintenance of their volume density by compensatory increase in capillary diameter. These observations could explain the fact that the gain of the heart weight was not accompanied by changes in the coronary flow in our study. Thus, a parallel adaptation of the coronary bed with the heart weight gain in normal aging is suggested. However, the coronary vasculature was apparently not able to respond adequately to the ischemic incident which could be explained by the impaired reactivity of the coronary microvasculature found at middle age.

A surprising and interesting finding of our study was that the DIO not only did not induce or worsen the age-related decline pattern of the coronary microvasculature reactivity but it appeared to ameliorate it. Indeed, an adaptation of the coronary microvascular reactivity was established at the beginning of the HF diet as evidenced by the enhanced EDD of the HF-fed hearts. This adapatation was also observed in the diabetic hearts of the ZDF animals but in a lesser degree, since their EDD was maintained and not enhanced, and due to different mechanisms. The enhanced EDD under HF conditions seemed to occur at the level of the endothelial cells for both young and middle aged adult animals while the maintained EDD of

ZDF animals was due to an enhanced VSMCs function. This could be related to an enhanced sensitivity of sGC to NO as a compensatory mechanism of NO diminished bioavailability [297, 298]. However, this parameter was not measured in our study. We cannot exclude the possibility that at an even earlier phase of T2D, EDD could have been found enhanced, as happened at the beginning of the high-fat diet and that the preserved EDD reflects a progressive reduction of this parameter as the disease advances. A progressive decrease in the EDD has already been demonstrated in isolated coronary vessels of ZDF rats [262]. Moreover, the diabetic ZDF rats demonstrated a severe glucose intolerance and insulin resistance that could prevent a better adaptation of the coronary system. These observations together with the data for the decreased *ex vivo* cardiac function of the DIO hearts suggest that in these hearts the need for oxygen and metabolites especially during periods of increased energy demand (e.g. exercise) is extremely important and could be mediated by an adaptation of their coronary microvasculature. Thus, the HF-induced increase in coronary reserve favors the upholding of tissue perfusion and welfare of obese individuals.

In this investigation we were also particularly interested in the vasoactive agents contributing to the phenomenon of the enhanced EDD in the HF-fed rats established at 6 months of age. According to the pharmacology experiments of our fourth study, this type of HF diet induced alterations at the level of NOS and COX pathway, which contributed together to the enhanced Ach response of the HF coronary microvessels. More specifically, the NOS pathway seemed to be enhanced in the HF-fed perfused hearts but it was not the only responsible for the increase in the EDD. Indeed, the results revealed that there is an altered regulation of the COX-derived vasoactive agents with the balance leaning more to the vasodilator than the vasoconstrictor agent production. This was also evidenced by the increase in the AA (C20:4n-6) of the HF rat hearts which could lead eventually to an increase in the COX-vasoactive agents and the PGI2 [299]. The investigation of the relative contribution of vasoactive agents at middle age after a HF diet would be of great interest to better understand this adaptation of the coronary system.

In conclusion, our work demonstrated that major changes concerning the body adiposity, mitochondrial energy metabolism and coronary microvascular reactivity occurred from youth to young adulthood. Thereafter, glucose intolerance together with increased circulating oxidative stress were developed contributing to further decline of the coronary reactivity despite the maintained cardiac function. These alterations contributed eventually to the middle

age-related susceptibility of the heart to ischemic injury. An intervention close to Western dietary habits, such as the HF diet chosen in our work, triggered a number of important alterations with particular interest the establishment of increased adiposity at the early beginning of the diet. Despite the negative effects on the oxidative stress status and *ex vivo* cardiac function this diet induced also a number of adaptations regarding the mitochondrial oxidative phosphorylation and the coronary microvascular reactivity. Whether the detrimental effects of a high-fat diet would predominate following a longer duration of high fat feeding is unknown.

Furthermore, the nutritional composition of this diet must be considered in light of our findings. The model of HF diet-induced obesity in our study is likely the result of the content of the diet and not of the increased caloric intake as happens with the Zucker rats, which are models of overfeeding-induced T2D [300]. The fat content of our diets was 37% SFAs, 46% MUFAs, 15% n-6 PUFAs and 1% n-3 PUFAs for the high fat while for the standard was 24% SFAs, 23% MUFAs, 48% n-6 PUFAs and 4% n-3 PUFAs. The fact that the fat content of the HF diet chosen was not consisted entirely by saturated fat might explain the state of obesity that we found in our rats. It could also explain any differences concerning basic characteristics of the animals from previous studies, such as body weight and glucose levels [297, 301]. The fact that the high-fat fed animals did not gain body weight but had increased adiposity could represent a case of the normal weight obesity (NWO) syndrome. This syndrome has been described recently and is defined as a normal body mass index associated with increased body fat [302, 303]. NWO has been also associated with increased inflammation due to the presence of increased adipose tissue. Even though in our HF-fed hearts we did not evaluate the inflammatory status, their low ratio EPA/AA suggests a predisposition to a balance of eicosanoids favoring platelet aggregation and inflammatory signaling. The NWO has been identified as risk factor for cardiometabolic dysregulation and cardiovascular mortality. Thus, it is extremely important to investigate its origins and consequences especially for the human subjects that have a normal BMI but can be characterized as metabolically obese and have increased risk of CVD [304].

Furthermore, our study revealed that habits that are adopted early in life, in our case in youth, impact multiple cellular processes and provokes metabolic changes that establish new conditions in the organism at their early beginning. These alterations probably affect functions eventually leading to complications apparent at middle age. These observations come in agreement with previous studies suggesting that dietary habits during early life (childhood or

adolescence) may affect the risk of developing obesity or diabetes mellitus later in life. It has been demonstrated that dietary patterns during adolescence increases the risk of type 2 diabetes in middle aged women [265]. Findings from the Bogalusa Heart study indicate that risk factors such as high blood pressure, hyperinsulinemia and dyslipidemia that begin to cluster during childhood due to unhealthy dietary habits can predict adult cardiovascular factors [266]. This clustering of risk factor has been linked to unhealthy dietary habits during childhood [267]. Moreover, it has been shown that postnatal overfeeding in rats can lead to moderate overweight in adult rats and higher susceptibility to cardiac injury [305]. Taken together these data, it appears extremely important, especially for the Westen societies, the type of dietary habits adopted in early life since they can lead to complications in adulthood. An interesting question is whether the modifications induced by this lifestyle habits could be inversed and at which extent this could prevent the health disturbances in later life.

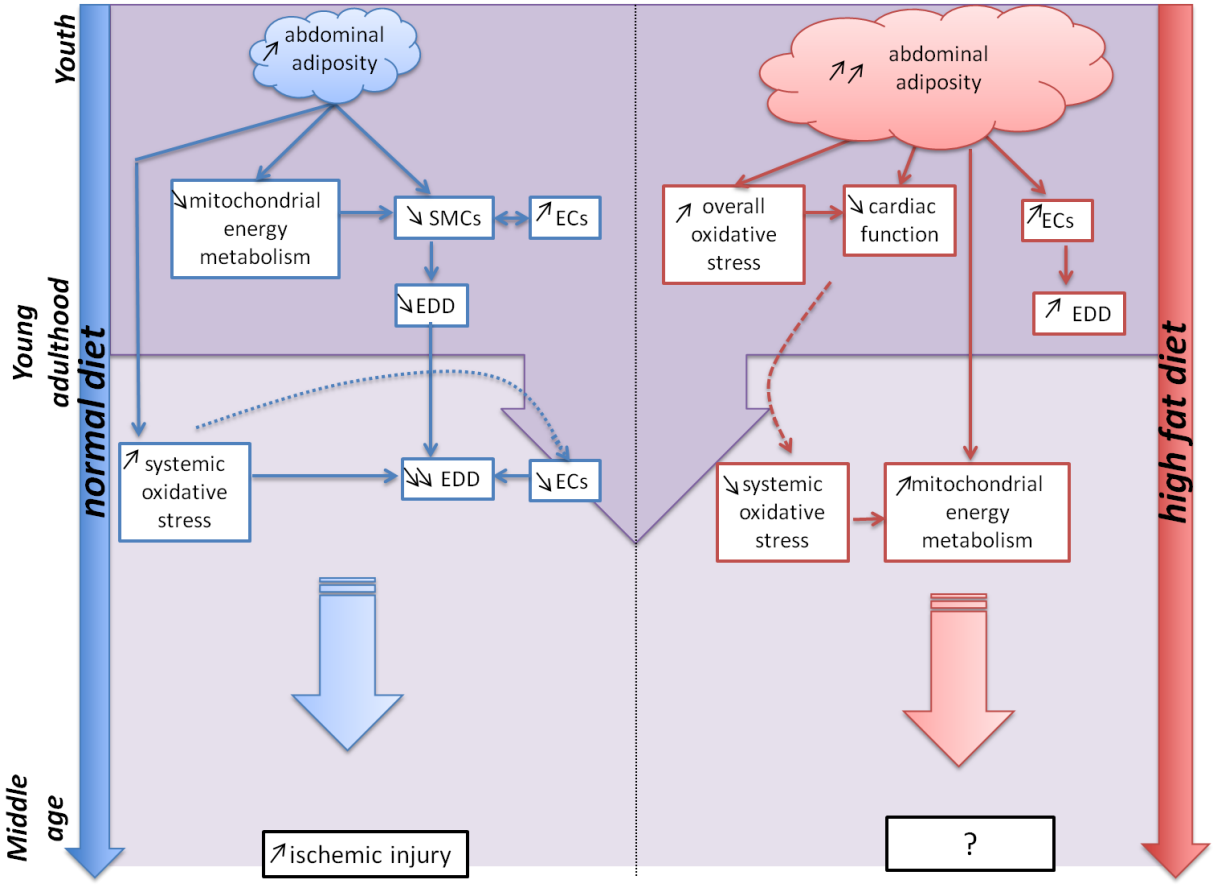

***Figure 26**. Representative diagram of the temporal pattern of changes occurring from youth to middle age in rat under normal or high-fat diet. SMCs: smooth muscle cells; ECs: endothelial cells; EDD: endothelial-dependent dilatation.*

Perspectives

The results of our studies regarding the progressive changes happening from youth to middle age as well as the effects of DIO on these aspects encourage further research.

One of the most interesting and yet surprising result of our work was the enhanced response to Ach of the coronary microvasculature induced by the high-fat diet. As already described this adaptation was established at the beginning of the diet and remained until middle age. Thus, it would be interesting to see how the heart reacts at middle age after this type of diet to ischemic incidents. A protocol of ischemia and reperfusion *ex vivo* would be helpful to understand if this enhanced reactivity of the coronary microvasculature serves as mechanism of protection to ischemic damage. It should be taken under consideration though the fat composition of our diet. In literature, it has been shown that the supplementation of red palm oil to a hypercholestermic diet reduces ischemia-reperfusion injury [306]. Interestingly, it has also been shown that the onset of diabetes in ZDF rats is not associated with increased susceptibility to ischemic injury [307], which could be also associated to the coronary adaptation that we observed in study 5. Finally, we observed that this enhanced response to Ach at the beginning of the high-fat diet is related to a different regulation of the NOS pathway and the balance between COX-derived vasodilatators and vasoconstrictors agents. Thus, to understand if these conditions remain or change in a way that other pathways are implicated in the enhanced reactivity of microvasculature at middle age would provide useful informations concerning the coronary system. Finally, the monitoring of the progression of this adaptation following a longer duration of high fat feeding would be of great interest.

Based on our finding concerning the age, it appears that the gain of adipose weight during youth triggers modifications that affect the cardiovascular function later in life, making the heart susceptible to damage at middle age. It would be interesting to examine if any interventions at this young age to prevent the adipose tissue gain could delay the cardiovascular incidents occurring at middle age. Such an intervention could be a protocol of physical activity applied from youth until middle age. However, the kind of physical exercise chosen would be of great importance since it has been demonstrated that habitual low-intensity exercise does not protect against myocardial ischemia-reperfusion injury [308] but endurance or resistance training does [309, 310]. Regarding our results concerning the reactivity of the vessels at middle age, it should be also noted that a physical training protocol should try to prevent the decline in EDD of the coronary microvasculature. Spontaneous running has been shown to have no effect on large vessels [311] while a training program has

been shown to enhance EDD of both large vessels and coronary resistance arteries [312-314]. Another possible intervention would be a protocol of caloric restriction since it has been shown to reverse vascular endothelial dysfunction in old mice [315]. Thus, it would be interesting to monitor the changes that happen from youth to middle age under these conditions and understand how the cardiovascular function is affected at middle age. An intervention such as exercise that aims at reducing the body adiposity would be also of great interest to see if we can inverse the changes that occur with high-fat diets.

Finally, our work revealed that both aging and DIO are closely related to the development of oxidative stress either at the systemic or the cellular and mitochondrial level. Thus, it would be interesting to test protocols regarding antioxidant treatments in an effort to eliminate the increased oxidative stress in aging and DIO.

References

1. Garrow, J.S., *Obesity and related diseases*. [Rev. ed1988, Edinburgh ; London [etc.]: Churchill Livingstone. X, 329 p.
2. Allison, D.B., et al., *Annual deaths attributable to obesity in the United States.* JAMA, 1999. **282**(16): p. 1530-8.
3. Flegal, K.M., et al., *Excess deaths associated with underweight, overweight, and obesity.* JAMA, 2005. **293**(15): p. 1861-7.
4. Fontaine, K.R., et al., *Years of life lost due to obesity.* JAMA, 2003. **289**(2): p. 187-93.
5. Must, A., et al., *The disease burden associated with overweight and obesity.* JAMA, 1999. **282**(16): p. 1523-9.
6. McTigue, K., et al., *Mortality and cardiac and vascular outcomes in extremely obese women.* JAMA, 2006. **296**(1): p. 79-86.
7. Han, T.S., et al., *The influences of height and age on waist circumference as an index of adiposity in adults.* Int J Obes Relat Metab Disord, 1997. **21**(1): p. 83-9.
8. Pouliot, M.C., et al., *Waist circumference and abdominal sagittal diameter: best simple anthropometric indexes of abdominal visceral adipose tissue accumulation and related cardiovascular risk in men and women.* Am J Cardiol, 1994. **73**(7): p. 460-8.
9. Ross, R., et al., *Quantification of adipose tissue by MRI: relationship with anthropometric variables.* J Appl Physiol, 1992. **72**(2): p. 787-95.
10. Han, T.S., et al., *Waist circumference action levels in the identification of cardiovascular risk factors: prevalence study in a random sample.* BMJ, 1995. **311**(7017): p. 1401-5.
11. Lean, M.E., T.S. Han, and P. Deurenberg, *Predicting body composition by densitometry from simple anthropometric measurements.* Am J Clin Nutr, 1996. **63**(1): p. 4-14.
12. Pischon, T., et al., *General and abdominal adiposity and risk of death in Europe.* N Engl J Med, 2008. **359**(20): p. 2105-20.
13. Shea, J.L., et al., *Body fat percentage is associated with cardiometabolic dysregulation in BMI-defined normal weight subjects.* Nutr Metab Cardiovasc Dis.
14. Berghofer, A., et al., *Obesity prevalence from a European perspective: a systematic review.* BMC Public Health, 2008. **8**: p. 200.
15. von Ruesten, A., et al., *Trend in obesity prevalence in European adult cohort populations during follow-up since 1996 and their predictions to 2015.* PLoS One, 2011. **6**(11): p. e27455.
16. Schemmel, R., O. Mickelsen, and Z. Tolgay, *Dietary obesity in rats: influence of diet, weight, age, and sex on body composition.* Am J Physiol, 1969. **216**(2): p. 373-9.
17. Ghibaudi, L., et al., *Fat intake affects adiposity, comorbidity factors, and energy metabolism of sprague-dawley rats.* Obes Res, 2002. **10**(9): p. 956-63.
18. Harrold, J.A., G. Williams, and P.S. Widdowson, *Early leptin response to a palatable diet predicts dietary obesity in rats: key role of melanocortin-4 receptors in the ventromedial hypothalamic nucleus.* J Neurochem, 2000. **74**(3): p. 1224-8.
19. Woods, S.C., et al., *A controlled high-fat diet induces an obese syndrome in rats.* J Nutr, 2003. **133**(4): p. 1081-7.
20. Levin, B.E. and A.A. Dunn-Meynell, *Defense of body weight depends on dietary composition and palatability in rats with diet-induced obesity.* Am J Physiol Regul Integr Comp Physiol, 2002. **282**(1): p. R46-54.
21. Zhang, Y., et al., *Positional cloning of the mouse obese gene and its human homologue.* Nature, 1994. **372**(6505): p. 425-32.
22. Ahima, R.S. and J.S. Flier, *Adipose tissue as an endocrine organ.* Trends Endocrinol Metab, 2000. **11**(8): p. 327-32.
23. Fruhbeck, G., et al., *The adipocyte: a model for integration of endocrine and metabolic signaling in energy metabolism regulation.* Am J Physiol Endocrinol Metab, 2001. **280**(6): p. E827-47.
24. Petrovic, N., et al., *Chronic peroxisome proliferator-activated receptor gamma (PPARgamma) activation of epididymally derived white adipocyte cultures reveals a*

population of thermogenically competent, UCP1-containing adipocytes molecularly distinct from classic brown adipocytes. J Biol Chem. **285**(10): p. 7153-64.
25. Ishibashi, J. and P. Seale, *Medicine. Beige can be slimming.* Science. **328**(5982): p. 1113-4.
26. Frayn, K.N., et al., *Integrative physiology of human adipose tissue.* Int J Obes Relat Metab Disord, 2003. **27**(8): p. 875-88.
27. Fain, J.N., et al., *Comparison of the release of adipokines by adipose tissue, adipose tissue matrix, and adipocytes from visceral and subcutaneous abdominal adipose tissues of obese humans.* Endocrinology, 2004. **145**(5): p. 2273-82.
28. Margetic, S., et al., *Leptin: a review of its peripheral actions and interactions.* Int J Obes Relat Metab Disord, 2002. **26**(11): p. 1407-33.
29. Flier, J.S., *Clinical review 94: What's in a name? In search of leptin's physiologic role.* J Clin Endocrinol Metab, 1998. **83**(5): p. 1407-13.
30. Chandran, M., et al., *Adiponectin: more than just another fat cell hormone?* Diabetes Care, 2003. **26**(8): p. 2442-50.
31. Diez, J.J. and P. Iglesias, *The role of the novel adipocyte-derived hormone adiponectin in human disease.* Eur J Endocrinol, 2003. **148**(3): p. 293-300.
32. Ruan, H. and H.F. Lodish, *Insulin resistance in adipose tissue: direct and indirect effects of tumor necrosis factor-alpha.* Cytokine Growth Factor Rev, 2003. **14**(5): p. 447-55.
33. Fernandez-Real, J.M. and W. Ricart, *Insulin resistance and chronic cardiovascular inflammatory syndrome.* Endocr Rev, 2003. **24**(3): p. 278-301.
34. Banerjee, R.R. and M.A. Lazar, *Resistin: molecular history and prognosis.* J Mol Med (Berl), 2003. **81**(4): p. 218-26.
35. Baum, C.L., 2nd and C.J. Ruhm, *Age, socioeconomic status and obesity growth.* J Health Econ, 2009. **28**(3): p. 635-48.
36. Bose, K., *Age trends in adiposity and central body fat distribution among adult white men resident in Peterborough, East Anglia, England.* Coll Antropol, 2002. **26**(1): p. 179-86.
37. Hebebrand, J., et al., *Epidemic obesity: are genetic factors involved via increased rates of assortative mating?* Int J Obes Relat Metab Disord, 2000. **24**(3): p. 345-53.
38. Hill, J.O., E.L. Melanson, and H.T. Wyatt, *Dietary fat intake and regulation of energy balance: implications for obesity.* J Nutr, 2000. **130**(2S Suppl): p. 284S-288S.
39. Martinez-Gonzalez, M.A., et al., *Physical inactivity, sedentary lifestyle and obesity in the European Union.* Int J Obes Relat Metab Disord, 1999. **23**(11): p. 1192-201.
40. Bouchard, C., *The causes of obesity: advances in molecular biology but stagnation on the genetic front.* Diabetologia, 1996. **39**(12): p. 1532-3.
41. Kernie, S.G., D.J. Liebl, and L.F. Parada, *BDNF regulates eating behavior and locomotor activity in mice.* EMBO J, 2000. **19**(6): p. 1290-300.
42. Rios, M., et al., *Conditional deletion of brain-derived neurotrophic factor in the postnatal brain leads to obesity and hyperactivity.* Mol Endocrinol, 2001. **15**(10): p. 1748-57.
43. Clement, K., et al., *Genetic variation in the beta 3-adrenergic receptor and an increased capacity to gain weight in patients with morbid obesity.* N Engl J Med, 1995. **333**(6): p. 352-4.
44. Jackson, R.S., et al., *Obesity and impaired prohormone processing associated with mutations in the human prohormone convertase 1 gene.* Nat Genet, 1997. **16**(3): p. 303-6.
45. Gray, J., et al., *Hyperphagia, severe obesity, impaired cognitive function, and hyperactivity associated with functional loss of one copy of the brain-derived neurotrophic factor (BDNF) gene.* Diabetes, 2006. **55**(12): p. 3366-71.
46. Frederich, R.C., et al., *Leptin levels reflect body lipid content in mice: evidence for diet-induced resistance to leptin action.* Nat Med, 1995. **1**(12): p. 1311-4.
47. Maffei, M., et al., *Leptin levels in human and rodent: measurement of plasma leptin and ob RNA in obese and weight-reduced subjects.* Nat Med, 1995. **1**(11): p. 1155-61.
48. Campfield, L.A., et al., *Recombinant mouse OB protein: evidence for a peripheral signal linking adiposity and central neural networks.* Science, 1995. **269**(5223): p. 546-9.
49. Chua, S.C., Jr., et al., *Phenotypes of mouse diabetes and rat fatty due to mutations in the OB (leptin) receptor.* Science, 1996. **271**(5251): p. 994-6.

50. Heo, M., et al., *A meta-analytic investigation of linkage and association of common leptin receptor (LEPR) polymorphisms with body mass index and waist circumference.* Int J Obes Relat Metab Disord, 2002. **26**(5): p. 640-6.
51. Huszar, D., et al., *Targeted disruption of the melanocortin-4 receptor results in obesity in mice.* Cell, 1997. **88**(1): p. 131-41.
52. Noben-Trauth, K., et al., *A candidate gene for the mouse mutation tubby.* Nature, 1996. **380**(6574): p. 534-8.
53. Fricker, L.D., et al., *Carboxypeptidase E activity is deficient in mice with the fat mutation. Effect on peptide processing.* J Biol Chem, 1996. **271**(48): p. 30619-24.
54. Ahima, R.S., et al., *Role of leptin in the neuroendocrine response to fasting.* Nature, 1996. **382**(6588): p. 250-2.
55. Chen, H., et al., *Evidence that the diabetes gene encodes the leptin receptor: identification of a mutation in the leptin receptor gene in db/db mice.* Cell, 1996. **84**(3): p. 491-5.
56. Phillips, M.S., et al., *Leptin receptor missense mutation in the fatty Zucker rat.* Nat Genet, 1996. **13**(1): p. 18-9.
57. Takaya, K., et al., *Molecular cloning of rat leptin receptor isoform complementary DNAs--identification of a missense mutation in Zucker fatty (fa/fa) rats.* Biochem Biophys Res Commun, 1996. **225**(1): p. 75-83.
58. Yamashita, T., et al., *Leptin receptor of Zucker fatty rat performs reduced signal transduction.* Diabetes, 1997. **46**(6): p. 1077-80.
59. Griffen, S.C., J. Wang, and M.S. German, *A genetic defect in beta-cell gene expression segregates independently from the fa locus in the ZDF rat.* Diabetes, 2001. **50**(1): p. 63-8.
60. Mutch, D.M. and K. Clement, *Unraveling the genetics of human obesity.* PLoS Genet, 2006. **2**(12): p. e188.
61. Vague, J., *Sexual differentiation. A determinant factor of the forms of obesity. 1947.* Obes Res, 1996. **4**(2): p. 201-3.
62. Vague, J., *The degree of masculine differentiation of obesities: a factor determining predisposition to diabetes, atherosclerosis, gout, and uric calculous disease. 1956.* Nutrition, 1999. **15**(1): p. 89-90; discussion 91.
63. Bjorntorp, P., *"Portal" adipose tissue as a generator of risk factors for cardiovascular disease and diabetes.* Arteriosclerosis, 1990. **10**(4): p. 493-6.
64. Gerich, J.E., et al., *Characterization of the glucagon response to hypoglycemia in man.* J Clin Endocrinol Metab, 1974. **38**(1): p. 77-82.
65. Reaven, G.M., *Pathophysiology of insulin resistance in human disease.* Physiol Rev, 1995. **75**(3): p. 473-86.
66. Opie, L.H. and P.G. Walfish, *Plasma free fatty acid concentrations in obesity.* N Engl J Med, 1963. **268**: p. 757-60.
67. Bjorntorp, P., H. Bergman, and E. Varnauskas, *Plasma free fatty acid turnover rate in obesity.* Acta Med Scand, 1969. **185**(4): p. 351-6.
68. Jensen, M.D., et al., *Influence of body fat distribution on free fatty acid metabolism in obesity.* J Clin Invest, 1989. **83**(4): p. 1168-73.
69. Pihl, E., et al., *Atherogenic inflammatory and oxidative stress markers in relation to overweight values in male former athletes.* Int J Obes (Lond), 2006. **30**(1): p. 141-6.
70. Chrysohoou, C., et al., *The implication of obesity on total antioxidant capacity in apparently healthy men and women: the ATTICA study.* Nutr Metab Cardiovasc Dis, 2007. **17**(8): p. 590-7.
71. Hartwich, J., et al., *Effect of supplementation with vitamin E and C on plasma hsCRP level and cobalt-albumin binding score as markers of plasma oxidative stress in obesity.* Genes Nutr, 2007. **2**(1): p. 151-4.
72. Fernandez-Sanchez, A., et al., *Inflammation, oxidative stress, and obesity.* Int J Mol Sci, 2011. **12**(5): p. 3117-32.
73. Ozata, M., et al., *Increased oxidative stress and hypozincemia in male obesity.* Clin Biochem, 2002. **35**(8): p. 627-31.
74. Fonseca-Alaniz, M.H., et al., *Adipose tissue as an endocrine organ: from theory to practice.* J Pediatr (Rio J), 2007. **83**(5 Suppl): p. S192-203.

75. Morrow, J.D., *Is oxidant stress a connection between obesity and atherosclerosis?* Arterioscler Thromb Vasc Biol, 2003. **23**(3): p. 368-70.
76. Shoelson, S.E., L. Herrero, and A. Naaz, *Obesity, inflammation, and insulin resistance.* Gastroenterology, 2007. **132**(6): p. 2169-80.
77. Wild, S., et al., *Global prevalence of diabetes: estimates for the year 2000 and projections for 2030.* Diabetes Care, 2004. **27**(5): p. 1047-53.
78. Kahn, S.E., R.L. Hull, and K.M. Utzschneider, *Mechanisms linking obesity to insulin resistance and type 2 diabetes.* Nature, 2006. **444**(7121): p. 840-6.
79. Reaven, G.M., *Banting lecture 1988. Role of insulin resistance in human disease.* Diabetes, 1988. **37**(12): p. 1595-607.
80. Despres, J.P., et al., *Abdominal obesity and the metabolic syndrome: contribution to global cardiometabolic risk.* Arterioscler Thromb Vasc Biol, 2008. **28**(6): p. 1039-49.
81. Park, Y.W., et al., *The metabolic syndrome: prevalence and associated risk factor findings in the US population from the Third National Health and Nutrition Examination Survey, 1988-1994.* Arch Intern Med, 2003. **163**(4): p. 427-36.
82. Katzmarzyk, P.T., et al., *Metabolic syndrome, obesity, and mortality: impact of cardiorespiratory fitness.* Diabetes Care, 2005. **28**(2): p. 391-7.
83. Romero-Corral, A., et al., *Relationships between leptin and C-reactive protein with cardiovascular disease in the adult general population.* Nat Clin Pract Cardiovasc Med, 2008. **5**(7): p. 418-25.
84. Lavie, C.J., R.V. Milani, and H.O. Ventura, *Untangling the heavy cardiovascular burden of obesity.* Nat Clin Pract Cardiovasc Med, 2008. **5**(7): p. 428-9.
85. Alpert, M.A., *Obesity cardiomyopathy: pathophysiology and evolution of the clinical syndrome.* Am J Med Sci, 2001. **321**(4): p. 225-36.
86. Messerli, F.H., et al., *Borderline hypertension and obesity: two prehypertensive states with elevated cardiac output.* Circulation, 1982. **66**(1): p. 55-60.
87. Messerli, F.H., et al., *Overweight and sudden death. Increased ventricular ectopy in cardiopathy of obesity.* Arch Intern Med, 1987. **147**(10): p. 1725-8.
88. Sjostrom, B. and R. Ettlinger, *[Suicide...serious behavior disorder independent of what may be the cause]*. Vardfacket, 1977. **1**(16): p. 22-3.
89. Messerli, F.H., *Cardiopathy of obesity--a not-so-Victorian disease.* N Engl J Med, 1986. **314**(6): p. 378-80.
90. Lavie, C.J., et al., *Left atrial abnormalities indicating diastolic ventricular dysfunction in cardiopathy of obesity.* Chest, 1987. **92**(6): p. 1042-6.
91. Chakko, S., et al., *Abnormal left ventricular diastolic filling in eccentric left ventricular hypertrophy of obesity.* Am J Cardiol, 1991. **68**(1): p. 95-8.
92. Garavaglia, G.E., et al., *Myocardial contractility and left ventricular function in obese patients with essential hypertension.* Am J Cardiol, 1988. **62**(9): p. 594-7.
93. Alpert, M.A., et al., *Cardiac morphology and left ventricular function in normotensive morbidly obese patients with and without congestive heart failure, and effect of weight loss.* Am J Cardiol, 1997. **80**(6): p. 736-40.
94. Grundy, S.M., et al., *Clinical management of metabolic syndrome: report of the American Heart Association/National Heart, Lung, and Blood Institute/American Diabetes Association conference on scientific issues related to management.* Circulation, 2004. **109**(4): p. 551-6.
95. Stary, H.C., *Evolution and progression of atherosclerotic lesions in coronary arteries of children and young adults.* Arteriosclerosis, 1989. **9**(1 Suppl): p. I19-32.
96. Ross, R., *Atherosclerosis--an inflammatory disease.* N Engl J Med, 1999. **340**(2): p. 115-26.
97. Mano, T., et al., *Endothelial dysfunction in the early stage of atherosclerosis precedes appearance of intimal lesions assessable with intravascular ultrasound.* Am Heart J, 1996. **131**(2): p. 231-8.
98. Quyyumi, A.A., *Endothelial function in health and disease: new insights into the genesis of cardiovascular disease.* Am J Med, 1998. **105**(1A): p. 32S-39S.
99. Williams, S.B., et al., *Impaired nitric oxide-mediated vasodilation in patients with non-insulin-dependent diabetes mellitus.* J Am Coll Cardiol, 1996. **27**(3): p. 567-74.

100. Lim, S.C., et al., *Soluble intercellular adhesion molecule, vascular cell adhesion molecule, and impaired microvascular reactivity are early markers of vasculopathy in type 2 diabetic individuals without microalbuminuria.* Diabetes Care, 1999. **22**(11): p. 1865-70.
101. King, G.L. and H. Wakasaki, *Theoretical mechanisms by which hyperglycemia and insulin resistance could cause cardiovascular diseases in diabetes.* Diabetes Care, 1999. **22 Suppl 3**: p. C31-7.
102. Pashkow, F.J., D.G. Watumull, and C.L. Campbell, *Astaxanthin: a novel potential treatment for oxidative stress and inflammation in cardiovascular disease.* Am J Cardiol, 2008. **101**(10A): p. 58D-68D.
103. Lavie, C.J., R.V. Milani, and H.O. Ventura, *Obesity and cardiovascular disease: risk factor, paradox, and impact of weight loss.* J Am Coll Cardiol, 2009. **53**(21): p. 1925-32.
104. Lavie, C.J., et al., *Body composition and prognosis in chronic systolic heart failure: the obesity paradox.* Am J Cardiol, 2003. **91**(7): p. 891-4.
105. Romero-Corral, A., et al., *Association of bodyweight with total mortality and with cardiovascular events in coronary artery disease: a systematic review of cohort studies.* Lancet, 2006. **368**(9536): p. 666-78.
106. McAuley, P., et al., *Body mass, fitness and survival in veteran patients: another obesity paradox?* Am J Med, 2007. **120**(6): p. 518-24.
107. Horwich, T.B., et al., *The relationship between obesity and mortality in patients with heart failure.* J Am Coll Cardiol, 2001. **38**(3): p. 789-95.
108. Halliwell, B., *Establishing the significance and optimal intake of dietary antioxidants: the biomarker concept.* Nutr Rev, 1999. **57**(4): p. 104-13.
109. Finkel, T. and N.J. Holbrook, *Oxidants, oxidative stress and the biology of ageing.* Nature, 2000. **408**(6809): p. 239-47.
110. Miller, D.M., G.R. Buettner, and S.D. Aust, *Transition metals as catalysts of "autoxidation" reactions.* Free Radic Biol Med, 1990. **8**(1): p. 95-108.
111. Cadenas, E. and H. Sies, *The lag phase.* Free Radic Res, 1998. **28**(6): p. 601-9.
112. Valko, M., et al., *Free radicals and antioxidants in normal physiological functions and human disease.* Int J Biochem Cell Biol, 2007. **39**(1): p. 44-84.
113. Tarpey, M.M. and I. Fridovich, *Methods of detection of vascular reactive species: nitric oxide, superoxide, hydrogen peroxide, and peroxynitrite.* Circ Res, 2001. **89**(3): p. 224-36.
114. Pastor, N., et al., *A detailed interpretation of OH radical footprints in a TBP-DNA complex reveals the role of dynamics in the mechanism of sequence-specific binding.* J Mol Biol, 2000. **304**(1): p. 55-68.
115. Valko, M., H. Morris, and M.T. Cronin, *Metals, toxicity and oxidative stress.* Curr Med Chem, 2005. **12**(10): p. 1161-208.
116. Liochev, S.I. and I. Fridovich, *The Haber-Weiss cycle -- 70 years later: an alternative view.* Redox Rep, 2002. **7**(1): p. 55-7; author reply 59-60.
117. De Grey, A.D., *HO2*: the forgotten radical.* DNA Cell Biol, 2002. **21**(4): p. 251-7.
118. Harrison, J.E. and J. Schultz, *Studies on the chlorinating activity of myeloperoxidase.* J Biol Chem, 1976. **251**(5): p. 1371-4.
119. Ghafourifar, P. and E. Cadenas, *Mitochondrial nitric oxide synthase.* Trends Pharmacol Sci, 2005. **26**(4): p. 190-5.
120. Bergendi, L., et al., *Chemistry, physiology and pathology of free radicals.* Life Sci, 1999. **65**(18-19): p. 1865-74.
121. Archer, S., *Measurement of nitric oxide in biological models.* FASEB J, 1993. **7**(2): p. 349-60.
122. Beckman, J.S., et al., *Apparent hydroxyl radical production by peroxynitrite: implications for endothelial injury from nitric oxide and superoxide.* Proc Natl Acad Sci U S A, 1990. **87**(4): p. 1620-4.
123. Milstien, S. and Z. Katusic, *Oxidation of tetrahydrobiopterin by peroxynitrite: implications for vascular endothelial function.* Biochem Biophys Res Commun, 1999. **263**(3): p. 681-4.
124. Fukai, T. and M. Ushio-Fukai, *Superoxide dismutases: role in redox signaling, vascular function, and diseases.* Antioxid Redox Signal, 2011. **15**(6): p. 1583-606.
125. Weisiger, R.A. and I. Fridovich, *Superoxide dismutase. Organelle specificity.* J Biol Chem, 1973. **248**(10): p. 3582-92.

126. Hsu, J.L., et al., *Catalytic properties of human manganese superoxide dismutase.* J Biol Chem, 1996. **271**(30): p. 17687-91.
127. Stralin, P., et al., *The interstitium of the human arterial wall contains very large amounts of extracellular superoxide dismutase.* Arterioscler Thromb Vasc Biol, 1995. **15**(11): p. 2032-6.
128. Mates, J.M., C. Perez-Gomez, and I. Nunez de Castro, *Antioxidant enzymes and human diseases.* Clin Biochem, 1999. **32**(8): p. 595-603.
129. Masella, R., et al., *Novel mechanisms of natural antioxidant compounds in biological systems: involvement of glutathione and glutathione-related enzymes.* J Nutr Biochem, 2005. **16**(10): p. 577-86.
130. Radak, Z., et al., *Effect of aging and late onset dietary restriction on antioxidant enzymes and proteasome activities, and protein carbonylation of rat skeletal muscle and tendon.* Exp Gerontol, 2002. **37**(12): p. 1423-30.
131. Wang, M., et al., *Lipid peroxidation-induced putative malondialdehyde-DNA adducts in human breast tissues.* Cancer Epidemiol Biomarkers Prev, 1996. **5**(9): p. 705-10.
132. Stadtman, E.R., *Role of oxidant species in aging.* Curr Med Chem, 2004. **11**(9): p. 1105-12.
133. Dalle-Donne, I., et al., *Proteins as biomarkers of oxidative/nitrosative stress in diseases: the contribution of redox proteomics.* Mass Spectrom Rev, 2005. **24**(1): p. 55-99.
134. Chance, B., H. Sies, and A. Boveris, *Hydroperoxide metabolism in mammalian organs.* Physiol Rev, 1979. **59**(3): p. 527-605.
135. Brandes, R.P., N. Weissmann, and K. Schroder, *NADPH oxidases in cardiovascular disease.* Free Radic Biol Med, 2010. **49**(5): p. 687-706.
136. Alderton, W.K., C.E. Cooper, and R.G. Knowles, *Nitric oxide synthases: structure, function and inhibition.* Biochem J, 2001. **357**(Pt 3): p. 593-615.
137. Bevers, L.M., et al., *Tetrahydrobiopterin, but not L-arginine, decreases NO synthase uncoupling in cells expressing high levels of endothelial NO synthase.* Hypertension, 2006. **47**(1): p. 87-94.
138. Vasquez-Vivar, J., et al., *The ratio between tetrahydrobiopterin and oxidized tetrahydrobiopterin analogues controls superoxide release from endothelial nitric oxide synthase: an EPR spin trapping study.* Biochem J, 2002. **362**(Pt 3): p. 733-9.
139. Heinecke, J.W., et al., *Tyrosyl radical generated by myeloperoxidase catalyzes the oxidative cross-linking of proteins.* J Clin Invest, 1993. **91**(6): p. 2866-72.
140. Funk, C.D. and T. Cyrus, *12/15-lipoxygenase, oxidative modification of LDL and atherogenesis.* Trends Cardiovasc Med, 2001. **11**(3-4): p. 116-24.
141. Kuhn, H. and V.B. O'Donnell, *Inflammation and immune regulation by 12/15-lipoxygenases.* Prog Lipid Res, 2006. **45**(4): p. 334-56.
142. Cyrus, T., et al., *Disruption of the 12/15-lipoxygenase gene diminishes atherosclerosis in apo E-deficient mice.* J Clin Invest, 1999. **103**(11): p. 1597-604.
143. Boveris, A. and E. Cadenas, *Mitochondrial production of superoxide anions and its relationship to the antimycin insensitive respiration.* FEBS Lett, 1975. **54**(3): p. 311-4.
144. Boveris, A. and B. Chance, *The mitochondrial generation of hydrogen peroxide. General properties and effect of hyperbaric oxygen.* Biochem J, 1973. **134**(3): p. 707-16.
145. Brand, M.D., et al., *Mitochondrial superoxide and aging: uncoupling-protein activity and superoxide production.* Biochem Soc Symp, 2004(71): p. 203-13.
146. Raimondi, L., et al., *Hydrogen peroxide generation by monoamine oxidases in rat white adipocytes: role on cAMP production.* Eur J Pharmacol, 2000. **395**(3): p. 177-82.
147. Droge, W., *Free radicals in the physiological control of cell function.* Physiol Rev, 2002. **82**(1): p. 47-95.
148. Zhang, Y., et al., *Oxidative and nitrosative stress in the maintenance of myocardial function.* Free Radic Biol Med, 2012.
149. Lounsbury, K.M., Q. Hu, and R.C. Ziegelstein, *Calcium signaling and oxidant stress in the vasculature.* Free Radic Biol Med, 2000. **28**(9): p. 1362-9.
150. Liu, Y., et al., *H2O2 is the transferrable factor mediating flow-induced dilation in human coronary arterioles.* Circ Res. **108**(5): p. 566-73.
151. Harman, D., *Aging: a theory based on free radical and radiation chemistry.* J Gerontol, 1956. **11**(3): p. 298-300.

152. Sonta, T., et al., *Evidence for contribution of vascular NAD(P)H oxidase to increased oxidative stress in animal models of diabetes and obesity.* Free Radic Biol Med, 2004. **37**(1): p. 115-23.
153. Dhalla, N.S., R.M. Temsah, and T. Netticadan, *Role of oxidative stress in cardiovascular diseases.* J Hypertens, 2000. **18**(6): p. 655-73.
154. Kukreja, R.C., R.L. Jesse, and M.L. Hess, *Singlet oxygen: a potential culprit in myocardial injury?* Mol Cell Biochem, 1992. **111**(1-2): p. 17-24.
155. Ha, H., et al., *A mitochondrial porin cDNA predicts the existence of multiple human porins.* J Biol Chem, 1993. **268**(16): p. 12143-9.
156. Kennedy, E.P. and A.L. Lehninger, *The products of oxidation of fatty acids by isolated rat liver mitochondria.* J Biol Chem, 1950. **185**(1): p. 275-85.
157. Lehninger, A.L. and S.W. Smith, *Efficiency of phosphorylation coupled to electron transport between dihydrodiphosphopyridine nucleotide and oxygen.* J Biol Chem, 1949. **181**(1): p. 415-29.
158. Chance, B. and G.R. Williams, *A method for the localization of sites for oxidative phosphorylation.* Nature, 1955. **176**(4475): p. 250-4.
159. Hackenbrock, C.R., B. Chazotte, and S.S. Gupte, *The random collision model and a critical assessment of diffusion and collision in mitochondrial electron transport.* J Bioenerg Biomembr, 1986. **18**(5): p. 331-68.
160. Bianchi, C., et al., *The mitochondrial respiratory chain is partially organized in a supercomplex assembly: kinetic evidence using flux control analysis.* J Biol Chem, 2004. **279**(35): p. 36562-9.
161. Kwong, L.K. and R.S. Sohal, *Substrate and site specificity of hydrogen peroxide generation in mouse mitochondria.* Arch Biochem Biophys, 1998. **350**(1): p. 118-26.
162. Lummen, P., *Complex I inhibitors as insecticides and acaricides.* Biochim Biophys Acta, 1998. **1364**(2): p. 287-96.
163. Lenaz, G. and M.L. Genova, *Structure and organization of mitochondrial respiratory complexes: a new understanding of an old subject.* Antioxid Redox Signal, 2010. **12**(8): p. 961-1008.
164. Shimokata, K., et al., *The proton pumping pathway of bovine heart cytochrome c oxidase.* Proc Natl Acad Sci U S A, 2007. **104**(10): p. 4200-5.
165. Wang, H. and G. Oster, *Energy transduction in the F1 motor of ATP synthase.* Nature, 1998. **396**(6708): p. 279-82.
166. Boyer, P.D., *Catalytic site occupancy during ATP synthase catalysis.* FEBS Lett, 2002. **512**(1-3): p. 29-32.
167. Schagger, H. and K. Pfeiffer, *Supercomplexes in the respiratory chains of yeast and mammalian mitochondria.* EMBO J, 2000. **19**(8): p. 1777-83.
168. Boekema, E.J. and H.P. Braun, *Supramolecular structure of the mitochondrial oxidative phosphorylation system.* J Biol Chem, 2007. **282**(1): p. 1-4.
169. Dudkina, N.V., et al., *The higher level of organization of the oxidative phosphorylation system: mitochondrial supercomplexes.* J Bioenerg Biomembr, 2008. **40**(5): p. 419-24.
170. Mitchell, P. and J. Moyle, *Respiration-driven proton translocation in rat liver mitochondria.* Biochem J, 1967. **105**(3): p. 1147-62.
171. Ricci, J.E., N. Waterhouse, and D.R. Green, *Mitochondrial functions during cell death, a complex (I-V) dilemma.* Cell Death Differ, 2003. **10**(5): p. 488-92.
172. Puchowicz, M.A., et al., *Oxidative phosphorylation analysis: assessing the integrated functional activity of human skeletal muscle mitochondria--case studies.* Mitochondrion, 2004. **4**(5-6): p. 377-85.
173. Kumaran, S., et al., *Age-associated decreased activities of mitochondrial electron transport chain complexes in heart and skeletal muscle: role of L-carnitine.* Chem Biol Interact, 2004. **148**(1-2): p. 11-8.
174. Torii, K., et al., *Age-related decrease in respiratory muscle mitochondrial function in rats.* Am J Respir Cell Mol Biol, 1992. **6**(1): p. 88-92.
175. Ferguson, M., et al., *Age-associated decline in mitochondrial respiration and electron transport in Drosophila melanogaster.* Biochem J, 2005. **390**(Pt 2): p. 501-11.

176. Wei, Y.H., et al., *Respiratory function decline and DNA mutation in mitochondria, oxidative stress and altered gene expression during aging.* Chang Gung Med J, 2009. **32**(2): p. 113-32.
177. Ungvari, Z., et al., *Dysregulation of mitochondrial biogenesis in vascular endothelial and smooth muscle cells of aged rats.* Am J Physiol Heart Circ Physiol, 2008. **294**(5): p. H2121-8.
178. Boudina, S. and E.D. Abel, *Diabetic cardiomyopathy revisited.* Circulation, 2007. **115**(25): p. 3213-23.
179. Boudina, S., et al., *Mitochondrial energetics in the heart in obesity-related diabetes: direct evidence for increased uncoupled respiration and activation of uncoupling proteins.* Diabetes, 2007. **56**(10): p. 2457-66.
180. van der Vusse, G.J., et al., *Fatty acid homeostasis in the normoxic and ischemic heart.* Physiol Rev, 1992. **72**(4): p. 881-940.
181. Gertz, E.W., et al., *Myocardial substrate utilization during exercise in humans. Dual carbon-labeled carbohydrate isotope experiments.* J Clin Invest, 1988. **82**(6): p. 2017-25.
182. Wang, X., et al., *Alterations in myocardial lipid metabolism during lactation in the rat.* Am J Physiol, 1998. **275**(2 Pt 1): p. E265-71.
183. de Jong, J.W. and W.C. Hulsmann, *A comparative study of palmitoyl-CoA synthetase activity in rat-liver, heart and gut mitochondrial and microsomal preparations.* Biochim Biophys Acta, 1970. **197**(2): p. 127-35.
184. Lopaschuk, G.D., et al., *Myocardial fatty acid metabolism in health and disease.* Physiol Rev, 2010. **90**(1): p. 207-58.
185. Kodde, I.F., et al., *Metabolic and genetic regulation of cardiac energy substrate preference.* Comp Biochem Physiol A Mol Integr Physiol, 2007. **146**(1): p. 26-39.
186. White, F.N. and G. Somero, *Acid-base regulation and phospholipid adaptations to temperature: time courses and physiological significance of modifying the milieu for protein function.* Physiol Rev, 1982. **62**(1): p. 40-90.
187. Brenner, R.R., *Effect of unsaturated acids on membrane structure and enzyme kinetics.* Prog Lipid Res, 1984. **23**(2): p. 69-96.
188. Hoch, F.L., *Cardiolipins and biomembrane function.* Biochim Biophys Acta, 1992. **1113**(1): p. 71-133.
189. Esrey, K.L., L. Joseph, and S.A. Grover, *Relationship between dietary intake and coronary heart disease mortality: lipid research clinics prevalence follow-up study.* J Clin Epidemiol, 1996. **49**(2): p. 211-6.
190. Kushi, L.H., et al., *Diet and 20-year mortality from coronary heart disease. The Ireland-Boston Diet-Heart Study.* N Engl J Med, 1985. **312**(13): p. 811-8.
191. Degirolamo, C. and L.L. Rudel, *Dietary monounsaturated fatty acids appear not to provide cardioprotection.* Curr Atheroscler Rep, 2010. **12**(6): p. 391-6.
192. Gillingham, L.G., S. Harris-Janz, and P.J. Jones, *Dietary monounsaturated fatty acids are protective against metabolic syndrome and cardiovascular disease risk factors.* Lipids, 2011. **46**(3): p. 209-28.
193. Demaison, L., et al., *Effects of dietary polyunsaturated fatty acids and hepatic steatosis on the functioning of isolated working rat heart under normoxic conditions and during post-ischemic reperfusion.* Mol Cell Biochem, 2001. **224**(1-2): p. 103-16.
194. Adkins, Y. and D.S. Kelley, *Mechanisms underlying the cardioprotective effects of omega-3 polyunsaturated fatty acids.* J Nutr Biochem, 2010. **21**(9): p. 781-92.
195. Brockerhoff, H., R.J. Hoyle, and P.C. Hwang, *Incorporation of fatty acids of marine origin into triglycerides and phospholipids of mammals.* Biochim Biophys Acta, 1967. **144**(3): p. 541-8.
196. Charnock, J.S., et al., *Differences in fatty acid composition of various tissues of the marmoset monkey (Callithrix jacchus) after different lipid supplemented diets.* Comp Biochem Physiol Comp Physiol, 1992. **101**(2): p. 387-93.
197. Ayre, K.J. and A.J. Hulbert, *Dietary fatty acid profile influences the composition of skeletal muscle phospholipids in rats.* J Nutr, 1996. **126**(3): p. 653-62.
198. Liautaud, S., et al., *Fatty acids of hearts from rats fed linseed or sunflower oil and of cultured cardiomyocytes grown on their sera.* Cardioscience, 1991. **2**(1): p. 55-61.
199. Das, U.N., *Essential Fatty acids - a review.* Curr Pharm Biotechnol, 2006. **7**(6): p. 467-82.

200. Julia, P., et al., *Studies of myocardial protection in the immature heart. II. Evidence for importance of amino acid metabolism in tolerance to ischemia.* J Thorac Cardiovasc Surg, 1990. **100**(6): p. 888-95.
201. Lommi, J., et al., *Blood ketone bodies in congestive heart failure.* J Am Coll Cardiol, 1996. **28**(3): p. 665-72.
202. Ferdinandy, P., R. Schulz, and G.F. Baxter, *Interaction of cardiovascular risk factors with myocardial ischemia/reperfusion injury, preconditioning, and postconditioning.* Pharmacol Rev, 2007. **59**(4): p. 418-58.
203. Bonventre, J.V., *Mechanisms of ischemic acute renal failure.* Kidney Int, 1993. **43**(5): p. 1160-78.
204. Stanley, W.C., F.A. Recchia, and G.D. Lopaschuk, *Myocardial substrate metabolism in the normal and failing heart.* Physiol Rev, 2005. **85**(3): p. 1093-129.
205. Salem, J.E., et al., *Mechanistic model of myocardial energy metabolism under normal and ischemic conditions.* Ann Biomed Eng, 2002. **30**(2): p. 202-16.
206. Opie, L.H., *Effects of regional ischemia on metabolism of glucose and fatty acids. Relative rates of aerobic and anaerobic energy production during myocardial infarction and comparison with effects of anoxia.* Circ Res, 1976. **38**(5 Suppl 1): p. I52-74.
207. Effros, R.M., et al., *In vivo myocardial cell pH in the dog. Response to ischemia and infusion of alkali.* J Clin Invest, 1975. **55**(5): p. 1100-10.
208. Rahimtoola, S.H., *The hibernating myocardium in ischaemia and congestive heart failure.* Eur Heart J, 1993. **14 Suppl A**: p. 22-6.
209. Clanachan, A.S., *Contribution of protons to post-ischemic Na(+) and Ca(2+) overload and left ventricular mechanical dysfunction.* J Cardiovasc Electrophysiol, 2006. **17 Suppl 1**: p. S141-S148.
210. Steenbergen, C., et al., *Correlation between cytosolic free calcium, contracture, ATP, and irreversible ischemic injury in perfused rat heart.* Circ Res, 1990. **66**(1): p. 135-46.
211. Henry, P.D., et al., *Myocardial contracture and accumulation of mitochondrial calcium in ischemic rabbit heart.* Am J Physiol, 1977. **233**(6): p. H677-84.
212. Marban, E., et al., *Quantification of [Ca2+]i in perfused hearts. Critical evaluation of the 5F-BAPTA and nuclear magnetic resonance method as applied to the study of ischemia and reperfusion.* Circ Res, 1990. **66**(5): p. 1255-67.
213. Orchard, C.H., et al., *Acidosis facilitates spontaneous sarcoplasmic reticulum Ca2+ release in rat myocardium.* J Gen Physiol, 1987. **90**(1): p. 145-65.
214. Hess, M.L. and N.H. Manson, *Molecular oxygen: friend and foe. The role of the oxygen free radical system in the calcium paradox, the oxygen paradox and ischemia/reperfusion injury.* J Mol Cell Cardiol, 1984. **16**(11): p. 969-85.
215. Ferri, K.F. and G. Kroemer, *Organelle-specific initiation of cell death pathways.* Nat Cell Biol, 2001. **3**(11): p. E255-63.
216. Majno, G. and I. Joris, *Apoptosis, oncosis, and necrosis. An overview of cell death.* Am J Pathol, 1995. **146**(1): p. 3-15.
217. Hearse, D.J., S.M. Humphrey, and E.B. Chain, *Abrupt reoxygenation of the anoxic potassium-arrested perfused rat heart: a study of myocardial enzyme release.* J Mol Cell Cardiol, 1973. **5**(4): p. 395-407.
218. Arroyo, C.M., et al., *Identification of free radicals in myocardial ischemia/reperfusion by spin trapping with nitrone DMPO.* FEBS Lett, 1987. **221**(1): p. 101-4.
219. Bolli, R., et al., *Direct evidence that oxygen-derived free radicals contribute to postischemic myocardial dysfunction in the intact dog.* Proc Natl Acad Sci U S A, 1989. **86**(12): p. 4695-9.
220. Walker, C.A. and F.G. Spinale, *The structure and function of the cardiac myocyte: a review of fundamental concepts.* J Thorac Cardiovasc Surg, 1999. **118**(2): p. 375-82.
221. Cadenas, E. and K.J. Davies, *Mitochondrial free radical generation, oxidative stress, and aging.* Free Radic Biol Med, 2000. **29**(3-4): p. 222-30.
222. Lemasters, J.J., et al., *Mitochondrial calcium and the permeability transition in cell death.* Biochim Biophys Acta, 2009. **1787**(11): p. 1395-401.
223. Kaminski, K.A., et al., *Oxidative stress and neutrophil activation--the two keystones of ischemia/reperfusion injury.* Int J Cardiol, 2002. **86**(1): p. 41-59.

224. Eltzschig, H.K. and C.D. Collard, *Vascular ischaemia and reperfusion injury.* Br Med Bull, 2004. **70**: p. 71-86.
225. Furchgott, R.F. and J.V. Zawadzki, *The obligatory role of endothelial cells in the relaxation of arterial smooth muscle by acetylcholine.* Nature, 1980. **288**(5789): p. 373-6.
226. Brutsaert, D.L., *Cardiac endothelial-myocardial signaling: its role in cardiac growth, contractile performance, and rhythmicity.* Physiol Rev, 2003. **83**(1): p. 59-115.
227. Landmesser, U., B. Hornig, and H. Drexler, *Endothelial function: a critical determinant in atherosclerosis?* Circulation, 2004. **109**(21 Suppl 1): p. II27-33.
228. Bonetti, P.O., L.O. Lerman, and A. Lerman, *Endothelial dysfunction: a marker of atherosclerotic risk.* Arterioscler Thromb Vasc Biol, 2003. **23**(2): p. 168-75.
229. Endemann, D.H. and E.L. Schiffrin, *Endothelial dysfunction.* J Am Soc Nephrol, 2004. **15**(8): p. 1983-92.
230. Le Brocq, M., et al., *Endothelial dysfunction: from molecular mechanisms to measurement, clinical implications, and therapeutic opportunities.* Antioxid Redox Signal, 2008. **10**(9): p. 1631-74.
231. Feletou, M. and P.M. Vanhoutte, *Endothelium-dependent hyperpolarizations: past beliefs and present facts.* Ann Med, 2007. **39**(7): p. 495-516.
232. Luksha, L., S. Agewall, and K. Kublickiene, *Endothelium-derived hyperpolarizing factor in vascular physiology and cardiovascular disease.* Atherosclerosis, 2009. **202**(2): p. 330-44.
233. Lundberg, J.O., E. Weitzberg, and M.T. Gladwin, *The nitrate-nitrite-nitric oxide pathway in physiology and therapeutics.* Nat Rev Drug Discov, 2008. **7**(2): p. 156-67.
234. Lincoln, T.M., N. Dey, and H. Sellak, *Invited review: cGMP-dependent protein kinase signaling mechanisms in smooth muscle: from the regulation of tone to gene expression.* J Appl Physiol, 2001. **91**(3): p. 1421-30.
235. Bolotina, V.M., et al., *Nitric oxide directly activates calcium-dependent potassium channels in vascular smooth muscle.* Nature, 1994. **368**(6474): p. 850-3.
236. Moncada, S., et al., *An enzyme isolated from arteries transforms prostaglandin endoperoxides to an unstable substance that inhibits platelet aggregation.* Nature, 1976. **263**(5579): p. 663-5.
237. Moncada, S., et al., *Differential formation of prostacyclin (PGX or PGI2) by layers of the arterial wall. An explanation for the anti-thrombotic properties of vascular endothelium.* Thromb Res, 1977. **11**(3): p. 323-44.
238. Busse, R., et al., *EDHF: bringing the concepts together.* Trends Pharmacol Sci, 2002. **23**(8): p. 374-80.
239. Bryan, R.M., Jr., et al., *Endothelium-derived hyperpolarizing factor: a cousin to nitric oxide and prostacyclin.* Anesthesiology, 2005. **102**(6): p. 1261-77.
240. Shimokawa, H. and K. Morikawa, *Hydrogen peroxide is an endothelium-derived hyperpolarizing factor in animals and humans.* J Mol Cell Cardiol, 2005. **39**(5): p. 725-32.
241. Liu, Y., et al., *H2O2 is the transferrable factor mediating flow-induced dilation in human coronary arterioles.* Circ Res, 2011. **108**(5): p. 566-73.
242. Beny, J.L. and O. Schaad, *An evaluation of potassium ions as endothelium-derived hyperpolarizing factor in porcine coronary arteries.* Br J Pharmacol, 2000. **131**(5): p. 965-73.
243. Sandow, S.L. and M. Tare, *C-type natriuretic peptide: a new endothelium-derived hyperpolarizing factor?* Trends Pharmacol Sci, 2007. **28**(2): p. 61-7.
244. Christ, G.J., et al., *Gap junctions in vascular tissues. Evaluating the role of intercellular communication in the modulation of vasomotor tone.* Circ Res, 1996. **79**(4): p. 631-46.
245. Shimokawa, H., et al., *The importance of the hyperpolarizing mechanism increases as the vessel size decreases in endothelium-dependent relaxations in rat mesenteric circulation.* J Cardiovasc Pharmacol, 1996. **28**(5): p. 703-11.
246. Ozkor, M.A. and A.A. Quyyumi, *Endothelium-derived hyperpolarizing factor and vascular function.* Cardiol Res Pract, 2011. **2011**: p. 156146.
247. Pearson, P.J. and P.M. Vanhoutte, *Vasodilator and vasoconstrictor substances produced by the endothelium.* Rev Physiol Biochem Pharmacol, 1993. **122**: p. 1-67.
248. Koga, T., et al., *Age and hypertension promote endothelium-dependent contractions to acetylcholine in the aorta of the rat.* Hypertension, 1989. **14**(5): p. 542-8.

249. Shimokawa, H., *Primary endothelial dysfunction: atherosclerosis.* J Mol Cell Cardiol, 1999. **31**(1): p. 23-37.
250. Schini, V.B. and P.M. Vanhoutte, *Endothelin-1: a potent vasoactive peptide.* Pharmacol Toxicol, 1991. **69**(5): p. 303-9.
251. Paterno, R., F.M. Faraci, and D.D. Heistad, *Age-related changes in release of endothelium-derived relaxing factor from the carotid artery.* Stroke, 1994. **25**(12): p. 2457-60; discussion 2461-2.
252. Delp, M.D., et al., *Ageing diminishes endothelium-dependent vasodilatation and tetrahydrobiopterin content in rat skeletal muscle arterioles.* J Physiol, 2008. **586**(4): p. 1161-8.
253. Poirier, P., et al., *Obesity and cardiovascular disease: pathophysiology, evaluation, and effect of weight loss: an update of the 1997 American Heart Association Scientific Statement on Obesity and Heart Disease from the Obesity Committee of the Council on Nutrition, Physical Activity, and Metabolism.* Circulation, 2006. **113**(6): p. 898-918.
254. Alpert, M.A., et al., *Relation of duration of morbid obesity to left ventricular mass, systolic function, and diastolic filling, and effect of weight loss.* Am J Cardiol, 1995. **76**(16): p. 1194-7.
255. Ridker, P.M., *Novel risk factors and markers for coronary disease.* Adv Intern Med, 2000. **45**: p. 391-418.
256. Tesfamariam, B. and R.A. Cohen, *Free radicals mediate endothelial cell dysfunction caused by elevated glucose.* Am J Physiol, 1992. **263**(2 Pt 2): p. H321-6.
257. Pieper, G.M., P. Langenstroer, and W. Siebeneich, *Diabetic-induced endothelial dysfunction in rat aorta: role of hydroxyl radicals.* Cardiovasc Res, 1997. **34**(1): p. 145-56.
258. Fulop, T., et al., *Adaptation of vasomotor function of human coronary arterioles to the simultaneous presence of obesity and hypertension.* Arterioscler Thromb Vasc Biol, 2007. **27**(11): p. 2348-54.
259. Auguet, M., S. Delaflotte, and P. Braquet, *Increased influence of endothelium in obese Zucker rat aorta.* J Pharm Pharmacol, 1989. **41**(12): p. 861-4.
260. Bhattacharya, I., et al., *Regional heterogeneity of functional changes in conduit arteries after high-fat diet.* Obesity (Silver Spring), 2008. **16**(4): p. 743-8.
261. Mundy, A.L., et al., *Fat intake modifies vascular responsiveness and receptor expression of vasoconstrictors: implications for diet-induced obesity.* Cardiovasc Res, 2007. **73**(2): p. 368-75.
262. Oltman, C.L., et al., *Progression of coronary and mesenteric vascular dysfunction in Zucker obese and Zucker diabetic fatty rats.* Am J Physiol Heart Circ Physiol, 2006. **291**(4): p. H1780-7.
263. Bagi, Z., *Mechanisms of coronary microvascular adaptation to obesity.* Am J Physiol Regul Integr Comp Physiol, 2009. **297**(3): p. R556-67.
264. Lakatta, E.G., *Age-associated cardiovascular changes in health: impact on cardiovascular disease in older persons.* Heart Fail Rev, 2002. **7**(1): p. 29-49.
265. Malik, V.S., et al., *Dietary patterns during adolescence and risk of type 2 diabetes in middle-aged women.* Diabetes Care, 2012. **35**(1): p. 12-8.
266. Bao, W., et al., *Persistence of multiple cardiovascular risk clustering related to syndrome X from childhood to young adulthood. The Bogalusa Heart Study.* Arch Intern Med, 1994. **154**(16): p. 1842-7.
267. Berenson, G.S., S.R. Srinivasan, and T.A. Nicklas, *Atherosclerosis: a nutritional disease of childhood.* Am J Cardiol, 1998. **82**(10B): p. 22T-29T.
268. Juhaszova, M., et al., *Protection in the aged heart: preventing the heart-break of old age?* Cardiovasc Res, 2005. **66**(2): p. 233-44.
269. Oudot, A., et al., *NADPH oxidases are in part responsible for increased cardiovascular superoxide production during aging.* Free Radic Biol Med, 2006. **40**(12): p. 2214-22.
270. Lesnefsky, E.J. and C.L. Hoppel, *Ischemia-reperfusion injury in the aged heart: role of mitochondria.* Arch Biochem Biophys, 2003. **420**(2): p. 287-97.
271. Clark, L.C., Jr., et al., *Continuous recording of blood oxygen tensions by polarography.* J Appl Physiol, 1953. **6**(3): p. 189-93.

272. Chance, B. and G.R. Williams, *Respiratory enzymes in oxidative phosphorylation. III. The steady state.* J Biol Chem, 1955. **217**(1): p. 409-27.
273. Mokdad, A.H., et al., *Prevalence of obesity, diabetes, and obesity-related health risk factors, 2001.* JAMA, 2003. **289**(1): p. 76-9.
274. Selvin, E., J. Coresh, and F.L. Brancati, *The burden and treatment of diabetes in elderly individuals in the u.s.* Diabetes Care, 2006. **29**(11): p. 2415-9.
275. Keaney, J.F., Jr., et al., *Obesity and systemic oxidative stress: clinical correlates of oxidative stress in the Framingham Study.* Arterioscler Thromb Vasc Biol, 2003. **23**(3): p. 434-9.
276. Furukawa, S., et al., *Increased oxidative stress in obesity and its impact on metabolic syndrome.* J Clin Invest, 2004. **114**(12): p. 1752-61.
277. Kakarla, S.K., et al., *Chronic acetaminophen attenuates age-associated increases in cardiac ROS and apoptosis in the Fischer Brown Norway rat.* Basic Res Cardiol, 2010. **105**(4): p. 535-44.
278. Asano, S., et al., *Aging influences multiple indices of oxidative stress in the heart of the Fischer 344/NNia x Brown Norway/BiNia rat.* Redox Rep, 2007. **12**(4): p. 167-80.
279. Shimomura, I., et al., *Enhanced expression of PAI-1 in visceral fat: possible contributor to vascular disease in obesity.* Nat Med, 1996. **2**(7): p. 800-3.
280. Yamauchi, T., et al., *Globular adiponectin protected ob/ob mice from diabetes and ApoE-deficient mice from atherosclerosis.* J Biol Chem, 2003. **278**(4): p. 2461-8.
281. Hotamisligil, G.S., N.S. Shargill, and B.M. Spiegelman, *Adipose expression of tumor necrosis factor-alpha: direct role in obesity-linked insulin resistance.* Science, 1993. **259**(5091): p. 87-91.
282. Bruun, J.M., et al., *Regulation of adiponectin by adipose tissue-derived cytokines: in vivo and in vitro investigations in humans.* Am J Physiol Endocrinol Metab, 2003. **285**(3): p. E527-33.
283. Meigs, J.B., et al., *The natural history of progression from normal glucose tolerance to type 2 diabetes in the Baltimore Longitudinal Study of Aging.* Diabetes, 2003. **52**(6): p. 1475-84.
284. Chen, M., et al., *Pathogenesis of age-related glucose intolerance in man: insulin resistance and decreased beta-cell function.* J Clin Endocrinol Metab, 1985. **60**(1): p. 13-20.
285. Dong, F., et al., *Impaired cardiac contractile function in ventricular myocytes from leptin-deficient ob/ob obese mice.* J Endocrinol, 2006. **188**(1): p. 25-36.
286. Ouwens, D.M., et al., *Cardiac contractile dysfunction in insulin-resistant rats fed a high-fat diet is associated with elevated CD36-mediated fatty acid uptake and esterification.* Diabetologia, 2007. **50**(9): p. 1938-48.
287. Vincent, A.M., et al., *Short-term hyperglycemia produces oxidative damage and apoptosis in neurons.* FASEB J, 2005. **19**(6): p. 638-40.
288. Ceriello, A., et al., *Acute hyperglycemia induces nitrotyrosine formation and apoptosis in perfused heart from rat.* Diabetes, 2002. **51**(4): p. 1076-82.
289. Yuill, K.H., D. Tosh, and J.C. Hancox, *Streptozotocin-induced diabetes modulates action potentials and ion channel currents from the rat atrioventricular node.* Exp Physiol, 2010. **95**(4): p. 508-17.
290. D'Amico, M., et al., *High glucose induces ventricular instability and increases vasomotor tone in rats.* Diabetologia, 2001. **44**(4): p. 464-70.
291. Gerhard, M., et al., *Aging progressively impairs endothelium-dependent vasodilation in forearm resistance vessels of humans.* Hypertension, 1996. **27**(4): p. 849-53.
292. Muller-Delp, J.M., et al., *Aging impairs endothelium-dependent vasodilation in rat skeletal muscle arterioles.* Am J Physiol Heart Circ Physiol, 2002. **283**(4): p. H1662-72.
293. Haines, R.J., et al., *Protein Kinase Calpha Phosphorylates a Novel Argininosuccinate Synthase Site at Serine 328 during Calcium-dependent Stimulation of Endothelial Nitric-oxide Synthase in Vascular Endothelial Cells.* J Biol Chem. **287**(31): p. 26168-76.
294. Headrick, J.P., *Aging impairs functional, metabolic and ionic recovery from ischemia-reperfusion and hypoxia-reoxygenation.* J Mol Cell Cardiol, 1998. **30**(7): p. 1415-30.
295. Willems, L., B. Garnham, and J.P. Headrick, *Aging-related changes in myocardial purine metabolism and ischemic tolerance.* Exp Gerontol, 2003. **38**(10): p. 1169-77.
296. Tomanek, R.J., M.R. Aydelotte, and R.J. Torry, *Remodeling of coronary vessels during aging in purebred beagles.* Circ Res, 1991. **69**(4): p. 1068-74.

297. Jebelovszki, E., et al., *High-fat diet-induced obesity leads to increased NO sensitivity of rat coronary arterioles: role of soluble guanylate cyclase activation.* Am J Physiol Heart Circ Physiol, 2008. **294**(6): p. H2558-64.
298. Brandes, R.P., et al., *Increased nitrovasodilator sensitivity in endothelial nitric oxide synthase knockout mice: role of soluble guanylyl cyclase.* Hypertension, 2000. **35**(1 Pt 2): p. 231-6.
299. Baber, S.R., et al., *Vasoactive prostanoids are generated from arachidonic acid by COX-1 and COX-2 in the mouse.* Am J Physiol Heart Circ Physiol, 2005. **289**(4): p. H1476-87.
300. Clark, J.B., C.J. Palmer, and W.N. Shaw, *The diabetic Zucker fatty rat.* Proc Soc Exp Biol Med, 1983. **173**(1): p. 68-75.
301. Cole, M.A., et al., *A high fat diet increases mitochondrial fatty acid oxidation and uncoupling to decrease efficiency in rat heart.* Basic Res Cardiol. **106**(3): p. 447-57.
302. Romero-Corral, A., et al., *Normal weight obesity: a risk factor for cardiometabolic dysregulation and cardiovascular mortality.* Eur Heart J, 2010. **31**(6): p. 737-46.
303. Marques-Vidal, P., et al., *Normal weight obesity: relationship with lipids, glycaemic status, liver enzymes and inflammation.* Nutr Metab Cardiovasc Dis, 2010. **20**(9): p. 669-75.
304. Shea, J.L., et al., *Body fat percentage is associated with cardiometabolic dysregulation in BMI-defined normal weight subjects.* Nutr Metab Cardiovasc Dis, 2012. **22**(9): p. 741-7.
305. Habbout, A., et al., *Postnatal overfeeding in rats leads to moderate overweight and to cardiometabolic and oxidative alterations in adulthood.* Biochimie, 2012. **94**(1): p. 117-24.
306. Kruger, M.J., et al., *Dietary red palm oil reduces ischaemia-reperfusion injury in rats fed a hypercholesterolaemic diet.* Br J Nutr, 2007. **97**(4): p. 653-60.
307. Wang, P. and J.C. Chatham, *Onset of diabetes in Zucker diabetic fatty (ZDF) rats leads to improved recovery of function after ischemia in the isolated perfused heart.* Am J Physiol Endocrinol Metab, 2004. **286**(5): p. E725-36.
308. Starnes, J.W., R.P. Taylor, and J.T. Ciccolo, *Habitual low-intensity exercise does not protect against myocardial dysfunction after ischemia in rats.* Eur J Cardiovasc Prev Rehabil, 2005. **12**(2): p. 169-74.
309. Fenning, A., et al., *Cardiac adaptation to endurance exercise in rats.* Mol Cell Biochem, 2003. **251**(1-2): p. 51-9.
310. Soufi, F.G., et al., *Role of 12-week resistance training in preserving the heart against ischemia-reperfusion-induced injury.* Cardiol J. **18**(2): p. 140-5.
311. Kingwell, B.A., et al., *Spontaneous running increases aortic compliance in Wistar-Kyoto rats.* Cardiovasc Res, 1997. **35**(1): p. 132-7.
312. Chen Hi, H., I.P. Chiang, and C.J. Jen, *Exercise Training Increases Acetylcholine-Stimulated Endothelium-Derived Nitric Oxide Release in Spontaneously Hypertensive Rats.* J Biomed Sci, 1996. **3**(6): p. 454-460.
313. Delp, M.D., R.M. McAllister, and M.H. Laughlin, *Exercise training alters endothelium-dependent vasoreactivity of rat abdominal aorta.* J Appl Physiol, 1993. **75**(3): p. 1354-63.
314. Muller, J.M., P.R. Myers, and M.H. Laughlin, *Vasodilator responses of coronary resistance arteries of exercise-trained pigs.* Circulation, 1994. **89**(5): p. 2308-14.
315. Rippe, C., et al., *Short-term calorie restriction reverses vascular endothelial dysfunction in old mice by increasing nitric oxide and reducing oxidative stress.* Aging Cell. **9**(3): p. 304-12.

PART IV. ANNEXE

Journal of Cardiovascular Pharmacology 2011 Sep;58(3):284-94.

"Disruption of chronic cariporide treatment abrogates myocardial ion homeostasis during acute ischemia reperfusion"

Bourahla V, Dubouchaud H, **Mourmoura E**, Vitiello D, Faure P, Migné C, Pujos-Guillot E, Richardson M, Demaison L.

Abstract

Cariporide, an Na/H exchanger inhibitor, is a drug with cardioprotective properties. However, chronic treatment with cariporide may modify the protein phenotype of the cardiomyocytes. Disruption of the equilibrium between a cariporide-modified phenotype and the supply of cariporide could be deleterious. The aim of this study was to test the effects of this equilibrium rupture (EqR) on cardiac function at baseline and acute ischemia reperfusion. Rats were chronically treated with cariporide (2.5 mg·kg·d) or with placebo for 21 days, after which isolated Langendorff-mode heart perfusion experiments utilized cariporide-free buffer. During this type of perfusion, the drug is rapidly cleared from the cellular environment. After 30 minutes of stabilization, the hearts were subjected to global zero-flow ischemia (25 minutes) followed by reperfusion (45 minutes). Measures of mechanical function, oxygen consumption, lactate plus pyruvate, CO2 and proton release into the coronary effluent were determined. The gene and protein expression of proton extruders was also evaluated. Chronic cariporide administration followed by EqR reduced the expression of the Na/H exchanger, increased the expression of the HCO3 or Na exchanger, decreased monocarboxylate/H carrier expression, reduced the lactate plus pyruvate release but did not change the glucose oxidation rate and mechanical function compared with baseline conditions. The resulting low glycolytic rate was associated with a stronger contracture during ischemia. During reperfusion, the early release of acidic forms was higher and redirected toward the use of the Na/H and HCO3 /Na exchangers to the detriment of the safe monocarboxylate/H carrier. Both phenomena were assumed to increase the Na uptake and activate the Na/Ca exchanger, resulting in Na and Ca overload and further cellular damage. This explains the impaired recovery of the contractile function observed in the EqR group during reperfusion. In conclusion, although cariporide is usually cardioprotective, a disruption of its chronic treatment followed by an ischemia/reperfusion event can become deleterious.

PMID: 21697734

Evangelia MOURMOURA
1, rue Paul Janet
38000 GRENOBLE
Tel: +33 (0)6 88 95 00 12
E-mail: evangelia.mourmoura@ujf-grenoble.fr
evoumour@hotmail.com
Date of birth: 29/02/1984
Nationality: Greek

Ph.D. student in Cardiovascular Physiology
(3rd year)

EDUCATION

2009-2012 ***Ph.D. Thesis*: « Effect of increased abdominal adipose tissue on the cardiovascular function studied *ex vivo*, the oxidative stress and mitochondrial function regarding the age»**

Supervisor: Dr. Luc DEMAISON (luc.demaison@ujf-grenoble.fr)

LABORATORY OF FUNDAMENTAL AND APPLIED BIOENERGETICS (LBFA-INSERM U1055, FRANCE)

Heart Perfusion at Langendorff mode (at constant flow/pressure, Coronary Reactivity, Ischemia/Reperfusion, Pulmonary Artery Catheterization) – Mitochondria isolation – Oxygraphy Measurements – Mitochondrial ROS production - Oxidtive stress determinations - Spectrophotometry – Fluorimetry – Western Blot – Animal Treatment: Oral Feeding, Blood Collection, Anesthesia, Organ and Tissue Extractions, Oral Glucose Tolerance Test – Statistical analyses

Scholarships: Research Scholarship (1/10/'09-30/09/'12) of the French Ministry of Education (MENRT)

2010 **Certificate for Animal Experimentation**
GRENOBLE UNIVERSITY, FRANCE

2008-2009 **Master: « Cellular and Integrative Biology »** (Grade: Good)
UNIVERSITY JOSEPH FOURIER, FACULTY OF BIOLOGY, GRENOBLE, FRANCE

2001-2007 **University Diploma in Biology** (Grade: Good)
NATIONAL AND KAPODISTRIAN UNIVERSITY OF ATHENS, GREECE

2001 **High School Diploma** (Grade 19.3/20)
3rd HELLENIC LYCEUM OF RHODES, GREECE

PROFESSIONAL EXPERIENCE

2010 ***Guidance*** of an Advanced Vocational Diploma student (2 months)
LBFA, INSERM U1055, FRANCE

2008-2009 ***Internship:* « The relative importance of the forced physical inactivity and obesity on the coronary vessel function regarding the age: Study of the Lou/C rat »**
LBFA- INSERM U1055, FRANCE

2004-2005	*Internship:* « **Histochemical and anatomical study of pharmaceutical plants of the greek flora** » Histochemistry –Microscopy *BOTANY DEPARTMENT, NATIONAL AND KAPODISTRIAN UNIVERSITY OF ATHENS, GREECE*
2004-2007	***Private biology lessons*** to secondary education students *ATHENS, GREECE*
2005, 2007	***Operator*** in the Departments of Telephone Directory Information and of Marketing *HELLENIC TELECOMMUNICATIONS ORGANIZATION (OTE S.A.), ATHENS, GREECE*
2007-2011	Member of Panhellenic Union of Bioscientists, *ATHENS, GREECE*

PUBLICATIONS

1. **Mourmoura E**, Leguen M, Dubouchaud H, Couturier K, Vitiello D, Lafond JL, Richardson M, Leverve X, Demaison L. ***Middle age aggravates myocardial ischemia through surprising upholding of complex II activity, oxidative stress, and reduced coronary perfusion***. Age. 2010 Sep 29.
2. Bourahla V, Dubouchaud H, **Mourmoura E**, Vitiello D, Faure P, Migné C, Pujos-Guillot E, Richardson M, Demaison L. ***Disruption of cariporide treatment abrogates myocardial ion homeostasis during acute ischemia reperfusion.*** J Cardiovasc Pharmacol. 2011 Sep;58(3):284-94.

CONFERENCES

- Physiology 2012, 2-5 July 2013, Edinburgh, United Kingdom
  Oral Presentation : " Aging and Reactivity of Coronrary Resistance arteries."
- Physiology 2012, 2-5 July 2013, Edinburgh, United Kingdom
  Poster Presentation:"Adaptation of the coronary microvascular system by a high-fat diet: cross-interaction study between diet and ageing"
- Journée G2L2, (**G**enève, **G**renoble, **L**yon, **L**ausanne), 30 Mars 2012, Lyon, France
  Oral Presentation (in French): **"The effects of a high-fat diet on the cardiovascular function studied *ex vivo*."**
- 9th International Congress on Coronary Artery Disease (ICCAD), 23-26 October 2011, Venice, Italy
  Poster Presentation: **"Adaptation of the coronary vascular function studied *ex vivo*."**
- 8th NSFA (Nouvelle Société Française d'Athérosclérose) Congress and 5th Joint meeting of French, German and Swiss Atherosclerosis Societies 2011, 16-18 juin 2011, Avignon, France
  Poster Presentation: **"Effects of obesity on the coronary vessel function studied *ex vivo*"**
- 5ème Colloque Meetochondrie, 2-5 Mai 2011, La Colle-sur-Loup (Alpes-Maritimes), France
  Poster Presentation: **"Increasing age, coronary reactivity and oxidative stress in the Wistar and anti-obese Lou/C rat."**
- Global Obesity Summit, 9-11 November 2010, Jackson, Mississipi, USA
  Poster Presentation: **"Aging of the anti-obese Lou/C rat, oxidative stress and coronary Reactivity."**

SKILLS & OUALIFICATIONS

Languages: 1. Greek: Native language

2. English: level C2 (Certificate of Proficiency in English, University of Cambridge)

3. French: level C2

4. German: level B2 (Zentrale Mittelstufenprufung,Goethe Institut)

5. Spanish: level A1

Computer skills: Word, Excel, Power Point, Access, Windows,
NCSS system, ISOHEART software

Artistic skills: Piano degree
HELLENIC CONSERVATORY OF ATHENS, GREECE

HOBBIES & INTERESTS

Classical music, Photography (black & white), Volleyball

« Ἓν οἶδα, ὅτι οὐδὲν οἶδα »

Σωκράτης

« Je ne sais qu’une chose, c’est que je ne sais rien »

Socrates